Influence of peroxisomes on development, maturation and adult functions of the testis

ANCA NENICU

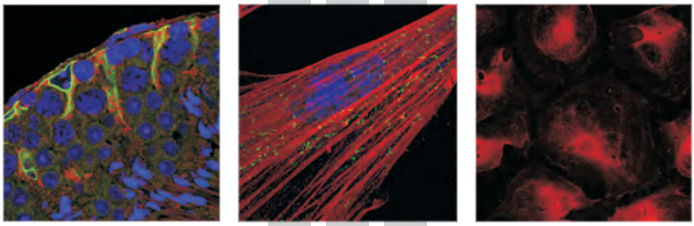

INAUGURAL DISSERTATION
submitted to the Faculty of Medicine
in fulfillment of the requirements
for the PhD-degree of the
Faculties of Veterinary Medicine and Medicine
of the Justus Liebig University Giessen

édition scientifique
VVB LAUFERSWEILER VERLAG

1. Auflage 2010

1st Edition 2010

édition scientifique
VVB LAUFERSWEILER VERLAG

STAUFENBERGRING 15, D-35396 GIESSEN
Tel: 0641-5599888 Fax: 0641-5599890
email: redaktion@doktorverlag.de

www.doktorverlag.de

Institute for Anatomy and Cell Biology II
Faculty of Medicine of the Justus Liebig University Giessen

Influence of peroxisomes on development, maturation and adult functions of the testis

Inaugural Dissertation

submitted to the
Faculty of Medicine
in fulfillment of the requirements
for the PhD-degree
of the Faculties of Veterinary Medicine and Medicine
of the Justus Liebig University Giessen

Anca Nenicu

Giessen 2010

From the Institute for Anatomy and Cell Biology II
of the Faculty of Medicine of the Justus Liebig University of Giessen
Director / Chairperson: Prof. Dr. Eveline Baumgart-Vogt

First Supervisor and Committee Member: Prof. Dr. Eveline Baumgart-Vogt

Second Supervisor and Committee Member: Priv.-Doz. Dr. Joachim Weitzel

Committee Members: **Prof. Dr. Martin Diener**
Priv.- Doz. Dr. Lutz Konrad

Date of Doctoral Defense: **20th August 2010**

My parents

“If you doubt you can accomplish something, then you can't accomplish it. You have to have confidence in your ability, and then be tough enough to follow through.”

Rosalyn Carter

Declaration

"I declare that I have completed this dissertation single-handedly without the unauthorized help of a second party and only with the assistance acknowledged therein. I have appropriately acknowledged and referenced all text passages that are derived literally from or are based on the content of published or unpublished work of others, and all information that relates to verbal communications. I have abided by the principles of good scientific conduct laid down in the charter of the Justus Liebig University of Giessen in carrying out the investigations described in the dissertation."

Giessen, April 30th 2010 Anca Nenicu

List of Abbreviations

3β-HSD	3β-hydroxysteroid dehydrogenase
17β-HSD	17β-hydroxysteroid dehydrogenase
17OH-P	17-hydroxypregnenolone
17OH-Pre	17-hydroxyprogesterone
ABC	ATP-binding cassette family of transporters
ACOX	Acyl-CoA oxidase
AMH	Anti-Müllerian hormone
APS	Ammonium persulfate
BSA	Bovine serum albumin
CAT	Catalase
cDNA	Complementary deoxyribonucleic acid
COX	Cyclooxygenase
CYP450arom	Cytochrome P450 aromatase
CYP450scc	Cytochrome P450 side-chain cleavage
°C	Degree celcius
Δ4-A	androstenedione
Δ5-A	androstanediol
DHEA	Dehydroepiandrosterone
DHT	Dihydrotestosterone
DMSO	Dimethyl sulfoxide
DNA	Deoxyribonucleic acid
DTT	1,4-dithio-DL-threitol
EDTA	Ethylene-diamine tetraacetate
ER	Endoplasmic reticulum
FSH	Follicle-stimulating hormone
GFP	Green fluorescent protein
h	Hour(s)
HSD	Hydroxysteroid dehydrogenase
HTZ	Heterozygote
IF	Immunofluorescence
IHC	Immunohistochemistry
IL	Interleukin
KH_2PO_4	Potassium dihydrogen phosphate
KO	Knockout
LCFA	Long-chain fatty acid
LH	Luteinizing hormone
min	Minute(s)
M	Molar
MFP-2	Multifunctional protein-2
mg	Milligram
ml	Millilitre
Na_2HPO_4	Disodium hydrogen phosphate
NaOH	Sodium hydroxide
ng	Nanograms
%	Percentage
PBD	Peroxisome biogenesis disorder
PBS	Phosphate-buffered saline
PBST	Phosphate-buffered saline with Tween
PCR	Polymerase chain reaction
Pex	Gene encoding a peroxin (peroxisome biogenesis protein)

PGE	Prostaglandin
PFA	Paraformaldehyde
PMP	Peroxisomal membrane protein
PPAR	Peroxisome proliferator activated receptors
PTS	Peroxisomal targeting signal
PUFA	Polyunsaturated fatty acids
RNA	Ribonucleic acid
ROS	Reactive oxygen species
RT	Room temperature
RXR	Retinoic X receptor
SDS-PAGE	Sodium dodecyl sulfate polyacrylamide gel electrophoresis
s	Second(s)
sER	Smooth endoplasmic reticulum
SF-1	Steroidogenic factor 1
siRNA	Small interfering RNA
SOD	Superoxide dismutase
StAR	Steroidogenic acute regulator protein
T	Testosterone
TAE	Tris acetate EDTA buffer
TEMED	N, N, N, N-tetramethylethylenediamine
THIOLASE	peroxisome 3-ketoacyl-CoA thiolase
Tris	Tris (hydroxymethyl) aminomethane
µg	Micrograms
µl	Microliter
µm	Micrometer
VLCFA	Very long-chain fatty acid
v/v	Volume/volume
WB	Western blot
WT	Wild-type
w/v	Weight/volume
X-ALD	X-linked Adrenoleukodystrophy
ZS	Zellweger syndrome

1. Literature overview 4
1.1. Overview on the male reproductive system 4
1.1.1. Structure of the adult testis 4
1.1.2. Development of the testis 4
1.1.3. The interstitial cells – Leydig cells 5
1.1.3.1. Leydig cells - Target for hormones and mediator of hormone effects 6
1.1.3.2. Growth factors – regulation of Leydig cells 6
1.1.3.3. Production of steroid hormones in Leydig cells 8
1.1.4. The testicular seminiferous tubule - structure and function 11
1.1.4.1. The Peritubular myoid cells 11
1.1.4.2. The Sertoli cell 11
I. Structure 11
II. Maintenance of the integrity of the seminiferous epithelium 12
III. Functions of Sertoli cells 13
1.1.5. Spermatogenesis 17
1.2. Peroxisomes 19
1.2.1. Nomenclature and morphology of peroxisomes 19
1.2.2. Biogenesis of peroxisomes 20
1.2.2.1. Peroxisomal matrix protein import and its receptors 21
1.2.2.2. Lipid transport through the peroxisomal membrane 21
1.2.2.3. Peroxisomal functions 22
1.2.2.4. Peroxisomal enzyme topology 22
1.2.2.5. Peroxisomes and its syndromes 23
Deficiencies in peroxisome biogenesis 23
Peroxisomal single-enzyme deficiencies 24
Peroxisomal dysfunction and male fertility 24
1.2.3. Mouse models for peroxisome dysfunction show impaired spermatogenesis 25
2. Materials and Methods 27
2.1. Human and animals tissue material used 27
2.1.1. Human 27
2.1.2. Mice 27
2.1.3. GFP-PTS1 transgenic mice 27
2.1.4. Necessary transgenic mouse lines for generation of Sertoli cell-specific *Pex13* knockout mice (scs*Pex13*KO) 27
- Pex13loxP – transgenic mice 27
- Amh-Cre – transgenic mice 28

2.2. Breeding strategy of generation scs*Pex*13KO mice using the *Cre-loxP* system 28
2.3. Genotyping with the polymerase chain reaction (PCR) 29
2.4. Laser micro-dissection of testes from 130 day-old mice scs*Pex13*KO, scs*Pex13*HTZ and scs*Pex13*WT 30
2.5. Morphological experiments 31
2.5.1. Fixation and embedding of the tissue 31
2.5.2. Fixation and processing of testes for frozen sections 32
2.5.3 Fixation and processing of tissue for electron microscopy – Cytochemical localization of catalase activity with the alkaline DAB-method 32
2.5.4. Immunoelectron microscopy 33
2.5.5. Immunohistochemistry (IHC) 33
2.5.6. Immunofluorescence (IF) 34
2.5.7. Analysis of the specificity of catalase antiserum by antigen competition 34
2.5.8. Hematoxylin and eosin (H&E) staining 35
2.5.9. Oil Red O staining 35
2.5.10 TUNEL assay 35
2.6. Primary culture of somatic testicular cells 36
2.6.1. Isolation and culture of Leydig cells 36
2.6.2. Isolation and culture of peritubular myoid and Sertoli cells 37

2.7. Subcellular fractionation by differential centrifugation for the isolation of enriched organelle fractions 38
2.7.1. Isolation of enriched peroxisomal fractions from primary cultures of Leydig-, peritubular myoid- and Sertoli cells 38
2.7.2. Isolation of enriched organelle fractions of interstitial, pertubular and tubular cells of the testes of 130 day-old scs*Pex13*KO, scs*Pex13*HTZ and scs*Pex13*WT mice 39
2.8. Western blot analyses and relative quantification of protein bands 41
2.9. RNA isolation and expression analysis by semi-quantitative RT-PCR 41
2.10. Blood collection 42
2.11. Testis homogenates for steroids measurements 42
2.12. Testis homogenate for very long chain fatty acid (VLCFA) and plasmalogen measurements 43
2.13. Fertility test for different scs*Pex13* mouse genotypes 43
2.14. *Pex13* silencing by RNA interference technology (RNAi) in primary Sertoli cell cultures 43
2.15. ROS-detection by staining with dihydroethidium 45
Secondary Antibodies 47
3. Aims of the study 56
PART I. Peroxisomes in different cell types of testis in human and mice 56
PART II. Physiological role of peroxisome in testis 56
4. Results 58
4.1. Peroxisomal proteins are heterogeneously distributed in distinct cell types of the mouse testis 59
4.2. Cell type-specific differences in abundance of peroxisomal proteins are conserved between mouse and man 61
4.3. Peroxisomes aggregate in clusters during spermatid maturation 62
4.4. The heterogeneity of peroxisomal enzymes is preserved in primary cell cultures and cytospin preparations of isolated Leydig, peritubular myoid- and Sertoli cells 67
4.5. Knockout of peroxisomal function in Sertoli cells 71
4.6. Fertility of scs*Pex13*KO males 73
4.7. Macroscopic differences between scs*Pex13*WT, scs*Pex13*HTZ and scs*Pex13*KO mice 73
4.8. Phenotypic differences of the testis and epididymis between scs*Pex13*WT, scs*Pex13*HTZ and scs*Pex13*KO mice at the microscopic level 74
4.9. Analysis of semithin sections revealed pathological alterations in the testis of 130 day-old scs*Pex13*KO animals 74
4.10. Electron microscopy confirms the severe pathological alteration in seminiferous tubules and reveals ultrastructural changes also in Leydig cells 76
4.11. Specification of the accumulation of peroxisome - metabolized lipids in the testis of scs*Pex13*KO animals 79
4.12. Impaired peroxisomal α – and β –oxidation induced accumulation of fatty acids primarily in Sertoli cells of scs*Pex13*KO animals 80
4.13. Sertoli cells, spermatogenesis and the testicular integrity are progressively affected during postnatal development of scs*Pex13*KO animals 83
4.14. Normal feature of prepubertal spermatogenesis in scs*Pex13*KO 83
4.15. Vacuolization of the cytoplasm of Sertoli cells in juvenile scs*Pex13*KO 84
4.16. Adult 60 day-old scs*Pex13*KO mice exhibit hyperplasia of interstitial cells 87
4.17. 90 day-old scs*Pex13*KO mice display hypospermatogenesis 89
4.18. *Pex13* gene deletion leads to “Sertoli cell only” syndrome in the testis of 130 day-old mice 90
4.19. Immunofluorescence detection of steroidogenic enzymes in the testis 96
4.20. The *in vivo* apoptosis rate of spermatogenic cells was strongly increased in 90 day-old scs*Pex13*KO mice 98
4.21. Western Blots reveal the good quality of the tubular and interstitial cell preparation 101

4.21.1. Interstitial and tubular cells exhibit a decrease of peroxisomal biogenesis proteins in scs*Pex13*KO testis 101
4.21.2. Proteins of peroxisomal lipid transport and enzymes of β-oxidation are altered in testicular fractions of scs*Pex13*KO..... 102
4.21.3. Alteration of the protein levels involved in ROS metabolism and inflammation in subcellular fractions of cell preparations from distinct genotypes of scs*Pex13* mice.. 103
4.21.4. Western Blot analysis of steroidogenic enzymes and the intermediate filaments marker - vimentin 105
4.22. Identification of affected genes by semi-quantitative RT- PCR in scs*Pex13*KO animals..... 107
4.22.1. Peroxisomal genes are affected by the knockout of *Pex13* gene in Sertoli cells 107
4.22.2. Significant alterations of mRNA levels of most antioxidant enzymes in scs*Pex13*KO mice 108
4.22.3. Increase in different pro-inflammatory genes in scs*Pex13*KO animals as detected by semi-quantitative RT- PCR 110
4.22.4. Activation of *Ppar* mRNA levels in scs*Pex13*KO mice 112
4.22.5. Alteration of testicular steroidogenesis and Sertoli cell homeostasis in scs*Pex13KO* mice 113
4.23. Measurements of the steroids reveal a strong accumulation of DHEA in the testis of scs*Pex13*KO animals 116
4.24. Detection of reactive oxygen species (ROS) in primary Sertoli cell cultures..... 118
4.24.1 Functional peroxisomes are required for ROS homeostasis in murine Sertoli cell primary culture 118
4.24.2. Mitochondrial ROS production is increased in Sertoli cells with *Pex13* knockdown..... 121
5. Discussion 124
Part I. Peroxisomes in wild type mice and man 124
5.1. Peroxisomes are present in all cell types of the testis..... 124
5.2. Peroxisomal enzyme content is heterogeneous, resulting in different metabolic functions of this organelle in distinct cell types of the testis 125
5.3. Calatase in Leydig cells as an antioxidative enzyme for the protection of steroid synthesis? 125
5.4. Peroxisomal metabolism in cells of the seminiferous epithelium: Sertoli cell peroxisomes as protectors against lipid toxicity 126
5.5. Peroxisomes are present in germ cells and undergo significant alterations during spermiogenesis 127
5.6. The heterogeneity in peroxisomal enzyme content is conserved in mouse and man 128
Part II: Physiological role of peroxisome in testis 129
5.7. Deficiency of peroxisomes in Sertoli cells and alterations of peroxisomal metabolic markers 129
5.8. Alterations of peroxisomal proteins in Sertoli cells and inducible expression of the ABCD-transporters in Leydig cells of the scs*Pex13*KO..... 132
5.9. Functional significance of peroxisomes in steroidogenesis and alteration of related signaling pathways in scs*Pex13*KO mice 134
5.10. DHEA and estradiol conversion by peroxisome β-oxidation..... 136
5.11. Alterations in different subcellular compartments and ROS metabolism induced by peroxisome deficiency in scs*Pex13*KO testis..... 139
5.12. Peroxisomal dysfunction in Sertoli cells leads to induction of constitutive and inducible cyclooxygenases, production of pro-inflammatory cytokines and local testicular inflammation..... 141
6. Summary ..... Error! Bookmark not defined.
7. Zusammenfassung 147
8. References 150

1. Literature overview

1.1. Overview on the male reproductive system

1.1.1. Structure of the adult testis

The male reproductive system consists of the two testes, a symmetric system of genital excurrent ducts, accessory sex glands, and the penis. The accessory sex glands include the seminal vesicles, the prostate and the bulbo-urethral glands. The testis is a complex organ that serves two crucial functions: 1) the synthesis of androgens - production of the male sex hormone (steroidogenesis) and 2) the production of sperms - the differentiation of the male gametes (spermatogenesis). Each differentiated adult testis is an oval structure housed in its separate compartment within the scrotum. Its fibromuscular connective tissue capsule, the tunica albuginea, is thickened at the mediastinum testis, from which septa are derived to subdivide the testis into approximately 250 small, incomplete compartments, the testis lobules. Each lobule houses one to four highly tortuous seminiferous tubules that function in the production of spermatozoa. The basal epithelium of the seminiferous tubule is formed by Sertoli cells and spermatogonia. The outside of the seminiferous tubules is surrounded by peritubular myoid cells also call peritubular cells which are residing in the basal membrane of the seminiferous tubules. The seminiferous tubules are surrounded by the connective tissue that contains in addition to neural, lymphatic and vascular elements, small groups of androgen-producing endocrine cells. These interstitial are called Leydig cells and produce the male sex hormone testosterone (T).

1.1.2. Development of the testis

The early undifferentiated gonad is characterized by onset of testis cord formation, which occurs at approximately 12.0 days post coitum (E12) in the mouse. The testis cords are derived from mesonephric cell migration from the yolk sac, and are composed of primordial germ cells, epithelialized pre-Sertoli cells, which are surrounded by a layer of peritubular cells and a smooth muscle cell lineage [1]. The *Sry* gene (Sex determining Region of the Y chromosome) [2, 3] expression occurs in pre-Sertoli cells between E10.5 and E12.5 in the cells of the XY gonad [4, 5]. A specific DNA-binding protein, called testis-determining factor (TDF), encoded by the SRY gene, and has been found to be directly responsible for testicular development and differentiation [6-8]. The pre-Sertoli cells that develop within the seminiferous cord also produce another important hormone, called Müllerian-inhibiting factor (MIF) or anti-Müllerian hormone (AMH), initiating the hormonal sex determination of the embryo [9, 10]. It is a large glycoprotein that inhibits cell division of the paramesonephric

(Müllerian) ducts, which in turn inhibits the development of the female reproductive organs. The AMH's molecular structure is similar to that of transforming growth factor-beta (TGF-β) [11, 12]. In male development the mesonephric stroma cells are separating the seminiferous cords, give rise to Leydig (interstitial) cells that produce T to stimulate the development of the indefinite primordium into a testis [13, 14]. Development and differentiation of the testis occur as a result from the action of dihydrotestosterone (DHT), a product of the conversion of testosterone by the 5α-reductase, which takes place in Sertoli cells. The appearance of AMH, T and DHT in the developing male embryo determines its male hormonal sex [15]. In the prenatal state AMH gene activation has been shown to involve various regulators, such as steroidogenic factor 1 (SF-1) [16, 17], GATA binding protein 4 (GATA4) [18] and SOX-9 [19], in conjunction with other putative Sertoli cell-specific factors. In postnatal period AMH production in Sertoli cells decreases and is closely related to an increase in GATA1 expression [20]. In the prepubertal mouse, GATA1 expression appears with the first wave of spermatogenesis and levels of its expression in the adult depend on changes in the spermatogenic cycle [21].

1.1.3. The interstitial cells – Leydig cells

During normal testicular development in all mammals, the ontogenesis of Leydig cell function involves at least two successive populations [22, 23]. The first (fetal) Leydig cells differ from the adult population in morphology, physiology and regulation [24, 25], originate from mesenchyme-like fibroblasts and produce androsterone [26]. They are not desensitised by luteinizing hormone (LH) and do not require LH for differentiation [22, 27]. The second Leydig (adult) cell population begins to differentiate in mice four days after birth and produces small amounts of T and also metabolize most of this hormone [28, 29]. The capacity to secrete T is increased significantly in mature Leydig cells during puberty [30-32]. At the onset of puberty the pituitary gland releases LH and follicle-stimulating hormone (FSH) and Leydig cells acquire more organelle components necessary for steroid production and enhanced responsiveness to circulatory LH [33, 34]. Leydig cells lie near blood vessels reflecting their endocrine function. They were described as polygonal or fusiform cells with a surface covered by a variety of filopodia or microvill [35]. Their nucleus is often ovoid or round with eccentric position in the cell. The cytoplasm of Leydig cell is densely packed with organelles, such as smooth endoplasmic reticulum (sER) that can appear in variety of configurations: randomly oriented tubular, cisternal, tubule sheets, fenestrated cisternae and swirls. Mitochondria occupy a substantial portion of the Leydig cell cytoplasm and posses the morphological features of steroid secreting cells (tubulovesicular structure). Peroxisomes, surrounding the lipid droplets of Leydig cell were observed for the first time by the cytochemical localization of the activity of their marker enzyme catalase [36]. The density of

peroxisomes in Leydig cell was described to correlate with the amount of T production [37]. The gradual increase in organelle volumes reflects the gain of steroidogenic enzyme activity from Leydig cells [38]. Lipid droplets of Leydig cells have attracted considerable attention because it has generally been assumed that they are the source of precursors for androgen biosynthesis. Some species have abundant lipids in Leydig cells including the mouse [35].

1.1.3.1. Leydig cells - Target for hormones and mediator of hormone effects

Cell-cell interactions characterize one of the testicular functions. The mammalian testis is under the overall control of pituitary hormones, the gonadotropins as luteinizing hormone (LH) and follicle stimulating hormone (FSH). The utilization of endocrine gonadotropin signals to achieve a normal testicular function involves in addition complex local paracrine interactions between *a)* Sertoli cells and germ cells, *b)* Sertoli cells and peritubular cells, *c)* Sertoli cells and Leydig cells, as well as *d)* local control of the testicular vasculature [39-41]. The paracrine interactions serve two purposes: (1) to coordinate the function of the three testicular compartments (seminiferous tubule, interstitium and vasculature) and (2) to control the complex sequence of events that constitutes the spermatogenic cycle [42-44]. The normal testicular function is dependent upon a functional pineal gland and the hypothalamic–pituitary–testicular (HPT) axis. The pineal gland secretes melatonin that acts on the hypothalamus to regulate the gonadotropin-releasing hormone (GnRH) output (see Fig.1). LH is secreted in pulses into the peripheral circulation by the pituitary gland in response to GnRH from the hypothalamus. T and its aromatized product estradiol, then feed back to the hypothalamus and pituitary gland to suppress transiently LH and thus T production. In response to reduced testosterone, GnRH and LH are again produced. Subsequently, the testicular hormones, inhibin, estrogen and T are pulsatile secreted back into the blood and act as classic feedback regulators of hypothalamic and pituitary output [43, 45-49]. A large number of studies have shown that LH is the chief regulator of adult Leydig cells and is also involved in Leydig cells development. Functionally, mature Leydig cells posses a higher LH receptor number and increased levels of androgen biosynthetic enzymes than immature Leydig cells [50].

1.1.3.2. Growth factors – regulation of Leydig cells

Leydig cell differentiation, proliferation, endocrine function, and regulation are modulated by various local factors such as cytokines and growth factors [23, 51-53]. Transforming growth factors (TGFs) and interleukin 1 regulate the proliferative activity of immature Leydig cells [54, 55]. The age-dependent stimulation of steroidogenesis in this cell type showed that interleukin 1 isoforms stimulated T production [56]. Growth factors that control their functions also include TGF-β, which plays an important role in signal transduction for cell–cell

interaction in testis, particularly as a potent inhibitor of Leydig cell functions [23, 52, 54]. Insulin-like growths factors I and II (IGF-I and IGF-II) are expressed differentially in fetal and adult Leydig cell in rat testis and are probably involved in different processes of their differentiation [57]. Periods of high IGF-I expression seem to coincide with periods of high T production [58].

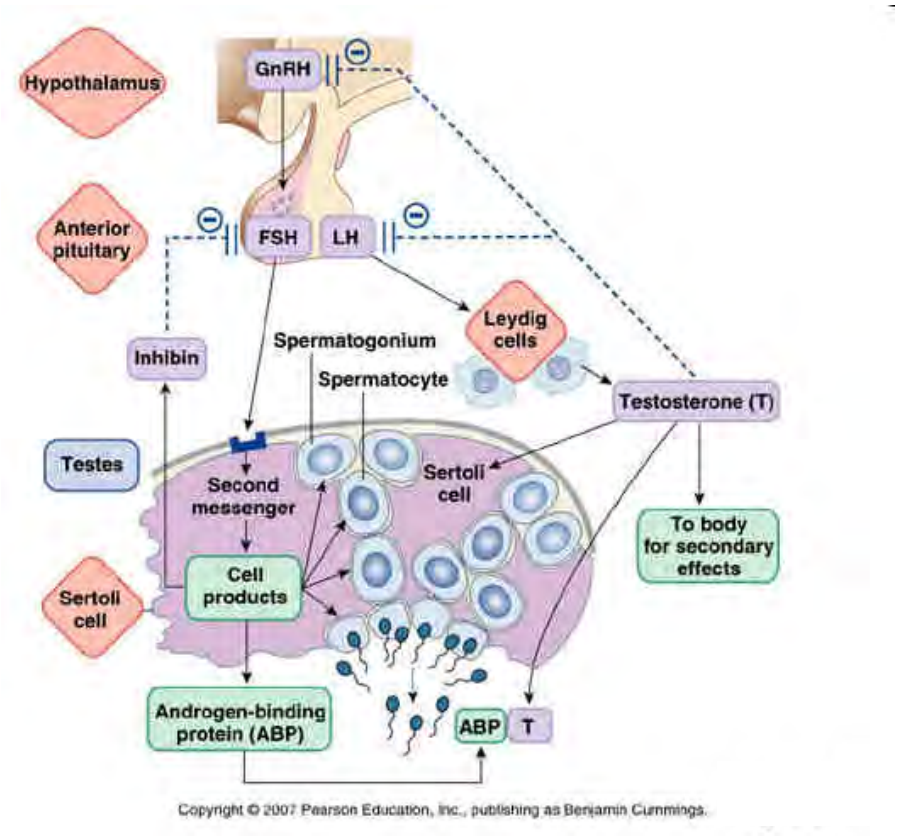

Figure 1. Hypothalamic-pituitary- testicular axis. Figure from [59]. LH and FSH are secreted by the pituitary gland. Receptors for LH and FSH are expressed in Leydig respectively Sertoli cells. LH stimulates Leydig cells to produce testosterone. FSH stimulates Sertoli cells to produce ABP, inhibin, DHT and estradiol. Those local products of the somatic cells of testis are representing the negative-feedback of the loops which are modulating of the gene expression in the pituitary gland. ABP binds to testosterone to stimulate spermatogenesis.

In addition, there are reports in the literature about relaxin-like factor (RLF) as a major secretory product of this cell type in various mammalian species [60, 61]. RLF is used as a marker for Leydig cells differentiation or function, however, which aspect of differentiation or function is exactly marked by RLF is still unknown [62]. Vitamin A (retinol) and its principal biologically active derivative, retinoic acid, regulate Leydig cell and as well as Sertoli and germ cells function [63]. Leydig cells contain retinoic acid receptors (RAR) and retinoic X receptors (RXR) [64]. The knockout of the receptor RXRβ2, present in Leydig cells in addition to Sertoli cells, induces sterility [64, 65]. Furthermore, prostaglandins, particularly PGE_2 and $PGF_{2\alpha}$, a group of bioactive substances derived from arachidonic acid by the action of the

cyclooxygenase (COX) isoenzymers type 1 and 2 (COX1 and COX2), have also been implicated in controlling Leydig cell development, production of proinflammatory cytokines such as interleukin 1 and 6 (IL1, IL6) by Leydig cells and Sertoli cells and for the autoregulation of spermatogenesis in the adult testis [66-69].

1.1.3.3. Production of steroid hormones in Leydig cells

The primary testicular and most well-known androgen is T. Besides T, other androgens in testis include: dehydroepiandrosterone (DHEA), androstenedione (Δ4-A), dihydrotestosterone (DHT) and andostanediol (Δ5-A). Furthermore, T is secreted into the blood and also carried to Sertoli cells and bound by the androgen receptor (AR). In Sertoli cells, T is reduced to DHT which is the most potent male steroid hormone, with an activity that is 10 times higher that of T. In addition, FSH stimulates Sertoli cells to express AR, which transports T and DHT from Leydig cells to the site of spermatogenesis.

Cholesterol provides the basic structure of all steroid hormones. The first chain of reactions in cholesterol biosynthesis from acetyl-CoA to the 3-hydroxy-3-methyl-glutaryl-coenzyme A reductase (HMG-CoA) can take place in the cytosol, mitochondria or peroxisomes [70]. Two acetyl-CoA are condensed to create acetoacetyl-CoA under the enzymatic reaction of an acetoacetyl-CoA thiolase, an enzyme that harbors a peroxisomal target signal 1 [71]. HMG-CoA reductase, the rate limiting enzyme of the cholesterol biosynthetic pathway, catalyzes the conversion of HMG-CoA into mevalonate. A number of studies indicate that HMG-CoA reductase is located in two compartments the endoplasmic reticulum (ER) and the peroxisomes [72-75]. The further steps of cholesterol synthesis are located solely in peroxisomes, since the following four enzymes possess peroxisomal targeting signals. The enzymes located in peroxisome are phosphomevalonate kinase (PMvK), mevalonate diphosphate decarboxylase (MPD) and isopentenyl phosphase (IPP) isomeriase and farnesyldiphosphate synthase (FPP) [76]. FPP is utilized further by the ER for squalene synthesis resulting final product cholesterol [77].

Leydig cells are responsible for the T production in the mammalian testis. Steroidogenic and trophic pathways depend upon stimulation of these cells by LH which binds to the LH-receptor on their plasma membrane, thereby initiating a cascade of intracellular: *a)* activation of adenylate cyclase, *b)* increase of intracellular cAMP formation [78, 79], *c)* translocation of cholesterol into the mitochondria, *d)* association of cholesterol with the cytochrome P450 side-chain cleavage enzyme (P450scc), *e)* production of pregnenolone from cholesterol into mitochondria, *f)* translocation of pregnenolone from mitochondria to the sER, and conversion of pregnenolone to T via a series of reactions in the sER and peroxisomes (Fig. 2) [80-82].

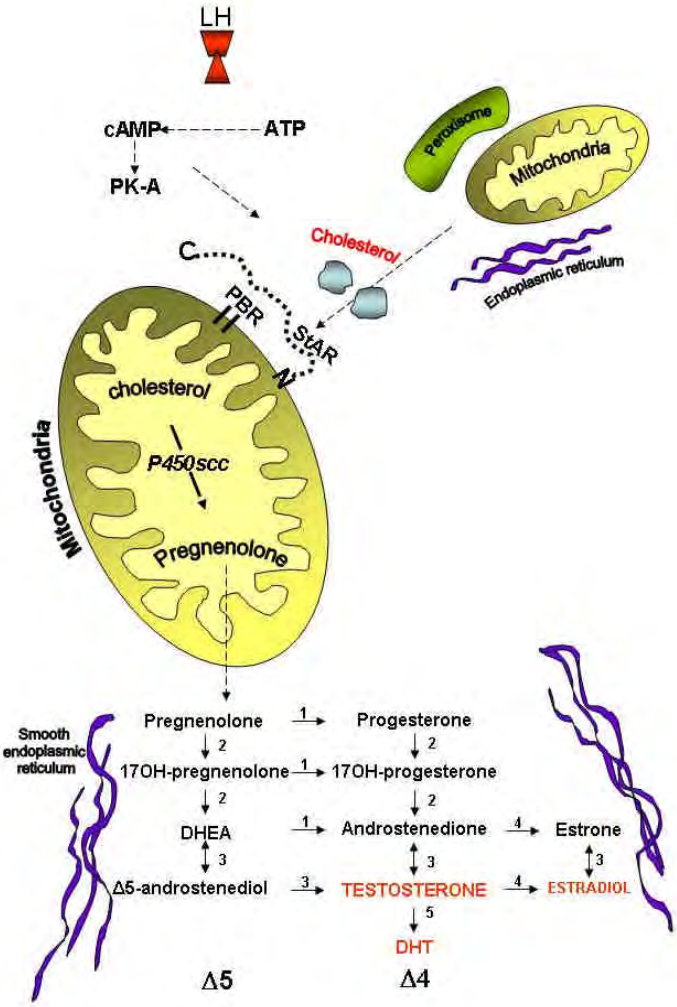

Figure 2. Summary of steroidogenesis in Leydig cells. Cholesterol biosynthesis takes place in mitochondria, peroxisomes and the endoplasmic reticulum. LH on binding with the receptor (LH-R) induces the synthesis of cAMP from ATP. cAMP catalyzes the activation of protein kinase A (PK-A), that is indirectly required for the transport of cytoplasmic cholesterol to mitochondria. StAR and PBR transfer cholesterol from the outer membrane to the inner mitochondrial membrane, where the P450scc enzyme resides. The N terminus of StAR is connected with the site of the mitochondrial import machinery at the outer mitochondrial membrane. The P450scc enzyme converts cholesterol into pregnenolone, which is ultimately transferred to the sER. In addition, peroxisomes house 17βHSD type 4 oxidizing 5-androstene-3beta, 17β-diol to DHEA, and estradiol to esterone. DHT (dihydrotestosterone); reaction 1: 3β-hydroxysteroid dehydrogenase; reaction 2: cytochrome P450 17α-hydroxylase; reaction 3: family of 17β-hydroxysteroid dehydrogenase; reaction 4: cytochrome P450 aromatase; reaction 5: 5α-reductase. Modified from [34, 80, 83, 84].

Several protein candidates have been postulated to be involved in the first rate-limiting and acutely-regulated step of steroidogenesis: sterol carrier protein 2 (SCP-2), steroidogenesis activating polypeptide, peripheral benzotropine receptor protein (PBR) and steroidogenic acute regulator protein (StAR) [23, 85, 86]. Indeed, the regulation of the StAR gene is controlled by the nuclear receptor steroidogenic factor (SF-1), which plays also an important role in mediating the transcriptional regulation of several steroid hydroxylase genes [87, 88]. The StAR protein is a member of a family of 37 and 30-kDa mitochondrial phosphoproteins, is acutely synthesized in response to LH or cAMP and is required for the transport of cholesterol from the outer membrane to the inner mitochondrial membrane [86, 89]. The cholesterol is cleaved on its side chain by the cytochrome P450 side chain cleavage (P450scc) enzyme, which is the first enzyme in the steroidogenic pathway that is located on the matrix side of the inner mitochondrial membrane [86]. Once formed in the mitochondria, pregnenolone moves to the membranes of the sER, and it is converted to progesterone by

the action of the 3β hydroxysteroid dehydrogenases (3βHSD). Thereafter, progesterone is modified by 17α-hydroxylation to 17-hydroxyprogesterone and thereafter converted to androstenedione. Androstenedione is a weak androgen which is converted to T by 17-ketosteroid reductase/17β-hydroxysteroid dehydrogenases. The synthesis from progesterone to T is named Δ4 pathway [90]. However, it is also well recognized that pregnenolone is transformed to 17α-hydroxypregnenolone followed by secretion of large amounts of an inactive steroid precursors named dehydroepiandrosterone (DHEA). Thereafter, DHEA is converted by the action of 17βHSD into androstenediol. This synthesis pathway is named Δ5. Further, androstenediol is converted to T by a 3βHSD enzyme. DHEA does not bind to the a AR [91], but exerts either estrogenic or androgenic action after its transformation into active androgens and/or estrogens in target cells [92]. The enzymes regulating sex steroid metabolism include steroid sulphatases, 3βHSD, 3αHSD, aromatase, 17βHSD and 5α-reductase (see Fig. 2) [22, 34, 93-95]. The family of 17βHSDs includes over ten enzymes [95] and Leydig cells contain a high level of 17βHSD type 4 also known as D-bifunctional protein or D-multifunctionalprotein (MFP2), which is localized in the peroxisomal matrix [81]. This enzyme was reported to oxidize 5-androstene-3β, 17β-diol to DHEA, and estradiol to esterone [81, 96-98]. The last step of conversion of the T to the most potent endogenous androgen dihydrotestosterone (DTH) is mediated by 5α-reductase enzymes. Other steroidogenic enzymes present in Leydig cells are located in the sER (microsomal): cytochrome P450c17 (CYP17), cytochrome P450aromatase (P450arom)/(CYP19), which catalyzes the aromatization of T to estradiol [5]. It was described that P450arom is present as well in Sertoli cells and in elongated spermatids [99]. In the fetal male mouse, serum T levels are rising 3 to 4 days prior birth and remain high (0.5 ng/ml) until 8 days after birth. T concentrations progressively decrease to about 0.2 ng/ml during postnatal days 8 to 24. From days 30, T levels rise to stable adult levels (3-8 ng/ml) [100]. The intra testicular concentration of T, in the adult mouse is approximately 50 to 100-fold higher than the one found in serum. The high intra testicular T concentration, (70 ng/ml) is required for full spermatogenic capacity. Spermatogenesis is dramatically affected at a T level below 20 ng/ml [101].

In the testis, only Leydig, peritubular and Sertoli cells express AR. No AR is expressed in germ cells of mature testis [102]. In adult testis, AR levels increase and decrease in a cyclic fashion, increasing during cell association stages II through VII of the spermatogenic cycle and then declining sharply during or immediately after stage VII to become barely detectable in stages IX – XII [103-105]. Studies using a tissue specific knock-out mouse of the AR gene demonstrated an alteration in the expression of several key steroidogenic enzymes in Leydig cells, suggesting that T is an autocrine factor regulating its own production. The AR knock-

out mouse also exhibited an arrest of spermatogenesis predominately at the round spermatid stage [106].

1.1.4. The testicular seminiferous tubule - structure and function

1.1.4.1. The Peritubular myoid cells

Peritubular myoid cells or peritubular cells (PTC) have been found in all mammalian species and their organization varies between species. In laboratory rodents, including rats, hamsters, and mice, only one layer of peritubular cells is located on the outside of the seminiferous tubules. On the other hand, several cellular layers exist in the lamina propria of the seminiferous tubule in humans and other animal species. The cells are joined by junctional complexes like epithelial cells. Peritubular cells contain abundant actin filaments which are distributed in the cells in a species-specific manner. In rodents, the filaments within peritubular cell are both longitudinal and circular and run along the long axis of the seminiferous tubule [107]. The arrangement of the actin filaments is affected by the disruption of spermatogenesis, such as in cryptorchidism. In the peritubular cells also other cytoskeletal proteins as myosin, desmin/vimentin and alpha-actin are found. Peritubular cells have been shown to be contractile, are involved in the transport of spermatozoa and the testicular fluid in the tubule. Several substances (prostaglandins, oxytocin, TGFβ, NO/cGMP) have been suggested to affect the contraction of this cell type [108, 109].

Recent in vitro studies have demonstrated that the cells secrete a number of substances, including extracellular matrix components (fibronectin, type I and IV collagens, proteoglycans) and growth factors (PModS, TGFβ, IGF-I, activin) [110]. PModS is a protein which modulates many of the metabolic activities of Sertoli cell along with peritubular cells, including androgen binding protein (ABP) and transferrin [111]. Furthermore, it has been reported that peritubular cells contain androgen receptors (AR) and are involved in retinol processing. Considering all this, it seems likely that peritubular cells not only provide structural integrity to the tubule but also take part in the regulation of spermatogenesis and other testicular functions [112].

1.1.4.2. The Sertoli cell

I. Structure

The Sertoli Cell (SC) is known as a supporting or sustentacular cell and is unique in many respects [113]. These cells do not replicate after puberty [114] and their number determines the testicular size, germ cell numbers per testis and spermatozoa output [115]. Sertoli cells are columnar cells with extensive apical and lateral processes, surrounding the adjacent spermatogenic cells and occupying the space between them. These cells provide the structural organization of the seminiferous tubules since they extend through the full

thickness of the germinal epithelium. Sertoli cells of adult mice show a characteristic nucleus with one large centrally located nucleolus, flanked by two chromocentres containing all the centromeric heterochromatin [116] [117]. The cytoplasm includes an extensive and continuous network of sER, polymorphous mitochondria, peroxisomes, an endosomal-lysosomal apparatus and a cytoskeleton composed of intermediate filaments (vimentin), microfilaments (actin) and microtubules. The cytoplasm contains lipid inclusions and protein crystals. Characteristic complexes formed by flattened cisternae of the ER and bundles of actin filaments are located next to the plasma membrane of Sertoli cells, facing either adjacent neighbouring Sertoli cells or spermatic cells. Morphological and functional evidence indicate a change in number and size of the intracellular organelles during the cycle of the seminiferouse epithelium. Mitochondria in Sertoli cells are characterized by a peak in volume at stages XII – XIV in rat seminiferous tubules [118]. Lysosomes vary in number, size and electron density, at stages IX – I are spherical in shape with a homogeneous granular content, and at stages II – VIII are heterogeneous with a greater electron density [119]. Frequently, in the cytoplasm small spherical lipid droplet, small dense bodies, and myelin figures are observed [120]. Also, a cyclic variation in volume density of both the smooth and rough ER, from stage IV – VIII have been described, suggesting that the synthetic and/or secretory roles of the Sertoli cells are cyclic in nature [121]. In contrast, the Golgi apparatus in this cell type does not undergo strong alterations throughout the cycle of the seminiferous epithelium [122].

II. Maintenance of the integrity of the seminiferous epithelium

The Sertoli cells provide a specialized, protected environment for germ cell development within the seminiferous tubules of the testis. Adjacent Sertoli cells are connected to each other by occluding junctions, establishing the blood-testis barrier (BTB), which protects the developing germ cells, against autoimmune reactions [123, 124] by preventing the passage of molecules larger than 1,000 Da. The BTB divides the seminiferous epithelium into a basal and an adluminal compartments. Sertoli cells are attached to the basal lamina via hemidesmosomes, and bound to each other by desmosomes [125], gap junctions and tight junctions [124]. Sertoli cells are attached to germ cells via desmosome like-junctions, gap junctions, ectoplasmic specializations [126] and tubulobulbar complexes [123]. Germ cells at the early stage of spermatogenesis, such as spermatogonia, are localized at the basal compartment [127, 128]. As the spermatogenic differentiation proceeds those cells move to the adluminal compartment, where they continue their development into spermatozoa [129]. Once beyond the BTB germ cells are dependent on the supply of nutrients and growth factors from Sertoli cells [130].

III. Functions of Sertoli cells

Sertoli cells are involved in: (1) mechanical support and nutrition of germ cells, (2) paracrine regulation of male germ cell proliferation and differentiation by secretion of regulatory proteins, including peptide growth factors and hormones, (3) phagocytosis, (4) steroid hormone synthesis and metabolism. The functions of this cell type change dramatically according to the stage of the spermatogenic cycle, and there are many Sertoli cell products which are produced and/or secreted in a cyclic pattern [131].

A. Delivery of nutrients to germ cells and secretion of proteins

As mentioned above the Sertoli cells are “nurse cells” and are providing nutrition and energy to the germ cells. As demonstrated in primary culture they predigest glucose to lactate for the use by germ cells. This process functions at the highest rate when it is stimulated by FSH [132]. In addition, Sertoli cells can also use glutamine or leucine as source of energy [133]. They are able to convert substantial amounts of glutamine to CO_2 and ATP. It is well accepted that under standard culture conditions Sertoli cells require media with glutamine [134]. In addition, the testis is one of the few organs in the body that can produce myoinositol (member of vitamin B), which also has been shown to be a function of Sertoli cells by converting glucose to this product. This process is inducing a 50-fold higher concentration of myoinositol in the tubular fluid in comparison to the serum [135] [136].

Further, secretory products of Sertoli cells are bioprotective proteins which are secreted in high amounts. These include metal ion transport proteins, such as transferrin (for iron transport) and coeruloprotein (for copper transport). One of the first secreted glycoprotein of Sertoli cells identified was the ABP. Its biochemical function is to serve as a binding protein for the androgens as T and DHT. ABP displays a stage-specific expression pattern within the seminiferous epithelium and its secretion has often been regarded as an index of Sertoli cell function [137]. In addition, secreted glycoproteins such as sulphated glycoprotein 1 (SGP1) and sulphated glycoprotein 2 (SGP2) which are thought to bind lipids and to be involved in immunosuppression are present in the Sertoli cell cytoplasm. SGP-1 was first isolated from cultured Sertoli cells and is the precursor of four sphingolipid proteins which are activacting glycosphingolipids and glycoglycerolipids in order to be effectively degraded [138].

Other important Sertoli cell products are the peptide hormones inhibin and activin. They are structurally related to the gonadal dimeric glycoproteins and appear to act back on the pituitary gland during development. Inhibin down-regulates the production of FSH, whereas activin is a potent releaser of FSH [139]. Both inhibin and activin can also influence steroidogenesis and are also produced by Leydig cells. In addition, α-inhibin acts as an intragonadal paracrine regulator, apparently functioning as a gonadal-specific tumor suppressor [140].

Steel factor (SF) or stem-cell factor is expressed on the Sertoli cell membrane [141]. SF is a ligand of the c-kit receptor tyrosine kinase present on the plasma membrane of the germ cells. c-Kit is absolutely necessary for meiotic development and is controlling male germ cell differentiation [142].

Sertoli cells secrete proteases and protease inhibitors which are important in tissue remodelling processes that occur during spermination. There are specific proteases, which consist of plasminogen activators (PA) of specific serine proteases, catalyzing the conversion of plasminogen to plasmin [143-145].

Furthermore, Sertoli cells secrete vitamin binding proteins, mainly for vitamins D and A [146] [147], the last one being very important for spermatogenesis. Vitamin A deficient male rats are sterile as the result of germ cell loss with accumulation of debris in the lumen of the seminiferous tubules [148]. The mechanism of vitamin A action is mediated by nuclear retinoid receptors which include a family of retinoic acid receptors (RAR alpha, beta and gamma) and a family of the retinoid X receptors (RXR alpha, beta and gamma). The RARs and RXRs bind short DNA sequences on vitamin A-responsive genes, called retinoic acid response element (RARE), to modulate gene expression. The RXRs are heterodimerize with numerous other nuclear receptors, including RARs, peroxisome proliferator-activated receptors (PPARs) and liver oxysterol receptors (LXRs). The Sertoli cells express RXR alpha in low levels and RAR beta was found exclusively in this cell type [149]. Moreover, the heterodimers RXR beta/RAR alpha may control spermatogenesis [65, 150].

B. Morphology of the lipid droplets in the cytoplasm of Sertoli cells

Lipid droplets are easily observed in Sertoli cells and the amount of these droplets differs with the stages of the cycle of the seminiferous epithelium [151]. These lipid droplets contain triacylglycerols which can be converted to free fatty acids for oxidation and production of energy by Sertoli cells [152]. Especially, by fatty acids such as the 22-carbon polyene fatty acids, derive from cis-linoleic acid (n:6) or linoleic acid (n:3) that are synthesized and accumulate in the testis after sexual maturation [153, 154]. In addition, Sertoli cells have a higher ratio of esterified to unsterified cholesterol than germ cells [155]. The testicular phospholipids and neutral lipids contain long-chain fatty acid (C:18)-(C:22) (LCFA), very long-chain fatty acid (C:24)-(C:32) (VLCFA) and polyunsaturated fatty acids (PUFA). The lipid alterations observed in cryptorchidism suggest a possible role for Sertoli cells in the turnover and conservation of PUFA within the seminiferous tubules [156]. The formation of LCFA, VLCFA and PUFA in isolated rat seminiferous tubules suggests that a PUFA chain shortening mechanism occurs in the testis involving alpha- and beta-oxidation [157].

C. Growth factors – regulation of Sertoli cells

Epithelial growth factor-α (EGF-alpha) and transforming growth factor-β (TGF-beta) are present in Sertoli cells to regulate germ cell proliferation and to promote or disrupt the blood-testis-barrier assembly [158]. Sertoli cells appear to secrete fibroblast growth factor (FGF) and EGF in response to FSH, influencing aspects of cellular growth and differentiation of germ cells [159]. In addition to growth factors, the cytokine interleukin-1alpha (IL-1alpha) and interleukin-6 (IL-6) are produced by Sertoli cells [160, 161], suggesting their involvement in the paracrine regulation of spermatogenesis [162]. Furthermore, phagocytosis of residual bodies by Sertoli cells is stimulated by cytokine action on Sertoli cells [142].

In addition, Sertoli cells secrete glycoproteins as well, which function as growth factors, such as the insulin-like growth factor I (IGF-I). IGF-1 stimulates DNA synthesis as well as increases transferrin and lactate production in immature Sertoli cells.

D. Secretion of fluid into the tubular lumen

Sertoli cells are well characterized as the responsible cell type for the secretion and modification of fluid, leading to the formation of the specialized luminal fluid microenvironment, which transports the spermatozoa into the epididymis [163]. For this purpose Sertoli cells also transport water from the interstitial space into the lumen, serving as the vehicle for moving spermatozoa from the testis to the epididymis. In addition to basolateral ion channels, aquaporins (water channels) are abundant in the testis, with some being localized in Sertoli cells [164, 165]. Interestingly, various members of the aquaporin gene family contain CRE motifs (CREB binding regions) and are under cAMP regulation, a second messenger that is activated upon FSH-R signalling [166].

E. Phagocytosis of residual bodies

In addition to its supporting role, Sertoli cells have the capacity to phagocytose apoptotic germ cells and lyse residual bodies which detach from the mature spermatids [167-170]. Residual bodies are surrounded by a plasma membrane rich in glycolipids and contain remnants of organelles and ribonucleoproteins that are degraded by Sertoli cells [171]. Such residual bodies contain large membrane-delimited vacuoles, multivesicular bodies, cluster of ribosomes, condensed mitochondria, lipid droplets [134] and shown by us also peroxisome-like structures. Prior to the release of step 16 spermatids in the lumen of the seminiferous tubule, a globular mass of the surplus cytoplasm called residual body detaches from these cells. Sertoli cells internalize these residual bodies, forming a double-membraned phagosome. The phagosomes characteristically migrate from the apex to the base of the Sertoli cells. This migration takes place during stage IX of the cycle of the seminiferous epithelium in the mouse [119]. Thus, the temporal relation between phagocytosis of residual

bodies and the increase in the volume and number of the lipid droplets at stage VIII to XII of spermatogenesis, is an indication that these droplets may arise from the degradation of residual bodies [172].

F. Sertoli cells - Target for hormones and mediator of hormone effects

Sertoli cells are targets for FSH in the male. FSH is a heterodimeric glycoprotein hormone secreted by the anterior pituitary gland that is essential for mammalian fertility. The hormone binds to its receptor on the membrane of the Sertoli cells and is known to activate at least 5 signaling pathways [173]. (1) *The cAMP-PKA pathway* – increasing cAMP concentration, leading to the release of the catalytic subunit of protein kinase A (PKA) from the repressor subunit, allowing the phosphorylation of numerous cellular proteins. One target of this pathway is a class of transcription factors that bind to cAMP response elements (CREs) [174]. (2) *The MAP kinase pathway* – which is limited to the period of Sertoli cell proliferation that occurs in the first 15 days after birth, being stimulated by FSH via this pathway. The FSH and ERK kinase-dependent induction of cyclin D1 and E2F, two promoters of entry into the cell-cycle, also suggests that mitogenic effects of FSH are at least partly mediated by the MAP kinase cascade during puberty [175]. (3) *The calcium pathway* – FSH (10-1000 ng/ml) causes an increase in intracellular Ca^{2+} within seconds of stimulation [176, 177]. One result of increased intracellular Ca^{2+} is the activation of calmodulin and CaM kinases that may affect the cytoskeletal structure of Sertoli cells and phosphorylation of transcription factors including CREB [178, 179]. (4) *The phosphatidylinositol 3-kinase (PI3-K) pathway* – the mechanism for PI3-K activation is mediated by FSH with increase in cAMP levels [180]. Dependent on PI3-K is the uptake of glucose that is converted to lactate for germ cell energy needs and transferrin secretion that is vital for maintenance of spermatogenesis [181]. (5) *The phospholipase A_2 (PLA_2) pathway* – FSH through the activation of the PLA_2 leads to the release of arachidonic acid as second messenger and its subsequent metabolism to PGE_2 and other eicosanoids that function as intracellular and extracellular signals. As a result, the adenylate cyclase activity and androgen aromatization are stimulated in Sertoli cells and germ cells may be affected via their G-protein coupled eicosanoid receptors [182]. In addition, PGE2 and PGF2alpha are produced by mature spermatozoa and play a role in the acrosome reaction [183].

The androgen receptor (AR) is also induced by FSH, thus FSH regulates the androgen responsiveness of Sertoli cells [184-187].

In contrast to FSH, it is well established that androgens are absolutely essential for the maintenance of spermatogenesis [188, 189]. Although DHT is crucial for the development of the male reproductive tract, T is the androgen in the testis that regulates spermatogenesis. T initiates pathways that contribute to the support of spermatogenesis as it activates the MAP

kinases in pubertal Sertoli cells and contributes to elevation of Ca^{2+} [190-192]. Although many genes can be regulated by androgens, only the gene encoding by the Pem transcriptionl factor is known to be induced by AR-DNA interactions in Sertoli cells [193].

G. Steroidogenesis and steroid metabolism in Sertoli cells

The Sertoli cell has the typical morphological characteristics of steroid-produceing cells [194], with numerous mitochondria, smooth ER and cholesterol-containing lipid droplets in the cytoplasm [195] as well as peroxisomes (as shown in this thesis). Other enzymes found in Sertoli cells are cholesterol ester hydrolase, aldose reductase, branched-chain amino acid transferase and the enzymes of inositol biosynthesis which are temperature sensitive [196, 197]. However, the main production of T is performed in Leydig cells that exhibit significant levels of cholesterol side-chain cleavage activity. Regulation of ABP by FSH and T has been demonstrated [198], although whether one or both are required for complete function remains to be resolved. In addition, Sertoli cell convert T to DHT, 5alpha-androstanediols, androsterone, and androstenedione. Furthermore, high levels of 3α-hydroxysteroid dehydrogenase activity in Sertoli cell preparations were confirmed by measuring the rates of formation of 5α-androstanediols from DHT [199, 200]. Observations during the past decade have led to the recognition of various testicular secretory products that modulate the FSH effect on the aromatase activity [154]. Furthermore, in Sertoli cells an EGF-like factor inhibits FSH stimulated aromatase activity while lactate production is stimulated [201].

Both Sertoli and Leydig cells are sites of estrogen (ER) biosynthesis in the testis. The support of the idea comes from isolation of biologically active estrogenic material from Sertoli cell tumors [202]. Two ER subtypes have been cloned, ERα and ERβ, and shown to be present in the hypothalamus, pituitary gland, testis and reproductive tract, suggesting the regulation of male reproduction by estrogen [203].

1.1.5. Spermatogenesis

Spermatogenesis in mammals is a precise cyclic and time-controlled process with stage-dependent gene expression, comprising extensive genomic and cellular remodelling from spermatogonia to haploid cells and the final release of spermatozoa [204].

Spermatogenesis starts by mitotic divisions inducing proliferation and differentiation of spermatogonia, meiotic divisions of spermatocytes (Fig.3). It is followed by the transformation of haploid round spermatids arising from the second meiotic division into spermatozoa, a process called spermiogenesis. Spermatogonia are diploid stem cells of spermatogenesis and can be divided in type A and type B. Meiosis starts with DNA synthesis of type B spermatogonia, which lose contact with the basal lamina (preleptotene). In the human, the prophase of the first meiotic division takes about 1-3 weeks and is divided into

several stages: the leptotene, zygotene, pachytene and diplotene. By these meiotic divisions primary and afterwards secondary spermatocytes are generated (Fig.3). Secondary spermatocytes undergo the second meiotic division in which the chromatids are finally separated, leading to round spermatids with a haploid number of chromosomes and DNA content (Fig.3). Spermiogenesis, the transformation of conventional round spermatids into spermatozoa, which have the capacity for motility and fertilization of an egg, includes a complex sequence of events: (1) formation of the acrosome, (2) condensation of the nucleus, (3) development of the sperm tail, (4) reorganization of cellular organelles such as centrioles and mitochondria (5) reduction of the cytoplasma. A dramatic reorganization of the peroxisomal compartment during spermiogenesis is for the first time described in this dissertation.

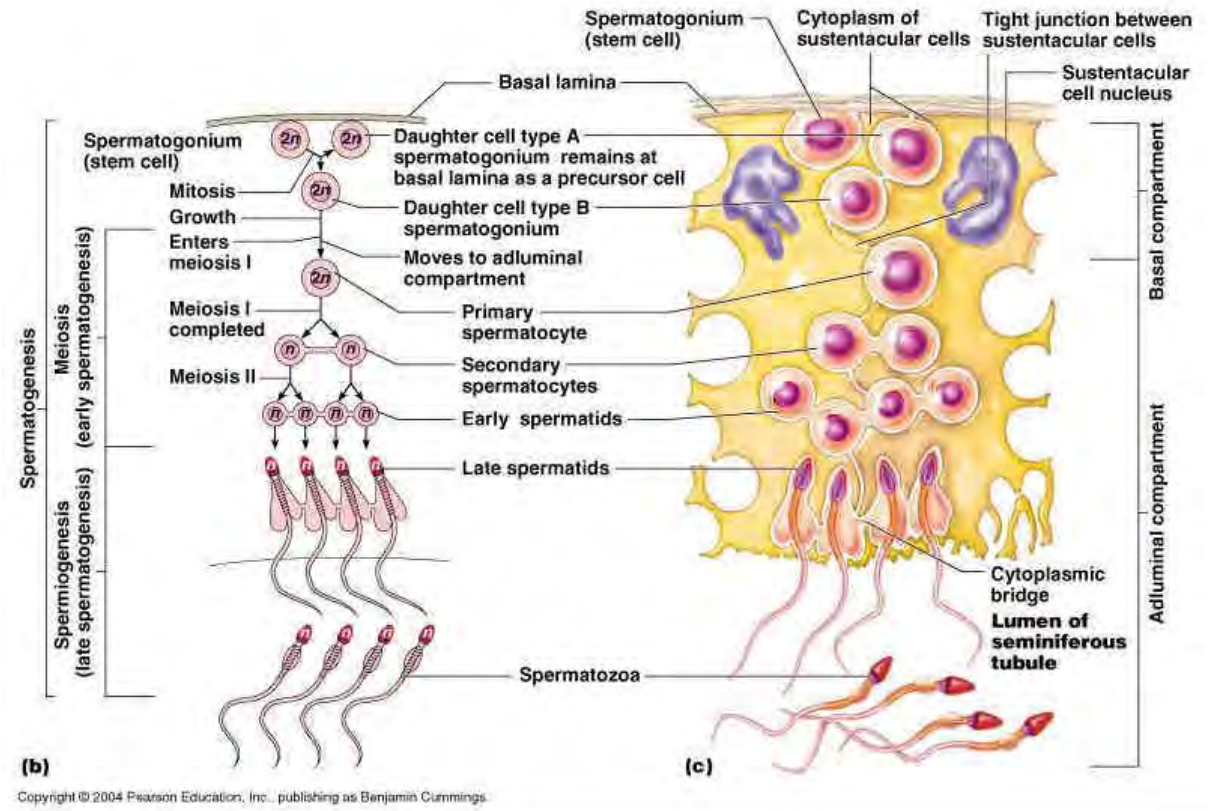

Figure 3. Spermatogenesis process. Figure according to Chase [59]. Spermatogonia undergo mitotic divisions forming the primary spermatocytes, diploid (2n) cells. Primary spermatocytes undergo first meiotic division giving rise to secondary spermatocytes, haploid (n) cells. They undergo the second meiotic divisions generating early spermatids. By several intracellular transformations, such as the condensation of the nucleus, the formation of the acrosome, development of the tail, late spermatids are developed. After their reorganization of the cellular organelles and reduction of the cytoplasm, mature spermatozoas are released into the seminiferous tubule.

Organization and localization of the germ cells within the seminiferous tubules vary at particular phases of the development. Each step of the development of the seminiferous epithelium with its associated germ cells can be divided into stages that show defined

physiological characteristics and cell associations - stages I – XII in the mouse. Stage I: at the basal part of the seminiferous epithelium spermatocytes are located with a not yet condensed chromosomes body. The inner part of the seminiferous epithelium is defined by the occurrence of early round spermatids. Stages II-III: spermatids are showing an acrosome vesicle on their nuclear surface. Stages IV: the acrosomal vesical flattens on the nuclear surface of the spermatids. Stage V: the angle subtended by the acrosome extends from 40º to maximum 95º on the nuclear surface of round spermatids. Stage VI: elongated spermatids remain within the crypts of the Sertoli cells. Stage VII: elongated spermatids move to the luminal aspect of the seminiferous epithelium and the angle subtended by the acrosome is bigger then 120º. Stage VIII: the nuclei of the eight spermatids make contact with the plasma membrane and the caudal end of the nucleus is slightly tapered. Stage IX: the spermatid nucleus becomes deformed from its round or ovoid shape. Stage X: the hook shape of spermatid head is formed. Stage XI: further elongation of the spermatid head takes place and chromatin condensation starts. In the seminiferous epithelium, diplotene spermatocytes that not yet progressed to metaphase are present. Stage XII: presence of anaphase or telophase of meiosis I, secondary spermatocytes, or any of the phases of meiosis II. Stages VI, VII, VIII and XII are characterized by the presence of secondary spermatocytes.
The process of spermatogenesis requires a continuous cross talk between germ cells and their somatic support, the Sertoli cells, which exert multiple functions critical for germinal differentiation [205].

1.2. Peroxisomes

1.2.1. Nomenclature and morphology of peroxisomes

Peroxisomes, glyoxysomes and glycosomes are microbodies, belonging to a single organelle family, often grouped under the generic name ‘peroxisome’, which are represented in virtually all eukaryotic cells. Peroxisomes were discovered by Rhodin [206] in a morphological study and were described as spherical oval organelles of 0.3-1.0 µm in diameter with a single limiting membrane and a finely granular matrix in the proximal convoluted tubular epithelium of the mouse kidney [206]. Due to the lack of a known function of this organelle, Rhodin named them “microbodies”. Rouiller and Bernard in 1956 identified a similar organelle, containing an additional crystalline core in parenchymal cells of rat liver, and suggested that the hepatic microbodies might be precursors of mitochondria. [207]. Only in 1960 De Duve and coworkers recognised “peroxisome” as a distinct organelle by establishing its biochemical characterization [208]. De Duve and Baudhuin observed that catalase, urate oxidase and D-amino acid oxidase were associated with particles different from lysosomes, microsomes or mitochondria. Therefore term “peroxisome” was introduced

by de Duve and Baudhuin, because these organelles contained both hydrogen peroxide producing (flavin-containing oxidases) and degrading (catalase) enzymes [208].
Peroxisomes were visualized with the cytochemical staining method, for the peroxidative reaction of catalase, using 3, 3'-diaminobenzidine (DAB) as a hydrogen donor [209]. By this method, peroxisomes have been identified in every tissue examined thus far with the exception of mature red blood cells and germ cells [210]. The presence of peroxisomes in all types of germ cells (except for spermatozoa) has been shown first in this thesis.
The size and shape of peroxisomes vary from organ to organ. They are relatively large in the kidney and liver (0.3–1.0 µm diameter) and are smaller in the brain and muscle (0.1–0.25 µm) where they were referred to as microperoxisomes [211]. Peroxisomes from animal liver often contain a crystalloid core, a nucleoid composed of urate oxidase [212] and xanthine oxidase [213]. Humans do not have peroxisome core in their liver cells, because of a mutation in the urate oxidase genes, occurring during the evolution at the level oh humanoids [214]. In the liver and kidney, peroxisomes are round or oval in shape, whereas in sebaceous and prepucial glands [215] and regenerating liver [216, 217], they are interconnected and organized into a peroxisomal reticulum. Peroxisomes can be differentiated from mitochondria by their single membrane, an electron dense core, a homogenous matrix and by the absence of cristae. They are differentiated from lysosomes by their homogeneous matrix and by histochemical staining for catalase, whereas the lysosomes are hetrogenous in content and stain for acid phosphatase [218]. The peroxisomal limiting membrane (6–8 nm) is permeable to small hydrophilic molecules. Enzymatic substrates of less than 800 daltons easily pass through non-specific pores. Two membrane proteins (22 and 28 kDa) have been identified and found to be associated with the formation of these non-specific pores [219].

1.2.2. Biogenesis of peroxisomes

Numerous proteins of the peroxin family are required for proliferation and regular biogenesis of mammalian peroxisomes. The classical model of peroxisome biogenesis describes that new peroxisomes arise through a budding and fission process from pre-existing ones. In recent years this view has been challenged by a numbers of groups who believe that peroxisomes may also be generated de novo [220]. The regular biogenesis and inheritance of peroxisomes requires the function of more then 30 proteins – the peroxins (Fig.4). Peroxin proteins are encoded by *PEX* genes (in the mouse *Pex*) and were numbered according to their date of discovery [221]. Peroxisome proteins can be divided into functional groups, e. g. for membrane biogenesis (PEX3, PEX16, PEX19), for cytoplasmic transport and sorting (PEX5, PEX7 and PEX19), for docking (PEX13, PEX14, PEX17) and import (PEX10, PEX12) of proteins into the peroxisome as well as for budding and fission of the organelles (PEX11) or for organelle degradation (PEX4) [222].

1.2.2.1. Peroxisomal matrix protein import and its receptors

Most peroxisomal proteins are synthesized on free ribosomes and are imported into the peroxisome without any further modification. Peroxisomal matrix proteins contain a peroxisomal targeting signal (PTS) either at their C-terminus (PTS1) with the consensus sequence (S/A/C)(K/H/R)(L/M) or at their N-terminus (PTS2) with the consensus sequence (R/K)(L/I/V)(X5)(H/Q)(L/A) that are recognized by specific cytoplasmic shuttling receptors (PEX5 for PTS1 and PEX7 for PTS2), which direct the proteins to the peroxisomes. These shuttling receptors, loaded with their cargo, bind to a docking complex at the peroxisomal membrane before the transported matrix proteins are imported in their folded conformation into the peroxisome [223].

1.2.2.2. Lipid transport through the peroxisomal membrane

The peroxisomal membrane contains multiple organelle specific proteins involved in the transport of matrix proteins into the organelle [224] and others whose function is required for transport of small molecule substrates and products across the organelle membrane [225, 226]. The peroxisomal ATP-binding cassette (ABCD), belong to the half adenosine-triphosphate transporters category, D sub-family, which are suggested to play a role in fatty acid beta-oxidation. The basic structure that defines the members of this protein family is the combination of a conserved ATP-binding and transmembrane domains. Four ATP-binding cassette (ABC) transporters have been identified in mammalian peroxisomes: the adrenoleukodystrophy protein ALDP / ABCD1, the adrenoleukodystrophy-related protein ALDRP / ABCD2, the 70-kDa peroxisomal membrane protein PMP70 / ABCD3 and the PMP70-related protein P70R / ABCD4. Relative to ABCD1 the human proteins display 63%, 36%, and 25% amino acid identity [227, 228], respectively and have the predicted structure of a half-transporter with one membrane spanning domain and one nucleotide binding fold. As most of the half-transporters identified to date function as dimers, it has been suggested that the peroxisomal ABCD transporters also need to assemble as homo- or heterodimers in order to form a functional unit [229, 230]. Hydrolysis of ATP is required to perform a directed transmembrane movement of their substrate. In order to be imported into peroxisomes, long-chain fatty acids are esterified to CoA esters in the cytoplasmic side of the peroxisome membrane by chain-length specific acyl-CoA synthetases [231]. This modification makes the molecule more polarized, preventing it from passing through membranes. Although the exact functions and substrates of the mammalian peroxisomal ABCD-transporters have yet to be defined, the detrimental effects of a transporter deficiency is demonstrated by mutations in the ABCD1 gene, leading to the lipid storage disorder X-linked adrenoleukodystrophy (X-ALD).

1.2.2.3. Peroxisomal functions

Peroxisomes are involved in the metabolism of reactive oxygen species (ROS) and of many lipid derivatives and couple with their enzymes system ROS and lipid metabolism (e.g. acyle-CoA oxidase 1-3) (see Fig.4; [232, 233]. They proliferate easily by interference with lipid metabolic pathways, e.g. after treatment with hypolipidemic drugs [234]. Peroxisomes house two pathways for ß-oxidation. They are generally involved in the biosynthesis of isoprenoids, such as retinoic acid derivatives and of important membrane lipids, such as cholesterol or plasmalogens - a group of ether lipids [235]. They are capable of metabolizing a range of bioactive lipids, such as leukotrienes and prostaglandins mediating inflammation or arachidonic acid and oxysterols which play a role in intracellular signalling. They are also involved in the synthesis of polyunsaturated fatty acids, which are implicated in signalling processes and apoptosis. In addition, peroxisomal β-oxidation takes part in the side-chain cleavage of cholesterol and could play a role in the conversion of gonadal steroids into inactive forms (Fig. 4). Thus, peroxisomal β-oxidation is essential for maintenance of the cellular homeostasis of lipids that are involved in the activation of many of ligand-activated nuclear receptors (PPARs, RXRs, and LXRs) [134, 236, 237].

1.2.2.4. Peroxisomal enzyme topology

Many scientific publications showed that the enzymatic composition of peroxisomes varies among species and among organs in the same species [238]. In recent years more than 130 proteins have been localized to peroxisomes [239]. The peroxisomal enzymes can be grouped as follows: *(1) antioxidants* (catalase, glutathione peroxidase 1 (GPX), peroxiredoxins 1, 5 (PRX1, PRX5) and superoxide dismutase 1 (SOD1) to degrade active oxygen species), *(2) oxidases* (acyl-CoA oxidases (ACOX1, ACOX2, ACOX3) urate, L-pipecolic acid, polyamine, D-amino acid) for saturated, unsaturated, branchedchain fatty acids, arachidonic acid metabolites, L-dihydroxy acids and cholestanoic acid, *(3) β-oxidation enzymes* (multi-functional protein 1 and 2 (MFP1,2) and peroxisome 3-ketoacyl-CoA thiolase (THIOLASE) A and B / SCPx, *(4) aminotransferases*, *(5) acyltransferases*, *(6) ether lipid syntheses enzymes* (dihydroxyacetone phosphate (DHAPA) acyltransferase, alkyl-DHAP-synthetase (DHAPS) and acyl-CoA reductase for the synthesis of plasmalogens [240] and *(7) enzymes of cholesterol synthesis* (3-Hydroxy-3-methyl glutaryl-CoA (HMGCoA) reductase, isopentenyl-diphosphate isomerase 2 (IDI), farnesyl pyrophosphate synthetase (FPP) and mevalonate kinase (Mvk), and *(8) other enzymes* associated with the synthesis of dolichol and bile acids as well as acyl-CoA hydrolase [241]. Furthermore, also a form of inducible nitric oxide synthase (iNOS) has been described in peroxisomes of hepatocytes [242]. In addition, it has been shown than more then half of the peroxisomal enzymes which

have been identified are located in the matrix, such as the β-oxidation enzymes. Others are membrane-bound, the enzymes involved in the activation of long- and very-long-chain fatty acids and the enzymes that catalyze the initial reactions in ether glycerolipid synthesis as well as the enzymes that catalyze the terminal reactions in cholesterol and dolichol synthesis. A few enzymes are associated with crystalline matrical inclusions (urate oxidase, xanthin oxidase, α-hydroxy acid oxidase B). Many observations suggest that peroxisomes with different enzyme compositions may be responsible for specific function in different tissues or cell types.

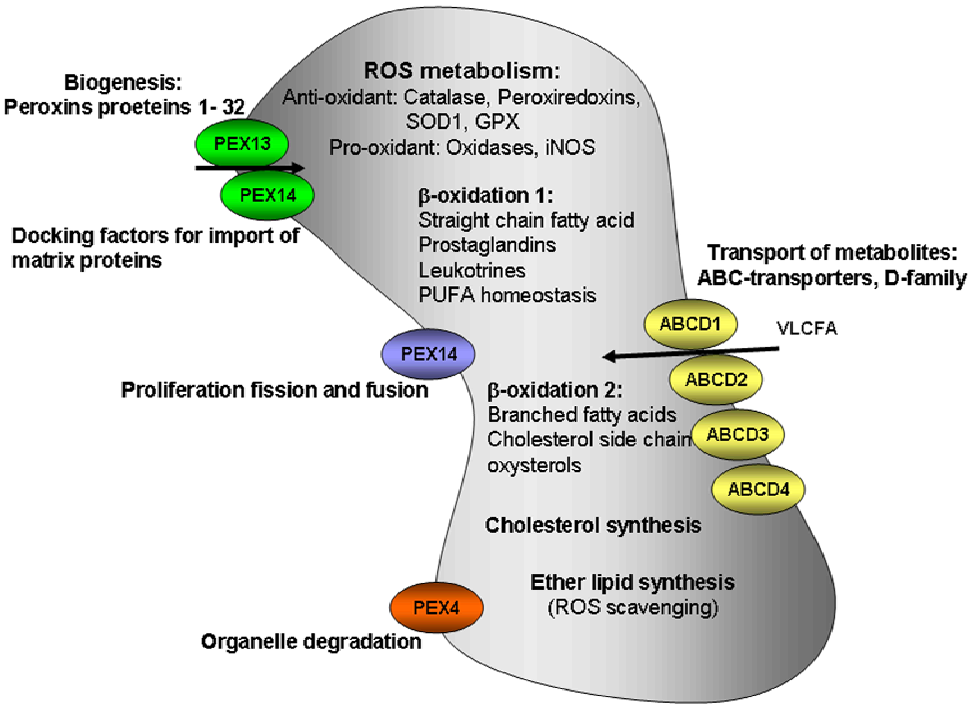

Figure 4: Model for a "general" peroxisome

1.2.2.5. Peroxisomes and its syndromes

There are two-group classifications of deficiencies based on organelle structure: (1) disorders of peroxisomal biogenesis (PBD) and (2) single-enzyme deficiencies with intact peroxisome structure.

Deficiencies in peroxisome biogenesis

Defective peroxisome biogenesis is associated with severe clinical manifestation, revealing the necessity and importance of regular peroxisomal metabolism for human health and survival. The diagnosis of a peroxisomal disease is made by the investigation of absent peroxisomal metabolic products, or the accumulation of "peroxisomal" intermediate, not oxidized derivatives due to deficient peroxisomal metabolism. The most severe peroxisomal biogenesis disorder is the cerbrohepatorenal syndrome of Zellweger (ZS) [243]. There are

other disorders included peroxisomal biogenesis disorder of ZS spectrum, exhibiting a less severe phenotype such as neonatal adrenoleukodystrophy (NALD) and infantile Refsum disease (IRD).

Diseases of ZS group are an autosomal recessive disorders, caused by defective PEX genes whose protein products (peroxins; PEX / Pex…p) are normaly involved in the regulator biogenesis of these organelles. Patients with ZS, the severe progressive form have embryological malformations in the central nervous system and kidney, and develop degenerative pathological defects, including lives cirrhosis and a degeneration of the adrenal cortex, leading to adrenal insufficiency. Children with ZS suffer from general muscular hypotonia and die usually in the first year of life. In these patients, regular peroxisomes are absent in tissues, wherefore cholic and chenodeoxycholic acid, docosahexaenoic acid and ether lipids (plasmalogens) are not produced, very long-chain fatty acids as well as branched-chain fatty acids are accumulated. It has become clear that certain metabolic pathways in peroxisomes are essential for efficient substrate channelling and to protect the cells against toxic metabolites that are normally degraded in peroxisomes, e.g., reactive oxygen species (ROS) [244].

Peroxisomal single-enzyme deficiencies

Based on biochemical abnormalities a number of monogenic peroxisomal single-enzyme deficiencies have been described, presenting different severity in phenotype. Peroxisomes are present in the tissues of the patients, but lack one enzyme. This group includes, *(1)* X linked adrenoleukodystrophy (X-ALD) in which boys are affected, who develops normally for the first few years of life and thereafter rapidly deteriorates. There is also adult variant *(2)* adrenomyeloneuropathy (ANM). Other diseases include *(3)* pseudo-neonatal ALD or acyl-CoA oxidase deficiency, *(4)* rhiztomelic chondrodysplasia punctata type 2 and 3, caused by mutations in *DHAPS* and *DHAPAT* genes, which encode the peroxisomal enzymes of the ether lipid syntheses pathway. Patients affected by these deficiencies show markedly lowered plasmalogen levels, which is in line with the notion that both enzymes play an indispensable role in ether-phospholipid biosynthesis [245].

Peroxisomal dysfunction and male fertility

Metabolic pathways of peroxisomes are of vital importance for normal spermatogenesis and regular functions of the human testis. This is accentuated by the impaired spermatogenesis and infertility in adult patients with peroxisomal single enzyme deficiencies, such as X-linked adrenoleukodystrophy (X-ALD) or adrenomyeloneuropathy (AMN, a milder phenotype of X-ALD) [246] [247]. Patients with X-ALD or AMN suffer from a defect of ABCD1 (formerly named “adrenoleukodystrophy protein” or ALDP), an ABC-transporter on the peroxisomal

membrane that is involved in the transport of very long-chain fatty acids (VLCFA) into the peroxisomal matrix [248]. Man with X-ALD exhibit an adreno-testiculo-leukomyelo-neuropathic-complex of symptoms [249] with impairment of the testicular functions in 80% of these patients. Many of the patients exhibit elevated serum LH levels and show a significantly lower testosterone/LH ratio, indicating an impairment of Leydig cells (see Fig. 2). In addition, other ALD-patients with defects in spermatogenesis also showed elevated serum levels of FSH (Fig. 2; [250]). Histological analysis of testicular tissue from 7 juvenile and 6 adult patients with X-ALD or AMN exhibited hypocellularity in the seminiferous tubules, a maturation arrest of spermatogenesis in distinct stages or a “Sertoli cells and Spermatogonia” only phenotype. Damage to Sertoli cells appeared to be the initial lesion of the seminiferous tubules. Germ cells showed vacuolization and necrosis, accompanied by slight tubular atrophy and thickening of the tunica propria [247]. In addition, Leydig cells were decreased in number and showed striations, suggestive for aggregates of VLCFA in the cytoplasm of these cells (Fig. 2; [247]). In ALD-patients, the decline of fertility can develop rapidly within only one year [251].

Similarly, patients with mild forms of peroxisomal biogenesis disorders (Zellweger spectrum patients), surviving to adolescence, show a complete degeneration of Leydig cells, resulting in hypocellular seminiferous tubules with spermatogenesis arrest and vacuolated Sertoli cells [252]. Severe forms of peroxisomal biogenesis disorders on the other hand lead to cryptorchidism [252], suggestive for an important function of peroxisomal metabolism also in the development of the testis and possibly the regulation of the androgen/estrogen balance or interference with androgen signalling [253][254].

Despite these deleterious effects of peroxisomal diseases on development, integrity and function of the adult testis, until the beginning of the experimented work of this thesis very little was known on peroxisomal metabolism in the testis. As indicated by the impaired spermatogenesis in peroxisomal diseases, however, normal function of peroxisomal metabolism is indispensable for male fertility. Thus, direct or indirect interference with peroxisomal metabolism might also play a role in the molecular pathogenesis of idiopathic infertility.

1.2.3. Mouse models for peroxisome dysfunction show impaired spermatogenesis

A number of mouse models have been generated to study the pathophysiology associated with peroxisome dysfunction in higher eukaryotes (for a review see [255]). Interestingly, several knockout mice with defects in single peroxisomal enzymes of anabolic and catabolic pathways of lipid metabolism were infertile, however, showed differences in the pattern of testicular pathologies and the level of spermatogenic arrest [256] [257] [258] [258].

Rodemer and colleagues described a mouse model disrupting plasmalogen synthesis by knockout of the gene encoding dihydroxyacetone-phosphate acyltransferase (GNPAT; formerly abbreviated DAPAT or DHAPAT). GNPAT is essential for one of the initial peroxisomal steps of plasmalogen synthesis. Adult GNPAT-deficient mice showed atrophic testes and an arrest of spermatogenesis. The germinal epithelium was disorganized exhibiting pachytene spermatocytes but a complete absence of elongated spermatids or spermatozoa [258].

Similarly, mice with defects in peroxisomal β-oxidation are infertile. According to reports in the literature, mice with a homozygous knockout of the acyl-CoA oxidase (ACOX1) gene showed reductions of the Leydig cell population and of spermatids, resulting in hypospermatogenesis [256]. However, the number and distribution of spermatogonia and spermatocytes was described as normal.

Furthermore, the knockout of the MFP-2 gene (17β-OH-DSH), encoding a multifunctional protein that catalyzes the subsequent steps in peroxisomal ß-oxidation, also caused infertility in homozygous mice [259]. An early sign of the testicular pathologies in these mice was lipid accumulation within cells of the seminiferous tubules, which was described already in prepubertal MFP-2 knockout mice. At the age of five weeks, large lipid deposits were present in Sertoli cells and a maturation arrest of germ cells with reduction of elongated spermatids and subsequent disintegration of the germinal epithelium was observed. In the same article [259], shortly results on Sertoli cell-specific *PEX5* knockout mice were reported. The phenotype in testes of these animals was similar to the one of MFP-2 deficient mice, suggesting that peroxisomal lipid metabolism of Sertoli cells is essential for regular spermatogenesis and integrity of the germinal epithelium. The testosterone levels in the serum of these animals was described as normal, however, there were no reports on the molecular pathogenesis of male infertility due to peroxisome deficiency.

In this dissertation work, however, several reasons for the induction of metabolic toxicity and stress were found Sertoli-cell-specific *Pex13* knockout mice (scs*Pex13*KO). These results present the first evidence of causative relationship between defects in peroxisomal metabolism and the development of male infertility due to the interference with steroid and ROS metabolism, lipid toxicity and alterations of important signal transduction pathways. The scs*Pex13*KO mouse generated and characterized during the experimental phase of this thesis periods is an excellent model system for male infertility due to peroxisome dysfunction.

2. Materials and Methods

All details for buffers, media, and solutions are given in the comprehensive Table 8 at the end of the Materials and Method section. All details for reagents and suppliers are given in the Table 10 at the end of the Materials and Method sections.

2.1. Human and animals tissue material used

2.1.1. Human: Testis biopsies were obtained after written informed consent, immersion-fixed with Bouin-fixative and embedded in paraffin. All biopsies used were from the biopsy and tissue repository of the Hessian Center for Reproductive Medicine in Giessen, Germany. General approval for the repository biopsy collection has been granted by the ethics committee of the Medical Faculty of the Justus Liebig University Giessen. The three biopsies analyzed were from 35- and 39-year old men and were diagnosed as "normal spermatogenesis" based on histopathological analysis.

2.1.2. Mice: Male C57Bl/6J mice (Charles River Laboratories, Sulzfeld, Germany) at the age of 4-6 months and 14-day-old animals (for isolation of cells) were used for all experiments in order to characterized peroxisomes in testis. The animals were delivered two days prior to the experiments and housed under standard conditions with free access to standard laboratory food and water and a 12h dark-/light-cycle. Experiments with laboratory mice were approved by the Government Commission of Animal Care Germany.

2.1.3. GFP-PTS1 transgenic mice: A fusion protein of the green fluorescent protein (GFP) and the peroxisomal targeting signal 1 (PTS1) is frequently used for visualization of peroxisomes in living cells [260]. The transgenic mouse line used in our study has been generated in the laboratory of Prof. Zimmer (Dept. Neurobiology, University of Bonn, Germany) by injecting a GFP-PTS1 cDNA fragment under the control of the murine *Rosa26* promoter into the pronucleus of CD1 mouse zygotes. Further details on this transgenic mouse line will be published elsewhere (Lüers et al., in preparation). The animals used were housed in the animal facility in Marburg, and testis biopsies were brought to our laboratory for experimental purpose only.

2.1.4. Necessary transgenic mouse lines for generation of Sertoli cell-specific *Pex13* knockout mice (scs*Pex13*KO)

- ***Pex13loxP – transgenic mice***

The *Pex13loxP* transgenic mouse line in C57Bl/6J background was obtained from the group of Denis I. Crane [1] for collaboration projects (cooperation agreement with Prof. Baumgart-

Vogt, Institute for Anatomy and Cell Biology II). The animals were delivered after the embryo transfers at the Transgenic Animal Facilities at the UKE Hamburg to the Central Animal Facility (Zentrales Tier Labor ZTL) of the Justus Liebig University, Giessen. Heterozygous animals of this line were crossed with C57Bl/6J (wild-type animals) and are now in the F12 generation of backcrosses in the ZTL Giessen. In the transgenic animals, the *exon 2* of the murine *Pex13* gene is flanked by *loxP* sites (*loxP*: locus of crossing over of the P1 phage), which are 35bp sequences recognized by the enzyme *Cre*-recombinase (*Cre*: “catalyses recombination” in the P1 phage).

- ***Amh-Cre* – transgenic mice**

The *Amh-Cre* transgenic animals in C57Bl/6J background were obtained from the central animal facility in Hamburg / Eppendorf after a user agreement with INSERM (Prof. Guillou) [10]. The heterozygous *AMH-Cre* animals were crossed with C57Bl/6J wildètype animals in the central animal facility of the Justus Liebig University, Giessen and are now in the F6 generation of the backcrosses in the ZTL. These animals express the *Cre*-recombinase under the control of the anti-Müllerian hormone promoter (*AMH-Cre*), which drives the *Cre* expression only in Sertoli cells of the testis.

2.2. Breeding strategy of generation scs*Pex*13KO mice using the *Cre-loxP* system

All experimental procedures using transgenic mice were performed in accordance with the guidelines of the German Government Commission of Animal Care and approved by the Regierungspräsidium Giessen (Allowance V54-19c 20/15c GI 20/23 to Prof. Baumgart-Vogt).

The Sertoli cell-specific deletion of *exon 2* of *the animals Pex13* gene was achieved by crossing *Pex13-floxed* mice with *AMH-Cre* transgenic. The parental generation consisted of homozygous male (or female) $Pex13^{loxP/loxP}$ mice in C57Bl/6J background, which was crossed with corresponding female (or male) animals expressing *Cre* recombinase exclusively in Sertoli cells. Heterozygous female (or male) (scs$Pex13^{WT/\Delta ex2}$ / $Amhcre^{+/-}$) from the F1 generation were then backcrossed to homozygous male (or female) (scs$Pex13^{loxP/loxP}$) mice in order to generate F2 offspring with the following genotypes: scs*Pex13*KO (scs$Pex13^{\Delta ex2/\Delta ex2}$/ $Amhcre^{+/-}$), scs*Pex13*HTZ ($Pex13^{WT/\Delta ex2}$/ $Amhcre^{+/-}$) and *Pex13*WT ($Pex13^{WT/loxP}$) mice. Mice of this F2 generation were born with the expected Mendelian frequency and were grossly indistinguishable from their non-KO littermates, after birth. For the experiments F2 male mice were used. The numbers of the mice used for each experiment are given in the different figure legends.

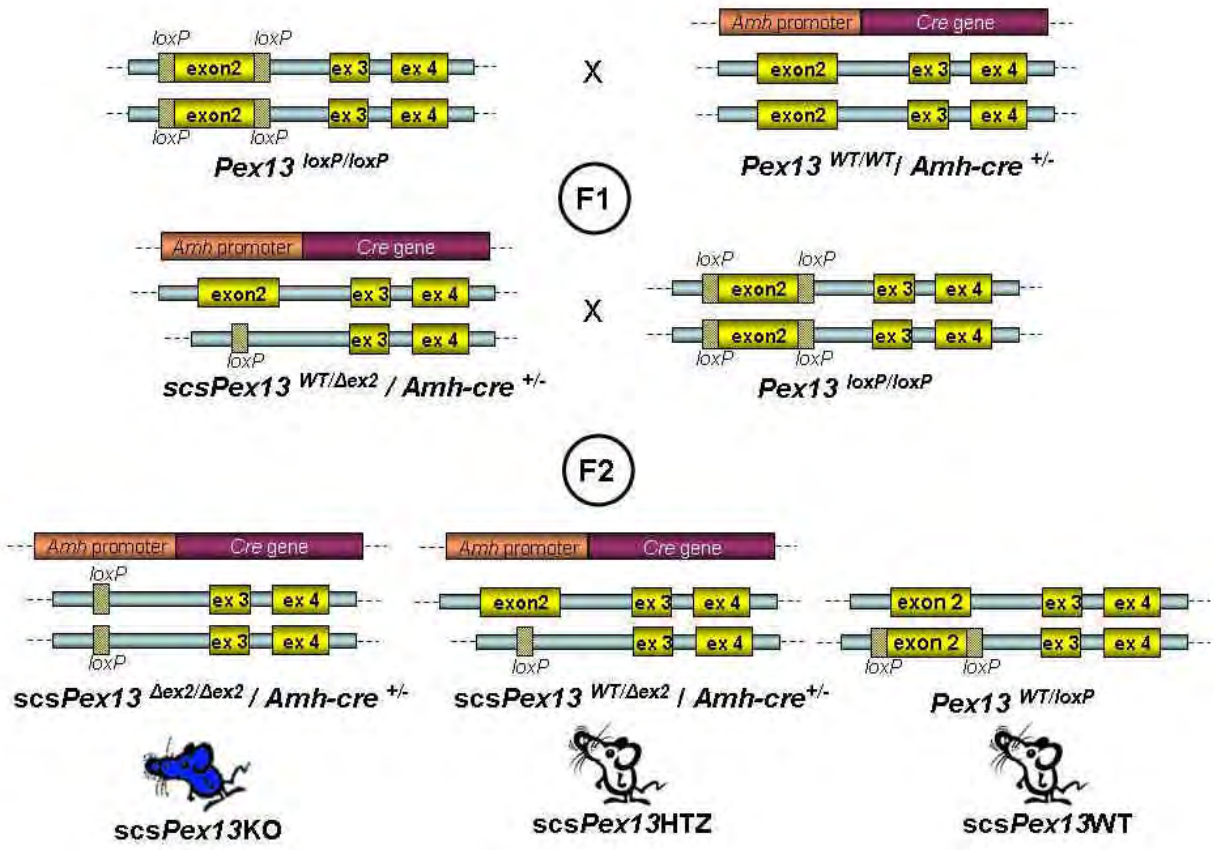

Figure 6. Strategy of mating to create tissue-specific scs*Pex13*KO mice. Parental generation: *Pex13* $^{loxP/loxP}$ (homozygous *Pex13loxP* mouse line) and *Pex13*$^{WT/WT}$ / *Amhcre*$^{+/-}$ (heterozygous *Amhcre* mouse line); First generation (F1 offsprings): heterozygous female (male) (scs*Pex13*$^{WT/\Delta ex2}$ / *Amhcre*$^{+/-}$) backcrossed to homozygous male (female) (*Pex13*$^{loxP/loxP}$); second generation (F2 offspring genotypes): scs*Pex13*KO (scs*Pex13*$^{\Delta ex2/\ \Delta ex2}$ / *AMHcre*$^{+/-}$), scs*Pex13*HTZ (scs*Pex13*$^{WT/\Delta ex2}$ / *AMHcre*$^{+/-}$) and scs*Pex13*WT (*Pex13*$^{WT/loxP}$) mice.

2.3. Genotyping with the polymerase chain reaction (PCR)

DNA for all genotyping experiments was prepared from mouse ear samples using a deproteinization procedure, salting out of the cellular proteins by dehydration and precipitation with a saturated NaCl solution. This procedure is an adapted method from Miller [261]. Over the samples 600 µl lysis buffer (50 mM Tris, 400 mM NaCl, 100 mM EDTA, 0.5% SDS) and 20 µl of protease K (15 mg/ml, Roche) solution were added. The samples were digested overnight at 55℃ with shaking at 900 rpm (Thermomixer comfort, Eppendorf). After the completion of the digestion 167 µl saturated 6 M NaCl was added to each tube and shaken vigorously for 15 sec, followed by centrifugation at 3,000 g for 5 min. The precipitated protein pellet was left at the bottom of the tube and the supernatant containing the DNA was transferred to a new 1 ml Eppendorf tube. In each tube 700 µl of absolute ethanol were added (RT) and the tubes were centrifuged at 3000 g for 2 min. The supernatant was removed from each tube. The DNA pellet was washed by addition of 1 ml of 70% ethanol

(RT) and subsequent centrifugation for 5 min at 3,000 g (RT). Thereafter the 70% ethanol was removed and the tubes were placed with open lid in the Thermomixer at 65℃ for 10 min for air drying. In each tube 20 µl of TE buffer (10 mM Tris-HCL, 0.2 mM Na_2EDTA, pH 7.5) in was added and the DNA was allowed to dissolve 10 min at 37℃ before quantification.
The *Cre*-PCR conditions were as follows: first denaturation at 94℃ for 3 min, followed by 34 cycles [denaturation at 94℃ for 30 s, annealing at 55℃ for 45 s, elongation at 72℃ for 1 min], and final elongation at 72℃ for 5 min. PCR p roducts were separated in a 1.5% agarose gel containing ethidium bromide for visualization (Sigma-Aldrich, Munich, Germany). For simultaneous detection of the *Pex13loxP* allele and the *Pex13* WT allele, appropriate primers (Table 6) were applied, generating a 504bp *Pex13*floxed amplicon and a 490bp *Pex13*WT amplicon. PCR conditions were as follows: first denaturation at 94℃ for 3 min, followed by 29 cycles [denaturation at 94℃ for 3 min, annealin g at 57℃ for 45 s, elongation at 72℃ for 1 min], and final elongation at 72℃ for 5 min. PCR products were separated in a 2% agarose gel containing xuM (xmg/ml) ethidium bromide.

Table 1. Reagents used to perform the genotyping PCR

Reagent	Cre-PCR Volume (in µl)	*Pex13*loxP-PCR Volume (in µl)	Final Concentration
10X Buffer	2.5	2.5	1X
10 mM dNTPs	0.5	0.5	200 µM
5 U Taq	0.2	0.2	1 U
10 µM primer 1	1.0	1.0	0.4 µM
10 µM primer 2	1.0	1.0	0.4 µM
DMSO	1.5		0.845 M
Braun-H_2O	QS 25 µl	QS 25 µl	-
DNA	Varies	Varies	200 ng
Final Volume	25.0	25.0	-

QS, Quantum Satis, the amount which is needed to reach

2.4. Laser micro-dissection of testes from 130 day-old mice scs*Pex13*KO, scs*Pex13*HTZ and scs*Pex13*WT

Three 130 day-old mice of each animal genotype (scs*Pex13*KO, scs*Pex13*HTZ and scs*Pex13*WT) were anesthetized as described (3.4.1.). The testes were embedded directly into a cryo-preservative solution (Optimal Cutting Temperature, OCT, Tissue-tek®) in freezing molds and placed in liquid nitrogen. The OCT-embedded tissue was stored at -80℃ prior to use. Frozen section were cut at 10 µm thickness and placed on 1 mm PEN membrane slide (cat no. 415101-4401-000, P.A.L.M. Microlaser Technologies GmbH,

Bernried, Germany) for UV laser cutting. The slides were stained immediately with Mayer's hematoxylin with the following procedure: 70% ethanol fixative for 3 sec, DEPC water for 5 sec, Mayer's hematoxylin for 15 sec, DEPC water for 5 sec, 70% ethanol for 5 sec, 95% ethanol for 10 sec, 2 times. The stained slides were air dried as quickly as possible. The testis sections were inspected with an Axio Observator microscope (Carl Zeiss) and microdissected with a P.A.L.M. laser-capture micro-dissection control unit using P.A.L.M RoboSoftware 4.0. (P.A.L.M. Microlaser Technologies GmbH, Bernried, Germany). 150 cross-sections from epithelial seminiferous tubules were catapulted into the lid of a 500 µl LPC-Microfuge tube (cat no. 1440-0200, P.A.L.M. Microlaser Technologies GmbH) and resuspended in RLT buffer (cat no. 56304, QIAamp DNA Micro Kit 50, QIAGEN). One thousand cells were the starting material for DNA isolation for each mouse phenotype. The DNA was isolated with QIAamp DNA Micro Kit 50 (cat no. 56304, QIAGEN) and its concentration was measured with a NanoDrop instrument (ND-1000 Spectrophotometer, Technology, Inc. USA). Two hundred nanograms of DNA were used for the genotyping PCRs as described in section 3.2. In addition, for comparison the DNA was isolated from tail and liver with the QIAGEN DNA MicroKit. Two hundred nanograms DNA was used for the subsequent genotyping PCR.

2.5. Morphological experiments

2.5.1. Fixation and embedding of the tissue

In the first set of experiments, wild type C57Bl/6J mice (Charles River) were anesthetized by intraperitoneal injection (100 mg/kg ketamine and 10mg/kg xylazine, sedastress) and perfused through the heart with 4% depolymerized paraformaldehyde (PFA) containing 2% sucrose in PIPES or PBS, pH 7.4. After fixation, testes were removed, the capsule was punctured at both poles and immersion-fixed in the same fixative overnight. The complete testes were embedded into paraffin (Paraplast®, Sigma, St. Louis, MO, USA), using a Leica TP 1020 automated vacuum tissue infiltration processor (1x 70%, 80%, and 90%, 3x 100% ethanol - each time for 90 min; 2x xylene, 2x paraffin - each time for 2 h).

In the second set of experiments, scs*Pex13*KO, scs*Pex13*HTZ and scs*Pex13*WT mice of postnatal days 15, 30, 60, 90 and 130 age were anesthetized in the same way as described above. After collection the blood directly from the heart, for lipid analyses, the testes were excised, fixed overnight in 4% (w/v) PFA containing 2% sucrose in PBS, pH 7.4 and processed for paraffin embedding exactly as described above. Paraffin blocks of testes were cut on a LEICA RM2135 rotation microtome into sections of 1-3 µm thickness.

2.5.2. Fixation and processing of testes for frozen sections

For the first set of experiments, testes of GFP-PTS1-transgenic mice were fixed by perfusion of the animals in Marburg (Institute of Anatomy and Cell Biology, Georg H. Lüerss) and the fixed testis samples were transferred to Giessen on the same day. Corresponding C57Bl/6J wild type mice were fixed by perfusion via the heart with 4% (w/v) PFA in 0.15 M HEPES, pH 7.4. The testes were excised, the capsule punctured at both poles with a needle and immersed in the same fixative overnight. Thereafter they were incubated in 25% sucrose for about 2 days, until they were completely penetrated and subsequently frozen and stored at -80℃. Cryosections obtained on a LEICA microtome (CM3050) were either directly analyzed by CLSM to monitor the GFP fluorescence or subjected to immunofluorescence using the antibody against Pex14p without antigen retrieval and lower detergent concentrations in the incubation buffers.

For the second set of experiments, testes of scs*Pex13*KO, scs*Pex13*HTZ and scs*Pex13*WT of 130 day-old mice were excised, the capsules punctured, and fixed by immersion overnight in 4% PFA containing 2% sucrose in PBS, pH 7.4. Fixed testes were snap-frozen in liquid nitrogen and stored at -80℃. Cryosections of 10 µm, obtained on a LEICA microtome (CM3050), were subjected to Oil O Red staining.

2.5.3 Fixation and processing of tissue for electron microscopy – Cytochemical localization of catalase activity with the alkaline DAB-method

C57Bl/6J wild type mice and scs*Pex13*KO, scs*Pex13*HTZ and scs*Pex13*WT mice (90 and 130 day-old) were anaesthetized and perfused via the left ventricle with a mixture of 4% PFA, 0.05% glutaraldehyde (GA) in 0.01 M cacodylate buffer (pH 7.4) and 2% sucrose. After fixation, the testes were carefully removed, cut in slices with razor blades, post-fixed in 1% (GA) in cacodylate buffer (pH 7.4) for 15 min, and washed 3 x for 5 min with 0.1 M cacodylate buffer. For cytochemical localization of catalase, specimens were incubated for 3 h at 45℃ in the alkaline 3,3'-diaminobenzidine (DAB) medium.[262] The DAB medium consisted of 0.2% DAB, 0.1% H_2O_2, 0.01 M Teorell-Stenhagen buffer, pH 10.5. Razor blade sections were stuck on agar-coated cover slips and incubated in a water bath shaker for 30 min at 45℃ in this solution without H_2O_2, followed by 1, 2, or 3h DAB rection at 45℃. After rinsing the sections with cacodylate buffer, post-fixation was done in 1-2% aqueous osmium tetroxide overnight. Samples were dehydrated in a series of graded ethanol (70%, 80%, 90%, 100% 3x 15 min each step) and embedded in Epoxy resin. After cutting of 1 µm semi-thin sections for the selection of the regions of interest, 80 nm-ultrathin sections were cut on a LEICA microtome (VT1000S) and inspected after contrasting with a LEO 906 electron microscope.

2.5.4. Immunoelectron microscopy

Three control C57Bl/6J and three GFP-PTS1-transgenic mice were anesthetized, perfused and testes were fixed as described above. Fixed testes were cut into slices with a razor blade and embedded into LR White resin (medium grade) according to the protocol of Newman and colleagues [4]. LR White-filled gelatin capsules were polymerized at 50℃ for three days. After cutting of 1 µm semithin sections, they were stained with methylene blue and analyzed to select the regions of interest (areas with defined stages of seminiferous tubules). After trimming of the blocks, ultrathin sections of 80 nm were cut, collected on 100 mesh nickel grids and coated on the back side with a 1% formvar film. The grids were dried at 37℃ overnight prior to immunostaining. The sect ions on the grids were incubated with blocking solution (1% BSA in TBST) for 30 min at RT. Incubation with the primary antibodies (anti-GFP 1:100 - 1:2000; anti-CAT 1: 500 - 1:10000 and anti-PEX13 1:500 – 1:5000) was performed on droplets overnight in TBST with 0.5% BSA at room temperature (RT) in a wet chamber. The sections were intensively washed on a series of TBS drops (10 drops each) and incubated with a protein A-gold solution (OD:0.45 1:75, 15 nm colloidal gold particles) for 1 h at room temperature [263]. Negative controls were processed in parallel a) by addition of TBST-buffer instead of the first antibodies or b) by antigen preabsorption of the first antibody (catalase preabsorption of the anti-catalase antibody). The grids were rinsed on droplets of TBST and subsequently contrasted with uranyl acetate for 2 min and lead citrate for 45 seconds. The sections were examined using a LEO 906 electron microscope.

2.5.5. Immunohistochemistry (IHC)

A three-step ABC-method with peroxidase detection was used for localization of peroxisomal catalase in mouse samples by IHC. For improved antigen retrieval and accessibility of epitopes, deparaffinized and rehydrated testis sections were subjected to digestion with trypsin for 10-15 min at 37°C, followed by microwaving in 10 mM citrate buffer at pH 6.0 for 3 x 5 min at 900 W in a conventional household microwave oven [264]. Cuvettes were filled up to the same volume with water between each microwaving step. The endogeneous peroxidase was blocked with 3% H_2O_2 for 5 min at RT. Non-specific binding sites were blocked with 4% bovine serum albumin (BSA) and in TBS with 0.05% Tween 20% (pH 7.4) (TBST) and avidin from an endogenous biotin blocking kit (Blocking kit, VECTOR, Burlingame USA). Subsequently, sections were incubated with primary antibodies for catalase (1:1,000) (Polysciences, Inc. Catalog no. 23728 Warrington, USA) in 1% BSA in TBST overnight at 4°C. In this solution, biotin (Blocking Kit, VECTOR, Burlingame U.S.A) was added to saturate the bound avidin. On the following day, the sections washed 3 x 5 min in TBST and incubated with the biotinylated goat anti-rabbit antibody (1:200) (Rabbit Extravidin Kit, Sigma, St. Louis, Missouri, USA) for 2 h. After washing 3 x 5 min with TBS,

sections were incubated with extravidin peroxidase (1:1,000) (Rabbit Extravidin Kit, Sigma, St. Louis, Missouri, USA) for 20 min. The antigen – anitibody complexes were visualized by peroxidase staining with NovaRed as substrate (VectorLab) for 5 min at RT. The nuclei were counter-stained with diluted 50% hematoxylin for 45 sec at RT.

2.5.6. Immunofluorescence (IF)

A two step IF-protocol was established for immunolabelling of paraffin sections. Sections were deparaffinized and rehydrated as follows: Xylene 3 x 10 min, absolute ethanol 2 x 5 min, 96% ethanol, 80% ethanol, 70% ethanol, and aqua dest, each step for 1 x 5 min at RT. For improved retrieval of peroxisomal antigens and accessibility of epitopes, deparaffinized and rehydrated testis sections were subjected to digestion with trypsin (in TBS) for 15 min at 37℃, followed by microwave trea tment for 15 min at 900 W in 10 mM citrate buffer at pH 6.0 (modified according to [264]). Nonspecific binding sites were blocked with 4% TBSA for 2 h at RT and the sections were incubated with primary antibodies in 1% BSA in TBST overnight at 4℃. On the following day, the sections were incubated after 3 x 5 min washing with TBST, with fluorochrome-conjugated secondary antibodies (diluted in 1% BSA TBS). For a complete summary of all antibodies, suppliers and functions of antigens see Table 5. Since individual, specific pre-immune sera were not available for most antibodies, negative controls were processed in parallel a) by addition of TBST-buffer instead of the first antibodies or b) by antigen pre-absorption of the first antibody (3.4.7). Nuclei were visualized with 1 µM TOTO-3 iodide for 30 min at RT (Molecular Probes/Invitrogen, Carlsbad, USA). Thereafter, samples were inspected with a LEICA fluorescence microscope and the best preparations were used for confocal laser scanning microscopy (CLSM) with a LEICA TCS SP2. Table 6 summarizes the antibodies used in this study. Images were processed with Adobe Photoshop CS. Figures were mounted in 300 pixels/inch resolution into figure plates and the text inserted in additional layers. Figure plates of the thesis were printed with a Lexmark HPColor Laser Jet2605dn printer on 90 g/m^2 paper (HP).

2.5.7. Analysis of the specificity of catalase antiserum by antigen competition

The polyclonal antiserum against catalase (Polysciences Inc., City, Country, dilution range 1:100 – 1:1000) was pre-incubated with bovine liver catalase at a final concentration of 6.45 mg/ml (Sigma) for 1h at RT, centrifuged at 13.000 x g for 15 min at 4℃ (Eppendorff centrifuge) and the depleted supernatant was used for immunostaining experiments. Paraffin sections were incubated overnight in parallel a) with supernatant from the catalase-preabsorption procedure or b) with the regular antiserum against catalase. After 3 x 5 min washing, the sections were incubated with AlexaFluor488-conjugated secondary anti-rabbit

antibodies (dilution 1:200) for 1h followed by washing in TBST and counter-staining for the nuclei with DAPI.

2.5.8. Hematoxylin and eosin (H&E) staining

Paraffin sections (5 µm thick) of testes from 15-, 30-, 60-, 90- and 130 day-old mice scs*Pex13*KO, scs*Pex13*HTZ and *Pex13*WT were stained with hematoxylin and eosin. Sections were deparaffinized and rehydrated as follows: Xylene 3 x 10 min, absolute ethanol 2 x 5 min, 96% ethanol, 80% ethanol, 70% ethanol, and aqua dest, each step for 1 x 5 min. The sections were stained for 7 min in 10% Mayer's Hematoxilin. After washing 10 min under the tap water for revealing the nuclei, the cytoplasm was stained for 5 min in 1% Eosin containing 0.2% glacial acetic acid. The slides were shortly washed with tap water and dehydrated short in 1 x 70%, 1 x 80%, 2 x 96%, 3 x in absolute alcohol, each step for 2 min, followed by 3 x 10 min in Xylene. The sections were examined with a LEICA CMRD microscope equipped with a LEICA CD 480 camera.

2.5.9. Oil Red O staining

Frozen sections of 130 day-old scs*Pex13*KO, scs*Pex13*HTZ and scs*Pex13*WT mice were stained with Oil Red O (ORO) in order to detect lipids. ORO staining was performed according to a standard protocol (www.ihcworld.com) using 0.5% ORO stock solution in isopropanol. The 0.3% ORO working solution had to be freshly prepared from the stock with bi-distilled water. Cryosections (10-15 µm) were cut with a LEICA microtome (CM 3050) and air dried for 30 min, followed by fixation with ice cold 10% formalin for 5 min. Thereafter, the sections were rinsed in 3 changes of distilled water and rinsed with 60% isopropanol to avoid carrying of water into the Oil Red O solution. The section were stained with the freshly prepared ORO working solution for 15 min at RT and rinsed ones with 60% isopropanol. Nuclei were lightly counter-stained with Mayer’s haematoxylin (5 dips for 5 sec) and rinsed thereafter with distilled water. The stained sections were mounted in glycerol gelatine medium (GG1 Sigma-Aldrich) and inspected with a LEICA DMRD microscope equipped with a LEICA CD480 camera.

2.5.10 TUNEL assay

Cell death was detected with a TUNEL assay on paraffin-sections from P90 and P130 scs*Pex13*KO and scs*Pex13*HTZ testes by using the Apoptosis *in situ* detection kit (Chemicon International, S7165). Sections were deparaffinized and rehydrated as follows: Xylene 3 x 10 min, absolute ethanol 2 x 5 min, 96% ethanol, 80% ethanol, 70% ethanol, and aqua dest, each step for 1 x 5 min. The rehydrated testis sections were subjected to digestion with trypsin for 15 min at 37℃, followed by microwave t reatment for 3 x 5 min at 900 W in 10 mM

citrate buffer at pH 6.0. The sections were washed in 2 changes of PBS for 2 min each. For positive controls, the sections were incubated for 10 min at RT with 1 unit of DNase I (Amplification grade, Invitrogen). The excess PBS was aspirated around the section and the equilibration buffer from the kit was immediately applied for 10 sec. After the buffer was removed, the terminal deoxynucleotidyl transferase enzyme (TdT), diluted 3:10 with reaction buffer, was applied onto the sections followed by an incubation for 1h in a humidified chamber at 37℃. The sections were transferred to coplin jars, containing the stop buffer from the kit for 10 min at RT and were thereafter washed 3 x 1 min in PBS. Finally, the anti-digoxigenin conjugate (rhodamine-conjugated) was applied to the sections for 30 min at RT in the dark. After 4 x 2 min washes with PBS, sections were counterstained with TOTO-3 iodide (Molecular Probes/Invitrogen, Carlsbad, USA) for 20 min at RT and embedded with Mowiol 4-88/n-propylgallate. The sections were inspected with a LEICA DMRD fluorescence microscope and pictures of region of interest were taken with a LEICA TCSSP2 CLSM (63x objective).

2.6. Primary culture of somatic testicular cells

Ten adult mice and fifteen 14-day-old mice in C57Bl/6J background were sacrificed by cervical dislocation and the testes excised aseptically and processed for the isolation of different somatic cell types.

2.6.1. Isolation and culture of Leydig cells

Isolation of Leydig cells was performed according to the method of Schumacher and colleges [265] with some modifications. All following procedures were carried out under sterile conditions. The tunica albuginea was carefully removed from the testis and seminiferous tubules and interstitial cells were dispersed by treating the decapsulated testis with collagenase A (1 mg/ml), hyaluronidase (1 mg/ml), and DNAse (20 µg/ml) in Dulbecco`s Modified Eagle Medium/Ham`s F-12 (DMEM/F12; 1:1, v/v) with 10 mM HEPES (pH 7.4) at 34℃ for 20 min in a shaking water bath. Seminiferous tubules were removed by sedimentation on ice for 2 min. The crude interstitial cells were collected by centrifugation at 1,000 x g for 5 min and resuspended in 6 ml DMEM/F12, supplemented with 2.2 µg/l sodium bicarbonate, 500 ng/ml insulin, 12 mg/l gentamicin and 1 mg/ml BSA. Two ml of the resuspended cells were loaded onto a five-layer discontinuous Percoll gradient (21, 26, 34, 40 and 60%) in isotonic Eagle's salt buffer containing 0.07% serum albumin and centrifuged at 800 x g for 30 min at 20℃. Highly purified Leydig cells were found in the third band of the Percoll gradient. The isolated Leydig cells were washed twice with serum-free medium DMEM/F12 with 10 mM HEPES (pH 7.4) and centrifuged at 100 x g for 8 min at RT. They were plated at a density of 1 x 10^5 /cm^2 in 12-well dishes in DMEM/F12 with 15% (v/v) horse

serum and supplemented with 2.2 µg/l sodium bicarbonate, 500 ng/ml insulin, 12 mg/l gentamicin, and 1 mg/ml BSA. The cells were cultivated at 34℃ in a humidified atmosphere of 5% CO_2 and 95% air. After 24 hours, Leydig cells were cultured in supplemented but serum-free DMEM/F12 for additional 3 days. The purity of the resulting Leydig cells preparation was determined by indirect immunofluorescence with an antibody against the mitochondrial cytochrome P450, cholesterol side-chain cleavage enzyme (CYP450scc), a marker specific for this cells type. 90-95% of the cells were cytochrome P450 positive, indicating a high enrichment and differentiation of Leydig cells within the preparation. These cells were taken for experiments after 3 days of culture. Leydig cells have been collected from three distinct sets of experiments.

2.6.2. Isolation and culture of peritubular myoid and Sertoli cells

Sertoli cells and peritubular cells from 15 mice of 14-day-old C57Bl/6J mice were isolated by a slightly modified protocol of Monssees and colleagues [266]. Decapsulated testes were minced into small fragments and incubated at 34℃ f or 15 min with collagenase A (1 mg/ml) in DMEM/12 with L-glutamine plus 15 mM HEPES and DNAse (20 µg/ml). Subsequently, the cells were dispersed by incubation with (2 mg/ml) collagenase A, hyaluronidase (2 mg/ml), and DNAse (20 µg/ml) in DMEM/F12 with L-glutamine plus 15 mM HEPES at 34℃ for 30 min. Enzymatic digestions were stopped by brief treatment with soybean trypsin inhibitor (400 µg/ml) in DMEM/F12, supplemented with 2 mg/ml BSA. The cell suspension was centrifuged for 45 sec at 50 x g. The supernatant, enriched with peritubular cells, was decanted. The cells from the supernatant were washed with RPMI 1640 medium and centrifuged at 50 x g for 10 min. Peritubular cells were resuspended and cultured in RPMI 1640 medium supplemented with 10% (v/v) fetal calf serum (FCS), 1000 IU/l penicillin and 50 mg/l streptomycin at 34°C in a humidified atmosphere of 5% CO_2 and 95% air. After splitting the cells 4 times, they were seeded at a density of 2 x 10^4 cells per ml onto either collagen- or poly-L-lysin-coated Petri dishes. The identity of these cells as peritubular cells was based on phase-contrast morphology and indirect immunofluorescence staining using anti-α-smooth muscle actin as specific cell marker. The purity of peritubular cell preparation was higher than 95%.

To separate the Sertoli cells and germ cells from each other the pellet with seminiferous tubules (see above) was further digested with (2 mg/ml) collagenase A, (2 mg/ml) hyaluronidase and (20µg/ml) DNAse in DMEM/F12 for 20 min at 34℃. Cell clusters were gently dispersed by homogenization using a potter. The cell suspension was filtered through a sterile (70 µm pore size) nylon mesh (BD Falcon, Bedford, USA). Cells were seeded at a density of 1.5-2 x 10^7 onto 100 mm^2 in matrigel covered culture dishes. They were cultured in DMEM/F12 GlutaMAX supplemented with 2 mM L-glutamine, 100 U/ml penicillin, 100 µg/ml

streptomycin, 10 ng/ml epidermal growth factor, 5 µg/ml human transferrin, 2 µg/ml insulin, 10 nM testosterone, 100 ng/ml follicle-stimulating hormone and 3 ng/ml cytosine arabinoside and incubated at 34℃ in a humidified atmosphere of 5% CO_2 and 95% air. After 3 days of culture the Sertoli cell monolayer was subjected to hypotonic shock to remove germ cells and increase the purity of the Sertoli cell preparation by incubation with 20 mM Tris-HCl (pH 7.5) for 5 min at RT [267]. The hypotonic solution was replaced with medium (without cytosine arabinoside). The medium was exchanged every day and the Sertoli cells were used for experiments after additional 3 days in culture. The identity of these cells as Sertoli cells was based on immunostaining for vimentin as specific cell marker. The purity of the cultures was higher than 95%. Sertoli cells and peritubular cells were collected from three distinct sets of experiments.

2.7. Subcellular fractionation by differential centrifugation for the isolation of enriched organelle fractions

2.7.1. Isolation of enriched peroxisomal fractions from primary cultures of Leydig-, peritubular myoid- and Sertoli cells

Distinct cell preparations (18 x 10^6 Sertoli cells, 12 x10^6 Leydig cells, 1 x10^7 peritubular myoid cells) were homogenized in homogenization medium (HM: 150 µl 5 mM MOPS, pH 7.4, 250 mM sucrose, 1 mM EDTA, 0.1 % (v/v) ethanol, 0.2 mM dithiothreitol, 1 mM 6-aminocapronic acid), supplemented with protease inhibitors (10% protease inhibitor mix M, Serva, Heidelberg, Germany) with a single stroke (2 min, 1,000 rpm) using a Potter-Elvehjem homogenizer (Potter-S, B. Braun, Melsungen, Germany). The homogenate was centrifuged at 1,900 x g for 10 min. The resulting supernatant (S1a) was kept on ice and the pellet was resuspended in 100 µl HM and recentrifuged at 1,900 x g, resulting in the supernatant (S1b) and a pellet (P1) with large mitochondria and nuclei. The combined supernatants S1 (S1a and S1b) were further subjected to centrifugation at 50,000 x g for 20 min to yield the enriched peroxisomal fraction (pellet) and the supernatant S2a. The enriched peroxisomal pellet was resuspended in 100 µl HM and recentrifuged again at 50,000 x g for 20 min, yielding the enriched peroxisomal fraction (P2) and the supernatant S2b. The supernatants S2a and S2b were combined (S2). Fractions S1, P1, S2, and P2 were analyzed by Western blotting. The enriched peroxisomal fraction is a mixed organelle fraction (= light mitochondrial fraction “LM”, also known as D-fraction), containing a high amount of peroxisomes as well as mitochondria, lysosomes and a lower amount of microsomal vesicles [268].

2.7.2. Isolation of enriched organelle fractions of interstitial, pertubular and tubular cells of the testes of 130 day-old scs*Pex13*KO, scs*Pex13*HTZ and scs*Pex13*WT mice

A pool of four testes was used from each phenotype to isolate interstitial cells (containing mainly Leydig cells, few macrophages, and few endothelial and smooth muscle cells), peritubular and tubular cells (containing Sertoli cells and germ cells) from 130 day-old scs*Pex13*KO, scs*Pex13*HTZ and scs*Pex13*WT mice. Decapsulated testes were minced into small fragments and processed by a first collagenase A and hyaluronidase digestion step as described above (3.6.1). The seminiferous tubules were removed by sedimentation for 2 min. The supernatant was subsequently centrifuged for 5 min at 1,000 x g to obtain the interstitial cells (= crude Leydig cells fraction). The interstitial cell pellet was gently dispersed in PBS for washing and re-centrifuged for 5 min at 1,000 x g.

Subsequently, the first tubular cell sediment was dispersed in a second digestion as described in chapter 3.7.2.

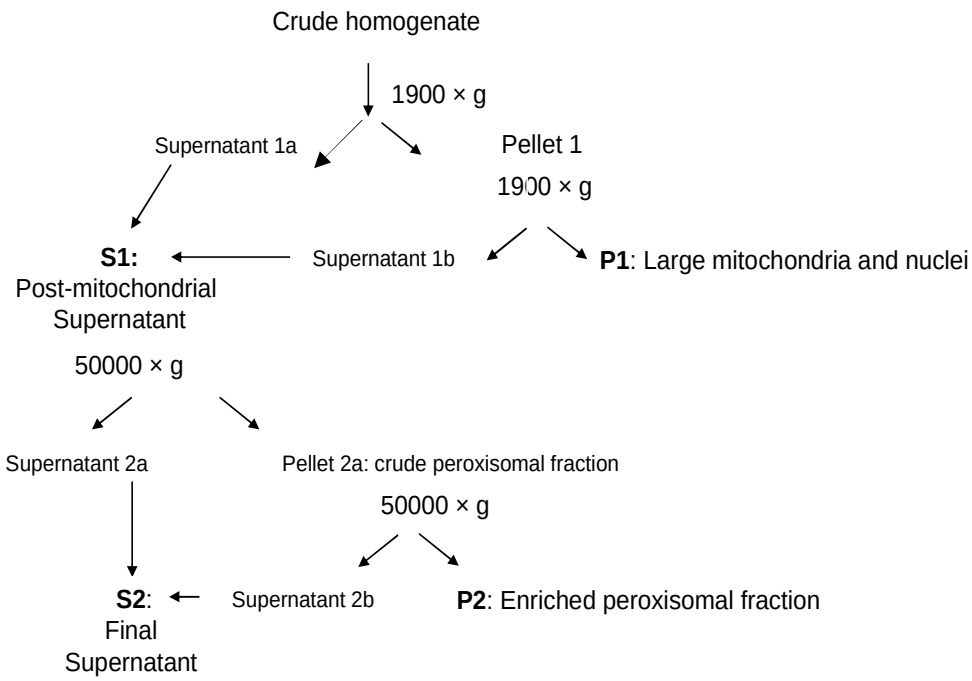

Figure 6. Subcellular fractionation and isolation of peroxisomes from primary cultures of Leydig, peritubular and Sertoli cells. The culture cells of the testis were homogenized in homogenization medium and the subcellular fractionation was done as shown in the diagram which is a modification after A.Völkl and HD Fahimi [268].

Thereafter, the cell suspension was centrifuged for 45 s at 500 x g yielding a pellet with seminiferous tubules. The supernatant containing peritubular cells was collected, centrifuged for 5 min at 1,000 x g, washed with PBS and re-centrifuged for 5 min at 1,000. The pellet with seminiferous tubules was gently dispersed by homogenization using a potter. The cell suspension was centrifuged for 5 min at 1,000 x g and the pellet was washed with PBS.

For the isolation of enriched organelle fractions, all cell preparations were homogenized in HM for 5 min according to the protocol described in chapter 3.8.1. In contrast to the procedure described in Fig. 6 (chapter 3.7.1.), one additional 300 x g centrifugation step for 10 min was introduced to the protocol to remove cell clumps. Thereafter, the protocol was followed as indicated in Fig.6. Since the subcellular fractionation protocol yielded pellets with different sizes for distinct cell preparations from scs*Pex13*WT and HTZ in comparison to scs*Pex13*KO mice, the resulting organelle pellets were resuspended in appropriate amount of HM according to the size of the pellets (*see* Table 2).

Table 2. Volume of the homogenization medium (HM) added to cell preparation.

Cell preparation	***scsPex13*WT**	**scs*Pex13*HTZ**	**scs*Pex13*KO**
Interstitial cells	200 µl	200 µl	150 µl
Tubular cells	300 µl	300 µl	100 µl

The fractions obtained from each centrifugation step and the amounts of HM that were added on each pellet are summarized in Table 3 and 4. Pellet 1 (P1) which contains the cell debris is not indicated in the table 3 and 4. The general fractionation procedure was the same as described in 2.7.2. yielding the supernatant S1 with all mixed organelles, the pellet P2 with heavy mitochondria and nuclei, the supernatant S2 with small organelles, the pellet P3 with enriched peroxisomes and light mitochondria and the final supernatant S3 with microsomes and the cytosolic proteins.

Table 3. Buffer volumes for subcellular fractionation of the testis of 130 day-old scs*Pex13*WT and scs*Pex13*HTZ mice

Centrifugation	*300 x g, 10 min* (2 times)	*1,900 x g, 10 min* (2 times)		*50,000 x g , 20 min* (2 times)	
Cellular Fractions	Supernatant with all organelles	**large mitochondria and nuclei**	**post-mitochondrial supernatant**	**enriched peroxisomes**	final supernatant
Interstitial cells	S1 225 µl	**P2** in 160 µl HB	**S2** 130 µl	**P3** in 150 µl HB	S3 75 µl
Tubular cells	S1 400 µl	**P2** in 300 µl HB	**S2** 275 µl	**P3** in 300 µl HB	S3 250 µl

Table 4. Buffer volumes for subcellular fraction of the testes of 130 day-old scs*Pex13*KO mice

Centrifugation	*300 x g, 10 min* (2 times)	*1,900 x g, 10 min* (2 times)		*50,000 x g , 20 min* (2 times)	
Cellular Fractions	Supernatant with all organelles	**large mitochondria and nuclei**	**post-mitochmdrial supernatant**	**enriched peroxisomes**	final supernatant
Intertitial cells	S1 180 µl	**P2** in 120 µl HB	**S2** 130 µl	**P3** in 100 µl HB	S3 80 µl
Tubular cells	S1 120 µl	**P2** in 100 µl HB	**S2** 80 µl	**P3** in 100 µl HB	S3 75 µl

Protein concentrations for all subcellular fractions were determined according to Bradford [269] using BSA as standard.

2.8. Western blot analyses and relative quantification of protein bands

Protein samples derived from cell cultures (10 µg) and from testicular interstitial and tubular cell preparations (25 µg) were separated on 12% SDS-polyacrylamide gels and transferred onto PVDF membranes (cat no:162-0218, BioRad, München, Germany) by electrotransfer with a Biorad blotter. Nonspecific protein binding-sites were blocked with Tris-buffered saline (TBS) containing 10% nonfat milk powder and 0.05% Tween-20 (blocking buffer). The blots were incubated for 2 h at RT with primary antibodies and after intensive washing for 1h at RT with alkaline phosphatase-conjugated secondary antibodies. The concentrations of the antibodies used for the Western blot analysis are given in Table 6. Alkaline phosphatase activity was detected using the Immun-StarTM AP (#170-5018) substrate from BioRad and exposure of the blots to Kodak Biomax MR films. Bands on films were quantified with the Gel Doc 2000 system from BioRad. The WB-membranes were stripped and reprobed several times with different antibodies as described in table 8. All Western blot analyses were performed three times with different membranes and therefore represent data from three individual experiments.

2.9. RNA isolation and expression analysis by semi-quantitative RT-PCR

Total RNA was prepared from juvenile and adult Leydig-, adult peritubular myoid- and juvenile Sertoli cells, from WT animals and also from preparations of adult interstitial peritubular and tubular cells derived from the scs*Pex13* transgenic mice using the RNeasy kit (cat. No 74104 Qiagen, Hilden, Germany). First-strand cDNA was synthesized from 3.5 µg total RNA with oligo(dT)12-18 primers using the Superscript II reverse transcriptase (#

18064-022, Invitrogen, Karlsruhe, Germany). The polymerase chain reaction (PCR) was set up in a final volume of 50 µl using 2 µl cDNA. All primers were tested and PCR conditions optimized with gradient PCRs on a BioRad iCycler prior to parallel analysis of cDNA samples from distinct testicular cells. Primer sequences are summarized in table 9. Bands on gels were quantified with the BioRad Gel Doc 2000 system. All RT-PCR experiments were performed three times and therefore represent data from three individual RNA isolation experiments.

2.10. Blood collection

All mice with different *Pex13* genotypes were anesthetized by intraperitoneal injection using a cocktail of 100 mg/kg ketamine and 10 mg/kg xylazine, and 2 mg/kg acepromazine (Sedastress®). Blood was collected from 130 day-old scs*Pex13*KO, scs*Pex13*HTZ and scs*Pex13*WT mice by direct cardiac puncture. For this purpose a 22-gauge needle, fitted onto a 1 ml-syringe, was inserted from the center of the thorax towards the animal's chin, 5-10 mm deep, and held at 25-30℃ away from the chest . When blood appeared in the syringe, the plunger was gently pulled back in order to obtain the maximum amount of blood (1 ml). Blood samples were immediately transferred to 2 ml anti-coagulating EDTA/KE tubes (Sarstedt Ag. & Co., Nürecht, Germany). The samples were centrifuged for 10 min at 13,000 x g and the plasma was stored at -80℃ until the hormonal measurements were performed.

2.11. Testis homogenates for steroids measurements

Dissected testis from scs*Pex13*WT and scs*Pex13*HTZ mice (10 to 11 mg) and scs*Pex13*KO mice (2 to 4 mg) were collected and stored at –80℃ prior to all homogenization and extraction procedures. For extraction, the two testes of the same animal were thawed and added to a glass tube containing 3 ml of PBS. The tissues were homogenized for 40 sec using a politrone homogenizer (T25basic IKA LABORTECHNIK) in a ice bath. All homogenates were subjected to diethyl ether extraction for 3 times. For this purpose 3 ml of diethyl ether was added in each tube. The tubes were vigorously mixed for 15 min, at 15℃, on a multi-tube shaker (Certomat IS, B Braun Biotech International) at 1,300 rpm, followed by centrifugation at 800 x g for 10 minutes at 4℃. Af ter each extraction with the diethyl ether the top organic layer was collected and transferred in new glass tubes and stored at -20℃ until they were subsequently measured with gas-liquid chromatography in collaboration with Dr. M. Hartmann and Prof. Dr. SA. Wudy, Department of Pediatrics, Pedriatic Endocrinology, University Hospital of Giessen and Marburg, Germany.

2.12. Testis homogenate for very long chain fatty acid (VLCFA) and plasmalogen measurements

VLCFA and plasmalogens were determined according to a modified protocol of Moser and Moser [270] by gas chromatography-mass spectrometry (GC-MS) in collaboration with Dr. Okun, Children Hospital, University of Heidelberg, Germany.

In brief, the testes were transferred into 10 ml glass tubes, suspended in 500 µl of sodium chloride (0.9% NaCl), and then homogenized with an ultraturax. Five ml of chloroform/methanol ($CHCl_3$/MeOH: 2/1, v/v) were added, gently mixed, incubated for 15 min, and mixed from time to time. The samples were centrifuged and the lower phase containing total lipids was transferred in a 25 ml reaction vessel. The remaining cell pellet was resuspended in 3 ml of $CHCl_3$/MeOH, mixed, and centrifuged. The lower phase was taken and pooled with the first fraction. The vessel was adapted to a rotating evaporator and the extracted and dried lipids (VLCFA and plasmalogens) were derivatised (methylisation) with 2 ml of methanolic HCl (3 M) at 80 ℃. After 1 h, the reaction was stopped by cooling down to room temperature. 2 ml of potassium carbonate solution (14 % w/v) and 2 ml of hexan were added and the mixture was shaken for 20 min. The hexan phase was transferred in a gas-chromatography vial and 500 µl of hexan were added prior to GC-MS analysis. For the GC-MS analysis the quadrupole mass spectrometer MSD 5972A (Agilent, Santa Rosa, California, USA) was run in the selective ion-monitoring mode. Gas chromatography separation was achieved on a capillary column (DB-5MS, 30 m x 0.25 mm; film thickness: 0.25; J&W Scientific, Folsom, California, USA) using helium as a carrier gas. A volume of 1 µl of the derivatized sample was injected in splitless mode.

2.13. Fertility test for different scs*Pex13* mouse genotypes

Three 90 day-old and 130 day-old males with scs*Pex13*KO and scs*Pex13*HTZ genotype were individually housed for 10 days with wild-type fertile C57Bl/6J female mice (Charles River). The female mice were then separated from the males and allowed to rest for additional 11 days since 19-21 days is the average gestation period in mouse. Males were considered to be fertile, when the female mice delivered pups.

2.14. *Pex13* silencing by RNA interference technology (RNAi) in primary Sertoli cell cultures

An RNAi approach was used to assess the effect of a *Pex13* gene knockdown in murine primary Sertoli cell cultures. A small interfering RNA for the mouse *Pex13* gene (siRNA ID#:176738) was synthesized and purified by Ambion (Austin, TX). The sequence of the silencing pre-designed siRNA targeted the exon 2 of the *Pex13* gene (NM_023651: *exon 2*, species: mouse) was used. One scrambled siRNA (scr-siRNA) that had no significant

sequence homology to mouse, rat or human gene sequences was used as a negative control. Primary Sertoli cells were isolated from 20 mice (15-day-old C57Bl/6J) according to the protocol described above (chapter 3.6.2). The cells were plated at a density of 350,000 per well in 12 well-plates. After 3 days of culture the Sertoli cell monolayer was subjected to hypotonic shock for 5 sec and replaced with DMEM/F12 GlutaMAX supplemented with 2 mM L-glutamine, 100 U/ml penicillin, 100 µg/ml streptomycin, 10 ng/ml epidermal growth factor, 5 µg/ml human transferrin, 2 µg/ml insulin, 10 nM testosterone, 100 ng/ml follicle-stimulating hormone (without cytosine arabinoside) and kept in culture for 1 more day prior to siRNA treatment. The effect of different concentrations of *Pex13* siRNA (15, 30 or 50 nM) and different compositions of the transfection reagent (1.5, 3, or 5 µl) on the *Pex13* mRNA expression and the PEX13 protein at distinct post-transfection time-points (12, 24, 48, and 72, 96 hours) were assessed using an array of techniques such as RT-PCR, Western blot and immunofluorescence. After several experiments the optimal conditions for the number of cells, the dilution of the siRNA and the amount of Lipofectamin RNAiMAX were found and are presented in Table 5. The siRNA knockdown had to be done with two consecutive transfections. Prior to the first transfection, the medium was replaced with Opti-MEM medium for 30 min and afterwards the cells were transfected for 24 h with *Pex13*-siRNA and control scr-siRNA using Lipofectamin RNAiMAX (Invitrogen). In a second control group only Opti-MEM medium was added to the cell cultures. The medium of the first transfection was replaced with normal Sertoli cell medium without antibiotic for 24 h. Thereafter, the second transfection was done with a longer incubation period of 72 h. Cultures with a second transfection at 48 h were supplied thereafter also with normal medium for Sertoli cells without antibiotic. After the siRNA transfection the cells were subjected to Western-blot, RT-RCR, and immunofluorescence analyses and ROS-measurements. These experiments were done three times under the same conditions.

Table 5. Optimal conditions for the transfection of primary Sertoli cells culture

	12 well-plate		
	***Pex13*-siRNA**	**scr-siRAN**	**Opti-MEM**
Lipofectamin	15nM in 100µl OPTI-MEM	15nM in 100µl OPTI-MEM	400µl
Density (cell/well)	350 000	350 000	350 000
RNAiMAX	1,5µl in 100µl OPTI-MEM	1,5µl in 100µl OPTI-MEM	-
Volume per well	400 µl	400 µl	400 µl

2.15. ROS-detection by staining with dihydroethidium

The oxidizable fluorescent probe dihydroethidium was used to evaluate intracellular ROS levels. Sertoli cells transfected with *Pex13*-siRNA, scr-siRNA or cells incubated solely with OPTI-MEM were used for this experiment. After transfection of cells and growth for different time points, 10 µmol of dihydroethidium (D-23107, Invitrogen) was added to 2 ml normal Sertoli cell medium, and incubated at 34℃ for 30 m in. Thereafter, the cells were washed two times with PBS and fixed with 4% PFA for 20 min at RT. Nuclei were counterstained with 1 µM TOTO-3 iodide for 20 min at RT. Images were taken with aLEICA TCS SP2 confocal laser scanning microscope (CLSM) and the average values of fluorescence intensity were measures from 450 cells using the LEICA software program of the CLSM. This experiment was performed two times under similar conditions.

Table 6. Primers sequences for genomic PCR of scs*Pex13* mouse line

Gene	Forward/reverse primers	Product length (in bp)	Ann. temp. (in °C)
Cre	For CCTGGAAAATGCTTCTGTCCG Rev GCAGGCGCAGGAGCTGGTGC	520	55
PEX13loxP	For ATGGCTCCCAAGTTAGTTCTG Rev TCTGTTTCCCTCCCACCTC	490 WT allele 517 loxP allele	57
PEX13Δ2	For TGGCTCCCAAGTTAGTTCTGTC Rev CCTCTCTATTTGTTGCTTACCCC	385	57

Table 7. Primary and secondary antibodies used in this dissertation

Host	Primary Antibodies	Con	Supplier	Function of Antigen
mouse	Human ABC-transporter D1 adrenoleukodystrophy protein, (ABCD1/ALDP), monoclonal antibody against a fusion protein aa 279-482 of ABCD1	IF 1:500 WB 1:200	Chemicon International, Temecula, 92590 CA, USA Cat. no. MAB2164	-ABC-transporter for VLCFA (very long-chain fatty acids -defective in X-linked ALD -marker for the peroxisomal membrane
sheep	Human ABC-transporter D3 70kDa Peroxisomal membrane protein (ABCD3 / PMP70) polyclonal antibody	IF 1:1,000	Gift from Steve Gould, Dept. Biol. Chem., Johns Hopkins Univ., Baltimore, MD, USA	-ABC-transporter for lipid derivatives -generally used as marker protein for the peroxisomal membrane
rabbit	Rat ABC-transporter D3 70kDa Peroxisomal membrane protein (ABCD3 / PMP70) polyclonal antibody	WB 1:100	Gift from Alfred Völkl, Dept. Anat. Cell Biol. II, Univ. Heidelberg	See above.
rabbit	Rat Acyl-CoA oxidase 1 (ACOX1) polyclonal antibody	IF 1:1,000 WB 1:5,000	Gift from Alfred Völkl, Dept. Anat. Cell Biol.II, Univ. Heidelberg	- first enzyme of peroxisomal β-oxdation pathway 1 -antibody labeling all subunits A, B, C
mouse	Mouse α-smooth muscle actin monoclonal antibody	IF 1:1.000	Sigma, Saint Louis, MO 63103, USA Cat. no: A2547	-cytoskeletal protein present in peritubular cells

rabbit	Human Catalase (CAT), polyclonal antibody	IHC 1:1,000 IF 1:1,000 EM 1:500	Polysciences, Inc. Warrington, PA 18976, USA Cat. no. 23728	-generally used as marker protein for the peroxisomal matrix -degradation of H_2O_2
rabbit	Mouse Catalse Catalase (CAT), polyclonal antibody	IF 1:2,000 WB 1:10,000	Gift from Denis I. Crane, Biomol. Biomed. Sci., Griffith Univ., Nathan, Brisbane, Qld 4111, Australia	See above.
rabbit	Mouse Cyclooxygenase 2 (COX2), polyclonal antibody	WB 1:400	Alexis Biochemicals, Enzo Life Sciences GmbH, 79539, Germany Cat. no: 2107121	-generally used as marker protein for inflammation
rabbit	Mouse Cytochrome P450 side chain cleavage enzyme (CP450scc) polyclonal antibody	IF 1:1,000 WB 1:5,000	Chemicon International, Temecula, 92590 CA, USA Cat. no. AB1244	-generally used as marker protein for Leydig cells -enzyme controlling steroidogenesis, responsible for the conversion of cholesterol to pregnenolone
mouse	Mouse Green fluorescent protein (GFP) (from jellyfish Aequorea victoria) monoclonal antibody	EM 1:800 IF 1:1,000	Santa Cruz Biotechnology Inc., Heidelberg 69115, Germany Cat. no: sc-9996	- used as a tag for in vivo fluorescence - in our study coupled to "-SKL", a peroxisomal targeting signal, to target GFP into peroxisomes
rabbit	Mouse Heme oxygenase 1 (HO-1) polyclonal antibody	WB 1:200	Assay Designs, Stressgen, MI 5777, USA Cat. no: SPA-895	-a heat shock/stress response protein, can be increased by heme and stimuli that induce cellular stress
mouse	Human Lysosome-associated membrane protein 2 (LAMP2), monoclonal antibody	IF 1:100	Research Diagnostics Inc., Flanders, NJ 07836 , USA Cat.. no: RDI-CD107b-H4B4	- lysosomal integral membrane protein generally used as marker protein for lysosomes and autophagic vacuoles
mouse	Mouse Oxidation Phosphorylation Complex III (OxPhosIII), monoclonal antibody	IF 1:2,000 WB 1:500	Molecular Probes/Invitrogen, Carlsbad, CA 92008, USA Cat. no: A11143	-complex 3 of the mitochondrial respiratory chain
mouse	Mouse Peroxin 5 (Pex5p) polyclonal antibody	WB 1:100	DB Biosciences, 69129 Heidelberg, Germany Cat. no: P10420-050	-cytoplasmic import receptor for peroxisomal matrix proteins (both PTS1 And PTS2)
rabbit	Mouse Peroxin 13 (Pex13p), polyclonal antibody	EM 1:500 IF 1:1,000 WB 1:5,000	Gift from Denis I. Crane (address see above)	-peroxisomal biogenesis protein 13 -integral peroxisomal membrane protein; involved in docking complex for matrix protein import
rabbit	Mouse Peroxin 14 (Pex14p), polyclonal antibody	IF 1:2,000 WB 1:30,000	Gift from Denis I. Crane (address see above)	-peroxisomal biogenesis protein 14 -function is similar to the one of Pex13p (see above)
mouse	Mouse Peroxisome proliferator-actgivated receptors γ (PPARγ) monoclonal antibody	WB 1:200	Santa Cruz Biotechnology Inc., Heidelberg 69115, Germany Cat. no: sc-7273	-nuclear hormone receptor that can be activated by fatty acids and ecosanoids
rabbit	Mouse Star domain-containing Protein1 (StARD1) polyclonal antibody	IF 1:25 WB 1:100	Protein Tech Group, Inc., Chicago, IL 60612, USA Cat. no: 12225-1-AP	-shuttle of cholesterol from outer to inner membrane of mitochondria

goat	Mouse Superoxide dismutase 1(SOD1) polyclonal antibody	WB 1:7,000	Abcam, 332 Cambridge Science Park, CG4 0WN, UK Cat. no: ab62800	-hemodimeric enzyme containing one Cu and Zn ion per subunit
rabbit	Mouse Superoxide dismutase 2 (SOD2) polyclonal antibody	IF 1:1,000 WB 1:5,000	Abcam, 332 Cambridge Science Park, CG4 0WN, UK Cat. no: ab13533	-tetra meric antioxidant enzyme involved in degradation of superoxide radical anion
rabbit	Mouse Thiolase A/B, polyclonal antibody	IF 1:1,000 WB 1:5,000	Gift from P. Van Veldhoven (Leuven, Belgium)	- third enzyme of peroxisomal β-oxdation pathway 1 -intermediate filament protein
goat	Mouse Vimentin, polyclonal antibody	IF 1,300	Sigma, St Louis, MO 63103, USA Cat. no: A2547	-generally used as marker for Sertoli cells
mouse	Mouse Vimentin, polyclonal antibody	IF 1:300 WB 1:200	Sigma, St Louis, MO 63103, USA Cat. no: A2547	See above.
Host	Secondary Antibodies		**Supplier**	
donkey	anti-Goat-IgG FITC	IF 1:200	Jackson Immuno Research Laboratories Inc., Dianova, Hamburg, Germany Cat. no: 705-095-147	
donkey	anti-Mouse-IgG TexasRed, Kit	IF 1:200 IF 1:300	VECTOR, Burlingame, CA 94010 USA Cat. no: Ti-2000	
donkey	anti-Rabbit-IgG AlexaFluor488	IF 1:300	Molecular Probes/ Invitrogen, Carlsbad, CA 92008, USA Cat. no: A21206	
donkey	anti-Sheep-IgG Rhodamine Red-X	IF 1:200	Jackson Immuno Research Laboratories Inc., Dianova, Hamburg 20354, Germany Cat. no: 713-295-147	
goat	anti-Rabbit IgG alkaline phosphatase conjugate	IHC 1:500 WB 1:20,000	Molecular Probes/ Invitrogen, Carlsbad, CA 92008, USA Cat. no: A0545	
goat	anti-Mouse IgG alkaline phosphatase conjugate	WB 1:20,000	Molecular Probes/ Invitrogen, Carlsbad, CA 92008, USA Cat. no: A3562	
goat	anti-Goat IgG alkaline phosphatase conjugate	WB 1:20,000	Molecular Probes/ Invitrogen, Carlsbad, CA 92008, USA Cat. no: A8438	
	Counterstaining of nuclei		**Supplier**	
	Hoechst 1:500			
	TOTO-3 nucleic acid staining 1:1,000	IF 1:1,000	Molecular Probes / Invitrogen, Carlsbad, CA, USA Cat. no:T-3604	
	Secondary detection system			
Staphylococcus aureus	Protein A	EM1:50	Self made according to [271]	

Table 8. Solutions, Media and Reagents

Solutions for Molecular Biology	
2% agarose gel, 50ml	1g of agarose , 50ml of 1x TAE, 1µl of ethidium bromide (10mg/ml)
Cell lysis buffer	50 mM Tris, 400 mM NaCl, 100 mM EDTA, 0.5% SDS
Formaldehyde gel 1x for RNA	100 ml 10x RNA Transfer buffer 10x, formaldehyde, 880 ml ddH_2O_2
Loading dye (10 ml)	16 µl saturated aqueous Bromophenol Blue, 80 µl 500 mM EDTA, pH 8.0, 720 µl 37% formalin stock solution, 4 ml 10X gel buffer fill up to 10 ml ddH_2O

NaCl	saturated 6 M NaCl
RNA Transfer buffer 10x	200 nM MOPS, 50 mM sodium acetate, 10 mM EDTA, pH 7.0
TE buffer	10 mM Tris-HCL, 0.2 mM EDTA, pH 7.5
Transfer buffer 10x (TAE)	40 mM Tris, 2 M glycin, 1% SDS
Solutions for Microscopy	
3-3'-diamino benzidine DAB	0.2% DAB, 0.01 M TS buffer, 0.15% H_2O_2, pH 10.5
Additional fixation for electron microscopy of wet sections	1% glutaraldehyde in cacodylate buffer (pH 7.4) for 15 min
Anti-fading agent (2.5%)	2.5 g N-propyl-gallate, 50 ml glycerol, 50 ml PBS
Buffer for diluting of antibody	1% TBST (50 mM Tris, 150 mM NaCl, 0.05% Tween 20, pH 7.4)
Citrate buffer	Buffer A: 1 mM $C_6H_8O_7$ H_2O; Buffer B: 50 mM $C_6H_5Na_3O_7$ $2H_2O$ Citrate buffer: 0.15 mM buffer A, 8.5 mM buffer B, pH 6.0
Epon / Epoxy resin Agar 812	24 g epoxy resin, 16g DDSA, 10 g MNA , stir 30 min, add drop by drop 1.5 g BBMA, stir 30 min
Fixation solution (testes for paraffin embedding)	4% depolymerized paraformaldehyde, containing 2% sucrose in PIPES or PBS, pH 7.4
Fixation solution (testes for frozen sections)	4% (w/v) paraformaldehyde in 0.15 M HEPES, pH 7.4
Fixation solution (electron microscopy)	4% depolymerized paraformaldehyde, 0.05% glutaraldehyde in 0.01 M cacodylate buffer (pH 7.4) and 2% sucrose
H_2O_2 (3%)	30% H_2O_2 10 ml, ddH_2O 90 ml
Hematoxylin and eosin staining	Xylene, absolute ethanol, 96% ethanol, 80% ethanol, 70% ethanol, and aqua dest., 10% Mayer's Hematoxylin, 1% acetic acid Eosin
IF blocking solution	4% bovine serum albumin (BSA) in Tris-buffered saline containing 0.05% Tween 20 (TBST)
IHC blocking solution	4% BSA , 0.05% TBST (pH 7.4) and extravidin from blocking kit (Avidin/Biotin Blocking kit, VECTOR)
Lead citrate (Reynold's)	0.19 mM lead nitrate, 0.22 mM sodium citrate, shake 30 min, ddH2O up to 25 ml, pH 10.0
Mounting medium	3 parts Mowiol 488, 1 part anti-fading agent
Mowiol 488 solution	16.7% Mowiol 488, 80 ml 1x PBS, stir overnight; add 40 ml glycerol stir again overnight; centrifuge at 15,000 g for 1h, store supernatant at -20ºC
Na-Cacodylate buffer	0.1 M sodium cacodylate, pH 7.4
Nuclear counter-staining (Oil red O staining)	alumn haematoxylin (5 short dips)
Oil red O stock solution	0.5 % Oil red O stock solution in 100% isopropanol
Oil red O working solution	0.3% Oil red O stock solution (30 ml stock and 20 ml distilled water)
Osmium post fixation for electron microscopy	1-2 % aqueous osmium tetroxide
PBS 10x	1.5 M NaCl, 131 mM K_2HPO_4, 50 mM KH_2PO_4, pH 7.4
PIPES buffer	0.1M PIPES, pH 7.4
TBS 10x	0.5 M Tris, 1.5 M NaCl, fill up to 1l ddH_2O_2, pH 7.4
Theorell-Stenhagen buffer (TS)	50 mM H_3PO_4, 75 mM boric acid, 35 mM citric acid, 345 mM NaOH, pH 10.5

Trypsin (0.01%)	0.01g trypsin in 1x TBS buffer
Uranyl acetate	1% uranyl acetate in ddH2O2; prior use centrifuge 15 min
Cell Culture Media	
Interstitial cell medium	DMEM/F12, supplemented with 2.2 µg/l sodium bicarbonate, 500 ng/ml insulin, 12 mg/l gentamicin and 1 mg/ml BSA
Leydig cell culture medium	DMEM/F12, supplemented with 15% (v/v) horse serum, 2.2 µg/l sodium bicarbonate, 500 ng/ml insulin, 12 mg/l gentamicin, and 1 mg/ml BSA
Leydig cell washing solution	serum-free DMEM/F12 medium with 10 mM HEPES (pH 7.4)
Percoll gradient	Percoll solution (21, 26, 34, 40 and 60%) in isotonic Eagle's salt buffer containing 0.07% serum albumin
Peritubula cell culture medium	RPMI 1640, supplemented with 10% (v/v) fetal calf serum (FCS), 1000 IU/l penicillin and 50 mg/l streptomycin
Sertoli cells culture medium	DMEM/F12, supplemented with 2 mM L-glutamine, 100 U/ml penicillin, 100 µg/ml streptomycin, 10 ng/ml epidermal growth factor, 5 µg/ml human transferrin, 2 µg/ml insulin, 10 nM testosterone, 100 ng/ml follicle-stimulating hormone and 3 ng/ml cytosine arabinoside
Solution for hypotonic shock	20 mM Tris-HCl (pH 7.5)
Stop of enzymatic digestions	soybean trypsin inhibitor (400 µg/ml) in DMEM/F12, supplemented with 2 mg/ml BSA
Testis enzymatic digestion for isolation of primary cells	collagenase A (1 mg/ml), hyaluronidase (1 mg/ml), and DNase (20 µg/ml) in DMEM/F12, supplemented with 10 mM HEPES (pH 7.4)
Washing medium for peritubular cells	RPMI 1640 medium
Solutions for Biochemistry	
10% blocking buffer	10 g fat free milk powder in 100 ml TBS
10x Electrophoresis buffer	250 mM Tris, 2 M glycin, 1% SDS
10x Sample buffer	3.55 ml ddH_2O, 1.25 ml 0.5 M Tris-HCl, pH 6.8, add 2.5 ml 50% glycerol, 2 ml 10% SDS, a tip of 0.05% Bromophenol Blue; prior to use add 50 µl β-mercaptoethanol
10x TBS	0.1 M Tris, 0.15 M NaCl in 1l ddH_2O, pH 8.0
12% resolving gel for 2 SDS-PAGE gels	30% acrylamide 4 ml, 5 ml buffer A, 1 ml ddH_2O, 65 µl 10% APS, 7.5 µl TEMED
1x TBST	0.1 M Tris, 0.15 M NaCl, 0.05% Tween 20, pH 8.0
20x transfer buffer	Bis-Tris-HCL buffer pH 6.4 polyacrylamide gel, NuPAGE transfer buffer (Invitrogen)
Homogenization medium for cell cultures and tissue fractions	150 µl 5 mM MOPS, pH 7.4, 250 mM sucrose, 1 mM EDTA, 0.1 % (v/v) ethanol, 0.2 mM dithiothreitol, 1 mM 6-aminocapronic acid, supplemented with 10% protease inhibitors mix M
Resolving gel buffer A	1.5 M Tris-HCl, pH 8.8, 0.4% SDS
SDS-PAGE solution:	
Stacking gel buffer B	0.5 M Tris-HCl, pH 6.8, 0.4% SDS
Stripping buffer (500ml)	62.5 mM Tris, 0.2% SDS, 500 ml ddH_2O

Table 9. Primers sequences for gene expression semi-quantitative PCR

Gene	Symbol	Also known as	Accession no.	Forward/reverse primers	Product length in bp	Ann. temp. in ℃
28 S ribosomal RNA	*28S rrna*	*28S RNA*	NR_003279	For CCTTCGATGTCGGCTCTTCCTAT Rev GGCGTTCAGTCATAATCCCACAG	254	65
3β-Hydroxysteroid dehydrogen	3b-HSD III	Hsd3b3	NM_001012306	For TCAATGTGAAAGGTACCC Rev ATCATAGCTTTGGTGAGG	499	55
3-Hydroxy-3-methylglutaryl-Coenzyme A reductase	*Hmgcr*	*HMG-CoAR*	NM_008255	For CCCACGAGCAAACATTGTC Rev TGAGCCCCACACTGATCAACC	741	54.3
3-Hydroxy-3-methylglutaryl-Coenzyme A synthase 1	*Hmgcs1*	*MGC36662*	NM_145942.4	For CTTTGCCTGACTGTGGTTCA Rev GACCACAGGGTACTCGGAGA	447	62.7
3-Ketoacyl-CoA thiolase A	*Thiolase A*	*pTH1*	AY273811	For TCAGGTGAGTGATGGAGCAG Rev CACACAGTAGACGGCCTGAC	241	60
Acyl-Coenzyme A oxidase 1, palmitoyl	*Acox1*	*ACOX1*	NM_015729	For CTGAACAAGACAGAGGTCCACGAA Rev TGTAAGGGCCACACACTCACATCT	565	60
Acyl-Coenzyme A oxidase 2, branched chain	*Acox2*	*ACOX2*	NM_053115	For CTCTTGCACGTATGAGGGTGAGAA Rev CTGAGTATTGGCTGGGGACTTCTG	688	58
Acyl-Coenzyme A oxidase 3, pristanoyl	*Acox3*	*ACOX3*	NM_030721	For GCCAAAGCTGATGGTGAGCTCTAT Rev AGGGGTGGCATCTATGTCTTTCAG	813	55
Alkylglycerone phosphate synthase	*Agps*	*DHAPS*	NM_172666	For TTTTGGGAAACAAAAGCTCAA Rev TTGGAGCAACACACTTCAGG	250	56
ATP-binding cassette, subfamily D, member 1	*Acbd1*	*ALDP*	NM_007435	For GAGGGAGGTTGGGAGGCAGT Rev GGTGGGAGCTGGGGATAAGG	440	63
ATP-binding cassette, subfamily D, member 2	*Abcd2*	*ALDPR*	AK134763	For TGCAAAATTCTGGGGAAGA Rev TGACATCAGTCCTCCTGGTG	405	58
ATP-binding cassette, subfamily D, member 3	*Abcd3*	*PMP70* *Pxmp1*	NM_008991	For CTGGGCGTGAAATGACTAGATTGG Rev GGGATAAGGTCCCCAGTCAAGTG	523	65
ATP-binding cassette, subfamily D, member 4	*Abcd4*	*PMP70R*	BC050102	For TGAAAGGCTCAGTGCAGATG Rev GGCTGCAGGTAGAAGAGACG	304	62
Catalase	*Cat*	*CAT*	NM_009804	For ATGGTCTGGGACTTCTGGAGTCTTC Rev GTTTCCTCTCCTCCTCGTTCAACAC	312	65
Cytochrome P450, family 11, subfamily a, polypeptide 1	*P450scc*	*Cyp11a1*	NM_019779	For GCTGGAAGGTGTAGCTCAGG Rev TTCTTGAAGGGCAGCTTGTT	432	58
Cytochrome P450, family 17, subfamily a, polypeptide 1	*P450c17*	*Cyp17a1*	NM_007809	For ACCAGCCAGATCGGTTTATG Rev AGGGCAGCTGTTTGTCATCT	204	58
Cytochrome P450, family 19, subfamily a, polypeptide 1	*P450arom*	*Cyp19a1*	NM_007810	For GACACATCATGCTGGACACC Rev CAAAGCCAAAAGGCTGAAAG	722	58
Enoyl-coenzyme A hydratase/3-hydroxyacyl coenzyme A dehydrogenase (multifunctional protein 1)	*Ehhadh*	*MFP1*	NM_023737	For ATGGCCAGATTTCAGGAATG Rev TGCCACTTTTGTTGATTTGC	211	56
Follicle stimulating hormone receptor	*Fshr*	*FSH-R*	NM_013523	For CCAGCCTTACCTACCCCAGT Rev CTGTGGTGTTCCCAGTGATG	345	58

GATA binding protein 1	*Gata1*	*Gf-1*	NM_008089	For TGTGTGAACTGTGGAGCAACGGC Rev AAATAGAGGCCGCAGGCATTGCA	350	58
GATA binding protein 4	*Gata4*	*Gata-4*	NM_008092	For CGGGTTGTTCAAACACCTTT Rev TGTGTGTGAAGGGGTGAAAA	250	58
Glutathione peroxidase1	*Gpx1*	*GpX-1*	BC086649	For GGGACTACACCGAGATGAACGA Rev ACCATTCACTTCGCACTTCTCA	430	55
Glutathione S-transferase 1	*Gsta1*	*Gst2-1*	BC132572	For GCAGACCAGAGCCATTCTCAACTAC Rev CTGCCAGGCTGTAGGAACTTCTTC	480	55
Heme oxygenase1	*Hmox1*	*HO-1*	MN_010442	For GCACTATGTAAAGCGTCTCCACGAG Rev CCAGGCAAGATTCTCCCTTACAGAG	610	55
Glyceronephosphate O-acyltransferase	*Gnpat*	*DHAPAT*	NM_010322	For CCGTCTCCTTGAGACCTCTG Rev AGGTGTGGGAATCTGAGTGG	198	60
17β–Hydroxysteroid dehydrogenase 4 (multifunctional protein 2)	*Hsd17b4*	*MFP2*	NM_008292	For GAGCAGGATGGATTGGAAAA Rev TGACTGGTACGGTTTGGTGA	223	60
Isopentenyl-diphosphate isomerase	*Idi1*	*MGC8139*	NM_145360	For GGGCTGACACCAAGAAAAAC Rev ACTGGCTGCCTTCTTCAAAA	470	62.7
Inhibin α	*Inha*		NM_010564	For GCAATGGATGGGGAAGGTGG Rev GGTGGCTGCGTATGTGTTGG	400	67
Interleukin 1α	*IL1a*	*IL-1a*	NM_010554.4	For CGTCAGGCAGAAGTTTGTCA Rev GTGCAAGTGACTCAGGGTGA	516	60.7
Interleukin 6	*IL6*	*IL-6*	AK150440	For GTTCTCTGGGAAATCGTGGA Rev GGAAATTGGGGTAGGAAGGA	339	60.7
Kit ligand Steel factor receptor	*Kitl*	*SF*	NM_013598	For CCGGATCCTGGAGCTCCAGAACAGCTAA Rev GCAGGCTGCAGACTGGACACACATGTTCTTGTC	200	58
Kit oncogene	*c-kit*	*Kit*	NM_001122733	For CAACAGCAATGGCCTCACGAGT Rev AGTGTGGCAGGACTTCTTGCC	500	64.5
Luteinizing hormone/choriogonadotropin receptor	*Lhr*	*LH-R*	NM_013582	For ATGGATCCCTCTCACCTATCTCCCTGT Rev AGTCTAGATCTTTCTTCGGCAAATTCCTG	702	58
Nitric oxide synthase 2, inducible	*Nos-2*	*iNOS*	NM_010927	For GTGTTCCACCAGGAGATGTTG Rev CTCCTGCCCACTGAGTTCGTC	576	56
Macrophage migration inhibitor factor	*Mif*	*GIF*	NM_010798.2	For CGGCAAGCCCGCACAGTACA Rev TCTCCCGGCTGGAAGGTGGG	357	62.7
Peroxiredoxin 1	*Prdx1*	*PAG*	NM_011034	For TCTCTTTCAGGGGCCTTTTT Rev CCAAAACACAGCTCAGACCA	396	35
Peroxiredoxin 5	*Prdx5*	*Pmp20*	NM_012021	For GAAAGAAGCAGGTTGGGAGTGT Rer CCCAGGGACTCCAAACAAAA	182	35
Peroxiredoxin 6	*Prdx6*	*GPx*	NM_007453	For TTGATGATAAGGGCAGGGAC Rev CTACCATCACGCTCTCTCCC	260	56
Peroxisome biogenesis factor 13	*Pex13*	*PEX13*	NM_023651	For GACCACGTAGTTGCAAGAGCAGAGT Rev CTGAGGCAGCTTGTGTGTTCTACTG	717	65
Peroxisome biogenesis factor 14	*Pex14*	*PEX14*	NM_019781	For CACCTCACTCCGCAGCCATA Rev CTGACAGGGGAGTGTCACTGCT	298	56

Peroxisome proliferator-activated receptor α	*Pparα*	*Ppara*	NM_001113418	For AGACCGTCACGGAGCTCACA Rev GGCCTGCCATCTCAGGAAAG	584	58
Peroxisome proliferator-activated receptor β / δ	*Pparβ*	*Pparb/d*	NM_011145	For CACCGAGTTCGCCAAGAACA Rev AGAGCCCGCAGAATGGTGTC	363	58
Peroxisome proliferator-activated receptor γ	*Pparγ*	*Pparg*	NM_001127330	For TCCGTAGAAGCCGTGCAAGA Rev CACCTTGGCGAACAGCTGAG	441	58
Cyclooxygenase 1 / Prostaglandin-endoperoxide synthase 1	*Ptgs1*	*Cox1*	NM_008969	For CTTTCCAGGAGCTCACAG Rev CAGTTTCTTCAGTGAGGC	271	55
Cyclooxygenase 2 / Prostaglandin-endoperoxide synthase 2	*Ptgs2*	*Cox2*	NM_011198	For GCAAATCCTTGCTGTTCC Rev GGAGGAAGGGCCCTGGTG	368	55
Retinoid X receptor α	*Rxrα*	*Rxra*	NM_011305	For CTCCTATCAGCACCCTGAGC Rev TCTAGGGGCAGCTCAGAAAA	739	64℃
Retinoid X receptor β	*Rxrβ*	*Rxrb*	NM_011306	For CTCCTCATTGCGTCCTTCTC Rev GAGACCCCGACAAATTCAGA	305	55℃
Retinoid X receptor γ	*Rxrγ*	*Rxrg*	NM_011307	For GGCAGCATTATGCGTGATTA Rev TCCATACATGTTGGCTGCTC	455	58℃
Steroidogenic acute regulatory protein	*StAR*	*Star*	NM_011485	For GTTCCTCGCTACGTTCAAGC Rev TTCCTTCTTCCAGCCTTCCT	292	58℃
Steroidogenic factor 1	*SF1*	*Ad4BP*	NM_139051	For GTGAAGTTCCTGAACAACCACAGC Rev GTCTGCTTGGCCTGCAGCATCTCG	300	60.7℃
Sterol-carrier protein X	*ScpX*	*SCPX*	M91458	For GGCCTTCTTTCAAGGGAAAC Rev ACCACAGCCCAATTAGCAAC	230	56℃
Sterol regulatory element binding transcription factor 1	*Srebf1*	*SREBP-1a*	NM_011480.3	For AGCCGTGGTGAGAAGCGCAC Rev TGCCCCAGCCGAAAAGCGAG	538	59.5
Sterol regulatory element binding transcription factor 2	*Srebf2*	*SREBP2*	NM_033218.1	For TCCCAGGCCGGCTTCTCTCC Rev GGCTGCAGGCCAAGTCCAGG	538	59.5
Sulfated glycoprotein 2 / Clusterin	*Sgp2*	*Clu*	NM_013492	For GACAATGAGCTCCA(G/A)GAA(A/C)TG Rev CAGGCATCCTGTGGAGTT(G/A)TG	1000	60℃
Superoxide dismutase 1	*Sod1*	*Cu-Zn-SOD*	BC86886	For AGCGGTGAACCAGTTGTGTTGT Rev CCACACAGGGAATGTTTACTGC	405	35
Superoxide dismutase 2	*Sod2*	*Mn-SOD*	NM_013671	For AAGTAGGTAGGGCCTGTCCGATG Rev CTAAGGGACCCAGACCCAACAAG	624	35
Superoxide dismutase 3	*Sod3*	*EC-SOD*	BC010975	For GGAGAGCGAGTGCAAGACCACTT Rev TCAAAGGTGCTCACTGGGAAGTC	485	35
Transferrin	*Trf*	*Cd176*	NM_133977	For ATCTGGGAGATTCTCAAAGTG Rev AGTGTGGCAGGACTTCTTGCC	960	56℃
Tumor necrosis factor	*Tnf*	*TNF-alpha*	NM_013693	For TGTCTACTGAACTTCGGGGTGA Rev GGCAGAGAGGAGGTTGACTTTC	356	59.6

Table 10. Reagents and Media Ingredients

Reagent	Catalogue Number	Manufacturer
10X PCR Buffer	DM2211	Promega GmbH
6-aminocapronic acid	8.00145	Merck
3,3' diaminobenzidine (DAB)	D5637	Sigma
ApopTag® Red *In Situ* Apoptosis Detection Kit	S7165	Chemicon
Blocking kit (avidin and biotin)	SP-2001	VECTOR
Bovine serum albumin (BSA)	A21153	Sigma
Sodium Cacodylate	42794	Fluka
Cytosine arabinoside	C-1768	Sigma
Chloroform (CH_3Cl)	25643	Sigma
Collagen Type I	C9791	Sigma
Collagenase Type I	C0130-1G	Sigma
DB Matrigel Matrix	354234	DB Biosciences
Deoxyribonuclease I, Amplification Grade	18068-015	Invitrogen
Diethyl ether	296082	Sigma-Aldrich
Dihydroethidium	D-23107	Molecular Probe
Dimethyl Sulfoxide (DMSO)	D2650	Sigma
Dithiotreitol (DTT)	D-9163	Sigma
DEPex	18245	Serva, D-69115 Heidelberg
DMEM/F12	11320-033	GIBCO
DMEM/F12 GlutaMAX	31331	GIBCO
Dulbecco`s Modified Eagle´s Medium/Ham`s F-12	31095029	GIBCO
DNase	D25	Sigma
Earle´s balanced salt solution 10x	E7510	Sigma
Earle´s balanced salt solution	E2888	Sigma
Ethylenediaminetetraacetic acid (EDTA)	O3690	Fluka, BioChemik
Epidermal growth factor (EGF)	E-1257	Sigma
Epoxy resin (AGAR 100kit)	R1031	Plano GmbH
Ethidium bromide	E7637	Sigma-Aldrich
Foetal calf serum	A15-043	PAA
Formalin	A5472	Sigma
Formvar	09818	Fluka – Biochemika
Follicle-stimulating hormone (FSH)	F-8174	Sigma
Gentamycin	G1397	Sigma
Glutaraldehyde	G7651	Sigma
Glycerol	GG1	Sigma-Aldrich
Hexan	448176	Aldrich
Horse serum	B15-021	PAA
Human transferrin	T-1147	Sigma
Hyaluronidase	H3506	Sigma

Hydrogen peroxide (H_2O_2)	371492	Aldrich
Isoflurane	FDG9623	Baxter
Immun-StarTM AP	170-5018	Biorad
Insulin	16634	Sigma
Isopropanol	59300	Sigma
Isotonic Eagle's salt buffer	D6946	Sigma
Kalium hexacyanoferrat(II)-thrihydrat	104984	Merck
Ketamine 100 mg/ml	14505	Pharmacia GmbH
Lead acetate	15326	Sigma
Lipofectamin RNAiMAX	13778075	Invitrogen
LR white resin	R1281	Plano GmbH
Matrigel	354234	DB Biosciences
Mayer's hematoxylin	109249	Merck
Methanol	15716	Fluka
Methanolic HCl (0.5N)	33354	Supelco
MOPS	M-8899	Sigma
NovaRed	SK-4800	VECTOR
Oil O Red	75087	Fluka
OPTI-MEM	31985-047	GIBCO
Osmium tetroxide	75632	Sigma
Paraffin (Paraplast®)	327204	Sigma
Paraformaldehyde (PFA)	604380	Sigma-Aldrich
Penicillin/Streptomycin	15140-122	Sigma
Percoll	P1644	Sigma
PIPES, analytical grade	32981	Serva
Poly-L-Lysine Hyrobromide	P2636	Sigma
Potassium carbonate	P5833	Sigma-Aldrich
Protease inhibitor mix M	39102	Serva
Protease K	P8044	Sigma
PVDF membranes	162-0218	Biorad
Rabbit Extravidin kit	EXTRA3A	Sigma
RNeasy kit	74104	QIAGEN
Rompun 2%	KP03J4W	BAYER
RPMI 1640	E15-840	PAA
dNTPs	U1515	Promega GmbH
Sedastress	6936	Medistar
Sodium bicarbonate	S5761	Sigma
Sodium chloride (NaCl)	S6191	Sigma
Sodium dodecyl sulfate (SDS)	L4390	Sigma
Soybean trypsin inhibitor	T9003	Sigma
Sucrose	1.07687	Merck
Taq polymerase	M166B	Promega GmbH
Testosterone	T-1500	Sigma

Tris	4855.2	Carl ROTH GmbH
Tris-HCL	93363	Sigma
Trypsin	T1426	Sigma
Tween 20	822184	Merck
Uranyl acetate	73943	Fluka
Xylene	97133	Carl ROTH GmbH

3. Aims of the study

Prior to this dissertation, peroxisomes were thought to be restricted only to somatic cells in the testis. Indeed, at the very beginning, peroxisomes have been identified by Fawcett & Burgos (1960) only in Leydig cells by routine electrone microscopy or by cytoplasmical visualization of there activity of the marker protein catalase. Reddy and Svoboda (1972) showed peroxisomes in Leydig cells proliferate upon LH treatment, whereas LH-deprivation results in a significant decrease in the number of these organelles. In addition, an increase of free cholesterol was noted in peroxisomes and mitochondria after LH treatment. Therefore, Mendis-Handagama & Ariyaratne (2005) have speculated that testicular steroid synthesis could occur at least in part in peroxisomes. Only recently work, from Luers and colleagues (2006) has revealed that peroxisomes are present in addition also in basal cells of the seminiferous tubules, Sertoli cells and spermatogonia respectively. However, little information is available on these organelles concerning its distribution and enzyme composition in mouse and human testis. The role of peroxisomal function in the testis and its influence in male fertility is not yet understood. Therefore, the goal of this study was to gain more insights into the presence of peroxisomes in different spermatic cells and to identify the physiological role of these organelles in the testis. The major aims of this study were:

PART I. Peroxisomes in different cell types of testis in human and mice

- To visualize and characterize peroxisomes in different cell types of testis in the wild type mice
- To identify germ cell peroxisomes in different steps of spermatogenesis, and characterize their alteration in distinct stages of the epithelial cycle of seminiferous tubules
- To exhibit analogies or differences of peroxisome compartment between human and mouse testis
- To characterize these organelles and the corresponding gene expression in primary cell cultures of distinct testicular somatic cells

PART II. Consequences of peroxisome deficiency in Sertoli cells

- To investigate the effects of peroxisomal dysfunction in the testis by generating a knock out of *Pex13* gene specifically in Sertoli cell by using *Cre-loxP* recombination system

- To investigate the effects of peroxisomal dysfunction in Sertoli cells and to study spermatogenesis and male fertility in this context
- To characterize the consequences and pathological alteration of structural integrity and the regulation of testis specific metabolism, hormone synthesis and signalling pathways
- To mimic the *Pex13* dysfunction in primary culture Sertoli cells by siRNA experiments and to compare its effects to the tissue alterations observed in Sertoli cell- specific *Pex13* gene knocked out

4. Results

Catalase (CAT) in general is the most abundant peroxisomal marker protein and has been frequently used for the detection of peroxisomes by immunohistochemistry (IHC) on paraffin sections or by cytochemical activity staining for this enzyme at the ultrastructural level in a variety of tissues [272]. However, the testis seems to be a big exception in this respect, since peroxisomes were only described in Leydig cells with this technique and seemed to be absent in germ cells. Even though, a highly sensitive peroxidise-based immunohistochemical technique (Avidin - Botin – complex: ABC) and optimal antigen retrieval was used [264], also in this dissertation, a punctuate staining pattern, indicating catalase positive peroxisomes could only be obtained in interstitial Leydig cells (Fig. 7). However, germ and Sertoli cells in seminiferous tubules were consistently labelled with a weak cytoplasmic staining in comparison to negative controls. Our group had already described that immunofluorescence techniques generally provide a more sensitive detection of peroxisomal antigens with precise subcellular location [264]. Therefore, this technique was adjusted to paraffin section of mouse and human testis tissue for the localization of a variety of peroxisomal antigens. In a series of preliminary experiments all necessary experimental conditions were elaborated to obtain optimal peroxisome localization in distinct testicular cell types. The ideal pre-treatment conditions found are described in detail in the Material and Methods chapter.

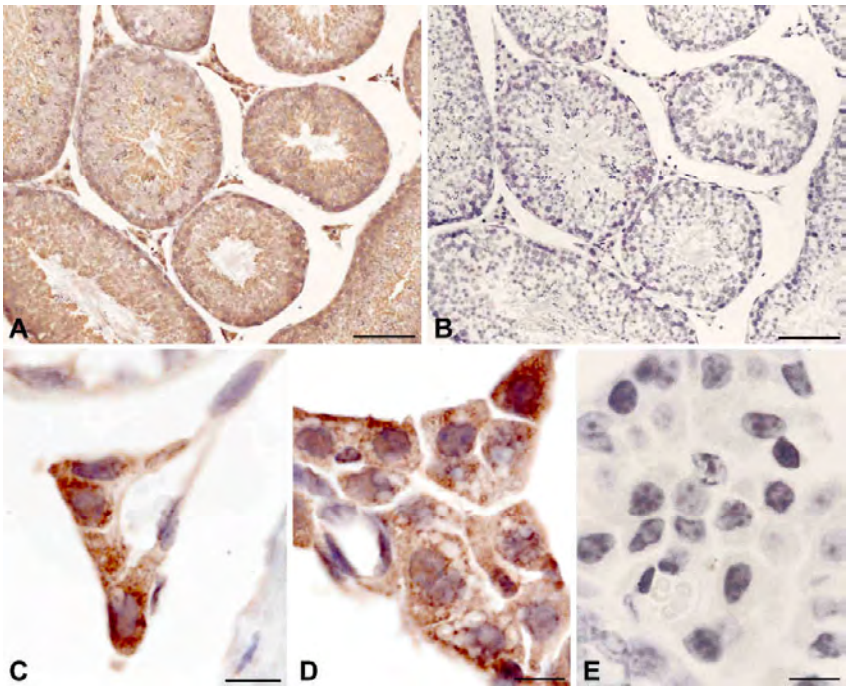

Figure 7: Immunohistochemical detection of catalase in adult mouse testis. (A) Overview of CAT staining in seminiferous tubules and interstitial cells. **(B)** Corresponding negative control without primary antibody. **(C,D)** Higher magnification views of CAT staining in interstitial cells, depicting the particulate localization of catalase in peroxisomes. **(E)** Corresponding high magnification without primary antibody. Bars represent 100µm in A and B and 20µm in C-E.

4.1. Peroxisomal proteins are heterogeneously distributed in distinct cell types of the mouse testis

By using immunofluorescence for the localization of several peroxisomal marker proteins, peroxisomes could be detected in addition in other testis–specific somatic cells (Sertoli cells and peritubular cells) and in germ cells (spermatogonia, spermatocytes, round and elongated spermatids) in the seminiferous tubules of the adult mouse testis (Fig. 8). In agreement with the peroxidase-based IHC results, catalase immunoreactivity was also most intense in Leydig cells in immunofluorescence preparations. In addition, a punctuate peroxisomal staining pattern could also be observed in the basal compartment of the germinal epithelium and in peritubular myoid cells (Fig. 8A). Only with very high concentrations of the CAT antibody (1:100) and prolonged exposure times, leading to overexposure of Leydig cells in the images, a weak punctuate staining for CAT was also seen in spermatocytes and spermatids.

A comparable distribution of immunoreactivity was observed for peroxisomal THIOLASE A with strong signal in Leydig cells and a fine punctuated staining of lower intensity in the germinal epithelium (Fig. 8B). However, in comparison to CAT, clear THIOLASE A immunoreactivity was present in a punctuate pattern also in suprabasal layers of the germinal epithelium. In contrast, the peroxisomal ABC transporter ABCD3, which is one of the most abundant integral membrane proteins of peroxisomes in hepatocytes, was expressed only in the periphery of seminiferous tubules, with highest abundance in Sertoli cells (Fig. 8C).

In Leydig cells, ABCD3 was barely detectable. In contrast, ABCD1, a second ABC transporter in the peroxisomal membrane, was selectively enriched in Sertoli cells as shown by a ABCD1/vimentin double-immunofluorescence staining (Fig. 8D). In comparison to the above-mentioned metabolic enzymes and transporters, the peroxisomal biogenesis proteins PEX13 and PEX14 were detected in all cell types of murine testis, except mature spermatozoa (Fig. 8E, F). However, the expression patterns of both proteins with respect to signal intensities were different in distinct cell types. PEX13 was most abundant in germ cells, with weaker staining of Sertoli-, peritublar myoid- and Leydig cells (Fig. 8E), whereas the staining for PEX14 was most prominent in the basal compartment of the germinal epithelium with significant labelling also of Leydig cells (Fig. 8F). In addition to individual small peroxisomes, large and strongly immunoreactive structures were observed with all antibodies against peroxisomal proteins at the luminal surface of the germinal epithelium in the region of late spermatids (Fig. 8E and Fig. 11).

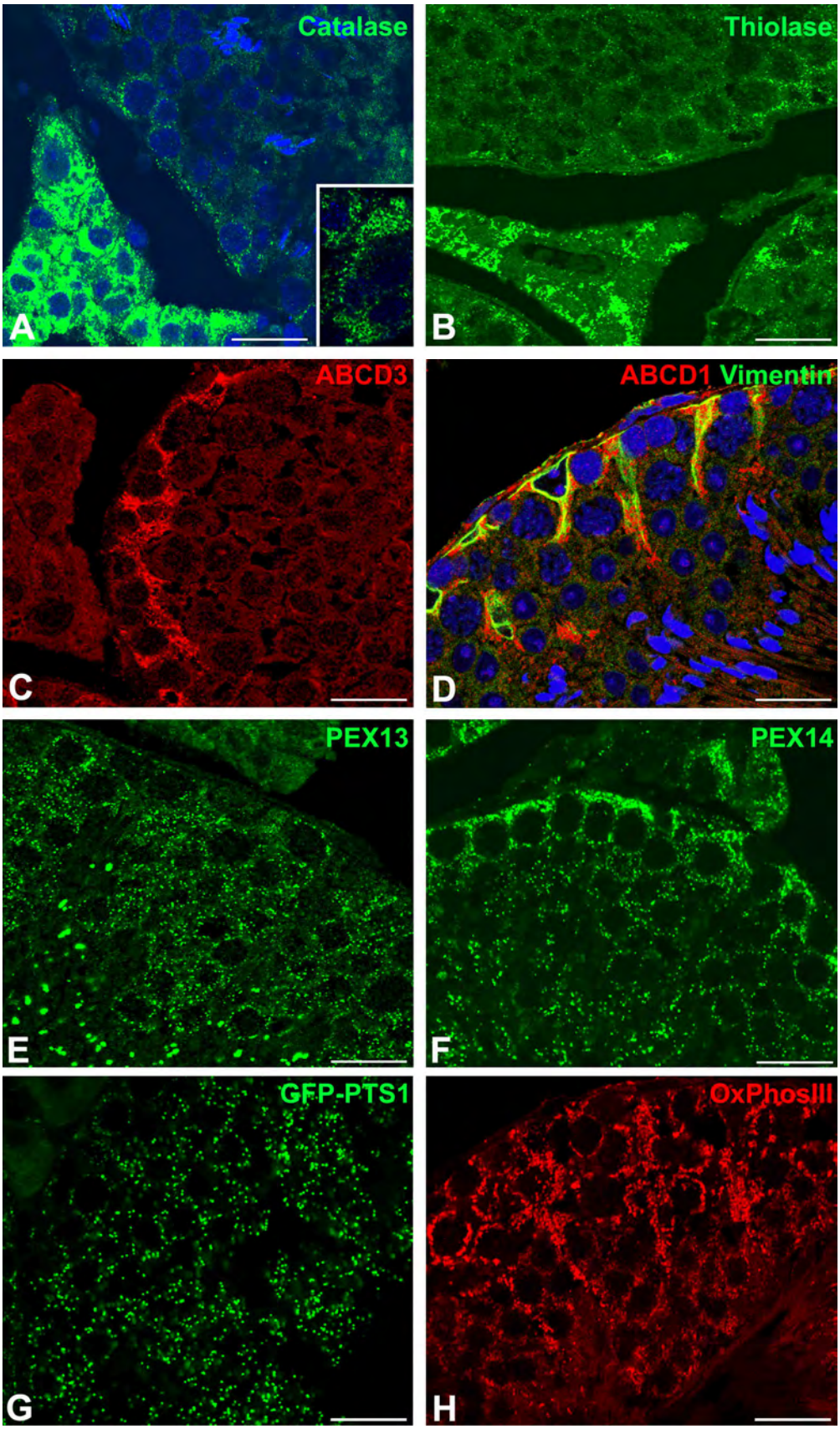

Figure 8: Fluorescence detection of peroxisomal and mitochondrial proteins in adult mouse testis. **Peroxisomal proteins: (A)** Catalase (inset shows Leydig cells at shorter exposure time). **(B)** Thiolase. **(C)** ABCD3. **(D)** ABCD1 (red). **(E)** PEX13. **(F)** PEX14. **(G)** GFP-PTS1 transgenic mouse. **Mitochondrial protein: (H)** OxPhosIII: Complex III of the mitochondrial respiratory chain. **(D)** Shows a double immunofluorescence labeling for ABCD1 (red) and VIM (green). Nuclei in A and D were counterstained with TOTO-3 iodide (blue). Note the difference in cell type-specific labelling intensities with highest abundance of catalase and thiolase in Leydig cells.

ABCD3 and ABCD1 show highest abundance in Sertoli cells. Pex13p and Pex14p are present in all cells shown. Bars represent 40 µm.

These results with antibodies against peroxisomal proteins were further substantiated by fluorescence analysis of cryosections of GFP-PTS1 transgenic mice, in which the green-fluorescent protein (GFP) is targeted to the peroxisomal matrix via the C-terminal peroxisomal targeting signal 1 (“SKL”). This transgenic mouse strain exhibits high expression levels of the GFP-transgene in all germ cells, allowing straight forward detection of peroxisomes in frozen sections without further embedding and antibody labelling procedures. As depicted in Fig. 8G, import competent peroxisomes are present throughout the germinal epithelium. As an internal control for organelle distribution, we also detected mitochondria with an antibody against complex III of the respiratory chain (OxPhosIII, Fig. 8H). In comparison to peroxisomal enzymes, mitochondrial complex III was enriched in spermatocytes I and also abundant in the middle piece region of step 16 spermatids (see also Fig. 9B).

4.2. Cell type-specific differences in abundance of peroxisomal proteins are conserved between mouse and man

Indirect immunofluorescence preparations of paraffin sections of human testis with antibodies against different peroxisomal marker proteins showed a similar staining pattern as observed in adult mouse testis (Fig. 9). CAT (1:1.000 dilution) was mainly detected in Leydig cells (inset) and the basal region of the seminiferous tubules (labelling in Sertoli cells, Fig. 9A,B). In contrast to CAT and similar to mouse samples, mitochondrial complex III was clearly detectable in spermatocytes I (Fig. 9B). The distribution pattern of Acyl-CoA oxidase I, the rate-limiting enzyme of the β-oxidation pathway I, was almost identical to that of CAT with strongest abundance in Sertoli cells (Fig. 9C). Similar to mouse preparations, peroxisomal THIOLASE A - the terminal enzyme of the β-oxidation pathway I, could be detected in addition to Sertoli cells also in suprabasal layers of the germinal epithelium in human testis (Fig. 9D). Furthermore, the peroxisomal biogenesis proteins PEX13 and PEX14 showed similar protein abundance patterns as in mouse testis with labelling of all cell types in different intensities (Fig. 9E, F, inset in G). Similar to murine testis ABC-transporters, D family, ABCD1 and ABCD3 (Fig. 9G, H) were selectively enriched in Sertoli cells. Double-IF with ABCD1 / VIM revealed an almost exclusive localization of ABCD1 in Sertoli cells (Fig. 9H). Large aggregates, similar to those seen in mouse testis, were also present in human samples in late spermatids (see in Fig. 9F: PEX14, Fig. 9G: ABCD3 and inset Pex13p). These clusters were never positive for lysosomal proteins (LAMP2). Specific staining of lysosomes and of autophagic vacuoles using anti-LAMP2 was strongest in Sertoli cells in

addition to the labelling of the acrosomes in spermatids (Fig. 9F), and did not colocalize with peroxisomal marker proteins (PEX13, PEX14).

In order to confirm the specificity of the antibodies used in the IF analyses on the mouse as well as on the human sections, negative controls without primary antibody were performed in all experiments in parallel, depicting the high quality of the secondary antibody-reaction in mouse (Fig. 10C,D) and human (Fig. 10E,F). In addition, the antigen specificity of the primary antibody was tested in immune competition experiments. For this purpose, the anti-CAT antibody (1:100) was depleted with bovine CAT protein. After immune precipitation, the CAT antigenicity in the solution was completely depleted and no specific reaction product was detected anymore on the sections (Fig. 10B).

4.3. Peroxisomes aggregate in clusters during spermatid maturation

For analysis of alterations of the peroxisomal compartment during spermatogenesis or different steps in spermiogenesis, distinct stages of the seminiferous tubules must be compared. In mice, the process of spermatogenesis progresses along the longitudinal axis of the seminiferous tubules and the synchronization of the spermatogenic cycle allows for the classification of different tubule segments in twelve distinct stages [273], (for a review see [274]). Since PEX14 labelling was most sensitive for the identification of peroxisomes in all cell types of the seminiferous tubules, we have used IF preparations of paraffin sections with this marker for analysis of peroxisomal alterations during the spermatogenic cycle (Fig. 11A-C) or a combination of fluorescence analysis of cryosections of GFP-PTS1 transgenic mice with PEX14 immunolabelling (Fig. 11D, E, G, H). During the course of spermiogenesis, peroxisomes could be clearly identified as single organelles in round and early elongating spermatids (step 1-13). In contrast, less numerous, large and intensely labelled peroxisomal structures appeared in late elongated spermatids (step 15 and 16). Colocalization of PEX14 and GFP-PTS1 in the same particles verified the peroxisomal nature of these structures (Fig. 11D, E). Similar structures were also labelled with CAT- and ABCD3-antibodies (Fig. 12A, B). Higher magnification images revealed aggregates and network-like structures positive for CAT and ABCD3. Similar peroxisomal aggregates were also found in PEX13 and PEX14 preparations (Fig. 8E and 9F, G inset). Upon careful analysis of peroxisomal aggregates in spermatids of distinct stages of the seminiferous epithelium, a significant difference in the number and spatial localization of peroxisomal structures with respect to the nuclei was noted (Fig. 11D-F). During the progress of spermatid maturation, peroxisomes disappeared as individual organelles (stage II-III, Fig. 11A, D), decreased in number and aggregated to larger clusters (stage VI-VII, Fig. 11B, E; Fig. 12A, B).

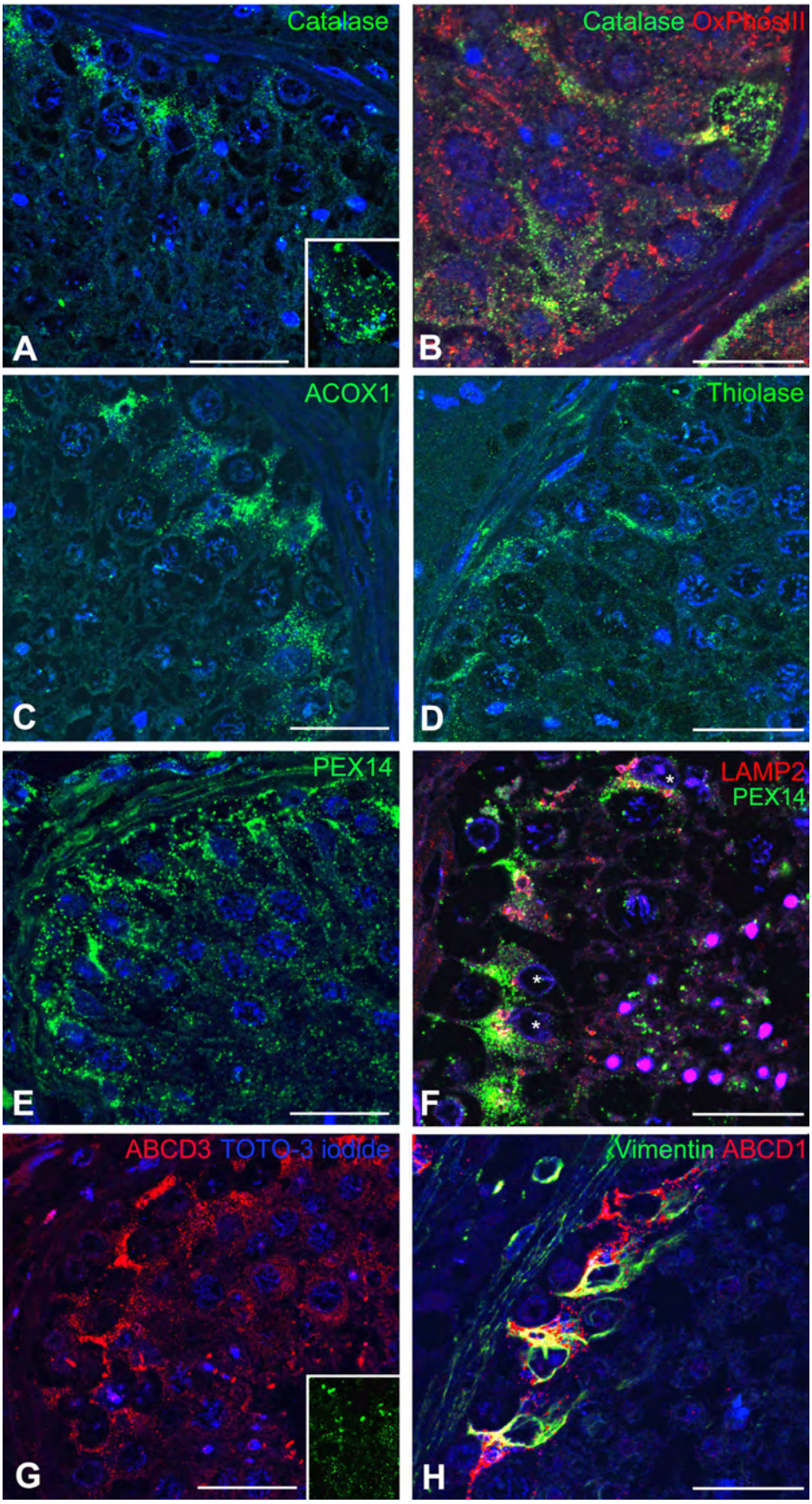

Figure 9: Immunofluorescence detection of organelle marker proteins in seminiferous tubules of human testis. All preparations are counterstained with TOTO-3 (blue) for labelling of nuclei. **(A)** Catalase (inset Leydig cells). **(B)** Double-IF for peroxisomal catalase (green) and mitochondrial complex III (red). **(C)** ACOX1: acyl-CoA oxidase 1,(β-oxidation pathway I). **(D)** Peroxisomal Thiolase A: peroxisome 3-ketoacyl-CoA thiolase. **(E)** Pex14p. **(F)** Double-IF for PEX14 (green) and LAMP2 (red). **(G)** ABCD3 (red) and PEX13 (inset, green). **(H)** Double- IF for vimentin (green, Sertoli cells) and ABCD1 (red). Bars represent 40 µm.

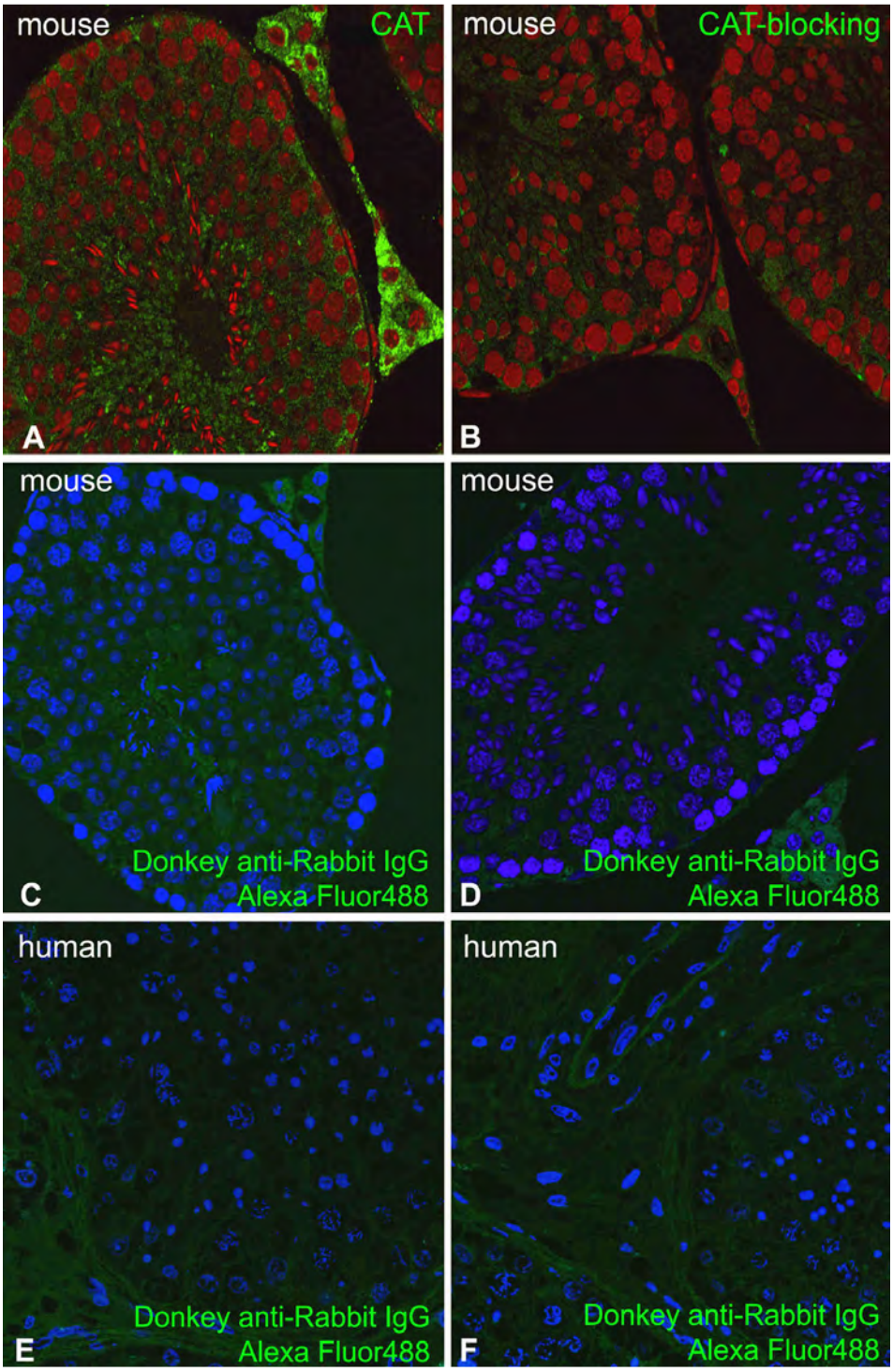

Figure 10: Catalase-competition experiment and other negative controls for immunofluorescence preparations of paraffin sections of mouse and human testis. (A) CAT-positive control with high antibody concentration (1:100). **(B)** Negative control with depletion of the anti-CAT antibody (1:100) with bovine CAT protein. Note that no reaction product is present despite the high primary antibody concentration in the competition experiment. **(C–F)** Negative controls without primary antibody, depicting the high quality of the secondary antibody-reaction in mouse **(C, D)** and human **(E, F)** seminiferous tubules of distinct stages.

Furthermore, they were transported from central regions in the spermatid cytoplasm to a basal location beneath the nuclei of the mature spermatids of step 16 (stage VIII, Fig. 11F). In addition, large peroxisomal aggregates were also found in residual bodies (Fig. 11G, arrows). All results obtained by fluorescence microscopy were corroborated by ultrastructural analysis. The specificities of all antibodies were high on the ultrastructural level in

immunocytochemical preparations as shown by selective staining of peroxisomes for CAT or PEX13 in various testicular somatic cell types (Fig. 12I, M, N). In addition, immunoreactivity of CAT in small, elongated peroxisomes in spermatogonia was shown (Fig. 12L). Furthermore, a specific labelling for GFP and PEX13 on membrane-bound structures resembling peroxisomes was found in all stages of spermato- and spermiogenesis (except for mature spermatozoa). Only rarely, single non-specific gold particles were found in appropriate negative controls for all antibodies (data not shown).

Peroxisomes in germ cells were often elongated, dump-bell shaped, and were similar or even smaller in diameter (50-100 nm) than segments of the endoplasmic reticulum. Similar to light microscopic results, their distribution and shape changed depending on the maturation of spermatids. In spermatid development up to step 13 (Fig. 12H, step 9) peroxisomes appeared as small individual structures. Individual peroxisomes in early stages of spermatid development were difficult to identify in post-embedding labelling experiments, since they are very small and were only rarely exposed on the surface of ultrathin sections in these cell types. To obtain a rough estimation about the probability for the presence of peroxisomes on the surface of these ultrathin preparations, we counted the peroxisome number in 100 round spermatids in a paraffin section stained for PEX14 using regular fluorescence microscopy (number of peroxisomes in 5 x 20 round spermatids of 5 distinct seminiferous tubules). In 100 spermatid profiles 1,874 fluorescent particles were present (range of 15 to 23 peroxisomes / spermatid profile). Thereafter, a thickness of 1.3 µm for this section was determined by a xzy-scan (vertical scan) with a CLSM (pinhole: airy 1, objective: 63 x, zoom: 8). By mathematical extrapolation this would implicate for a DAB-stained ultrathin section of 80 nm thickness a value of 0.92 to 1.42 peroxisomes/round spermatid profile and a minimum probability of 0.0115-0.0178 (= value for DAB sections divided by 80 nm section thickness) on the surface of post-embedding labelling preparations (= a single peroxisome on the section surface / 56-87 spermatids). These derived, nonempirical values help to explain the scarcity of peroxisomal profiles on the electron-microscopic images in comparison to the enumerated abundance in the paraffin-sectioned material.

In contrast to early spermatids, in later stages of spermiogenesis (step 15-16 spermatids) aggregation of peroxisomal profiles was noted. These clusters were positively labelled with gold particles in immunocytochemical preparations stained for detection of catalase, PEX13 or GFP (testis sections of transgenic animals) (Fig. 12E, F). Labelling was present on round or tubular profiles and also on double-membraned loop structures (Fig. 12G). Cytochemical detection of CAT activity on the ultrastructural level also revealed large clusters of CAT positive profiles in step 16 spermatids, including CAT-positive double-membraned loops (Fig. 12C, D).

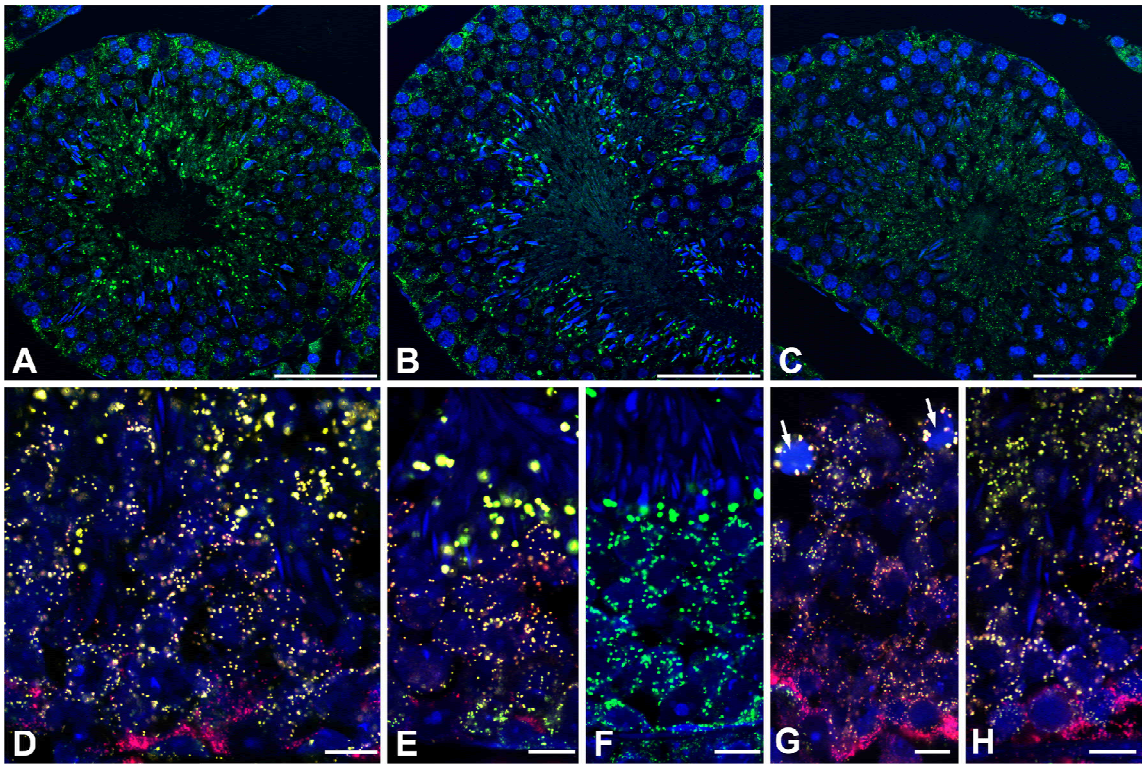

Figure 11: Localization of peroxisomal marker proteins in distinct stages of the seminiferous tubules of the mouse testis (A: stage II; B: stage VI-VII; C: stage XII). (A-C) Immunofluorescence staining for Pex14p (green) and nuclear counterstaining with TOTO-3 (blue) in paraffin sections. (D-H) GFP-fluorescence in cryosection of testes of GFP-PTS1 transgenic mice. Pex14p immunoreactivity is shown in red in D, E, G, H. Note that GFP and Pex14p colocalize in all germ cells indicating that these structures are peroxisomes. (G) Large peroxisomal structures in residual bodies (arrows). Nuclei in frozen sections (D-H) are also counterstained with TOTO-3 (blue). Bars represent: A-C: 50 µm; D-H: 10 µm.

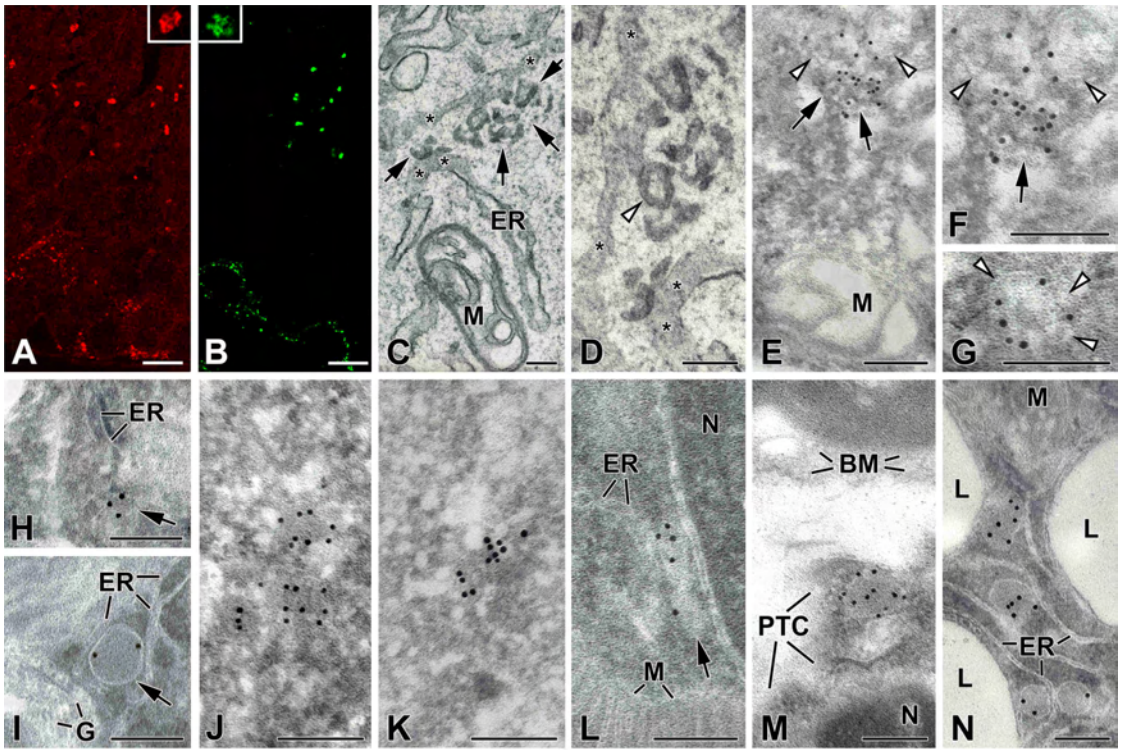

Figure 12: Localization of peroxisomal marker proteins in peroxisomes in germ cells and somatic cell types of the mouse testis of control (A-D, H, I, K-N) and GFP-transgenic mice (E-G, J). IF staining of paraffin sections for ABCD3 (A) and CAT (B). Insets in A and B are magnified views of large immunostained structures in late spermatids. (C, D). Electron micrographs of a late mouse spermatid (step 16) from a cytochemical preparation for catalase activity with DAB. D shows a higher magnification view of the cluster of DAB-stained

profiles from C. For better orientation, asterisks in C and D mark identical regions of the endoplasmic reticulum. (E-G). GFP immunoreactivity in a similar region of a GFP-PTS1 transgenic mouse. (C-G) Arrows mark clusters of peroxisomal profiles and arrowheads depict double-membraned loop structures. (H) Peroxisome (arrow) in a step 9 spermatid labelled for PEX13. (J, K). Peroxisomes in late spermatids labeled for GFP (step 16) (J) and CAT (step 15) (K). (I) PEX13 immunoreactivity of a Leydig cell peroxisome (arrow). (L-N) CAT staining of peroxisomes in a spermatogonium (*arrow* in L), a peritubular- (M) and a Leydig cell (N) depicting the high specificity of the CAT antibody and of the protocol used for post-embedding protein A-gold labelling. BM – basement membrane, ER – endoplasmic reticulum, G – Golgi apparatus, L – lipid droplets, M – mitochondria, N – nuclei , PTC – peritubular cell. Bars represent: A, B: 10 µm; C-N: 0.2 µm.

4.4. The heterogeneity of peroxisomal enzymes is preserved in primary cell cultures and cytospin preparations of isolated Leydig, peritubular myoid- and Sertoli cells

After isolation of primary Leydig-, peritubular myoid-, and Sertoli cells from 14-day-old (P14) mice and Leydig cells from adult mice, the purities of the cultures were determined by immunofluorescence stainings using antibodies against cell type-specific markers (Fig. 13). The Sertoli cells cultures were labelled with specific marker vimentin (Fig. 13A), α-smooth muscle actin (αSMA) was used for peritubular cells (Fig. 13C) and cytochrome P450scc for Leydig cells (Fig. 13E,G). More than 95% of Sertoli and peritubular cell cultures and more than 98% of juvenile and adult Leydig cell cultures were positive for cell type-specific markers. In addition, the specific testicular somatic cells in primary culture were immunolabelled with different antibodies against peroxisomal proteins. The results confirmed the presence of peroxisomes in all somatic cell types of the testis in culture and revealed similar individual differences as in tissue sections. The peroxisomal membrane transporter ABCD3 was strongly present in cultured Sertoli cells (Fig. 13B), whereas PEX13 was a better marker for peritubular cell cultures (Fig. 13D). Double immunostaining was used to distinguish between distinct subcellular organelle compartments. In juvenile Leydig cells, peroxisomes were positive for PEX14 and mitochondria for OxPhosIII (Fig. 13F). Peroxisomes in adult Leydig cells were stained best with an antibody against CAT (Fig. 13H). To confirm the morphological results obtained in situ and in isolated cell cultures by immunofluorescence, Western blot analysis was performed using distinct subcellular fractions obtained by differential centrifugation from homogenized cell preparations. The peroxins PEX13 and PEX14 were detected in adult Leydig cells and P14 Sertoli and peritubular myoid cells, whereas the protein levels of both peroxins were low in P14 Leydig cells (Fig. 14A). In accordance with the results obtained by immunofluorescence, ABCD1 was mainly present in Sertoli cells (Fig. 14B). In contrast, high levels of catalase were present in adult Leydig- and peritubular myoid cells, whereas the abundance of this enzyme was low in Sertoli cells (Fig. 14A). CAT was barely detectable under these conditions in P14 Leydig cells, however, a specific band of expected size could be observed after prolonged exposure times of films (Fig. 14B).

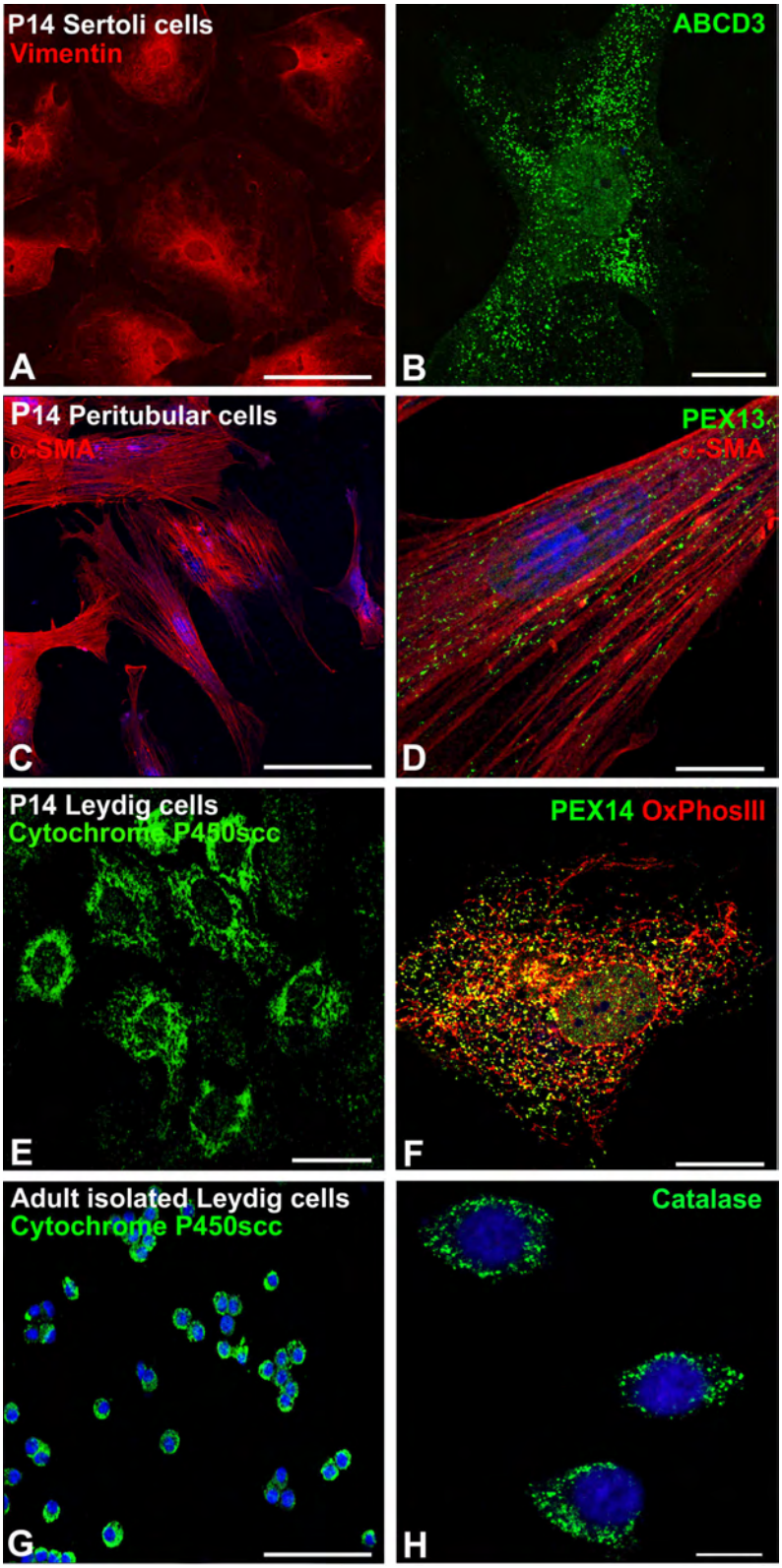

Figure 13: Primary cultures of distinct somatic cell types of the mouse testis. (A – F) Cell cultures isolated from P14-testis. **(A, C, E)**. Overviews of cell cultures labeled with cell-type specific markers, **(A)** vimentin for Sertoli cells, **(C)** α-smooth muscle actin (αSMA) for peritubular myoid cells, and **(E)** cytochrome P450scc for Leydig cells. **(B, D, F)** Higher magnification views of corresponding cells stained for different peroxisomal marker proteins, **(B)** ABCD3, **(D)** Pex13p, **(F)** PEX14 **(G)** Immunofluorescence for mitochondrial cytochrome P450scc of cytospin preparations of Leydig cells isolated from adult mouse testis. **(H)** CAT localization in the isolated adult Leydig cells. Bars represent in A, G,F,G 25µm in B, E, H 18µm and in D 21µm.

Using semi-quantitative RT-PCR, the steady-state levels for the mRNAs encoding peroxisomal proteins were determined in isolated cell cultures. For calculations of differences

in mRNA expression levels, the RT-PCR band intensities of peroxisome-related genes were normalized for the band intensity of the *28S rrna* of the same cDNA preparation (Fig. 15A). mRNAs for *Abcd1* and *Abcd3* (Fig. 15B) were present in high amounts in Sertoli and peritubular myoid cells (1.4-fold higher to the value of adult Leydig cells).

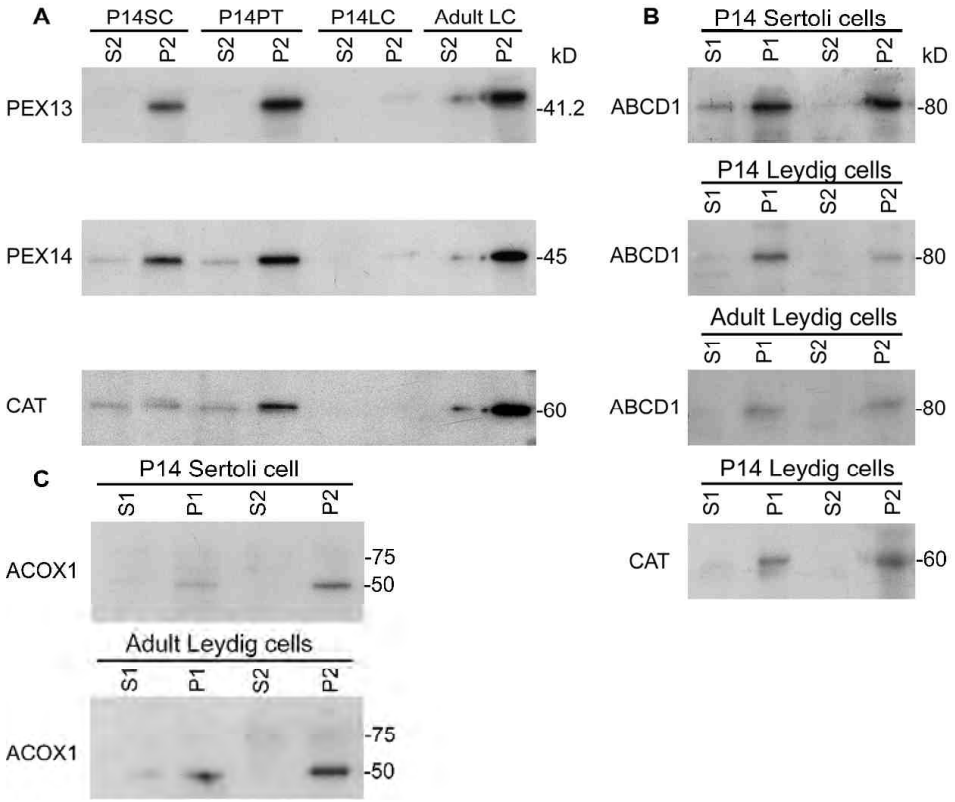

Figure 14: Western blot analysis of enriched organelle fractions isolated from somatic testicular cell types. Ten micrograms of proteins have been loaded in 12.5% SDS gels in each lane and the same blots **(A, B, C)** were reprobed several times with specific antibodies for the indicated peroxisomal marker proteins. PEX13: peroxin 13; PEX14: peroxin 14; ABCD1: adrenoleukodystrophy protein; CAT – catalase, ACOX1 – acyl-CoA oxidase 1.

In contrast, the expression of *Abcd2* mRNA was strongest in Leydig cells, whereas expression levels of *Abcd4* and the genes encoding the peroxins *Pex13* and *Pex14* were similar in all cell types (Fig. 15B,C). Catalase (*Cat*) mRNA levels were comparable in adult Leydig-, P14 Sertoli- and peritubular myoid cells. However, the expression level of *Cat* in P14 Leydig cells was only about 20% of that of adult Leydig cells (Fig. 15D).

Most mRNAs for peroxisomal β-oxidation enzymes (*Acox1*, *Ehhadh*, *Thiolase A* for the β-oxidation pathway I and *Hsd17β4*, *ScpX* for the β-oxidation pathway II) were expressed at comparable levels in distinct cell types (Fig. 15D,E). However, the mRNA levels for acyl-CoA oxidase 2 (*Acox2*), the rate-limiting enzyme for cholesterol side-chain cleavage, was elevated about 4- and 6-fold in P14 Leydig- and P14 Sertoli cells, respectively, compared to

adult Leydig cells, whereas *Acox2* expression in P14 peritubular myoid cells was decreased to 20% of that of adult Leydig cells (Fig. 15E). The mRNA for acyl-CoA oxidase 3 (*Acox3*), which is the rate-limiting enzyme for the β-oxidation of branched-chain fatty acids, was not altered. The expression of mRNAs of two enzymes involved in the biosynthesis of ether lipids, glyceronephosphate dihydroxyacetonephosphate acyltransferase (*Gnpat / Dhapat*) and of glyceronephosphate alkyl-dihydroxyacetone-phosphate synthase (*Agps / Dhaps*) was about 1.3-fold higher in P14- compared to adult Leydig cells (Fig. 15F).

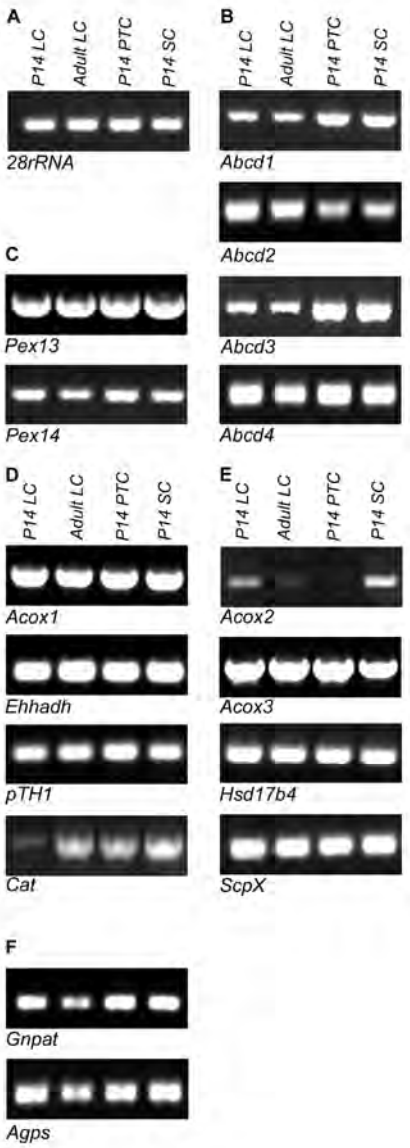

Figure 15: Semiquantitative RT-PCR analysis on cDNAs prepared from total RNA of distinct somatic cell types of the mouse testis. (A) *28S rrna* as internal control. **(B)** Peroxisomal ABC-transporters *Abcd1-4*. **(C)** Peroxisomal biogenesis genes *Pex13, Pex14*. **(D)** Enzymes of the β-oxidation pathway 1, *Acox1:* acyl-CoA oxidase I, *Ehhadh* multi-functional protein 1, *Thiolase A: peroxisome 3-ketoacyl-CoA thiolase; Cat: catalase.* **(E)** Enzymes of the β-oxidation pathway 2, *Acox2 and 3*: acyl-CoA oxidase 2 and 3, *Hsd17β4:* multifunctional protein 2 and *ScpX:* sterol carrier protein X. **(F)** Enzymes of ether lipid synthesis: *Gnpat* : glyceronephosphate O acyltransferase and *Agps*: glyceronephosphate alkyl-dihydroxyacetonephosphate synthase.

4.5. Knockout of peroxisomal function in Sertoli cells

To understand the specific roles of peroxisomes in Sertoli cells of the testis, a tissue specific *Pex13*KO mouse line has been generated by the *cre-loxP* technology (Sertoli cell specific *Pex13*KO – scs*Pex13*KO). The expected Mendelian breeding patterns, an apparently normal phenotype of the mice homozygous for the floxed *Pex13* gene, and apparently normal phenotype of mice containing the *Cre* gene driven by the *Amh* promoter, were all indications for normal gene expression in the presence of *loxP* sites or *Cre* recombinase. Heterozygous animals - scs*Pex13*HTZ, showing a deletion of the *exone 2* of one Pex13 allele, were generated by crossing homozygous animals carrying the *floxed exon 2* of the *Pex13* allele [275] with transgenic mice in which the *Cre* recombinase was driven under *Amh* promoter control, that is expressed specifically in Sertoli cells during development [276]. In a second mating scs*Pex13*KO pups were generated by back-crossing scs*Pex13*HTZ animals with homozygous *floxed Pex13* mice. The generated mice were genotyped by genomic PCR for the *Pex13* and *Cre* genes, and the DNA was prepared from tail biopsies, to reveal their gene composition for scs*Pex13*KO, scs*Pex13*HTZ and scs*Pex13*WT and the presence or absence of *Cre* gene. For the genotyping the PCR primers *Pex13loxP*-F1 (P1 in Fig. 17A) and *Pex13loxP*-R1 (P2 in Fig. 17A) were used, which produce a band at 490bp, representing the wild-type allele and a band of 540bp, which represents the *floxed Pex13* allele with two *loxP* sites flanking *exon 2* (Fig. 16A - C). New born pups with distinct genotypes (scs*Pex13*KO, scs*Pex13*HTZ, scs*Pex13*WT) did not present any phenotypic difference. The animals with one *floxed Pex13* allele in the non deleted state were phenotypically identical to WT animals, scs*Pex13*WT (*Pex13* $^{WT/loxp}$) (Fig. 16A and Fig. 17B). The animals with one wild type *Pex13* allele, one deleted *Pex13* allele and *Amh-cre* expressed were considered scs*Pex13*HTZ, (scs*Pex13* $^{WT/\Delta ex2}$*/Amh-cre*$^{+/-}$) (Fig. 16B and Fig. 17B). The scs*Pex13*KO animals were shown both deleted *exone 2* of *floxed Pex13* gene and *Amh-cre* expressed (scs*Pex13* $^{\Delta ex2/\Delta ex2}$ / *Amh-cre*$^{+/-}$) (Fig. 16B and Fig. 17B). PCR analyses of genomic testis DNA confirmed the homozygous disruption of the *Pex13* allele in this tissue, whereas other tissues analyzed such as liver or tail, never exhibited the band for identifying the *exon 2* disruption of *Pex13* gene (Fig. 17B). Male progeny underwent excision of one or both alleles of the *exon 2* of the *Pex13* gene in Sertoli cells because of the specific *Cre* expression driven by the *Amh* promoter in this type of cells (Fig. 17B). The disruption of the *Pex13* gene was demonstrated by PCR to confirm the *Cre*-mediated excision at *loxP* sites using primers immediately 5´ to the first *loxP* site in the front of *exon 2* (P3 in Fig. 17A) and 3´of the second *loxP* site after the *exon 2* (P4 in Fig. 17A). This reaction produces a 385bp product for the disrupted allele. The 385bp amplicon was seen also in the scs*Pex13*HTZ, however, with a lower intensity due to excision of only one *Pex13* allele (Fig. 17B).

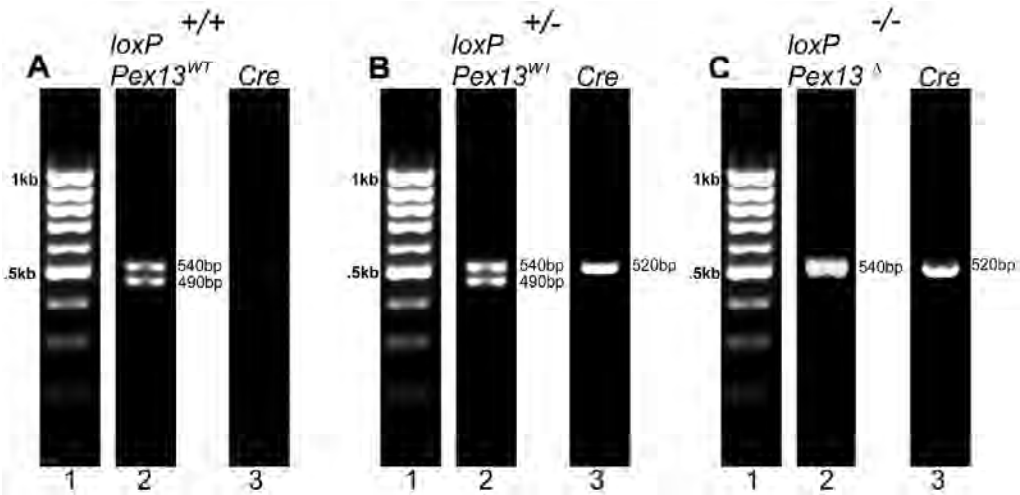

Figure 16: Confirmation of the correct genotypes by PCR with primers for *Pex13* flox/ WT allels and the Cre transgene using DNA, isolated from mouse tails of representative animals. PCR genotyping shows **(A, 2)** the WT bands for *Pex13* floxed at 540bp and *Pex13*WT at 490bp and **(A, 3)** no band for Cre. These animals were further named scs*Pex13*WT. **(B, 2)** Animals were named scs*Pex13*HTZ are exhibited the double bands for *Pex13* floxed at 540bp and *Pex13*WT at 490bp and in addition **(B, 3)** the *Cre* band at 520bp indicating heterozygosity. **(C, 2)** Animals were named scs*Pex13*KO, when they exhibited single band of *Pex13* floxed at 540bp indicating homozygosity and in addition, **(A-C, 1)** the Cre band at 520bp confirming the present of the *Cre* gene. 100-bp DNA ladder.

In order to confirm the excision of *Pex13* in the Sertoli cells, microdissected seminiferous tubules from 130day-old scs*Pex13*KO, scs*Pex13*HTZ and *Pex13*WT were used for DNA extraction. The same set of primers P1/P2, P3/P4 (Fig. 17A) was used. Due to the excision of *Pex13Δexon2* solely in Sertoli cells the 385bp amplicon of the *Pex13*Δ allele was highly increased in microdissected seminiferous tubules of scs*Pex13*KO compared to scs*Pex13*HTZ animals. In scs*Pex13*HTZ the 385bp amplicon of the *Pex13*Δ allele was present at lower intensity since the excision just took place on one allele (Fig. 18).

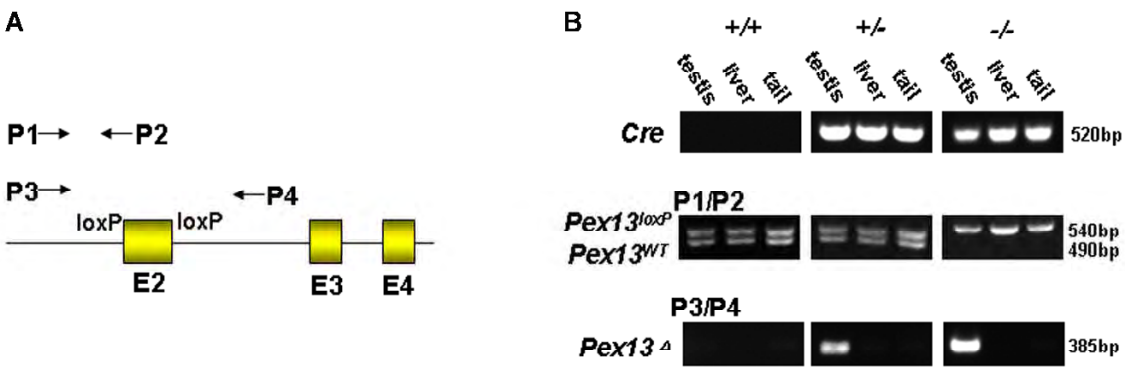

Figure 17: Targeted disruption of the *Pex13* gene. (A) Schematic representation of the floxed *Pex13* allele. The positions of *exons 2* to 4 (E2-E4) and the directions and positions of genotyping PCR primers P1 to P4 are indicated. **(B)** Genotyping by PCR screening of genomic DNA of different tissues (testis, liver, tail). The PCR confirming the presence of the *Cre* gene showed an amplicon of 520bp in the testis, liver and tail for scs*Pex13*HTZ (+/-) and scs*Pex13*KO (-/-), but no in scs*Pex13*WT (+/+). The P1/P2 primer pair generated an amplicon of 490 bp for the *Pex13*WT (+/+) and 540 bp for the floxed *Pex13* allele. The P3/P4 primer pair generated an amplicon of 385 bp for the *Pex13*Δ allele, following *Cre* mediated excision of the *floxed exon 2.*

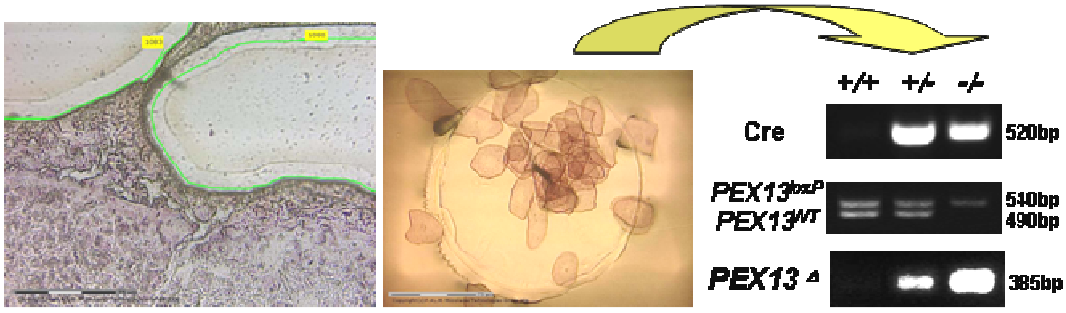

Figure 18. Confirmation of the *Cre*-mediated *exon 2* of *Pex13* excision via genotyping PCR of microdissected seminiferous tubules. Frozen sections (10µm) of OCT-embedded testis tissue from scs*Pex13*KO, scs*Pex13*HTZ and scs*Pex13*WT were shortly stained with H&E and cut out by P.A.L.M. laser-capture microdissection. 1.050 cells for each genotype were used for DNA extraction and subsequent PCR reactions. The PCR confirmed the presence of the *Cre* gene showing an amplicon of 520bp for scs*Pex13*HTZ (+/-) and scs*Pex13*KO (-/-), but no for *Pex13*WT (+/+) animals. The *floxed Pex13* allele (including the *loxP* sites) was represented by a 540 bp amplicon, the wild-type *Pex13* allele with 490 bp amplicon. *Cre*-mediated excision of *exon 2* of the *Pex13* gene was represented by a 385 bp amplicon, which was only present in scs*Pex13*HTZ and to under strong extent in scs*Pex13*KO animals.

4.6. Fertility of scs*Pex13*KO males

Male scs*Pex13*KO animals were tested for their fertility (90 and 130 day-old), by mating them with fertile wild type females up to 2 weeks. Mutant male mice of P90 were fertile as indicated by the pregnancies and delivery of pups by the female animals. However, the number of the offspring was of 3 or 4 pups per litter. The number of the pups was approximately reduced by half, since mating wild type female mice produced an average size of eight pups per litter. Wild type females that were mated with the P130 scs*Pex13*KO male produced no offsprings, indicating that these males were completely sterile.

4.7. Macroscopic differences between scs*Pex13*WT, scs*Pex13*HTZ and scs*Pex13*KO mice

Even though new born pups showed no clear phenotypic differences between the distinct phenotypes, a clear distinction could be made at P130 post partum between wild type and mutant animals. The body weight of 130 day-old scs*Pex13*KO mice was significantly reduced compared to the scs*Pex13*WT and scs*Pex13*HTZ animals (Fig. 19A). Male 130 day-old scs*Pex13*HTZ and scs*Pex13*KO mice showed no gross abnormalities of external genitalia. As noted during dissection, also, the testes of the scs*Pex13*KO mice were located in the correct position when compared to WT and HTZ mice. Epididymis, deferent ductus, seminal vesicles and prostate glands appeared to be normal. In contrast, the testes of scs*Pex13*KO mice were atrophic, with their size and total weight being drastically reduced compared with testes of scs*Pex13*HTZ and WT littermates (Fig. 19B,C). Statistical analysis confirmed that the total testis weight was significantly reduced ($P<0.001$) to 1/3 of the wild type volume in 130 day-old scs*Pex*13KO compared to scs*Pex*13HTZ and scs*Pex13*WT controls.

4.8. Phenotypic differences of the testis and epididymis between scs*Pex13*WT, scs*Pex13*HTZ and scs*Pex13*KO mice at the microscopic level

P130 male mice of the scs*Pex13*WT and scs*Pex13*HTZ genotype exhibited quantitative and qualitative normal spermatogenesis, with regular formation of the seminiferous epithelium, containing all generations of germ cells up to elongated spermatids (Fig. 20A,B,D,E). The histological examination of scs*Pex13*KO mice revealed in 99% of seminiferous tubules a "Sertoli cell only" syndrome (SCO), with the presence of big intratubular vacuoles in the testis and azoospermia in the epididymis. In interstitial spaces Leydig cells were massively proliferated and macrophages showed signs of activation (Fig. 20C,F).

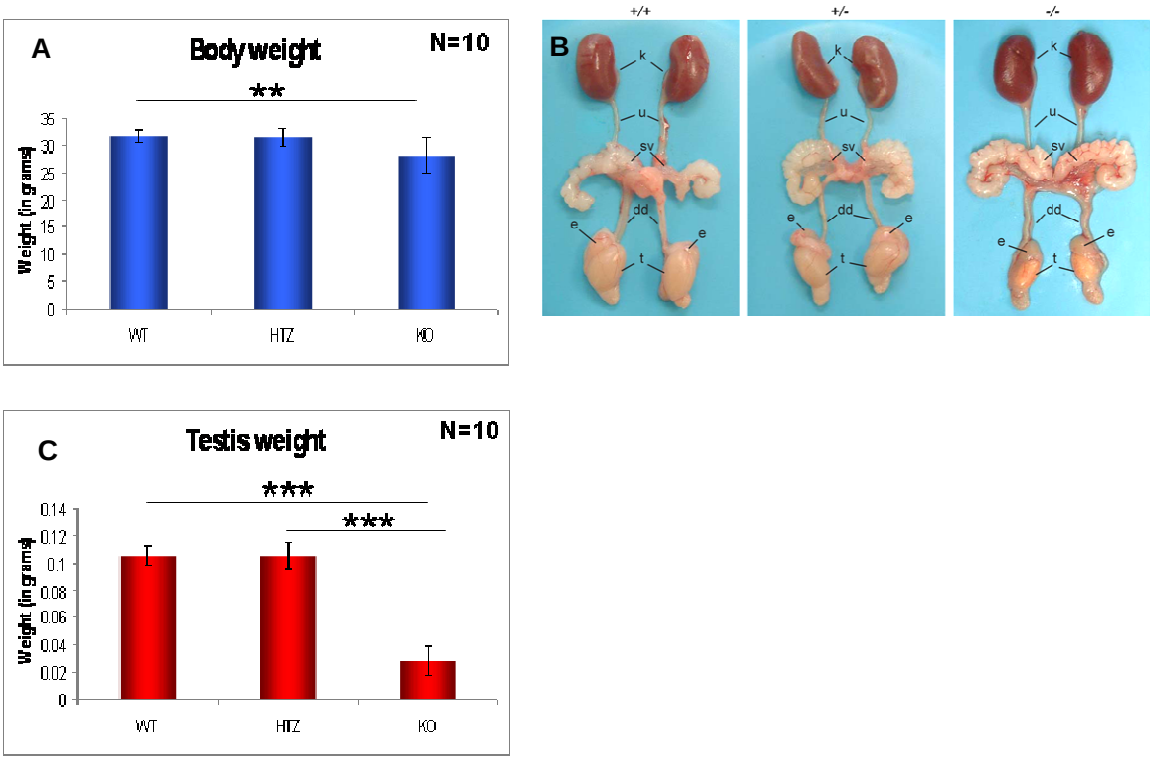

Figure 19: Macroscopic differences between the genotypes of the scs*Pex13* mouse line (A) Comparison of the body weight of 130 day-old scs*Pex13* mice. The body weight of P130 scs*Pex13*KO mice was significantly reduced (P< 0.01). **(B)** Dissection of the urogenital tract (urinary bladder removed) of scs*Pex13*WT (+/+), scs*Pex13*HTZ (+/-) and scs*Pex13*KO (-/-) mice at P130. **(C)** Note that, the size of the testes in scs*Pex13*KO animals was significantly reduced (*P< 0.001*) compared to the one of scs*Pex13*HTZ and scs*Pex13*WT mice. k: kidney; u: ureter; SV: seminal vesicle, dd: deferens ductus, e: epididymis, t: testis. (* p ≤ 0.05, ** p ≤ 0.01, **** p ≤ 0.001).

4.9. Analysis of semithin sections revealed pathological alterations in the testis of 130 day-old scs*Pex13*KO animals

Semithin cross-sections of the testis of P130 scs*Pex13*KO mice revealed a 50% decrease in the average diameter of the seminiferous tubules and a disorganization of the multilayered epithelium. Regular germ cells were completely absent and giant phagosomes dominated in

Sertoli cells, exhibiting phagocytosed cells in different apoptotic stages. In addition, abundant large lipid inclusions were identified within the Sertoli cells cytoplasm of scs*Pex13*KO, which were not present in scs*Pex13*HTZ and scs*Pex13*WT mice. These globular lipid inclusions were sometimes surrounded by numerous smaller osmiophilic lipid droplets. The latter small lipid droplets were normal constituents of Sertoli cells also in the scs*Pex13*HTZ and WT testis (Fig. 21B,C).

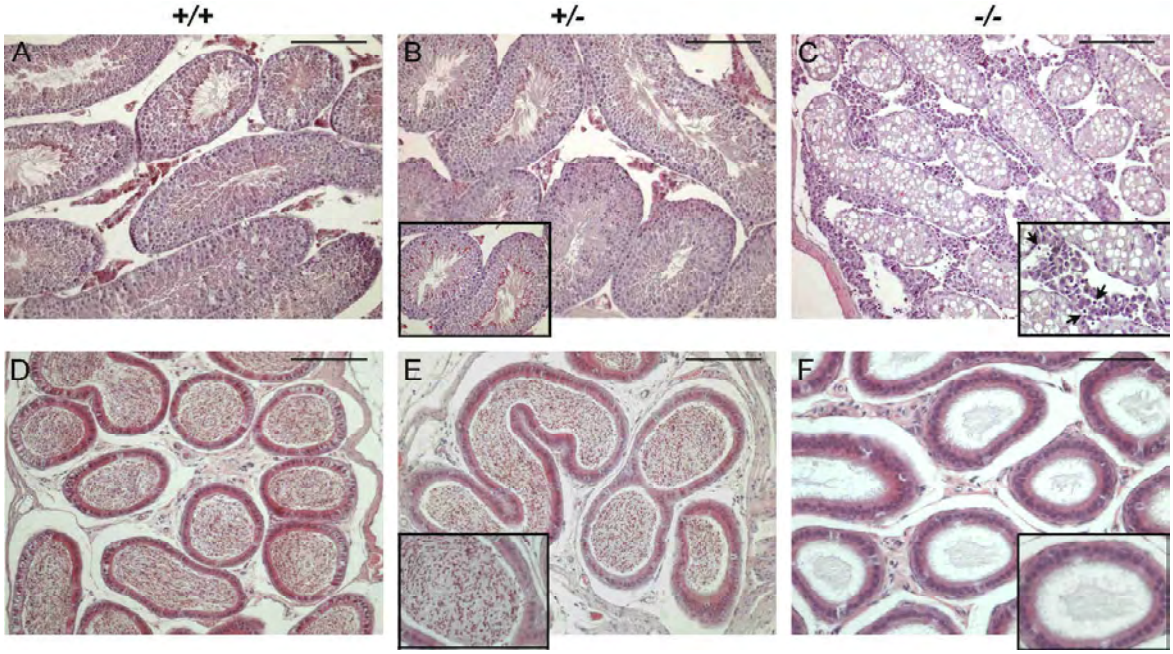

Figure 20: H&E staining of the testis and the Cauda epididymidis obtained from 130 day-old *Pex13*WT (+/+), scs*Pex13*HTZ (+/-) and scs*Pex13*KO (-/-) animals. (A) Regular complete spermatogenesis was observed in scs*Pex13*WT, **(B)** scs*Pex13*HTZ animals. In contrast, smaller tubules with "Sertoli cell only" syndrome and many vacuoles were present in **(C)** scs*Pex13*KO in conjunction with proliferation of Leydig cells and the presence of many immune cells, indicated by *arrowheads* in the insert picture. Corresponding sections of the caudal epididymis revealed that spermatozoa could only be detected in **(D)** scs*Pex13*WT, as well as **(E)** scs*Pex13*HTZ, but not in **(F)** scs*Pex13*KO animals. Bars represent in A-F 100 µm.

In controls and scs*Pex13*HTZ mice (Fig. 21G,H), the lamina propria was composed of a single continuous layer of flat elongated peritubular cells, separated by a rather thin basal lamina from both seminiferous tubules and endothelium of lymphatic capillaries. A slight thickening of the lamina propria was observed surrounding the SCO seminiferous tubules of scs*Pex13*KO animals (Fig. 21A-D). Proliferation of peritubular cells correlated with an increase in the thickness of the basement membranes of seminiferous tubules (Fig. 21D). In contrast to controls (Fig. 21F), the intertubular space in the scs*Pex13*KO mice was occupied by proliferating Leydig cell clusters of all developmental stages (Fig. 21A,D,E). The cytoplasm of the Leydig cells in scs*Pex13*KO animals showed an increased number of lipid droplets (Fig. 21A,D,E) in contrast to the Leydig cells of the scs*Pex13*HTZ animals (Fig. 21F).

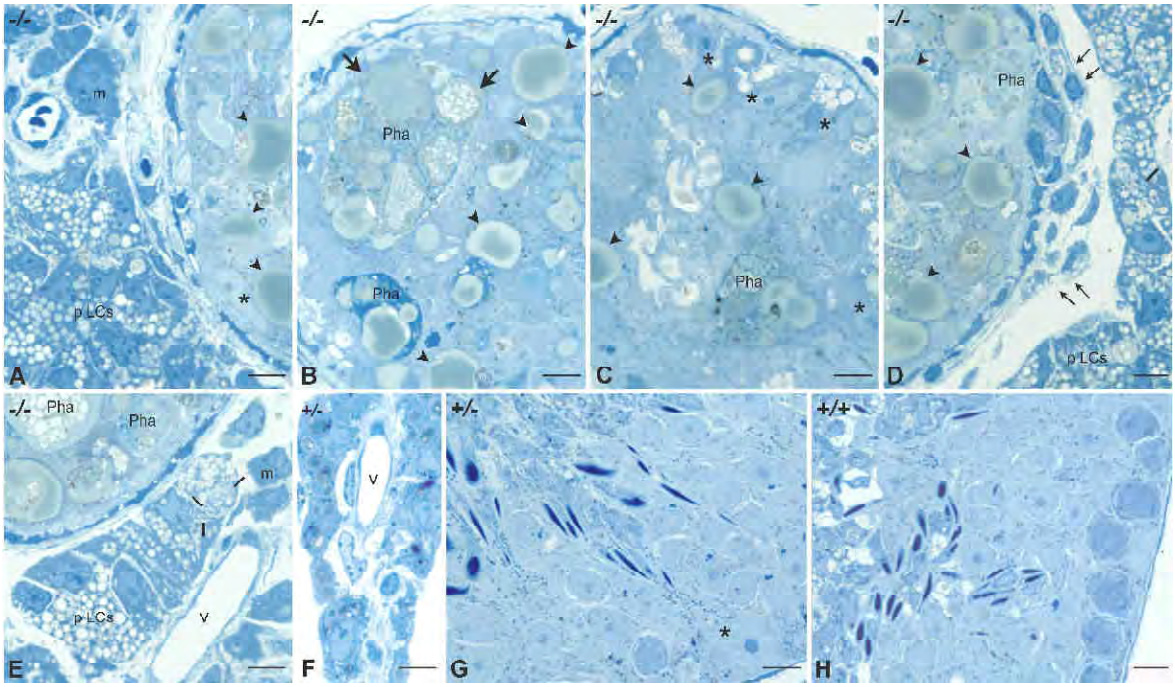

Figure 21: Semithin sections of scs*Pex13*KO and scs*Pex13*HTZ testes from 130 day-old mice stained with Methylene blue. (A – E) The disorganization of the seminiferous epithelium in scs*Pex13*KO animals was accompanied by the presence of big phagosomes (pha) with apoptotic cells (indicated by *big arrows)* and inclusions of large lipid droplets (marked by *arrowheads)*. The predominant cell types of the seminiferous epithelium were vacuolated Sertoli cells (marked by *asterisks)*. **(A – D)** Proliferated peritubular cells leading to thickening of basement membranes (indicated by *small arrows)*. **(E)** In addition, the interstitial space was filled with proliferated Leydig cells (p LCs), containing increased number of lipd droples and structures resembling VLCFA crystals (marked by *lines)*. Around proliferating Leydig cells activated macrophags (*m*) were present. **(F)** Normal Leydig cells from scs*Pex13*HTZ. **(G,H)** Seminiferous tubules of scs*Pex13*HTZ mice contained an intact multilayered seminiferous epithelium, composed of Sertoli cells and all spermatogenic cell type, comparable to WT animals. Bars represent in A-H 50 µm.

4.10. Electron microscopy confirms the severe pathological alteration in seminiferous tubules and reveals ultrastructural changes also in Leydig cells

Detailed ultrastructural analysis of ultrathin sections of the testis of P90 and P130 scs*PEX13*KO mice by transmission electron microscopy revealed severe pathological alterations of different cell types in the germinal epithelium and of Leydig cells.

Ultrastructural alterations were observed in the seminiferouse epithelium already in 90 day-old scs*Pex13*KO animals. Whereas, peroxisomes were clearly identifiable by their catalase staining in Sertoli cells of scs*Pex13*HTZ (Fig. 22A-E), these organelles were absent in any Sertoli cells of scs*Pex13*KO animals (Fig. 22F-L), confirming the *Pex13* gene KO in these cells. In contrast, peroxisomes were present in neighbouring peritubular cells and strongly stained for CAT of their matrix (Fig. 22F insert). Sertoli cells of control scs*Pex13*HTZ animals revealed peroxiosmes often closely associated with cisternae of the sER and mitochondria (Fig. 22A,B,C,E) or were located on the surface of small lipid droplets (Fig. 22D). In P90

scs*Pex13*KO testis the ultrastructure of epithelium of many seminiferous tubules revealed a disorganization, exhibiting vacuoles of different sizes in the Sertoli cells, most probably resulting form the loss of germ cells (Fig. 22F), whereas in other tubules large confluent empty spaces were already observed in the cytoplasm of Sertoli cells (Fig. 22J). Most germ cells still present in the seminiferous tubules showed a relatively normal appearance. In contrast, several alteration in the Sertoli cell cytoplasm were observed such as proliferation of pleomorphic mitochondria (Fig. 22F,G) as well as increased number of lipid droplets, lysosomes and phagosomes (Fig. 22G,H). In addition, lamellae of sER were closely associated with the large lipid droplets as well as with mitochondria (Fig. 22I).

The morphology of the seminiferous epithelium and Sertoli cells of 130 day-old scs*Pex13*KO was dramatically altered (Fig. 22K). The seminiferous epithelium was strongly disorganized, showing massive lipid accumulation in the Sertoli cell cytoplasm (Fig. 22K). Only residual parts of apoptotic germ cells were present in large phagosomes (Fig. 22L). No viable germ cells could anymore be identified.

Leydig cells of P90 scs*Pex13*HTZ mice, taken as the control group, showed the typical morphological characteristics of this cell type, such as areas of the cytoplasm rich in anastomosing tubules of the sER, large mitochondria and lipid droplets surrounded by peroxisomes. DAB positive peroxisomes were proliferated in the cytoplasm of Leydig cells at P130 scs*Pex13*KO mice (Fig. 23J,K). The tubular cristae in mitochondria were homogenously distributed in the organelles (Fig. 23A,B). Whorled sER was only seldom detected in Leydig cells of scs*Pex13*HTZ (Fig. 23A,D). In the P90 scs*Pex13*KO animals, Leydig cells contained an increased number of lipid droplets as well as giant whorl-like sER, some of which engulfed lipid droplets (Fig. 23E,F) and contained many peroxisomes between their lamellae (Fig. 23G,H). In Leydig cells of P130 scs*Pex13*KO most mitochondria were larger and longer and exhibited proliferated and dense tubular cristae. (Fig. 23I,J,K). Some mitochondria showed a rearrangement of their cristae to the external surface and a rarefaction of cristae in internal matrix areas, leading to the empty spaces (Fig. 23F *asterisk*). Large groups of lysosomes with DAB-positive electron dense deposits were frequently observed in Leydig cells of P130 scs*Pex13*KO animals (Fig. 23J). In these cells lipid crystals were present on the surface of lipid droplets (Fig. 23K). In the interstitial space besides the Leydig cells many macrophages were seen that exhibited an activated appearance with extending filopodia on their surface and large phagosomes in their cytoplasm (Fig. 23I).

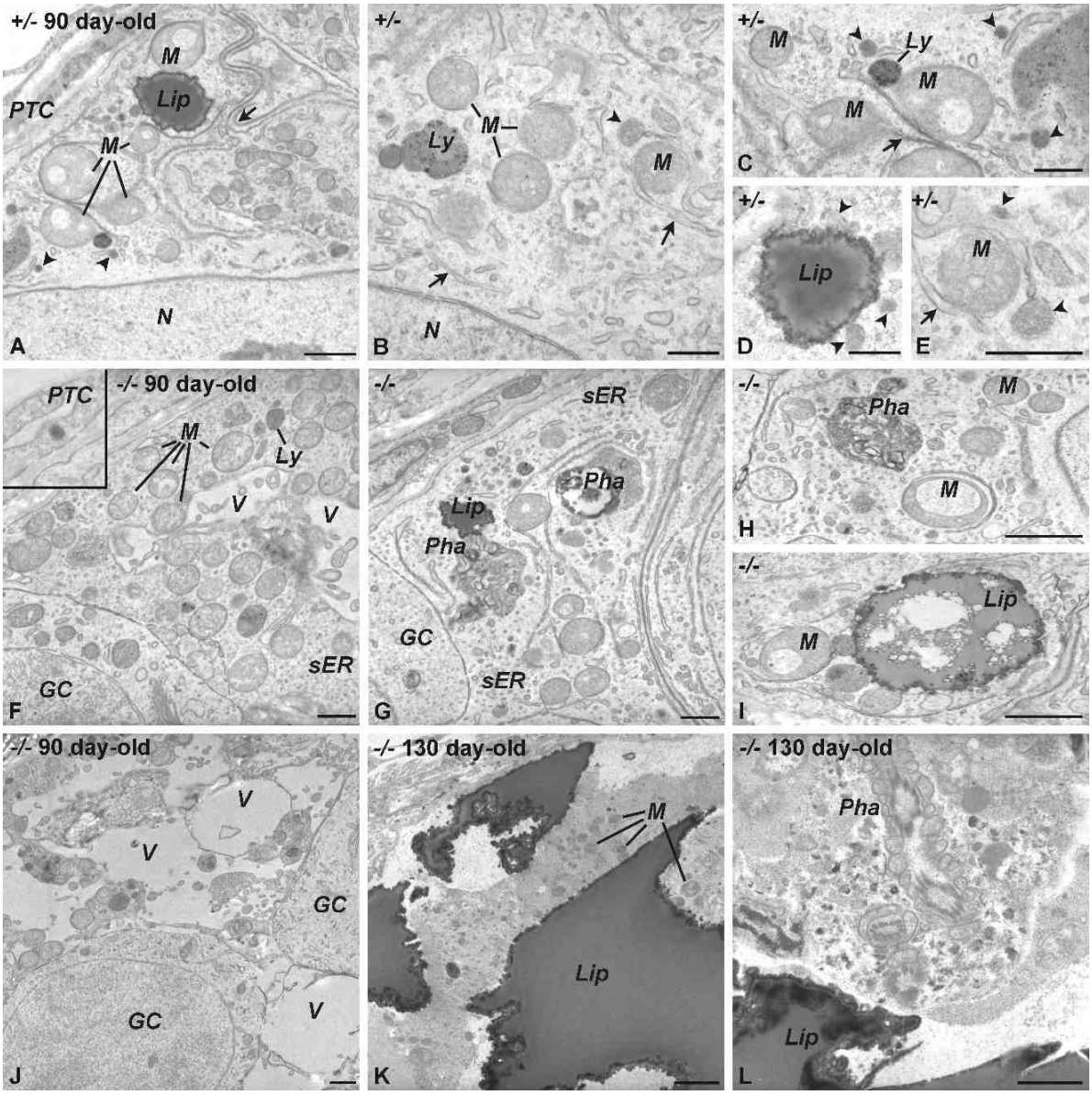

Figure 22: Electron microscopy of Sertoli cells from P90 and P130 scs*Pex13*KO (-/-) and scs*Pex13*HTZ (+/ -) animals. Sections were incubated for 3h in DAB medium for the detection of CAT activity in peroxisomes. **(A,B)** Regular ultrastructure of basal part of Sertoli cell from P90 HTZ animals, depicting peroxisomes (*arrow heads*), lipid droplets (*Lip*), lysosomes (*Ly*) and mitochondria (*M*) and peritubular cell (*PTC)*. **(C)** High magnification of HTZ Sertoli cell with peroxisomes (*arrow heads*), sER (*arrows*), lysosomes (*Ly*) and mitochondria (*M*). **(D)** Peroxisomes (*head arrows*) of Sertoli cells are in close contact to lipid droplets (*Lip*). **(E)** High magnification showing the close association of peroxisomes (*arrow heads*) and sER (*arrows*) in a HTZ Sertoli cell. (**F,G**) Sertoli cell of P90 scs*Pex13*KO animal with small vacuoles (*V*), proliferated mitochondria (*M*), cytoplasmic areas with sER and phagosomes (*Pha*) and neighboring lipid droplet (*Lip*). GC: germ cell. The insert in picture **(F)** depicts a DAB positive peroxisome in PTC. **(H)** Higher magnification of a P90 Sertoli cell of scs*Pex13*KO showing strong pleomorphism of the mitochondria population (*M*) and a big phagosome (Pha). **(I)** Sertoli cell of a P90 scs*Pex13*KO animal exhibiting a big lipid droplet (*Lip*) with mitochondria (*M*) on its surface. **(J)** Low magnification of a seminiferous tubule of a 90 day-old scs*Pex13*KO animals depicting several vacuoles (*V*) in a Sertoli cell. Germ cell (*GC*) lost their contacts with the altered Sertoli cells. **(K)** Seminiferous tubule in a P130 scs*Pex*13 testis revealing massive lipid accumulation (*Lip*) in a Sertoli cell. **(L)** KO Sertoli cell with a large phagosome, containing the residual structures of apoptotic spermatids still identifiable by the mitochondrial sheath around the axial filament. Bars represent in A, B: 1 µm, C-E: 0.5 µm, F-I: 0.5 µm, H-I: 1 µm, J-L: 1 µm.

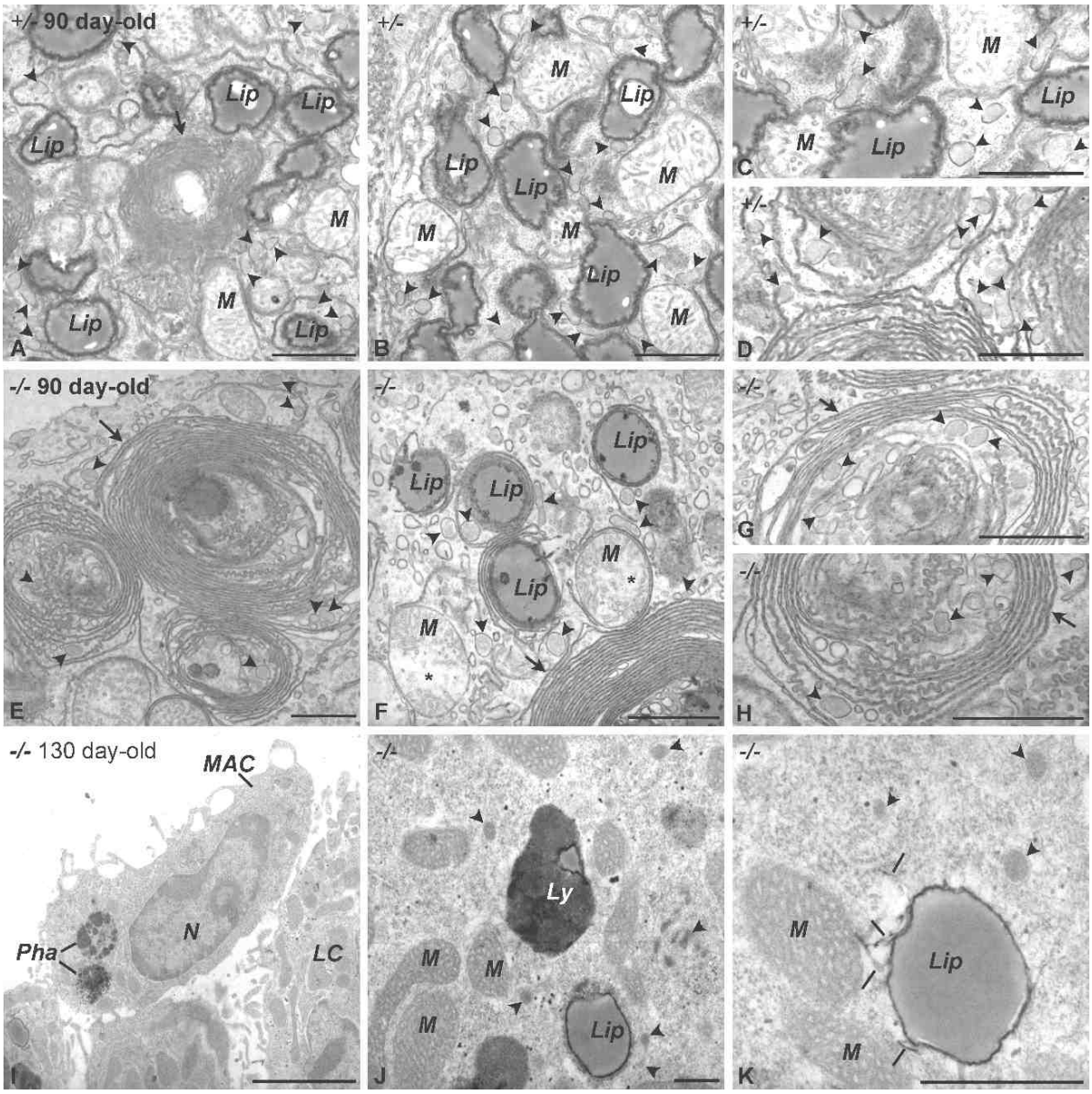

Figure 23: Electron microscopy of Leydig cells from P90 and P130 scs*Pex13*KO (-/-) and scs*Pex13*HTZ (+/ -) animals. Sections were incubated for 3h in DAB medium for the detection of catalase in peroxisomes. Leydig cell (*LC*) ultrastructure of a 90 day-old HTZ animal **(A,B,C,D)** showing the typical features of steroid producing cells with ER (*arrow*), lipid droplets (*Lip*), mitochondria with tubular cristae (*M*) and peroxisomes (*arrow heads*). **(E, F)** Leydig cells of 90 day-old scs*Pex13*KO animals with giant whorl-like ER (*arrow*) engultiong the lipid droplets (*Lip*). **(G, H)** Leydig cells of 90 day scs*Pex13*KO with peroxisomes (*arrow heads*) integrated into whorl lamellar of the ER (*arrow*). **(I)** Activated macrophage (*MAC*) with two big phagosomes (*Pha*). **(J, K)** Leydig cells of a 130 day-old scs*Pex13*KO showing mitochondria densely packed with tubular cristae in their matrix (*M*), many peroxisomes (*arrow heads*), lysosomes (*Ly*), as well as small lipid crystals (*small lines*) on lipid droplets (*Lip*). Bars represent: A-J: 1µ, H: 0.5 µm.

4.11. Specification of the accumulation of peroxisome - metabolized lipids in the testis of scs*Pex13*KO animals

To decipher the nature of the lipid accumulation in the testes from scs*Pex13*KO mice, all distinct mouse genotypes were analyzed in parallel with different techniques for lipid identification. The presence of large lipid inclusions, as suggested by light- and electron microscopy, within the seminiferous epithelium of scs*Pex13*KO animals was confirmed by Oil Red O using frozen sections from P130 scs*Pex13*WT, scs*Pex13*HTZ and scs*Pex13*KO mice.

This type of staining was indicating mainly of neutral lipids such as triglycerides and cholesteryl esters. Small deposits of lipid material could already be clearly identified within the cytoplasm of late spermatids at stage VII and residual bodies at stage VIII of the spermatogenesis cycle of the seminiferouse epithelium in scs*Pex13*WT and scs*Pex13*HTZ animals. During stage IX – XI of the seminiferous epithelial cycle, the lipid droplets were found in the basal regions of the Sertoil cells, in these animals. These lipid droplets in Sertoli cells most probably resulted from heavy lipid load due to phagocytosis of cytoplasmic bodies with lipids droplets and storage of the lipids in the cytoplasm of these cells (Fig. 24A, B). Lipid droplets were also present in abundant number in cytoplasm of interstitial Leydig cells, which are involved in steroid synthesis, explaining the Oil Red O staining of scs*Pex13*WT and scs*Pex13*HTZ animals (Fig. 24A, B).

In scs*Pex13*KO mice the seminiferous tubules the regular spermatogenic cells were absented (SOS) and Sertoli cells were completely filled with lipids stained positively with Oil Red O (Fig. 24C). Interstitial spaces of these animals contained the proliferating Leydig cells which were much weaker stained for Oil Red O, indicating that Leydig cells were still functional. In contrast to scsPex13WT and HTZ animals, the lipid droplets in Leydig cells of scs*Pex13*KO animals were smaller and less intensively stained with Oil Red O.

4.12. Impaired peroxisomal α – and β –oxidation induced accumulation of fatty acids primarily in Sertoli cells of scs*Pex13*KO animals

In agreement with the histological findings of lipid distribution in the scs*Pex*13KO animals, severe accumulation of “peroxisome-specific” lipid substrates was found in these animals. Peroxisomes are involved in the breakdown of fatty acids, like VLCFA (C22:0, C24:0, C26:0) and different branched-chain fatty acids such as pristanic acid (2-methyl branched chain C26:0 fatty acid) and phytanic acid (3-methyl precursor of pristanic acid). They are involved in the biosynthesis of plasmalogen, as well. These typical “peroxisomal” substrates were analyzed in the neutral lipid fraction from scs*Pex13*KO, HTZ and WT testes of 130 day-old mice.

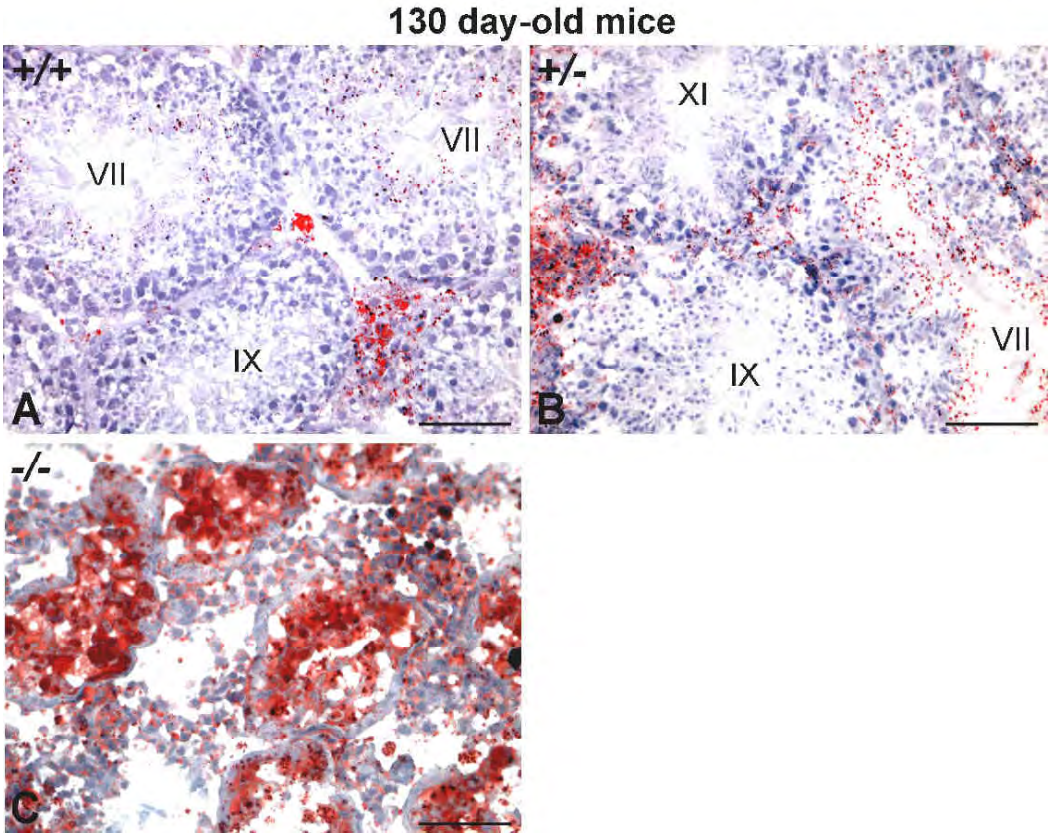

Figure 24: Lipid accumulation in P130 scs*Pex13*KO mice. Frozen sections of testis from **(A)** scs*Pex13*WT (+/+), **(B)** scs*Pex13*HTZ (+/-), **(C)** scs*Pex13*KO (-/-) mice were stained with Oil Red O. **(A, B)** In control testis the neutral lipids in the seminiferous epithelium accumulated according to the stage of spermatogenesis. Leydig cells were also Oil Red O positive. **(C)** The testis from scs*Pex13*KO exhibited massive accumulation of lipids within the seminiferous tubules. Proliferating Leydig cells were less intensively stained. Bars represent in A-C 50 µm.

The concentration of VLCFA were significantly increased for hexacosanoic acid (C26:0) ($p \leq 0.001$) and for lignoceric acid (C24:0) ($p \leq 0.01$) in scs*Pex13*KO animals, showing a testis-specific accumulation of VLCFA. Since fatty acids are degraded by peroxisomal β-oxidation the results suggest the disruption of this pathway due to the peroxisomal biogenesis defect in Sertoli cells of mutant animals (Fig. 25A). In addition, the pristanic and phytanic acid levels were significantly increased in scs*Pex13*KO mouse testis ($p \leq 0.01$) (Fig. 25B), suggesting that the Sertoli cell specific peroxisomal biogenesis defect also led to an α and β-oxidation defect of branched chain fatty acids. Furthermore, plasmalogen levels in the testis were detected as the dimethylacetal (DMA) derivative of C16:0 and C18:0 fatty acids. Unexpectedly, the ratio of C18:0-DMA / C18:0 was significantly increased ($p \leq 0.05$) in the testis of scs*Pex13*KO mice (Fig. 25C), suggesting an overall compensation of plasmalogen synthesis in other cell types of the testis or a delivery via lipoproteins of the blood.

A

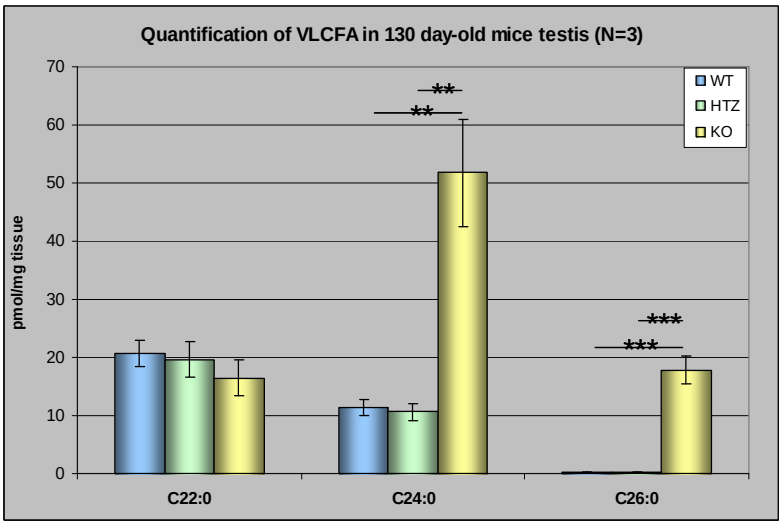

B

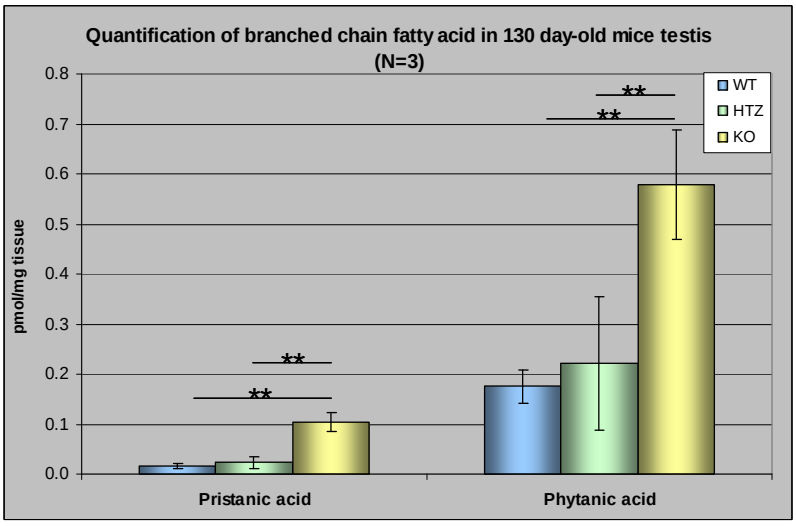

C

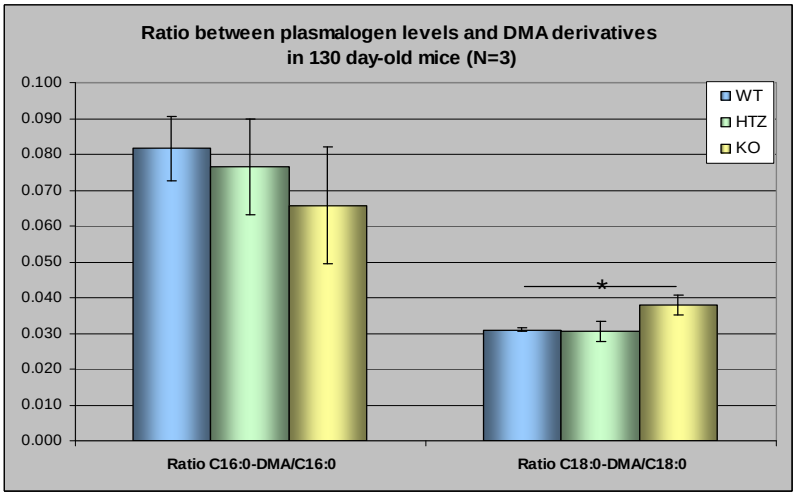

Figure 25: Levels of VLCFA, branched chain fatty acids, plasmalogens in neutral lipids. Measurements in testes of 130 day-old scs*Pex13*WT/HTZ/KO mice were performed by gas chromatography (*n=3* for all genotypes). **(A)** The levels of C24:0 / C26:0 VLCFA were significantly increased in scs*Pex13*KO. **(B)** The levels of branched chain fatty acids (pristanic and phytanic acid) were also significantly increased in scs*Pex13*KO. **(C)** Plasmalogens and their dimethylacetal derivatives (DMA) were measured and the ratio of C18:0-DMA / C18:0 was slightly, but significantly increased in the testis of scs*Pex13*KO. (* $p \leq 0.05$, ** $p \leq 0.01$, *** $p \leq 0.001$) (N=3)

4.13. Sertoli cells, spermatogenesis and the testicular integrity are progressively affected during postnatal development of scs*Pex13*KO animals

To evaluate and follow the pathological alterations in the testis, a comparative analysis of tissues sections from 15, 30, 60, 90 and 130 day-old mice of all genotypes was performed. The IF analyses were studied for each genotype of the scs*Pex13* mouse line, but for space reasons only the results of scs*Pex13*HTZ and scs*Pex13*KO are depicted. IF analyses were used in order to compare the localization, distribution and alterations of peroxisomal and testis-specific marker proteins. All incubations of testis sections from distinct genotypes for the localization of a specific antigen were done in parallel and all pictures were taken with the same CLSM settings to achieve comparable and standardized results.

4.14. Normal feature of prepubertal spermatogenesis in scs*Pex13*KO

Spermatogenesis is initiated only shortly after birth. In consequence, during the prepubertal period at 15 day-old, most seminiferous tubules contain only Sertoli cells, spermatogonia type A and B and primary spermatocytes. Some tubules also contain early spermatids, but later spermatids are still absent at this age [277]. The peroxisomal biogenesis proteins of the docking complex PEX13 and PEX14 were detected in all testicular cell types of P15 scs*Pex13*HTZ animals. Corresponding to the results of the adult animals, PEX13 was most abundant in germ cells, whereas the staining for this protein was weaker in all somatic cells (Fig. 26A). PEX14 was most abundant in the basal compartment of the germinal epithelium, exhibiting a weaker staining of prepubertal Leydig cells (Fig. 23C). In comparison to the results obtained for adult animals, the testis of P15 scs*Pex13*KO animals presented a relatively “normal” appearing architecture. However, most of the seminiferous tubules were significantly smaller in diameter. The signal intensity for PEX13 was reduced in spermatogonia and primary spermatocytes from 15 day-old scs*Pex13*KO mice. PEX13 was not detectable in Sertoli cells and only weakly expressed in peritubular cells (Fig. 26B). In scs*Pex13*KO animals PEX14 was barely detectable in the basal compartment of the germinal epithelium including Sertoli cells, although the staining for this marker was increased in the germ cells, especially in primary spermatocytes (Fig. 26D). The peroxisomal ABCD3 transporter was highly abundant in the cytoplasm of Sertoli cells from scs*Pex13*HTZ mice, while barely detectable in Leydig cells (Fig. 26E). In contrast, only few positive spots labeling for ABCD3 were noted in the cytoplasm of Sertoli cells from 15 day-old scs*Pex13*KO animals (Fig. 26F). Interestingly, the expression of ABCD3 was increased in “normal” appearing Leydig cells in these animals. The mitochondrial proteins, complex III of the respiratory chain (OxPhosIII) and superoxide dismutase 2 (SOD2) were used to evaluate pathologic mitochondrial alterations induced by the absence of peroxisomes in Sertoli cells. The mitochondrial complex III was detected in somatic cells as well as in spermatogonia and

in primary spermatocytes in all genotypes (Fig, 26E,F). The enzyme SOD2, that efficiently catalyzes the dismutation of superoxide anions to H_2O_2, was found in a punctuate pattern in somatic cells and was present an abundance in germ cells (Fig. 26G). However, in P15 scs*Pex13*KO mice, SOD2 was increased in Sertoli cells (Fig. 26H).

4.15. Vacuolization of the cytoplasm of Sertoli cells in juvenile scs*Pex13*KO

At the onset of the juvenile period, the first wave of spermatogenesis occures and the first appearance of spermatozoa is observed at ~ 35 days of age [278, 279]. In 30 day-old mice the seminiferous epithelium showed elongating spermatids (step 11-13) in scsPex13HTZ as well as in scsPex13KO mice (Fig. 27A,B,D,E,G,H,K). This result demonstrates that the first wave of spermatogenesis is not affected in the scsPex13KO. However, at this time of development for the first time an area within the cross section of testis was observed presenting morphological modifications in the seminiferous epithelium. However, these alterations were just found in one of the three mutant testes examinated (Fig. 27C,F,L). Interestingly, pathological altered seminiferouse tubules were surrounded by hyperplasic Leydig cells (Fig. 27C,F,L). The cytoplasm of Sertoli cell from 30 day-old scsPex13KO mice was lacked for immunoreactvity for PEX13, confirming the complete absence of this protein due to Cre-mediated gene excision of exon 2 of the Pex13 gene (Fig. 27B). In contrast, the intensity and distribution of the PEX13 IF in the germ cells of seminiferous tubules of scs*Pex13*KO mice (Fig. 27B) was comparable with that of scs*Pex13*HTZ animals (Fig. 27A). In addition, the germ cells of scs*Pex13*KO were immunopositive for PEX14 while the cytoplasm of Sertoli cells was negative for this marker (Fig. 27E), which is distinct from the PEX14 pattern in scs*Pex13*HTZ sections (Fig. 27D). Indeed, also ABCD3 staining revealed only very few peroxisome membrane ghosts in these mutant Sertoli cells (Fig. 27H,I). ABCD3 – positive peroxisomal membrane ghost structures surrounded big vacuoles that were not present in scs*Pex13*HTZ animals. The vacuoles most probably are big accumulation of lipids in the Sertoli cells cytoplasm, appearing as gaps or vacuoles due to the dehydratation procedure for paraffin embedding. In contrast to scs*Pex13*HTZ animals, a strong ABCD3 immunoreaction was also found in Leydig cells (Fig. 27H,I). This finding suggested that already Sertoli cells in 30 day-old scs*Pex13*KO animals presented metabolic problems and lipid accumulation due to the lack of peroxisomes. In addition, the immunoreactivity for mitochondrial SOD2 was increased in Sertoli cells of scs*Pex13*KO mice compared with HTZ animals. In contrast, germ cells of scs*Pex13*KO contained less SOD2 protein. At this age the OxPhosIII staining in “normal appearing” seminiferous tubules of both phenotypes was comparable (Fig. 27D,E), however, in pathological altered areas a weaker staining in seminiferous tubules as well as in adjacent proliferated Leydig cells was noted (Fig. 27F).

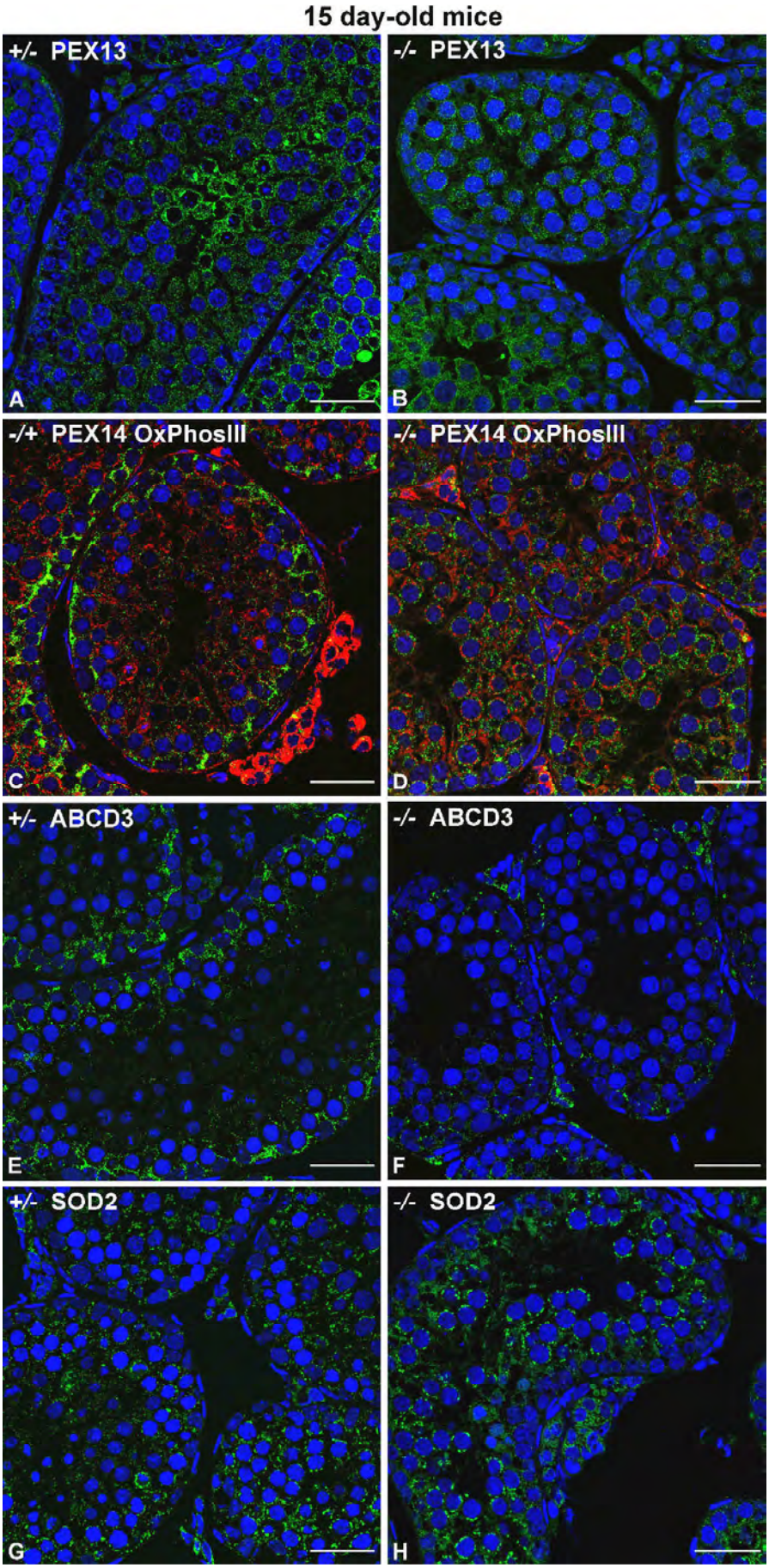

Figure 26: Immunofluorescence detection of peroxisomal and mitochondrial proteins in the testis of 15 day-old scs*Pex13*HTZ (+/-) and scs*Pex13*KO (-/-) animals. Testes were fixed with 4% PFA, paraffin embedded and 2µm sections were cut. **(A-F)** Peroxisomal proteins. **(A)** PEX13 in a control testis section. **(B)** The seminiferous tubules of scs*Pex13*KO animals were smaller in diameter and the PEX13 staining was weaker.

(C,D) Double staining for PEX14 / OxPhosIII (peroxisomes/ mitochondria). **(D)** In scs*Pex13*KO animals only a weak staining for PEX14 was noted in the cytoplasm of Sertoli cells. **(E)** Whereas the ABCD3 staining was clear visible in the basal part of seminiferous tubules of scs*Pex13*HTZ animals. **(F)** The ABCD3 staining was reduced in some area in scs*Pex13*KO animals. In contrast, in adjacent Leydig cells it was increased. **(G)** The section of scs*Pex13*HTZ stained for mitochondrial protein SOD2 being presented in all germ cells. **(H)** The staining of SOD2 n the germ cells was increased in scsPex13KO animals. In addition, Sertoli cells were weakly positive for SOD2. Nuclei were counterstained with TOTO-3 iodide (blue). Bars represent in A-H 100 µm. Representative pictures obtained from 3 experiments.

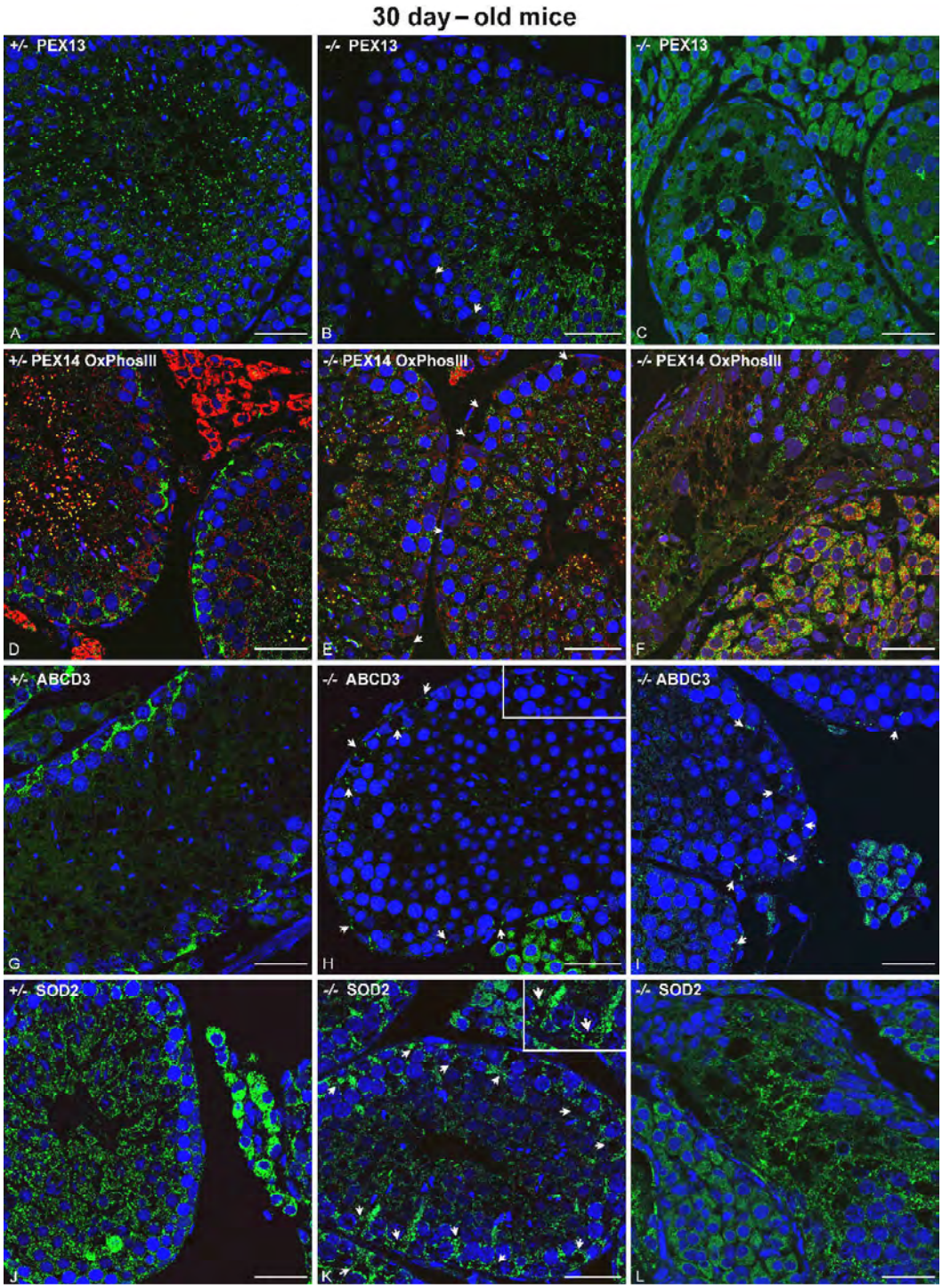

Figure 27: Immunofluorescence analysis of peroxisomal and mitochondrial proteins in paraffin section of the testis from 30 day old mouse. Testes were fixed with 4% PFA, paraffin embedded, 2 µm sections were cut and stained with specifically antibodies. **(A)** PEX13 distribution (green) in control testis section. **(B)** The seminiferous tubules of scs*Pex13*KO revealed a normal diameter. However, vacuoles (*arrowhead*) were present

in some of the Sertoli cells. PEX13 staining distribution was similar as in the control section. **(C)** An area of the mutant testis showing four seminiferous tubules with large empty spaces and vacuoles in Sertoli cells. The pathological altered tubules are surrounded by proliferated Leydig cells. **(D-F)** Double staining for PEX14 (green) / OxPhosIII (red) (peroxisomes / mitochondria). **(D)** Sections of scs*Pex13*HTZ animals depicting PEX14 immunoreactivity. **(E)** scs*Pex13*KO sections showed a weak PEX14 staining in the cytoplasm of Sertoli cells. **(F)** The disturbed region exhibited a weak staining for both markers compared to other regions of the same section. **(G)** ABCD3 staining in scs*Pex13*HTZ testis. **(H-I)** In basal part of the seminiferous epithelium of scs*Pex13*KO animals ABCD3 staining (green) was reduced to few dots engulfing large vacuoles in Sertoli cells. In contrast Leydig cells were strongly stained for ABCD3. **(J)** scs*Pex*13HTZ testis section stained for the mitochondrial protein SOD2 (green) which was present in all germ cells, Sertoli and Leydig cells. **(H)** SOD2 showed a strong increase in Sertoli cells and the staining of germ cells as well as of Leydig cells was reduced. **(L)** SOD2 staining was prominent in strongly affected tubules. Nuclei were counterstained with TOTO-3 iodide (blue). Bars represent in 100 µm. Representative pictures obtained from 3 experiments.

4.16. Adult 60 day-old scs*Pex13*KO mice exhibit hyperplasia of interstitial cells

Under normal conditions spermatogenic differentiation occurs in a highly organized and synchronized manner in 60 day-old adult mice. Seminiferous tubules of P60 mice show complete spermatogenesis with mitotic expansion of the spermatogonia, meiotic divisions of spermatocytes and spermiogenesis of the spermatids to form spermatozoa. This process occurs periodically along the tubules, known as the spermatogenic wave [274]. Also in P60 testis of scs*Pex13* KO animals in most seminiferous tubules there were no visible differences concerning the spematogenetic process between the two genotypes studied. In the cytoplasm of Sertoli cells, however, lipid vacuoles with increased size compared to the ones from pubertal animals were found (Fig. 28B). A major histological modification was the overall hyperplasia of the interstitial Leydig cells in sections of the testis from 60 day-old scs*Pex13*KO animals (Fig. 28B,D,H). Interestingly, some of the proliferated Leydig cells exhibited an increased staining for mitochondrial SOD2, while the seminiferous tubules showed a similar staining pattern as in the pubertal testis of scs*Pex13*KO animals (Fig. 28H). Immunofluorescence preparations of paraffin sections from scs*Pex13*KO showed a remarkable decreased of PEX13 staining in the seminiferous epithelium, in the cytoplasm of Sertoli cells as well as in spermatogonia and spermatocytes, respectively (Fig. 28B). The cytoplasm of Sertoli cells was only positively stained for mitochondrial OxPhosIII, whereas peroxisomal PEX14 was not detectable in double-immunofluorescence preparations in Sertoli cells of scs*Pex13*KO animals (Fig. 28D). In all tubules a reduced amount of ABCD3 was detected, revealing an unusual pattern since few small immuno-positive dots were located around the lipid vacuoles within the cytoplasm of Sertoli cells. The highest level of ABCD3 expression was observed in Leydig cells in the mutant testis (Fig. 28F).

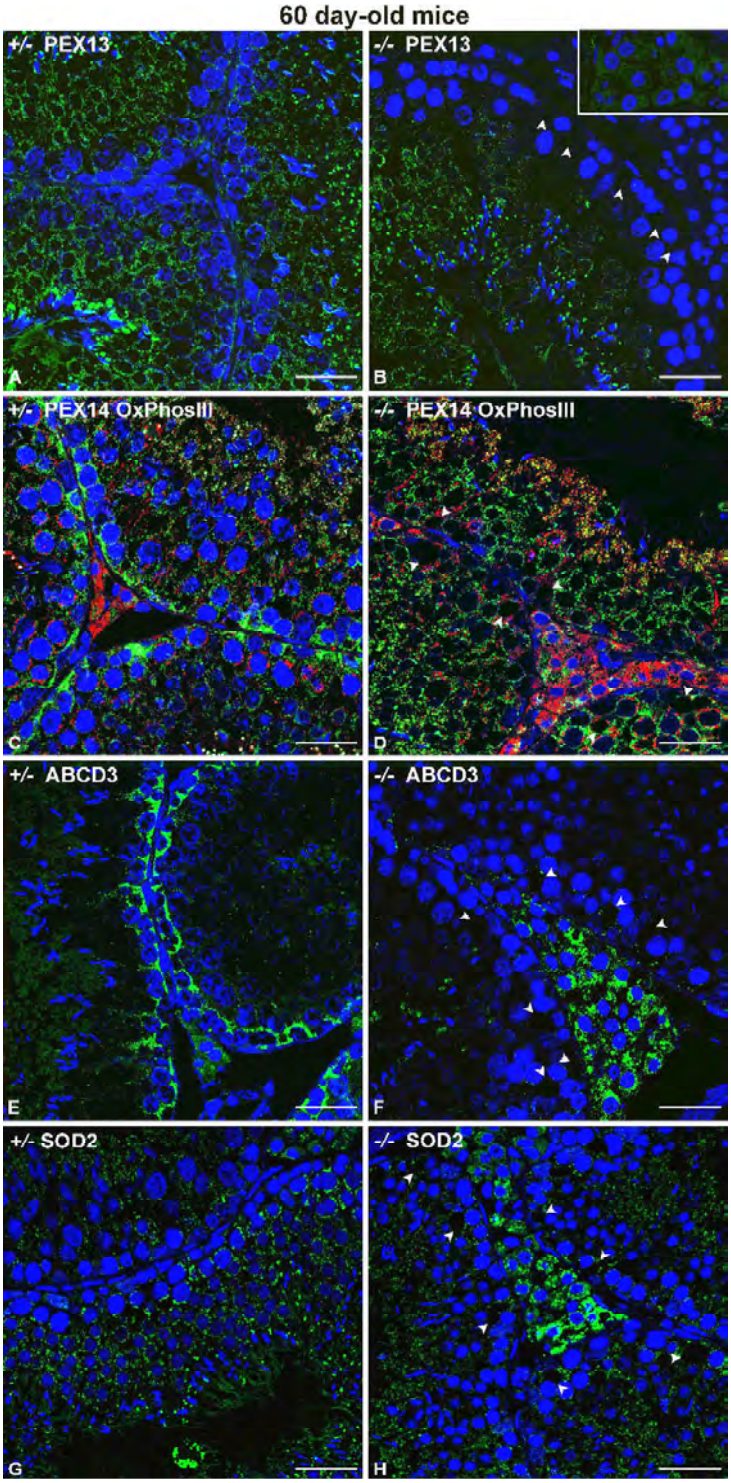

Figure 28: **Immumofluorescence analyses of peroxisomal and mitochondrial proteins in paraffin sections of the testis from 60 day old mouse.** Testes were fixed with 4% PFA, paraffin embedded, 2µm sections were cut and stained with specifically antibodies. **(A)** PEX13 (green) in a testis section of scs*Pex13*HTZ animals. **(B)** The Sertoli cells of scs*Pex13*KO animals revealed large vacuoles (*arrow head*). PEX13 staining was absent in Sertoli cells and also reduced in spermatogonia and spermatocytes of the seminiferous epithelium. Leydig cells were proliferated. **(C,D)** Double staining for PEX14 (green) / OxPhosIII.(red) (peroxisomes / mitochondria) **(C)** scs*Pex13*HTZ section. **(D)** scs*Pex13*KO sections showed only a weak staining for PEX14 in Sertoli cells. **(E)** ABCD3 staining in scs*Pex13*HTZ testis. **(F)** Whereas, ABCD3 staining (green) was strong reduced (minimized) in Sertoli cells of scs*Pex13*KO testis sections, whereas this protein was strongly up-regulated in proliferated Leydic cells. **(G)** scs*Pex13*HTZ testis section showing mitochondrial SOD2 staining (green) in all germ cells, Sertoli and Leydig cells. **(H)** In the testis of scs*Pex13*KO animals the SOD2 expression was extremely induced in Sertoli cells, meanwhile the germ cells exhibited lower SOD2 contrary to germ cells of HTZ sections. Some of the proliferated Leydig cells also revealed an increased expression of the SOD2 protein. Nuclei were counterstained

with TOTO-3 iodide (blue). Bars represent in A-H: 100 µm. Representative pictures of obtained from 3 experiments.

4.17. 90 day-old scs*Pex13*KO mice display hypospermatogenesis

Testis sections of 90 day-old mice were examined by immunofluorescence analyses to evaluate the further progress of the pathological alterations in the testis of scs*Pex13*KO animals. Careful histological examination revealed a mixture of normal appearing seminiferous tubules and others with clear pathological modification in scs*Pex13*KO mice. The diameter of the pathologically modified seminiferous tubules was smaller than the one of normal tubules from the same sample. The finding of only a few mature spermatids in some of the tubules points to a condition of hypospermatogenesis in 90 day-old scs*Pex13*KO mice. In addition, there was a strong variability of different cell layers within the epithelium of the same seminiferous tubule, revealing areas with the complete set of germ cells up to spermatozoa (functioning spermatogenesis), adjacent to areas within the tubules lined only by Sertoli cells, indicating germ cell loss (Fig. 29B, E,F).

Other tubules showed an almost complete loss of germ cells or a “Sertoli cell only” syndrome (Fig. 29H). In the majority of the Sertoli cells huge lipid-vacuoles surrounded by intermediate filaments were observed (as identified by vimentin staining, marker for Sertoli cells) (Fig. 29B,C,E,F,H,I). Since the heterogeneous appearance of the seminiferous epithelium was associated with a completed spermatogenesis process, the degeneration of the seminiferous tubules seemed to be a progressive process in 90 day-old scs*Pex13*KO mice (Fig. 29B,C,E,F,H,I). In intertubular spaces, Leydig cell aggregates were visible in a similar manner as in sections from 60 day-old scs*Pex13*KO mice (Fig. 28, 29).

Staining for PEX13 and PEX14 proteins in P90 scs*Pex13*KO animals showed a similar distribution pattern and intensity in the germ cells, whereas the Sertoli cell cytoplasm was completely immunonegative for PEX13 (Fig. 29B,C,E,F). Peroxisomal PEX14 could be detected with a cytoplasmic distribution in Sertoli cells (Fig. 29E,F right tubule). Furthermore, the peroxisomal lipid transporter ABCD3 could be hardly detected by imunofluorescence in the Sertoli cell cytoplasm in P90 scs*Pex13*KO animals. In contrast, proliferating Leydig cell were intensely stained for ABCD3 (Fig. 29H,I).

To provide further insight into the peroxisomal biogenesis defect and disruption of matrix protein import, the localization of different peroxisomal matrix enzymes, such as CAT and ACOX1, was investigated by immunofluorescence analysis on paraffin sections. In P90 scs*Pex13*KO testis CAT was highly abundant in proliferating Leydig cells as well as in peritubular cells (Fig. 30B,C). In contrast to HTZ control section, CAT was increased in intensity and also visible in a punctuate pattern in primary spermatocytes of scs*Pex13*KO animals. In contrast, staining pattern was dramatically altered in Sertoli cells, exhibiting an

intracytoplasmic distribution. However, this enzyme revealed a visible distribution, in a punctuate pattern, in primary spermatocytes (Fig. 30B,C).

The distribution for ACOX1 was changed as well in 90 day-old mutant testis, exhibiting a strong staining in the intraluminal compartment that was absent from the periphery of the seminiferous tubules. Leydig cells exhibited a strong signal for ACOX1 (Fig. 30E,F). In addition, SOD2, an antioxidant protein was strongly increased in the Sertoli cells, as shown by colocalization of SOD2 / VIM (Fig. 27H,I). Interestingly, SOD2 displayed a weak staining in the peripheral region of altered tubules and was also less abundant in the luminal compartment of relatively normal appearing seminiferous tubules of the scs*Pex13*KO testis, compared to scs*Pex13*HTZ testis (Fig. 27H). Many of hyperplasia Leydig cells SOD2 was detected in high level by IF analysis, while some of the Leydig cells were found to be almost completely negative for this protein (Fig. 30F).

4.18. *Pex13* gene deletion leads to “Sertoli cell only” syndrome in the testis of 130 day-old mice

Progressive accumulation of lipids and a compete loss of germ cell upset a “Sertoli cell only” syndrome (SCO) were observed in most seminiferous tubules in 130 day-old scs*Pex13*KO mice (Fig. 31). The lipid vacuoles were much larger than the nucleus, and were surrounded by stabilizing vimentin intermediate filaments.

Disruption of normal adhesion complexes between Sertoli cells and germ cells over time and germ cells death (as shown by TUNEL staining later) most probably contributed to the loss of spermatogenesis and male infertility. Markedly reduced tubule diameters, no germ cells and Sertoli cells filling the lumen of the seminiferous tubules were observed by a double-immunofluorescence staining for PEX13 and VIM (Fig. 31B). The seminiferous tubules were surrounded by two layers of peritubular cells, whose nuclei appeared closely adjacent to each other (Fig. 31B,D,F,H). Leydig cells were strongly proliferated and were dominant in the testis of scs*Pex13*KO mice, since at the same time as the tubule volume was markedly reduced (Fig. 31F,H). Leydig cells seemed to be metabolically disturbed, since an intense immunoreactivity for ABCD3 was observed within the interstitial cells of scs*Pex13*KO testis (Fig. 31H). In Sertoli cells, ABCD3 could be identified in remaining peroxisomal membrane ghosts, located around huge lipid vacuoles. The staining intensity of ABCD3 in 130 day-old mutant mice, was similar to that observed in 90 day-old scs*Pex13*KO animals (Fig. 30B,H,I and Fig. 31H). In contrast, the expression patterns of PEX13 and PEX14 toward signal intensity were different in Sertoli cell cytoplasm. PEX13 was completely absent verifying the knockout of the corresponding gene in Sertoli cells.

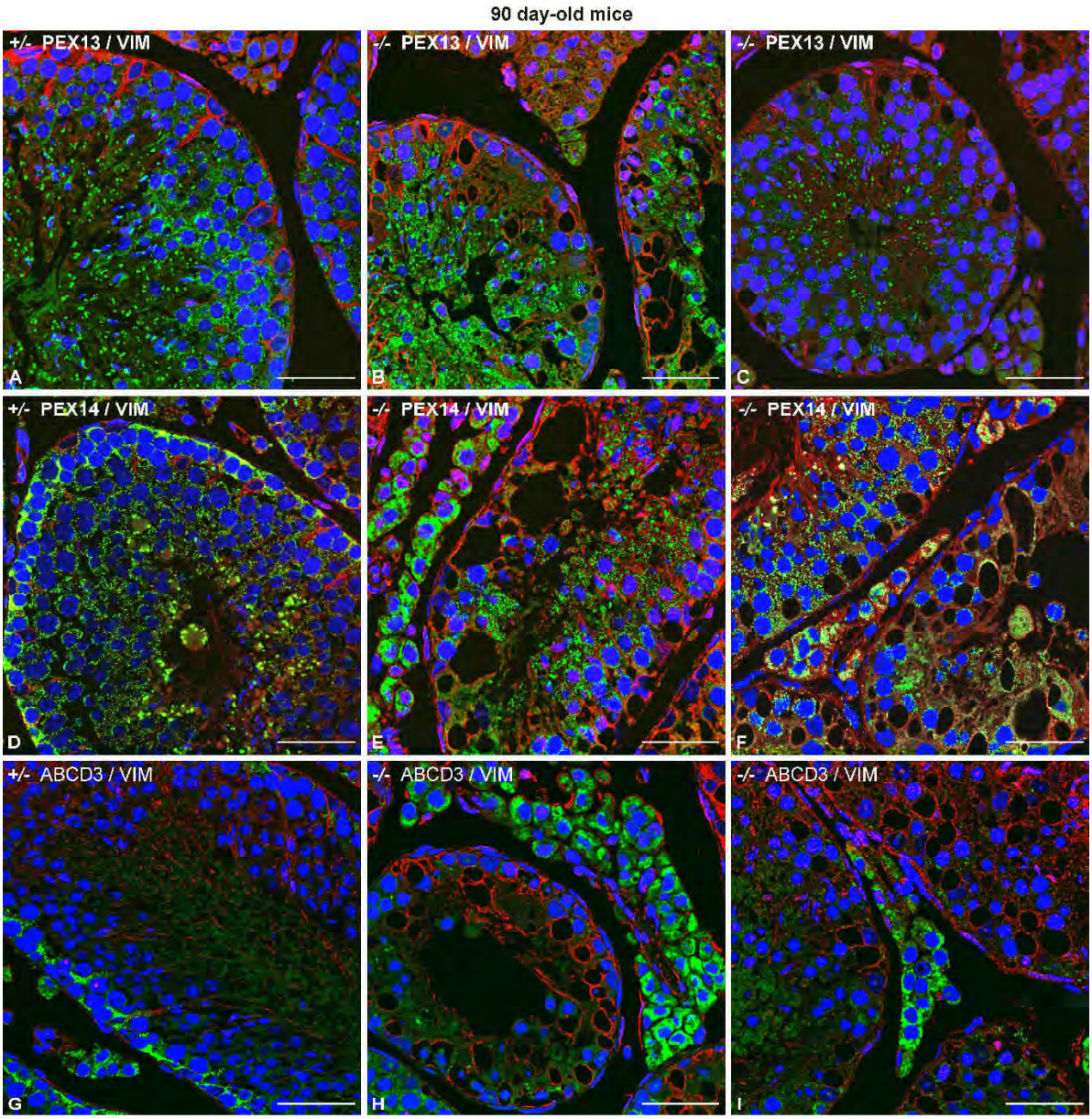

Figure 29: Immunofluorescence analyses of peroxisomal, mitochondrial and intermediate filamental proteins in paraffin sections of the testis from 90 day-old mice. Testes were fixed with 4% PFA, paraffin embedded, 2µm sections were cut and double-staining for specifically antigens. **(A)** PEX13 (green) in HTZ control testis section. **(B)** In some areas of the scs*Pex13*KO testis the basal epithelium of the seminiferous tubules was lined only by Sertoli cells stained for VIM (red) **(C)** A mixed population of differently altered seminiferous tubules was present with some of them exhibiting almost normal appearing spermatogenesis in scs*Pex13*KO mice **(D)** PEX14 (green) / VIM (red) in HTZ testis. **(E,F)** PEX14 staining (green) showed intracytoplasmic distribution in Sertoli cells. Germ cells from the mutant testis were positive for PEX14. Proliferated Leydig cells showed a strongly increased expression of PEX14. **(G)** ABCD3 staining in HTZ control testes. **(H,I)** ABCD3 expression was up-regulated in proliferated Leydig cells. The staining for ABCD3 was almost negative in Sertoli cells. Nuclei were counterstained with TOTO-3 iodide (blue). Bars represent A-I: 100 µm Representative pictures of obtained from 3 experiments.

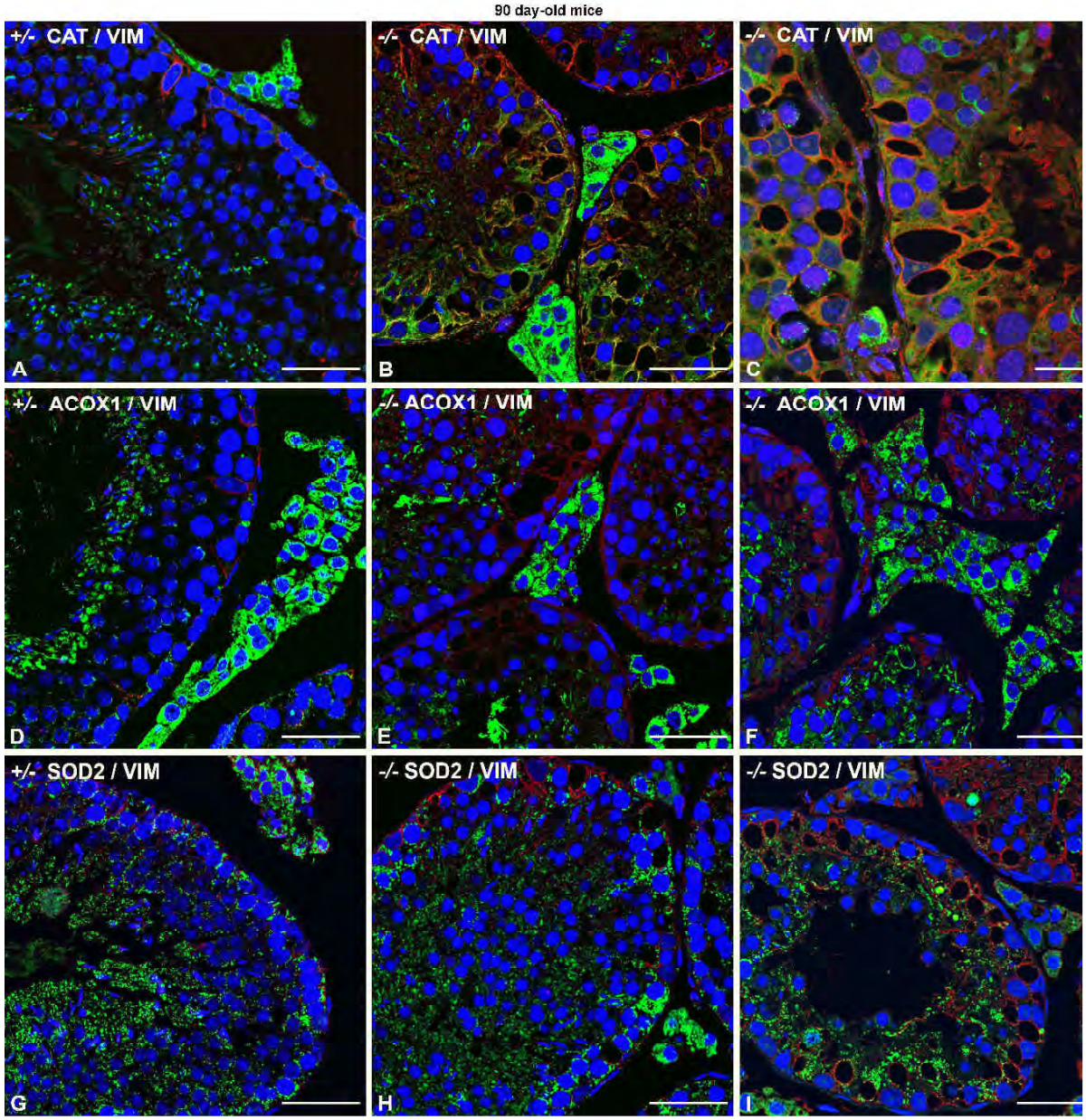

Figure 30: **Immunofluorescence analyses of anti-oxidants peroxisomal, mitochondrial enzymes and intermediate filamental proteins in paraffin sections of the testis from 90 day-old mice** Testes were fixed with 4% PFA, paraffin embedded, 2µm sections were cut and double stained for specifically antigens. **(A)** Double staining for CAT (green) / VIM (red) in HTZ control testis section. **(B)** Seminiferous tubule of a scs*Pex13*KO mouse with relatively normal spermatogenesis, revealing vacuolated Sertoli cells with intracytoplasmic of CAT distribution. **(C)** Many seminiferous tubules of scs*Pex13*KO exhibit disturbed spermatogenesis and huge vacuoles in Sertoli cells cytoplasm **(D)** ACOX1 (green) / VIM (red) in HTZ control testis. **(E,F)** ACOX1 staining was cytoplasmic in Sertoli cells of scs*Pex13*KO. Germ cells from the scs*Pex13*KO animals showed a weak staining for ACOX1 in peroxisoms. Hyperplasia Leydig cells showed ACOX1 protein expression in the scs*Pex13*KO testis. **(G)** Mitochondrial SOD2 staining in HTZ control testes. **(H,I)** SOD2 expression was strongly up-regulated in mitochondria of Sertoli cells of scs*Pex13*KO animals. In some of proliferated Leydig cells the staining for SOD2 appeared strong labeled. Nuclei were counterstained with TOTO-3 iodide (blue). Bars represent A-I: 100 µm, C: 50 µm. Representative pictures were obtained from 3 experiments.

PEX14 showed a diffuse accumulation near lipid droplets in the cytoplasm with an additional punctuate staining of peroxisomal membrane ghosts (Fig. 31D,F). In a few tubules, PEX13 and PEX14 were identified with a punctuate “peroxisome” staining pattern in some apoptotic germ cells or residual bodies (Fig. 31D,F). Proliferating Leydig cells showed only a weak IF

reaction for PEX13 (Fig. 31B,D). In the same type of cells, PEX14 was slightly increased in 130 day-old scs*Pex13*KO mice in comparison to scs*Pex13*HTZ animals (Fig. 31F). ROS are the normal by-products of cellular metabolism and are usually decomposed by cellular defense mechanisms provided by antioxidant enzymes, such as peroxisomal CAT and mitochondrial SOD2, which were detected by IF reactions in testis of scs*Pex13* WT mice (Fig. 32A,D). In 130 day-old scs*Pex13*KO testis, CAT exhibited a complete intracytoplasmic distribution in Sertoli cells, depicting the peroxisomal biogenesis defect (Fig. 32B,C). The intensity of the cytoplasmic CAT staining varied significantly between neighboring Sertoli cells within the same seminiferous tubule with some of the Sertoli cells exhibiting high cytoplasmic levels of this enzyme (Fig. 32B,C). Proliferating Leydig cells showed a high CAT expression in peroxisomes, revealed by the punctuate staining pattern in the IF preparations (Fig. 31B,C). Complex III of the mitochondrial respiratory chain was strongest expressed in primary spermatocytes and germ cells until step 16 spermatids as well as in Leydig cells of scsPEX13HTZ animals (Fig. 32A). In scs*Pex13*KO testis, this protein had a weak expression and was encircled large lipid-vacuoles in many Sertoli cells (Fig. 32B,C). Some Sertoli cells exhibited positive mitochondria for complex III protein accumulated in large organelle aggregates, indicating a different distribution and proliferation of this organelle in this cell type. Interestingly, in Sertoli cells with high intracytoplasmic CAT expression only a weak signal for complex III was observed, indicating heterogeneous alteration of mitochondria in Sertoli cells of scs*Pex13*KO testis. In Leydig cells of scs*Pex13*HTZ testis, complex III was located in bright IF dots, representing mitochondria (Fig. 32A), while scs*Pex13*KO Leydig cells were less intensely stained for this protein (Fig. 32B,C). In testis of scs*Pex13*HTZ animals, Leydig cells were strongest stained for SOD2, followed by germ cells and low a expression in Sertoli cells. Similarly to the expression of complex III, SOD2 was heterogeneously distributed in mitochondria of Sertoli cells of scs*Pex13*KO animals (Fig. 32E,F). In contrast to scs*Pex13*HTZ sections, the intensity of SOD2 labeling was strongly increased in scs*Pex13*KO Sertoli cells, and surpassed the one of proliferating Leydig cells. High expression of SOD2 was found in Sertoli cell mitochondria around the lipid droplets (Fig. 32E,F). Among proliferating Leydig cells in scs*Pex13*KO mice, SOD2 was strongly expressed in mitochondria of a few cells, whereas the rest of Leydig cells appeared almost negative (Fig. 32E,F). The ACOX1 enzyme, known to be responsible for the rate-limiting step of the peroxisomal β-oxidation pathway I, was highly expressed in the cytoplasm of Sertoli cells in scs*Pex13*KO testis (Fig. 33B). In contrast to Sertoli cells, all proliferating Leydig cells of scs*Pex13*KO animals were stained for ACOX1 in the same manner as in scs*Pex13*HTZ mice (Fig. 33A,B). The last enzyme of the β-oxidation pathway I, THIOLASE A, could not be visualized in the cytoplasm of Sertoli cells of scs*Pex13*KO mice, whereas the reaction for THIOLASE A localization was clearly positive in proliferating Leydig cells (Fig. 30 D).

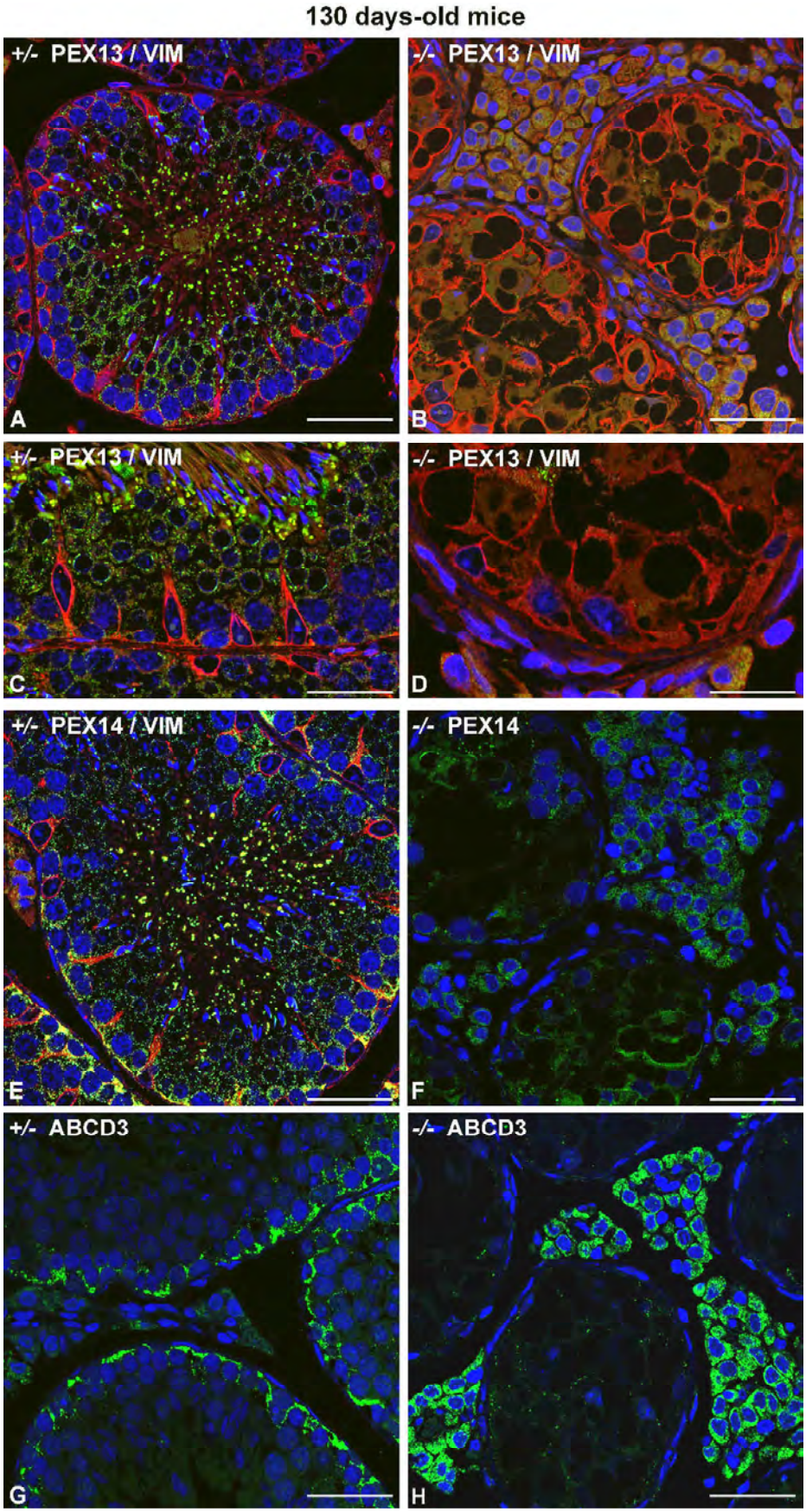

Figure 31: **Immunofluorescence analyses of peroxisome proteins on paraffin sections of the P130 testis of scs*Pex13*HTZ and scs*Pex13*KO mice.** Testes were fixed with 4% PFA, paraffin embedded, cut in 2µm sections stained for peroxisomal markers (green) and the Sertoli cell marker vimentin (red). **(A)** scs*Pex13*HTZ control testis section with double staining for VIM (red) revealing a typical staining of intermediate filaments in the Sertoli cells cytoplasm and PEX13 showing the highest protein expression in germ cells. **(B)** scs*Pex13*KO

seminiferous tubule with vacuolated Sertoli cells, depicting the absence of PEX13 protein; PEX13 (green) was present in low amount in proliferated Leydig cells **(C,D)** High magnification of a scs*Pex13*HTZ and of the scs*Pex13*KO testes sections. Few residual apoptotic germ cells (*arrow*) were still positive for PEX13, whereas the surrounding Sertoli cells were completely negative. **(E)** Double staining for PEX14 (green) and VIM (red) in HTZ testis. **(F)** PEX14 (green) was localized in large punctuate structures, most probably membrane ghosts of peroxisomes, surrounding large vacuoles. In addition, PEX14 showed a cytoplasmic staining in these areas. Proliferated Leydig cells exhibited a weak punctuate pattern staining for PEX14. **(G)** ABCD3 staining in HTZ control testis was characterized by basal distribution of the staining in seminiferous tubules **(H)** In scs*Pex13*KO mice ABCB3 expression was strongly up-regulated in proliferated Leydig cells. Only few membrane ghost like structures were positive for ABCD3 in Sertoli cells. Nuclei were counterstained with TOTO-3 iodide (blue). Bars represent in A-H: 100 µm, C and D: 50 µm. Representative pictures of obtained from 3 experiments.

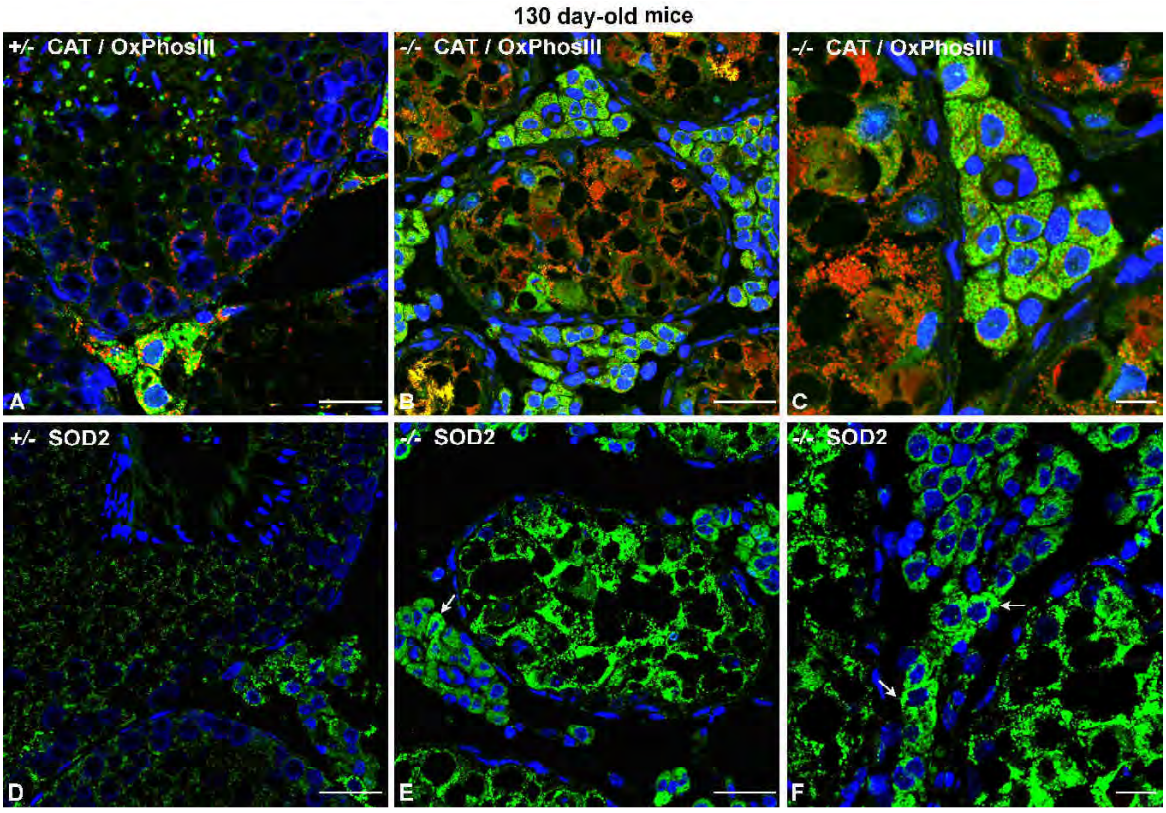

Figure 32: **Immunofluorescence analyses of anti-oxidative peroxisomal and mitochondrial enzymes and compex III of the mitochondrial respiratory chain in paraffin sections of the testis of 130 day old mouse.** Testes were fixed with 4% PFA, paraffin embedded, cut in 2µm sections and stained with specifically antibodies. **(A)** Double staining for CAT (green) and OxPhosIII (red) in scs*Pex13*HTZ testis section. **(B)** Seminiferous tubule reduced in size from scs*PEX13*KO with vacuolated Sertoli cells. CAT revealed a cytoplasmic and heterogeneous distribution in Seroli cells. The staining intensity of complex III / OxPhosIII was weak in Sertoli cells and also in proliferated Leydig cells. **(C)** High magnification of seminiferous tubules and proliferated Leydig cells from scs*Pex13*KO testis sections **(D)** Staining of SOD2 (green) in cells of scs*Pex13*HTZ seminiferous tubules and interstitial cells. **(E)** SOD2 staining (green) was high in Sertoli cells as well as in some of the proliferated Leydig cells (*arrow*). **(F)** High magnification of proliferated Leydig cells showing highly expressed SOD2 in these cells types. Nuclei were counterstained with TOTO-3 iodide (blue). Bars represent in A, B, D, E: 100 µm, C and in F: 50 µm. Representative pictures of obtained from 3 experiments.

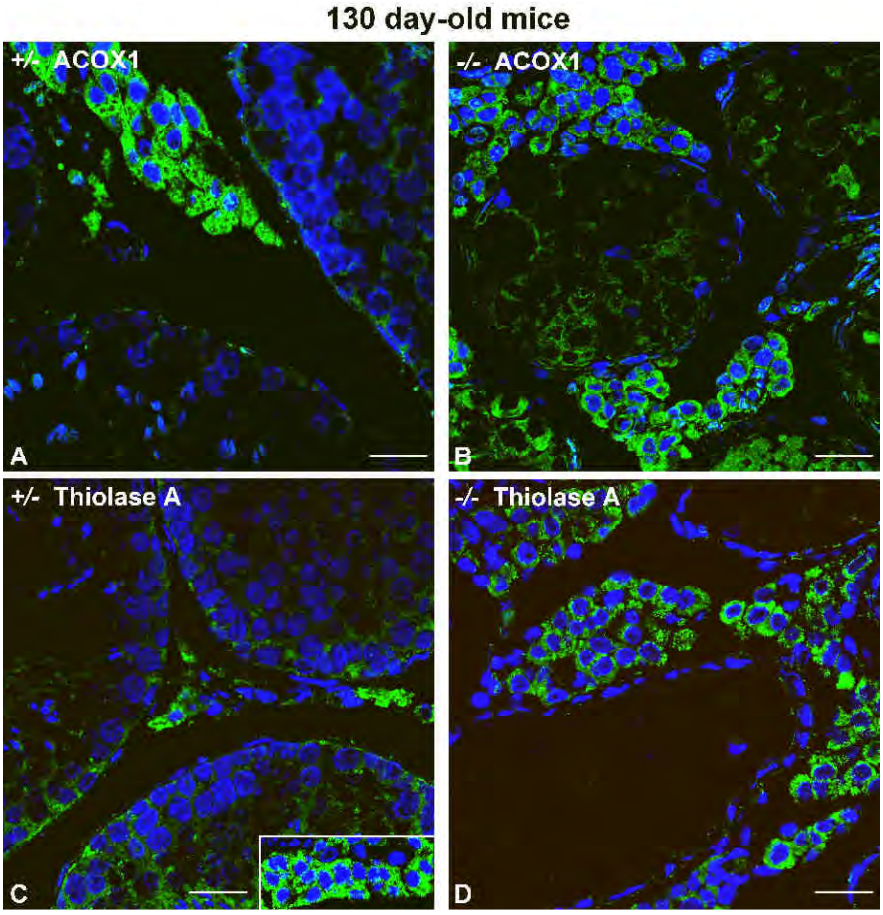

Figure 33: Immumofluorescence analyses of β-oxidation enzyme on paraffin sections of testis of P130 testis sections. Testes were fixed with 4% PFA, paraffin embedded, 2µm sections were cut. **(A)** ACOX1 (green) staining in HTZ control sections of the testis **(B)** Testis of scs*Pex13*KO mice exhibited cytoplasmic ACOX1 staining in Sertoli cells. Proliferated Leydig cells showed a slightly reduced ACOX1 staining intensity in comparison to ones in scsPex13HTZ animals. **(C)** Thiolase A (green) in the testis of scs*Pex13*HTZ animals of scsPex13HTZ animals. Insert shows HTZ Leydig cells. **(D)** Seminiferous tubules of scs*Pex13*KO were almost immunonegative for Thiolase A and some proliferated Leydig cells exhibited a slightly weak staining in scs*Pex13*KO animals. Nuclei were counterstained with TOTO-3 iodide (blue). Bars represent in A-D: 100 µm. Representative pictures of obtained from 3 experiments.

4.19. Immunofluorescence detection of steroidogenic enzymes in the testis

Sections of 130 day-old WT animals were used to establish the optimal conditions for antibody labeling of distinct enzymes involved in steroid synthesis, because staining of paraffin sections with these antibodies had not been performed and characterized in previous publications [134, 235]. With the optimal conditions, it was possible to label the scsPex13HTZ and KO sections for the steroidogenic acute regulatory protein, domain containing protein 1 (StARD1). In wild type animals some of interstitial Leydig cells were strong positive for StARD1 and contained big fluorescence dots labeled for StARD1 (Fig. 34A, B, F). In addition, strong StARD1 labeling was noted in the internal layer of the seminiferous epithelium of stages VI to VII of spermatogenic cycle, indicating that spermatids of step 15 to 16 exhibited a high abundance of StARD1 in the mitochondrial sheath of the mid piece of their tail (Fig. 34A, B, F right tubule). In the same tubules (stages VI to VII), the

Sertoli cells exhibited only a low amount of StARD1 in a punctuate pattern, representing the mitochondrial distribution (Fig. 34A,B). In contrast to other stages, Sertoli cells of stage VIII tubules showed a clear StARD1 labeling in a punctuate pattern, suggesting a stronger abundance of this protein in the mitochondria (Fig. 34D,E). Furthermore, in stage VIII, in which the cytoplasm of step 16 spermatids is removed to form residual bodies, StARD1 was identified in these structure in a dual localization with a diffuse cytoplasmic staining in addition to big dots in small numbers (Fig. 34D,E). In the IF staining of step 16 spermatids from stage VIII, individual mitochondria could not be distinguished as separated dots anymore, corresponding to the strong compaction of the mitochondrial sheath, leaving only small space between adjacent organelles that were too small to be resolved by IF microscopy (Fig. 34D,F). StARD1 was identified also into the cytroplasm of the step 10 spermatids of stage X tubules, however showing a punctuate staining pattern with weak fluorescence intensity (Fig. 34C,F left tubule). As mentioned above, in the Sertoli cells StARD1 staining was strongest in stage VIII tubules, whereas in stages IX to XII the labeling was much weaker (Fig. 34C and F left tubule) and in stages I to V tubules the StARD1 protein could not be clearly visualized in a punctuate staining pattern in Sertoli cell mitochondria (Fig. 34F upper tubule).

In 130 day-old scs*Pex13*HTZ animals, StARD1 staining showed an identical pattern as in the testis sections of WT mouse (Fig. 35A,B). In testis sections from P130 scs*Pex13*KO mice, StARD1 was detected in the cytoplasm of Sertoli cells (Fig. 35C,D). Furthermore, StARD1 could be identifed with high intensity in large dots-like structure only in few Leydig cells, whereas all other proliferated Leydig cells exhibited lower staining intensities (Fig. 35C,D).

The next steroidogenic enzyme studied was cytochrome P450 side chain cleavage enzyme (CYP450scc), a marker generally used for Leydig cells, which was identified solitarily in interstitial cells of scs*Pex13*HTZ testis sections (Fig. 35E). In testis sections of scs*Pex13*KO, the CYP450scc expression was up-regulated in all proliferating Leydig cells (Fig. 35F). In contrast to scs*Pex13*HTZ animals, also the Sertoli cells from scs*Pex13*KO tubules showed a weak mitochondrial staining for CYP450scc (Fig. 35F).

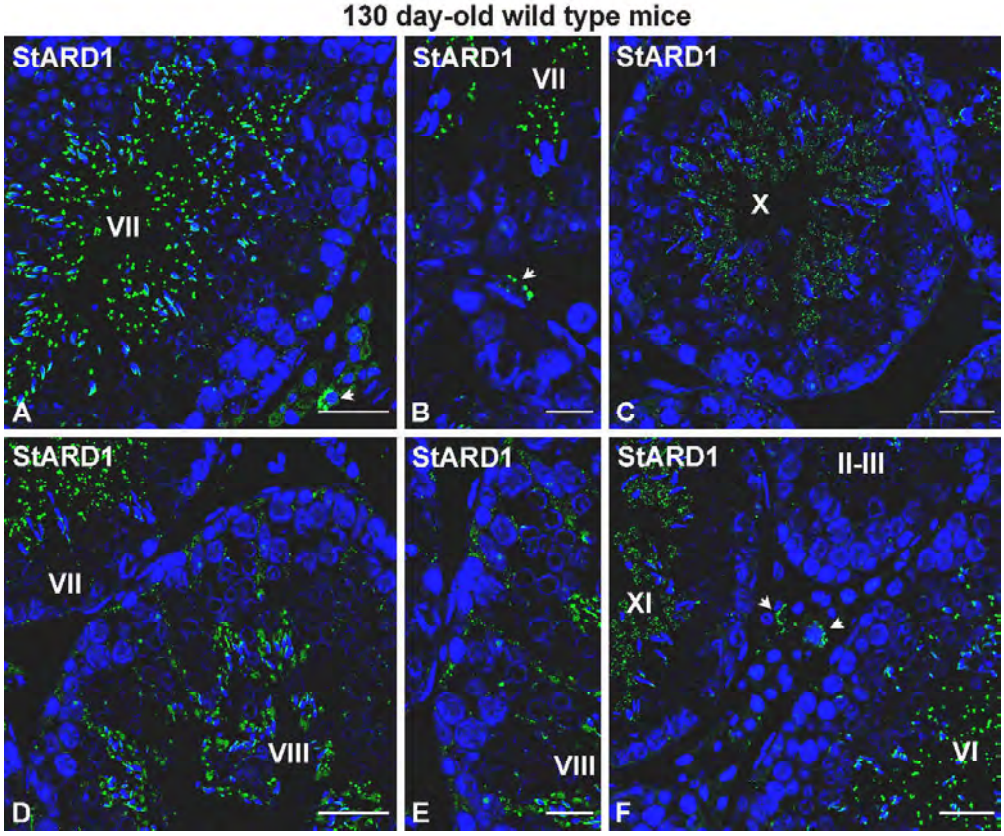

Figure 34: Localization of StARD1 protein in germ cells and somatic cell types of wild-type mouse testis. Testes were fixed with 4% PFA, paraffin embedded, 2µm sections were stained for StARD1 in different areas and stages in the testis. **(A)** StARD1 (green) in stage VII of a seminiferous tubule presented step 16 spermatids. Some Leydig cells were strongly positive for StARD1 (*arrow head*) **(B)** Big StARD1 immunopositive dots along the tail of step 16spermatids. Leydig cell strongly positive for StARD1 (*arrowhead*) **(C)** Stage X seminiferous tubule with step 10 spermatids, exhibiting a punctuat staining pattern with weaker fluorescence intensity. **(D)** Stage VIII seminiferous tubule revealed StARD1 step 16 spermatides showing a strong cytoplasmic staining. Sertoli cells of stage VIII tubules were immunopositive for StARD1. **(E)** High magnification of the basal side of stage VIII germinal epithelium, revealing a punctuate staining pattern for StARD1 in the Sertoli cell cytoplasm. **(F)** Overview of the difference in StARD1 protein expression in seminiferous tubules of different stages (II-III, VI, XI). Some Leydig cells were strong positive for StARD1 (*arrowheads*). Nuclei were counterstained with TOTO-3 iodide (blue). Bars represent in A-F 100 µm, in B and E: 50 µm. Representative pictures obtained from 3 experiments.

4.20. The *in vivo* apoptosis rate of spermatogenic cells was strongly increased in 90 day-old scs*Pex13*KO mice

Cells death was examined on testis sections of P90 and P130 of scs*Pex13*HTZ and scs*Pex13*KO mice by using a TUNEL assay (terminal dUTP nick end labelling) which detects DNA fragmentation resulting from activation of apoptotic signaling cascades and caspase cleavage. Treatment with DNase I was used as a positive control as shown in Fig. 36B,F,I. In scs*Pex13*HTZ animals only few meiotic germ cells were TUNEL positive (Fig. 36C-G). In contrast, severe cell death of germ cells during different phases of meioses was noted in P90 scs*Pex13*KO animals. Hardly any Sertoli cell nuclei were TUNEL positive in the same area were most of the germ cells death occurred in P90 scs*Pex13*KO animals (Fig. 36D). In P130 mutant animals, some of Sertoli cell nuclei became TUNEL-positive, suggesting that a complete degeneration of seminiferous tubules will occur in these animals (Fig. 36J). Leydig

cells were not TUNEL-positive in P90 or P130scs*Pex13*KO animals. This finding suggests that the severe cell death might take place at the around P90, leading to the Sertoli cell only syndrome of the P130 scs*Pex13*KO animals and further testicular degradation later.

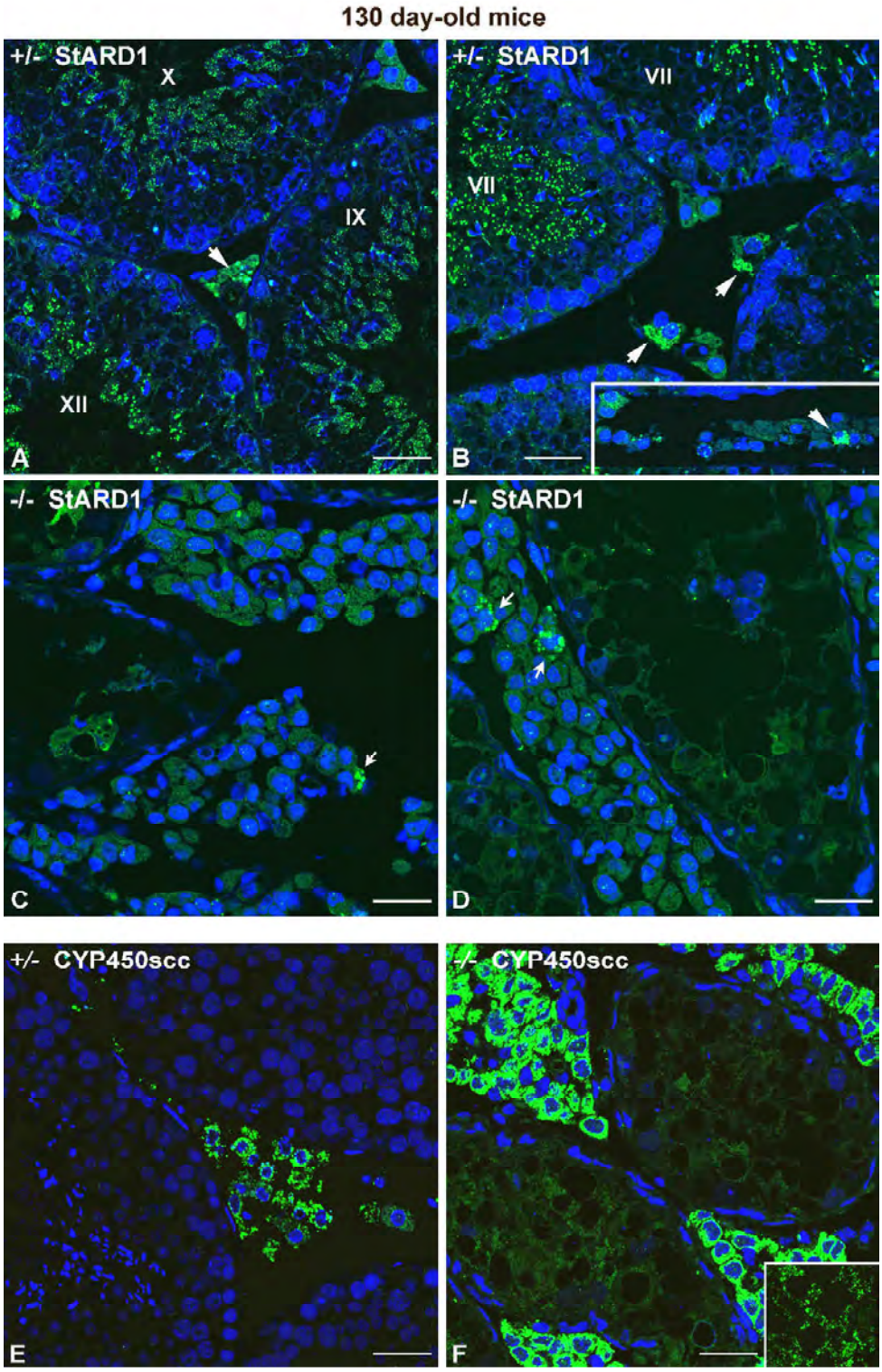

Figure 35: Localization of steroidogenic proteins in testis sections of 130 day-old animals with distinct scs*Pex13* genotypes. Testes were fixed with 4% PFA, paraffin embedded, 2µm sections were cut. **(A, B)** StARD1 protein (green) showed different expression patterns and distribution in various stages (VI, VII, VIII, IX, XII) of the seminiferous tubules in scs*Pex13*HTZ animals, corresponding to WT staining pattern. Some Leydig cells were clearly positive for StARD1 (*arrow head*). **(C, D)** Many Sertoli cells of the scs*Pex13*KO animals showed

a higher StARD1 expression in comparison to scs*Pex13*HTZ control sections. Leydig cells were a heterogeneously stained for StARD1 (*arrow head*) in scsPex13KO animals. **(E)** CYP450scc protein (green), a marker for Leydig cells, was specifically expressed in Leydig cells in scs*Pex13*HTZ sections. **(F)**. In scs*Pex13*KO animal, all proliferated Leydig cells were stronger positive for CYP450scc. Nuclei were counterstained with TOTO-3 iodide (blue). Bars represent in A-F: 100 µm. Representative pictures of obtained from 3 experiments.

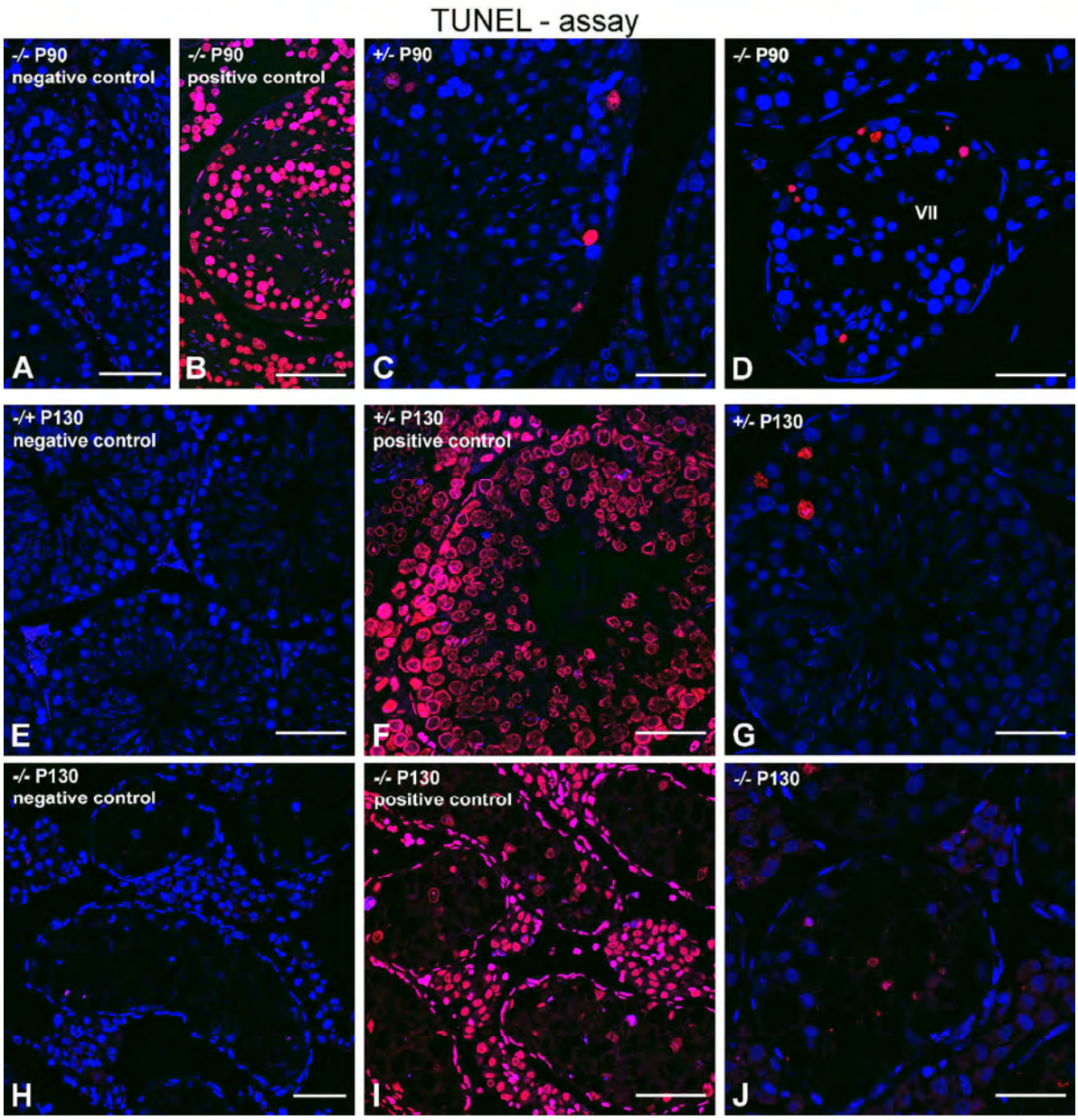

Figure 36: TUNEL assay on paraffin sections of testis from 90 and 130 day old scs*Pex13*KO and scs*Pex13*HTZ. Testes were fixed with 4% PFA, paraffin embedded, 2µm sections were cut. *In situ* staining of DNA strand breaks by the TUNEL assay was detected. **(A,E,H)** Negative controls sections, without the TdT enzyme, depicting the high specificity of the detection reaction (anti-dioxigenin conjugate-rhodamine). **(B,F,I)** Positive control sections, treated with DNase for 10 min RT. **(C)** Testis section of P90 scs*Pex13*HTZ showing very few apoptotic germ cells in stage VII of seminiferous tubules. **(D)** Testis section of P90 scs*Pex13*KO exhibiting germ cells death during different phases of meioses. **(G)** scs*Pex13*HTZ seminiferous tubules were showing very few apoptotic germ cells. **(J)** Sertoli cell only syndrome revealed by seminiferouse tubules of the 130 day-old scs*Pex13*KO, presenting remaining DNA breaks fragment from the germ cells or some of Sertoli cells detected by the TUNEL assay. Nuclei were counterstained with TOTO-3 iodide (blue). Bars represent in A-I: 100 µm. Representative pictures obtained from 3 experiments.

4.21. Western Blots reveal the good quality of the tubular and interstitial cell preparation

To confirm the morphological results obtained *in situ*, Western blot (WB) analyses were performed using distinct subcellular fractions from interstitial and tubular cell preparations. Distinct subcellular fractions (P2: heavy mitochondria containing also big peroxisomes, P3: light mitochondria and enriched peroxisomal fraction, S3: microsomes and cytosol) were obtained by differential centrifugation after homogenization of isolated enriched interstitial cells, peritubular and enriched tubular cells from testis of mice of different genotypes (scs*Pex13*WT, scs*Pex13* HTZ and scs*Pex*13KO animals). The isolated peritubular cells were not used for comparative WB analyses, since the cell pellet was too small to be subjected to differential centrifugation.

4.21.1. Interstitial and tubular cells exhibit a decrease of peroxisomal biogenesis proteins in scs*Pex13*KO testis

In scs*Pex13*WT and scs*Pex13*HTZ animals all peroxisomal biogenesis proteins were present in the pellet fractions, with highest intensity in P3, which corresponds to the highest enrichment of peroxisomes in the light mitochondrial fractions. Large peroxisome sediments were already at lower g – forces in the heavy mitochondrial fractions. The high quality of the isolation procedure is shown by the fact that almost no organelle breakage occurred and only very small peroxisomes are present in the microsomal / cytoplasmic fractions. In contrast to scs*Pex13*WT and scs*Pex13*HTZ animals, PEX13 was completely absent in tubular cells – mainly Sertoli cells of scs*Pex13*KO animals, whereas it was clearly detectable in the interstitial cell preparation in the same animals (Fig. 37A). The absence of the PEX13 protein in the WB of the tubular fractions of mutant animals confirms the disruption of the *Pex13* gene in these mice. In addition, PEX14 was also strongly reduced in tubular cells of P130 day-old scs*Pex13*KO, which can be easily explained by the low number of membrane ghosts in scsPex13KO Sertoli cells (Fig. 37B).

Interestingly, also the protein levels of these two peroxins were considerably decreased in the interstitial cell in subcellular fractions of scs*Pex13*KO genotype compared with the subcellular fraction of the scs*Pex13*WT and HTZ animals (Fig. 37A,B). Furthermore, PEX5 a peroxisomal biogenesis protein with cytoplasmic localization and attachment also on the outer surface of the peroxisomal membrane was strongly reduced in scs*Pex13*KO animals. At similar protein concentrations, PEX5 was more abundant in tubular cells of scs*Pex13*WT as well as scs*Pex13*HTZ animals in comparison to interstitial cells of the same animals (Fig. 37C).

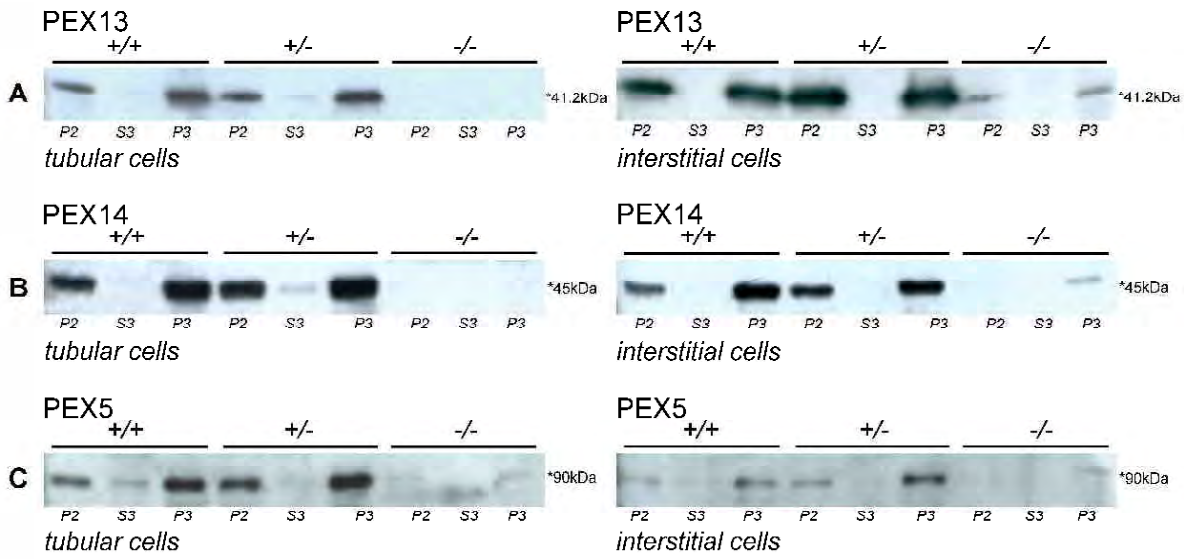

Figure 37: Western blot analyses of enriched subcellular fractions isolated from different testicular cell preparations. Twenty-five microgram of proteins were loaded in each lane on 12.5% SDS gels. The same blots were stripped and reprobed several times with specific antibodies. **(A)** PEX13 – peroxin 13 **(B)** PEX14 - peroxin 14 **(C)** PEX5 – peroxin 5 *(tubular cells – Sertoli cells along with germ cells; interstitial cells – enriched Leydig cells; P2: enriched heavy mitochondrial fraction; S3: microsomes and cytosolic fraction; P3: enriched peroxisome and light mitochondria fraction).*

4.21.2. Proteins of peroxisomal lipid transport and enzymes of β-oxidation are altered in testicular fractions of scs*Pex13*KO

The peroxisomal ABCD3 membrane transporter for lipid substrates was also drastically reduced in subcellular fractions of tubular cells from scs*Pex13*KO animals, suggesting a removal of peroxisomal membrane ghosts in Sertoli cells (Fig 38A). In contrast this transporter was significantly induced in interstitial cells of the scs*Pex13*KO animals corresponding to the strong induction in the morphological staining.

Furthermore, the expression of acyl-CoA oxidase 1 (ACOX1), the first and rate-limiting enzyme of the fatty acid beta-oxidation pathway I in peroxisome, was studied. The immunoblot analysis revealed that a 50 kDa band (B-subunit of ACOX1) was present with a similar distribution pattern in subcellular fractions of both tubular and interstitial cell preparations from scs*Pex13*WT and HTZ testes, but with higher expression in tubular cells. The amount of the cleaved 50 kDa form was reduced in the tubular cells of scs*Pex13*KO animals. In contrast, this form was significantly induced in the enriched peroxisomal fraction (P3) of interstitial cells (Fig. 38B). Whereas most of ACOX1 protein seemed to be bound to filaments or the outer surface of membranes, it was mainly present in the P3 fractions of scsPex13KO tubular cells. A part of THIOLASE A, the third enzyme of the peroxisomal β-oxidation pathway I, showed a shift into the cytosolic fraction, indicating the misstargetting of this enzyme in Sertoli cells of the tubular cells preparation from scs*Pex13*KO animals. Surprisingly, a reduction of THIOLASE A protein level was observed in interstitial cells of scs*Pex13*KO animals, while ACOX1 was induced in these preparations (Fig. 38B,C).

In addition to the alteration of the peroxisomal lipid transporters and the β-oxidation enzymes, the PPARγ protein was up-regulated in the cytosolic S3 fraction of tubular cells in scs*Pex13*KO animals in comparison to *Amh-cre* positive scs*Pex1*3HTZ animals (Fig. 38D). Unfortunately, the PPARγ protein abundance in interstitial cells preparation was too low to be detected, when identical protein concentrations were used for WB analyses.

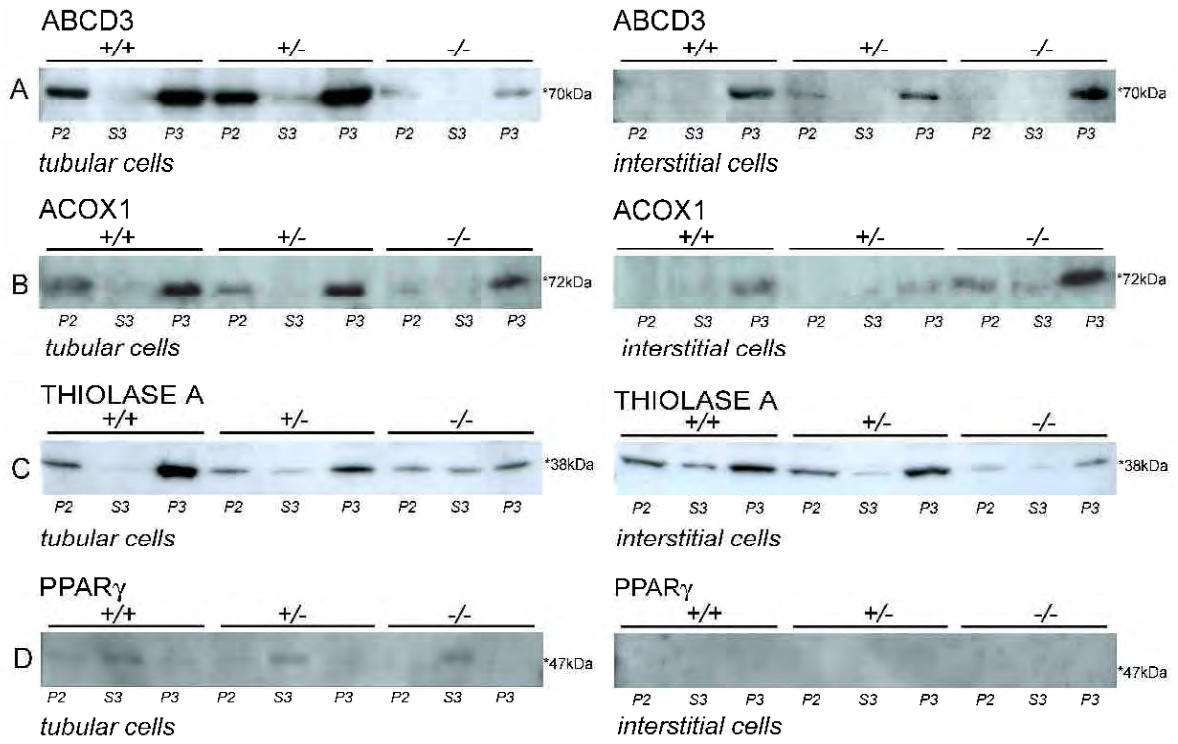

Figure 38: Western blot analysis of enriched subcellular fractions isolated from different testicular cell preparations. Twenty-five micrograms of proteins were loaded in each lane on 12.5% SDS gels. The same blots were stripped and reprobed several times with specific antibodies. **(A)** ABCD3 – peroxisomal membrane protein 70, member D3 of the ATP binding cassette transporters). **(B)** ACOX1, Acyl-CoA oxidase 1, 51kDa B subunit. **(C)** THIOLASE A **(D)** PPARγ - peroxisome proliferator activated receptor gamma *(tubular cells – Sertoli cells along with germ cells; interstitial cells – enriched Leydig cells; P2: enriched heavy mitochondrial fraction containing large peroxisomes; S3: microsomes and cytosolic fraction; P3: light mitochondrial fraction and enriched peroxisome).*

4.21.3. Alteration of the protein levels involved in ROS metabolism and inflammation in subcellular fractions of cell preparations from distinct genotypes of scs*Pex13* mice

Peroxisomal CAT, the enzyme with highest capacity to degrade H_2O_2 was increased significantly in the cytosolic fraction (S3) from tubular cells of scs*Pex13*KO mice in comparison to scs*Pex13*WT and scs*Pex13*HTZ mice, reflecting the peroxisome import deficiency due to *Pex13* gene defect. This enzyme was drastically induced in interstitial cells and interestingly also a significant part of the enzyme was present in the S3 fraction of the interstitial cell preparation of scs*Pex13*KO animals (Fig. 39A).

The reason for this phenomenon it is not clear, but could be explained *a)* by partial import deficiency in Leydig cells, reflected by the low PEX5, PEX13 and PEX14 protein levels in peroxisomal fractions or *b)* a higher fragility of the organelles during the isolation procedure in these cells type.

The cytoplasmic distribution of CAT which was revealed by WB analysis (Fig. 39A) was in agreement with the IF results in Sertoli cells from testis sections from scs*Pex13*KO mice (Fig. 32B,C).

Similarly, the mitochondrial SOD2, involved in the dismutation of the superoxide anions into H_2O_2 was increased in P3 and more strongly in the S3 fractions (cytosolic and microsomal fraction) most probably also due to broken mitochondria in the tubular cell preparation of the scs*Pex13*KO mice. The SOD2 protein was also shifted, but to a lesser extent into the cytosolic fraction (S3) in the interstitial cell preparation of scs*Pex13*KO animals (Fig. 39B). Since a clear mitochondrial staining pattern was achieved in IF preparation, the cytosolic increase of SOD2 indicates breakage of long fragile mitochondria during the isolation procedure Complex III of the mitochondrial inner-membrane, was dramatically decreased in the tubular cell preparation of scs*Pex13*KO animals (Fig. 39C). A slight band was noted in the S3 fraction of this cell preparation, suggesting also the breakage of mitochondria in scs*Pex13*KO animals.

The heme oxygenase-1 (HO-1) is the rate-limiting enzyme of heme catabolism present in ER and has been assumed to be important in cellular response against oxidative stress, by producing CO as messenger molecule and for the resolution of inflammation. Immunoblotting revealed that the HO-1 protein expression was dramatically reduced in tubular cell preparation of scs*Pex13*KO mice in comparison to scs*Pex13*HTZ and WT mice. Only a slight reduction of the HO-1 protein level occurred in testicular interstitial cell fractions of the same genotype (Fig. 39D).

Finally, the expression of another proinflammatory ER protein the cyclooxygenase 2 (COX-2) was studied. The Western blot analysis revealed a dramatic up-regulation of the COX2 protein in P2, S3 and P3 fractions of testicular tubular cells of scs*Pex13*KO mice. In contrast, no decrease of over all COX-2 level was observed in interstitial cells (Fig. 39E).

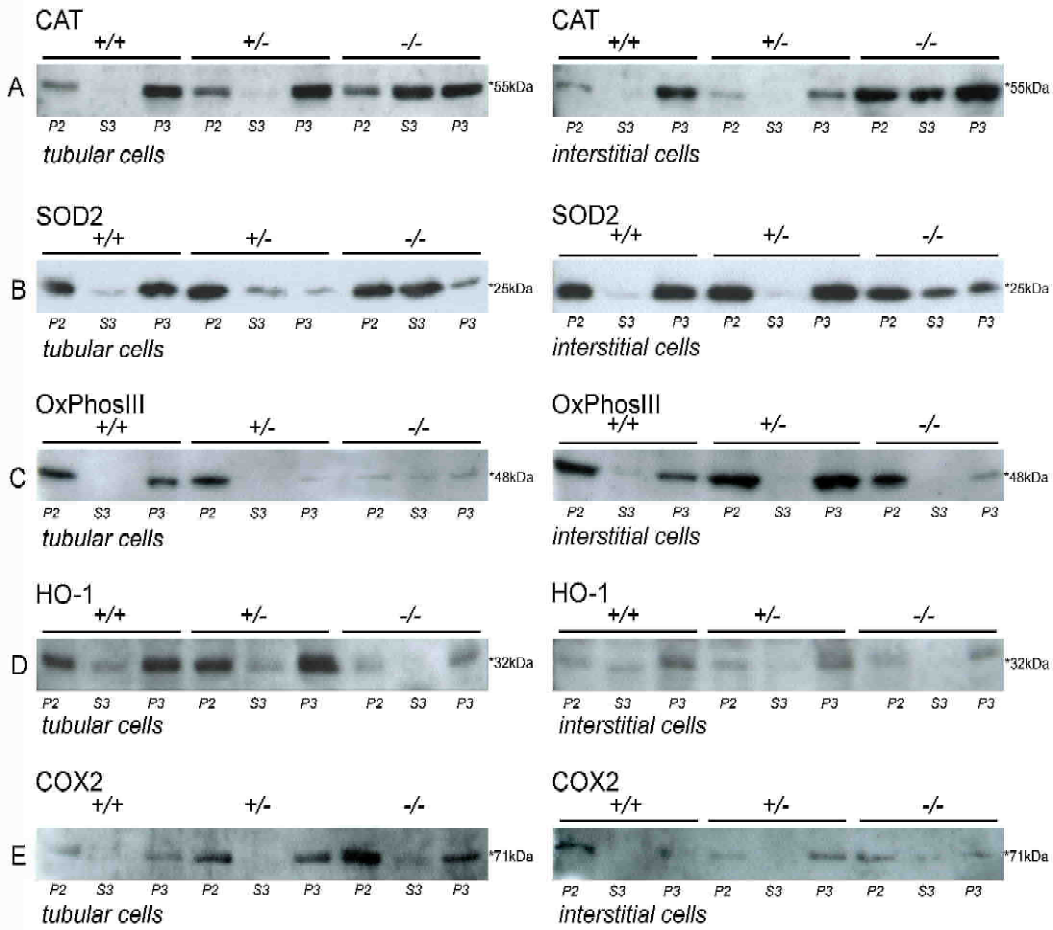

Figure 39: Western blot analysis of enriched subcellular fractions isolated from different testicular cell preparations Twenty-five micrograms of proteins were loaded in each lane on 12.5% SDS gels. The same blots were stripped and reprobed several times with specific antibodies. **(A)** CAT- catalase **(B)** SOD2 - superoxide dismutase 2 **(C)** OxPhosIII - complex III of the respiratory chain (oxidat Phosphorylation) **(D)** HO-1 - heme oxygenase 1 **(E)** COX2 – cyclooxygenase 2 (prostaglandin H synthase 2). *(tubular cells - Sertoli cells along with germ cells; interstitial cells – enriched Leydig cells; P2: enriched heavy mitochondrial fraction containing large peroxisomes; S3: microsomes and cytosolic fraction; P3: light mitochondrial fraction and enriched peroxisome).*

4.21.4. Western Blot analysis of steroidogenic enzymes and the intermediate filaments marker - vimentin

In scs*Pex13*WT and scs*Pex13*HTZ controls interstitial cell fractions StARD1 were visualized in P2 (weak) and P3 (strong) as a double band of 37 kDa and 32 kDa. In contrast in corresponding scs*Pex13*KO fractions, only a single band for StARD1 immunoactivity was revealed in P3 at 37 kDa and most probably in P2 fraction at 32 kDa band. In tubular cell preparation, only very weak bands were visible (by using the same exposure time for the blots) mainly in P2, of WT and HTZ protein preparations (Fig. 40A). A strong increase of the 32kDa band of StARD1 was noted in tubular cell fractions of scs*Pex13*KO (strongest signal in P2), suggesting an upregulation of the StARD1 protein. There was a significant increase in the expression of StARD1 protein in large mitochondrial fraction of the tubular cells from the scs*Pex13*KO animals (Fig. 40A). The low staining for StARD1 in mitochondria of mixed tubular cells of scs*Pex13*WT and scs*Pex13*HTZ animals might be explained by the fact that only a minority of elongated spermatids in the seminiferous tubules are positive for StARD1

protein. In accordance with the results obtained by IF, CYP450scc was mainly present in the interstitial cell fractions, depicting also the purity of the testicular cell preparation meaning that the interstitial cell pool contained really enriched Leydig cells and the one for tubular, peritubular, Sertoli and germ cells). In addition CYP450scc exhibited a clearly higher expression level in the subcellular fractions of interstitial cells of scs*Pex13*KO (Fig. 40B). CYP450scc was barely detectable in tubular cells from WT and scs*Pex13*HTZ mice, however, a weak but clear band in P2 of scc*Pex13*KO mice could be observed at the expected 78 kDa, indicating an increase of CYP450scc enzyme also in Sertoli cells mitochondria (Fig. 40A).

Western blot analysis was also carried out to determine the expression pattern of the VIM protein, which was enriched also in P2 of WT and scs*Pex13*HZT tubular cell fractions of testis. In contrast, only a weak band was seen in the interstitial cell preparations of these genotypes. In distinct subcellular fractions from tubular cells of scs*Pex13*KO, VIM was present in P2 as well as in P3 fractions, indicating a different arrangement of these filaments in the KO animals. In addition, VIM protein was increased in the interstitial cell preparation of scs*Pex13*KO animals, suggesting the presence of more peritubular cells or macrophages and immune cells or fibroblast or endothelial cells in the interstitial cell preparation (Fig. 40C).

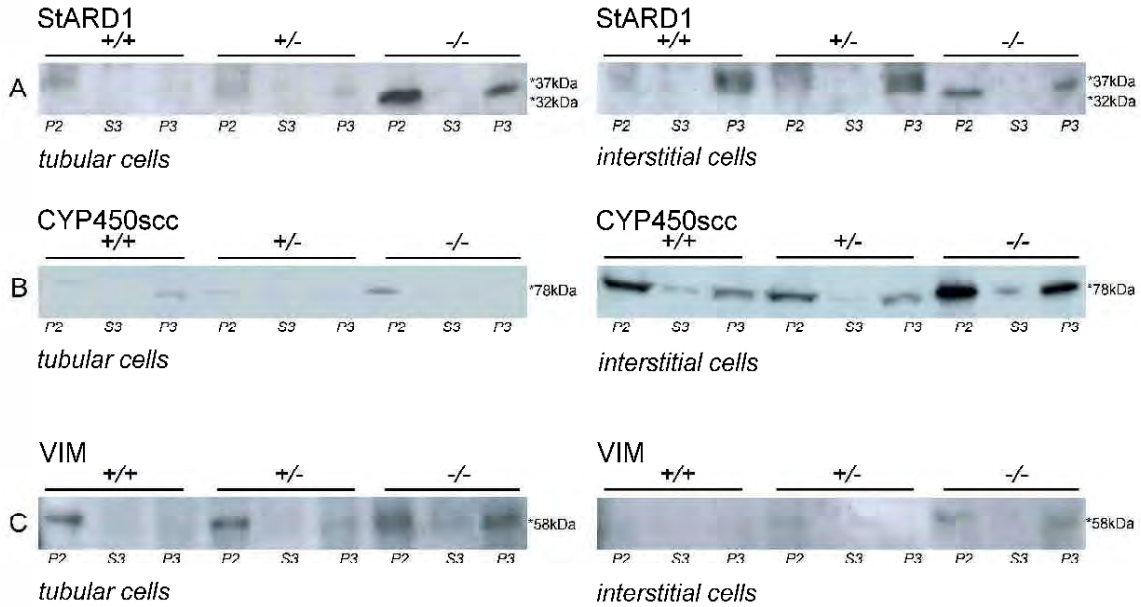

Figure 40: Western blot analysis for steroidogenic enzymes and vimentin of enriched subcellular fractions isolated from different testicular cell preparations. Twenty-five micrograms of proteins were loaded in each lane on 12.5% SDS gels. The same blots were stripped and reprobed several times with specific antibodies. **(A)** StARD1 - steroidogenic acute regulatory, domain containing protein 1. **(B)** CYP450scc – cytochrome P450 side chain cleavage enzyme. **(C)** VIM – intermediate filaments vimentin. *(tubular cells - Sertoli cells along with germ cells; interstitial cells – enriched Leydig cells; P2: enriched heavy mitochondrial fraction containing large peroxisomes; S3: microsomes and cytosolic fraction; P3: light mitochondrial fraction and enriched peroxisome).*

4.22. Identification of affected genes by semi-quantitative RT- PCR in scs*Pex13*KO animals

4.22.1. Peroxisomal genes are affected by the knockout of *Pex13* gene in Sertoli cells

The steady-state levels of mRNAs encoding peroxisomal proteins were determined by RT-PCR in total RNA preparations of isolated tubular, peritubular and interstitial cells of testis of animals with distinct scs*Pex13* genotypes. Thereafter, the RT-PCR band intensities of peroxisome-related genes were normalized to the band intensity of *28S ribosomal RNA* of the same cDNA preparation (Fig. 41A).

The mRNA for *Abcd1* was present in similar amounts in tubular, peritubular and interstitial cells of the mice of all three genotypes. In contrast, the mRNA for *Abcd2* was strongest expressed in tubular cells and lower in peritubular cells and showed a very weak induction in both cells preparation in scs*Pex13*KO mice. *Abcd3* was also expressed at highest level in Sertoli cells, however, was not altered in tubular cells of scsPex13KO animals. Abcd3 showed its strongest up-regulation in interstitial cells from scs*Pex13*KO mice. In contrast to the widespread expression of *Abcd1-3* mRNAs, *Abcd4* was only expressed in tubular cells of WT and scs*Pex13*HTZ animals, whereas it was not present in peritubular and interstitial cells in these animals. However, *Abcd4* was strongly induced in interstitial cells of scs*Pex13*KO animals. In addition, the level of *Abcd4* mRNA was significantly increased in tubular cells of the scs*Pex13*KO animals (Fig. 41B).

The mRNA levels of enzymes involved in the peroxisomal β-oxidation pathway I (*Acox1, Ehhadh*, *Thiolase A)* and II (*Acox2, Acox3, Mfp2* and *ScpX*) were investigated. Except for the mRNAs of *Acox1*, *Acox2* and *Thiolase A*, the one for other β-oxidation enzyme were expressed at similar high levels in all cell preparations and were not significantly altered in scsPex13Ko animals. *Acox1* showed a similar expression level in tubular and interstitial cells, but was less abundant in peritubular cells in testicular cell fractions of the scs*Pex13*WT and HTZ animals. The *Acox1* mRNA was induced in all cell types in scs*Pex13*KO testis with highest upregulation in interstitial cells (Fig. 41D). The mRNA of *Thiolase A* was expressed also at slightly lower levels in peritubular cells in scs*Pex13*WT animals and was up regulated in interstitial cells of scs*Pex13*KO mice (Fig. 41D). The *Acox2* mRNA levels were highest in tubular cells scs*Pex13WT* and scs*Pex13HTZ*, followed by peritubular cells and lowest in interstitial cells (Fig. 41C). In contrast to other genes, the mRNA for *Acox2* was strongly down-regulated in tubular cells of scs*Pex13*KO mice and to a lesser extent also in the interstitial cells, but it was up-regulated in peritubular cells of the scs*Pex13*KO animals (Fig. 41C).

The mRNA expression of genes involved in the biosynthesis of ether lipids (*Gnpat* and *Agps*) were also altered differently. Whereas, *Gnpat* mRNA was present at similar levels in cellular fractions of all genotypes, the *Agps* mRNA was slightly elevated in tubular cells and stronger

upregulated in peritubular cells in scs*Pex13*KO mice. The mRNA of *Agps* was not altered in interstitial cells of the scs*Pex13*KO animals (Fig. 41E).

Furthermore, the mRNA levels for sterol regulatory element binding factor 1 and 2 (*Srebf1, Srebf2*), involved in fatty acid and cholesterol metabolism were studied. The mRNA levels of *Srebf1 and Srebf2* showed higher expression in tubular cells, followed by interstitial cells and the lowest expression was detected in peritubular cells of scs*Pex13*WT and scs*Pex13*HTZ animals. In scs*Pex13*KO testis, the *Srebf1 and Srebf2* mRNA levels were strongly up-regulated in tubular cells, whereas the levels were only slightly up-regulated in interstitial and tubular cells (Fig. 41F).

Finally, the genes associated with cholesterol biosynthetic pathway, such as isopentenyl-diphosphate isomerase (*Idi1*), 3-hydroxy-3-methylglutaryl-Coenyme A reductase (*Hmgcr*) and 3-hydroxy-3-methylglutaryl-Coenyme A synthase 1 (*Hmgcs1*) were investigated. The corresponding proteins of *Idi1*, *Hmgcr* are *Hmgcs1* are located in the peroxisome, ER and peroxisomes and the cytoplasm, respectively. The mRNA expression of all three genes revealed an equal distribution in all testicular cell fractions in the scs*Pex13*WT and HTZ. The *Idi1* and *Hmgcr* mRNA levels were slightly down-regulated in tubular cells, while in peritubular and interstitial cells their mRNA expression was increased in the scs*Pex13*KO testis. In contrast, the *Hmgcs1* mRNA showed a slight up-regulation in all testicular cell preparations of the scs*Pex13*KO animals (Fig. 41G).

4.22.2. Significant alterations of mRNA levels of most antioxidant enzymes in scs*Pex13*KO mice

The mRNA levels of the major antioxidant enzymes catalase (*Cat*), glutathione peroxidase 1 (*Gpx1*), glutatione S – transferase 1 (*Gsta1*), peroxiredoxins 1, 5 and 6 (*Prdx1, 5, 6*), and superoxide dismutases 1 to 3 (*Sod1, 2, 3*) as well as heme oxygenase I (*Ho-1*) were determined by semi-quantitative RT-PCR. The expression level of catalase was massively up-regulated in all testicular cell preparations of scs*Pex13*KO animals (Fig. 42A). The mRNA levels of *Prdx 1, 5* and *6* were differently affected. The amount of *Prdx1* mRNA was increased in tubular and peritubular cell preparations of scs*Pex13*KO animals, whereas no significant increase the *Prdx1* mRNA level was observed in interstitial cells from KO animals (Fig. 42B). The mRNA levels of *Prdx5* were not altered at all and those for *Prdx6* were only slightly up-regulated in tubular cell preparations of KO animals (Fig. 42B). The *Gpx1* mRNA levels were strongest increased in tubular, followed by interstitial cells and peritubular cells in scs*Pex13*KO animals (Fig. 42D).

The *Gsta1* mRNA levels showed no major alterations between scs*Pex13*HTZ and scs*Pex13*KO in distinct cell preparations. The expression of the *Ho-1* mRNA was significantly

up-regulated in peritubular and interstitial cell preparations in scs*Pex13*KO mice, whereas it was only slightly changed in tubular cells in scs*Pex13*KO cell preparation (Fig. 42E).

In distinct testicular cell preparations the *Sod1* mRNA levels were not significantly altered, while the *Sod2* mRNA was increased in all cell preparations of scs*Pex13*KO animals (Fig. 42C). The mRNA encoding the extracellular *Sod3* was expressed at high levels in tubular cells, followed by interstitial and peritubular cells in the testis of scs*Pex13*WT and HTZ mice. The *Sod3* mRNA levels were significantly increased in tubular cells and interstitial cells and hardly altered in scs*Pex13*KO in comparison to scs*Pex13*HTZ and WT animals (Fig. 42C).

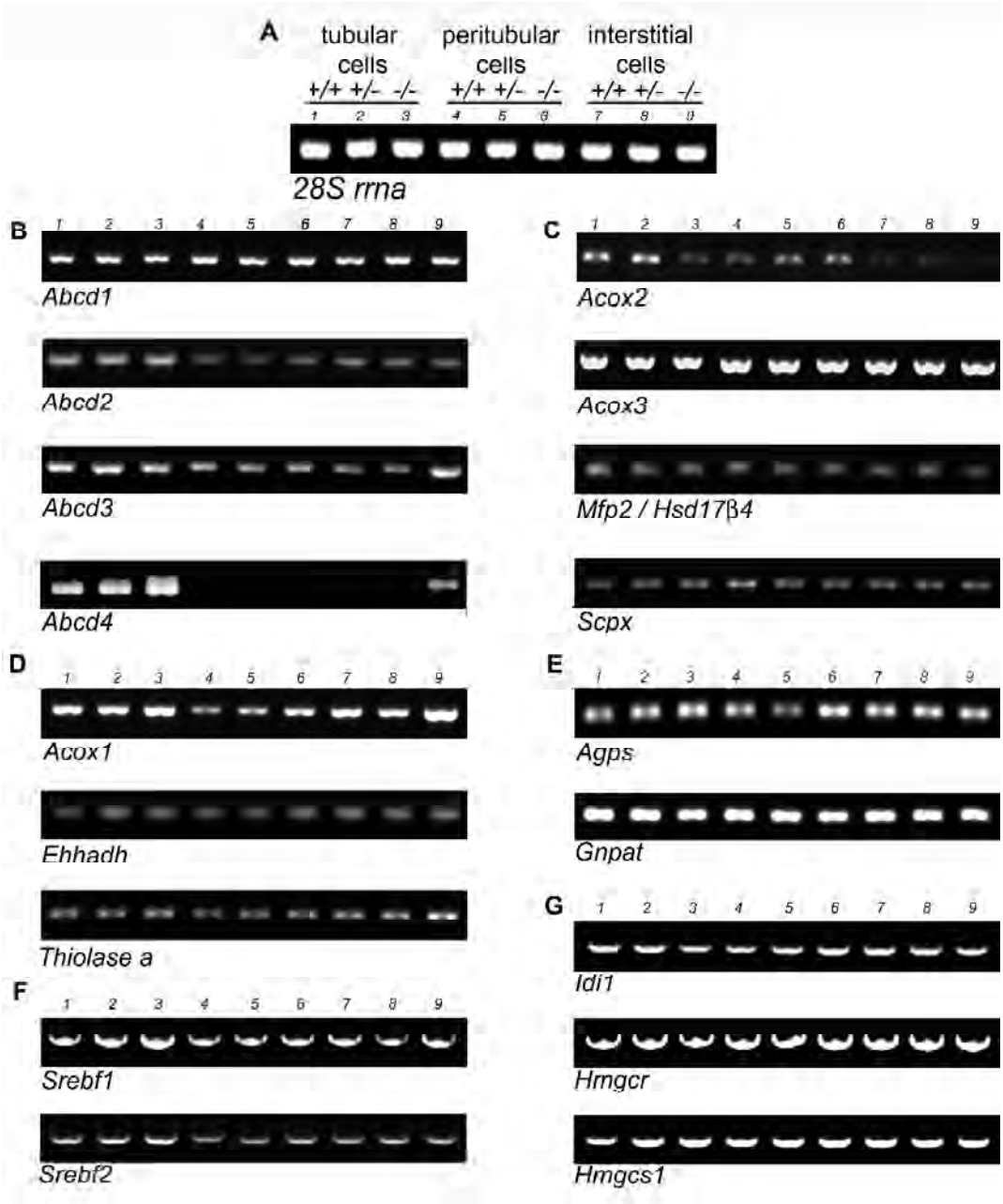

Figure 41: Semiquantitative RT-PCR analyses of genes encoding for the peroxisomal enzymes and *Srebf1* and *2* from the total RNA of distinct cell fractions from testis of the mice. (A) *28S rrna*: 28S ribosomal *RNA* as internal control. **(B)** *Abcd1-4: p*eroxisomal ABC-transporters **(C)** mRNA of enzymes of the β-oxidation pathway 2, *Acox2 and 3:* acyl-CoA oxidase 2 and 3, *MFP2 / HSD17β4:* multifunctional protein 2, *Scpx:* sterol carrier protein X **(D)** mRNAs encoding enzymes of the β-oxidation pathway 1, *ACOX1:* acyl-CoA oxidase I, *Mfp11*: multi-functional protein 1 / Hsd17β4, *Thiolase A* (**E)** mRNAs of enzymes of ether lipid synthesis, *Gnpat* glicerone

(dihydroxyacetone) phophate acyltransferase, *Agps*: alkyl-glicerone (dihydroxyacetone) phosphate synthase. **(G)** *Idi1*: isopentenyl-diphosphate isomerase, *Hmgcr:* 3-hydroxy-3-methylglutaryl-Coenyme A reductase, *Hmgcs1:* 3-hydroxy-3-methylglutaryl-Coenyme A synthase 1 (+/+: scs*Pex13*WT; +/-: scs*Pex13*HTZ; -/-: scs*Pex13*KO; *tubular cells – Sertoli cells along with germ cells; peritubular cells – enriched myoid cells; interstitial cells – enriched Leydig cells).*

4.22.3. Increase in different pro-inflammatory genes in scs*Pex13*KO animals as detected by semi-quantitative RT- PCR

Cytokines are polypeptide mediators that function as immune modulators and also have a wide range of other biological activities, such as regulation of differentiation in the testis and orchestration of immune-endocrine interactions in distinct cell types.

In addition, cyclooxygenase 1 and 2 (Co*x1, Cox2*) and their pro-inflammatory products such as prostaglandin E2 (*Pge2*) are implicated in the inflammatory pathogenesis, being involved in the production of interleukins during inflammation. The cyclooxygenases are usually expressed at low undetectable levels in most tissues and cells, but are significantly abundant in inflammatory cells and other cell types after treatment with various stimuli such as lipopolysaccharide (LPS), cytokines, and chemicals [66, 280].

Pro-inflammatory cytokines, interleukins 1α and 6 (*Il1α and Il6*), produced by Sertoli and germ cells, are known to regulate Sertoli cell secretory function and promote germ cell survival. Moreover, *Il1α* secreted by Sertoli [281], is known as mediator of inflammation stimulate Sertoli cell *Trf* (transferin) production, and inhibits Leydig cell steroidogenesis.

Interestingly, *Cox1* and *Cox2* mRNA levels were significantly induced in tubular, peritubular and interstitial cell preparations of testis in scs*Pex13*KO animals (Fig. 42E). In contrast to *Cox* mRNA levels, the *iNos* mRNA was much less expressed in tubular cells than in peritubular or interstitial cells. In the scs*Pex13*KO testis, the *iNos* mRNA levels were slightly increased in peritubular and interstitial cells, but hardly altered in tubular cells (Fig. 42E).

The cytokines *Il1α* and *Il6* were already expressed at high levels in tubular cells of scs*Pex13*WT and scs*Pex13*HTZ animals, but only at lower levels in peritubular and interstitial cells (Fig. 42E). The deletion of one *Pex13* allele (HTZ phenotype) did not alter the expression of these cytokines (Fig. 42E). However, the *Il1α* mRNA level was remarkably increased in peritubular and interstitial cells and less pronounced in tubular cells of scs*Pex13*KO mice (Fig. 42E). The mRNA levels for *Il1* and *Il6* were significantly up-regulated in all testicular cell preparations in scsPex13KO animals, indicating proinflammatory conditions in the testis of mutant animals with a defective *Pex13* gene in Sertoli cells (Fig. 42E). Interestingly, the induction of the cytokine mRNA was much more pronounced in comparison to wild type and scs*Pex13*HTZ animals in peritubular and Leydig cells. A similar pattern for mRNA expression of the tumor necrosis factor alpha (*Tnfα*) was observed, with highly basal expression levels in tubular cells of control and HTZ animals and a strong induction in all testicular cell preparations of scsPex13KO mice (Fig. 42E). The mRNA

encoding the macrophage migration inhibitory factor (*Mif*) also showed the highest basal expression level in tubular cells in scs*Pex13*WT and HTZ animals. The *Mif* mRNA level was strongly induced in tubular cells, but less in peritubular and interstitial cells of scs*Pex13*KO animals (Fig. 42E).

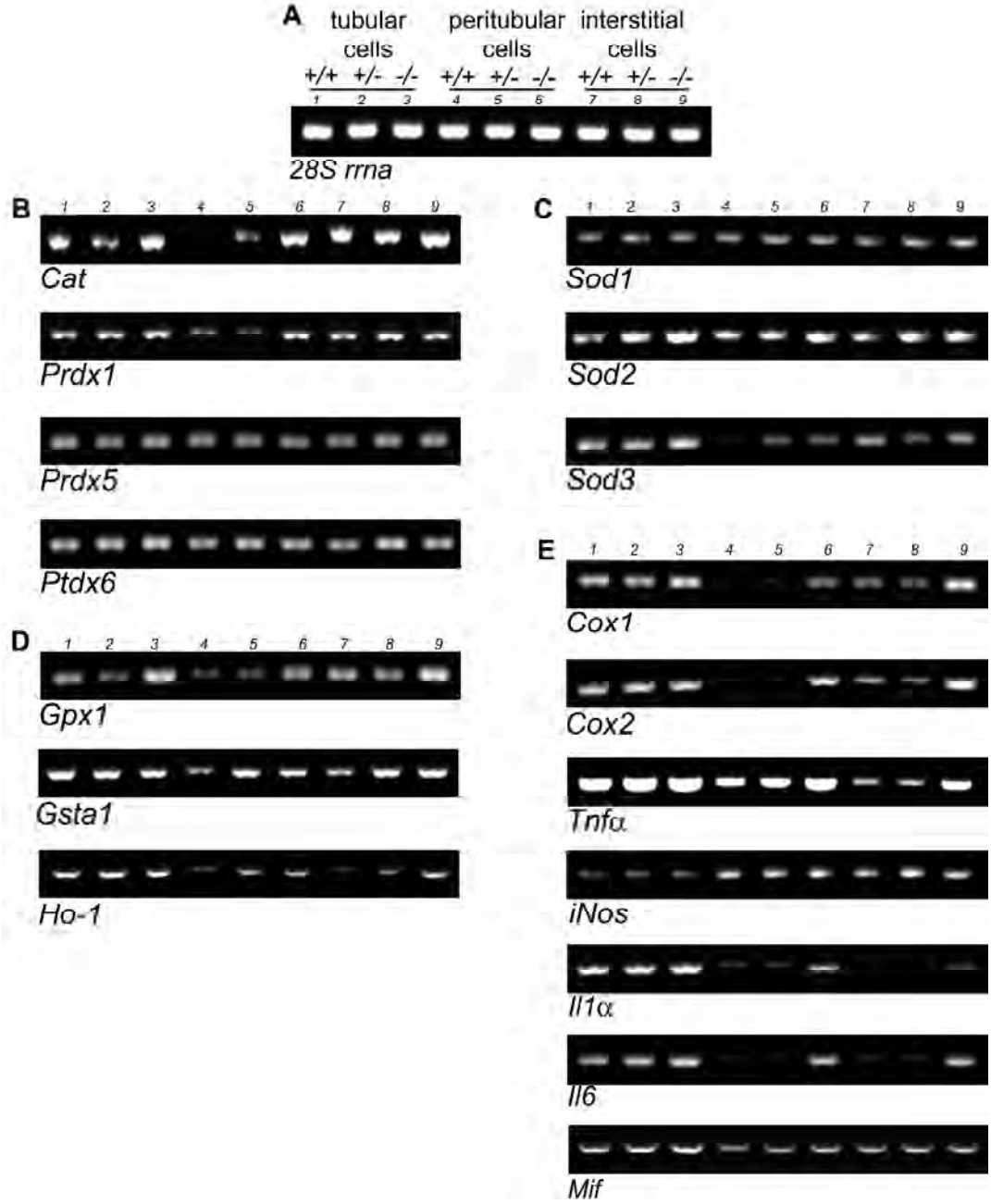

Figure 42: Semiquantitative RT-PCR analysis of total RNA preparations of distinct testicular cell preparation of mice with distinct genotypes. (A) *28Sr rna* as internal control. **(B-D)** mRNAs encoding anti-oxidant enzymes: **(B)** mRNAs encoding peroxisomal catalase *(Cat);* mRNA of peroxiredoxins 1, 5, 6 *(PrdX1, 5, 6)*; **(C)** mRNAs encoding superoxide dismutases 1-3 (*Sod1-3*) **(D)** mRNAs encoding glutatione peroxidase1 (*Gpx1*); Glutatione S - transferase1 (*Gsta1*) and Heme oxygenase-1 (*Ho-1*) **(E)** mRNAs encoding pro-inflammatory genes: cyclooxygenase 1, 2 *(Cox1, 2)*; tumor necrosis factor alpha (*Tnfα*); inducible nitric oxide synthase *(iNos)*; cytokines: interleukin-1α (*Il1α*) and interleukin-6 (*Il6*); macrophage migration inhibitory factor (*Mif*). (+/+: scs*Pex13*WT; +/-: scs*Pex13*HTZ; -/-: scs*Pex13*KO; *tubular cells – Sertoli cells along with germ cells; peritubular cells – enriched myoid cells; interstitial cells – enriched Leydig cells).*

4.22.4. Activation of *Ppar* mRNA levels in scs*Pex13*KO mice

The PPAR nuclear hormone receptor family constitutes of three distinct subtypes *Pparα*, *Pparβ* /*Pparδ* and *Pparγ,* encoded by separate genes [282]. Their activation leads to altered expression of genes with roles in cell metabolism, cell growth and stress response (e.g. fatty acid oxidation is regulated by activation of *Ppars* [283]). These nuclear hormone receptors form heterodimers with *Rxrβ,* after ligand binding allowing the nuclear translocation and the activation of gene transcription. The expression of the *Ppars* and *Rxrs* was studied at the mRNA level in cell preparations of 130 day-old mice from all three genotypes. The three *Ppar* transcripts were present in all cell types under baseline conditions. *Pparα* showed the highest expression in interstitial cells, followed by tubular cells. The highest baseline level of *Pparβ* mRNA was noted in tubular cells. *Pparγ* showed a similar baseline distribution as *Pparα*, however, with lower levels in all cell types, especially in peritubular cells. In all cell types of scsPex13KO animals the mRNA levels of *Pparα* and *Pparγ* were significantly increased. Interestingly, *Pparβ* mRNA, the PPAR family member that is thought to be constitutively expressed in most tissues showed the strongest up-regulation of all *Ppars* members. *Pparβ* was drastically upregulated in tubular cells of scsPex13KO animals, whereas it was weaker induced in interstitial cells and not at all in peritubular cells (Fig. 43). The mRNA levels of the receptors of *Rxr* family (α, β, γ) were not clearly altered. In scs*Pex13*KO, *Rxrα* was inconsistently up- or down-regulated in comparison to scs*Pex13*HTZ animals.

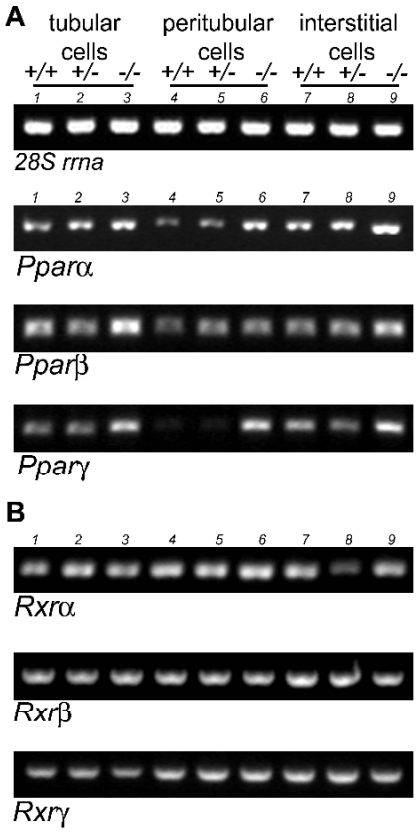

Figure 43: Semiquantitative RT-PCR analysis on total RNA of distinct cell preparations of mice with different genotypes. (A) *28S rrna* as internal control; *PPAR α, β, γ:* peroxisome proliferator-activated receptors; **(B)** *RXR α, β, γ:* retinoid X receptors. (+/+: scs*Pex13*WT; +/-: scs*Pex13*HTZ; -/-: scs*Pex13*KO; *tubular cells – Sertoli cells along with germ cells; peritubular cells – enriched myoid cells; interstitial cells – enriched Leydig cell)*

4.22.5. Alteration of testicular steroidogenesis and Sertoli cell homeostasis in scs*Pex13KO* mice

The process of spermatogenesis, steroidogenesis and the overall testicular functions are regulated by a complex interplay of the endocrine system (hypothalamus-pituitary-gonad axis) in which GnRH stimulates the secretion of the pituitary hormones, LH and FSH, which in turn act at the level of the testis on Leydig and Sertoli cells respectively. In addition to the endocrine control of testicular function, local testicular steroids, proteins and peptides called paracrine–autocrine factors coordinate the various functions of the different testicular cell types and/or modulate the testicular actions of pituitary gonadotropins according to local conditions and requirements. Furthermore, secretory functions of Sertoli cells are often modulated by the presence or absence of particular germ cell types [52, 284].

Quantitative RT-PCR analysis of the FSH-receptor (*Fsh-r*), LH-receptor (*Lh-r*), mast/stem cell growth factor receptor *(Kit)* and *3β-Hsd* using tubular, peritubular and interstitial cell preparation demonstrated the high quality of the cellular isolation procedure. The tubular cells specifically exhibited high levels of *Fsh-r* and *Kit* mRNA, while the interstitial cells showed abundant *Lh-r* and 3*β-Hsd* mRNA expression in scs*Pex13*WT and HTZ mice. The peritubular cells were not labeled *for Kit*-ligand *(Kitl), Lh-r* or *3β-Hsd* (Fig. 44A).

In scs*Pex13*KO mice, transferrin (*Trf*) which is a paracrine–autocrine regulator of testicular function was up-regulated in all cell preparations. The mRNA of another regulator, α-inhibin (*Inha*), was increased in the tubular cell preparation but was decreased in interstitial cells from the testis of the mutant mice. Furthermore, the level of sulphated glycoprotein 2 (*Spg2*) was studied revealing significant differences of basal mRNA levels in distinct cell preparations. In addition, the *Sgp2 mRNA* level was strongly induced in tubular and interstitial cell preparation of scs*Pex13*KO animals, in contrast to peritubular cells in which it was not altered at all (Fig. 44B).

Futhermore, important regulators of steroidogenesis, belonging to the transcription factors of *Gata* family were studied. The level of *Gata1* mRNA was slightly increased in tubular cells and was not altered in peritubular and interstitial cells in scs*Pex13*KO animals (Fig. 44B). The mRNA level for *Gata4*, was present in higher amounts in tubular cells and showed an increase in tubular cells of scs*Pex13*KO animals. An up-regulation of *Gata4* mRNA occurred also in interstitial cells of scs*Pex13*KO animals in comparison to scs*Pex13*HTZ animals, whereas in peritubular cells this mRNA showed the lowest basal expression level and was not altered in scs*Pex13*KO animals. The transcription factor Gata4 can also regulate some promoters via a synergistic interaction with the nuclear receptor steroidogenic factor 1 (Sf1) [285]. The basal *Sf1* mRNA levels were highest in tubular cells, followed by interstitial cells and peritubular cells in scs*Pex13*WT and HTZ animals. The *Sf1* mRNA levels were up-

regulated in all testicular cells preparations of scs*Pex13*KO mice compared to the WT and HTZ mice (Fig. 44B).

Thereafter, the mRNA levels of several key enzymes involved in steroid metabolism were analyzed. The PCR reactions revealed a significant increase in *Star* and *CYP450scc* mRNA levels in testicular tubular, peritubular and interstitial cells of the scs*Pex13*KO mice (Fig. 44C). Whereas, the *CYP450scc* mRNA was induced at similar levels in all cell types, the Star mRNA was strongly up-regulated in tubular and peritubular cells, while its mRNA was only slightly elevated in interstitial cells. The *CYP450c17* mRNA level was significantly increased in testicular tubular and peritubular cells fractions of the mutant animals and was hardly altered in interstitial cells (Fig. 44B). Furthermore, the *CYP450arom* mRNA was a significantly down-regulated in scs*Pex13*KO testicular tubular cells compared to a slight increase in peritubular and no change in interstitial cell preparations (Fig. 44C). Although the *3β-Hsd* mRNA is a specific marker for Leydig cells (interstitial cell preparations) under control conditions, the expression level of *3β-Hsd* mRNA was increased in all testicular cell preparation of the scs*Pex13*KO mice. The induced bands of the *3β-Hsd* mRNA were however much weaker in tubular and peritubular cells in comparison to the interstitial cell preparation of scs*Pex13*KO mice (Fig. 44B).

In addition, some of the genes exerting a crucial role in germ cell differentiation were studied. In the adult testis, *Kit* mRNA expression was observed in type A spermatogonia as well as in late primary spermatocytes, secondary spermatocytes and round spermatids. In contrast, somatic Sertoli cells that support the growth and differentiation of germ cells express kit ligand *(Kitl)* [286]. Expression of *KIT* mRNA was noted in tubular and peritubular cells of scs*Pex13*WT and HTZ mice. In scs*Pex13*KO animals, this mRNA was drastically reduced, revealing the absence of germ cells. *Kit* mRNA was not expressed in interstitial cells in all distinct genotypes. Examination of *Kitl* mRNA in scs*Pex13*WT and HTZ testicular cell fractions indicated the purity of the cell fractions and confirmed the expression pattern of *Kitl* mRNA in the tubular cell fractions. In contrast to control mice, *Kitl* mRNA was detected in the interstitial cell preparation of scs*Pex13*KO animals (Fig. 44B).

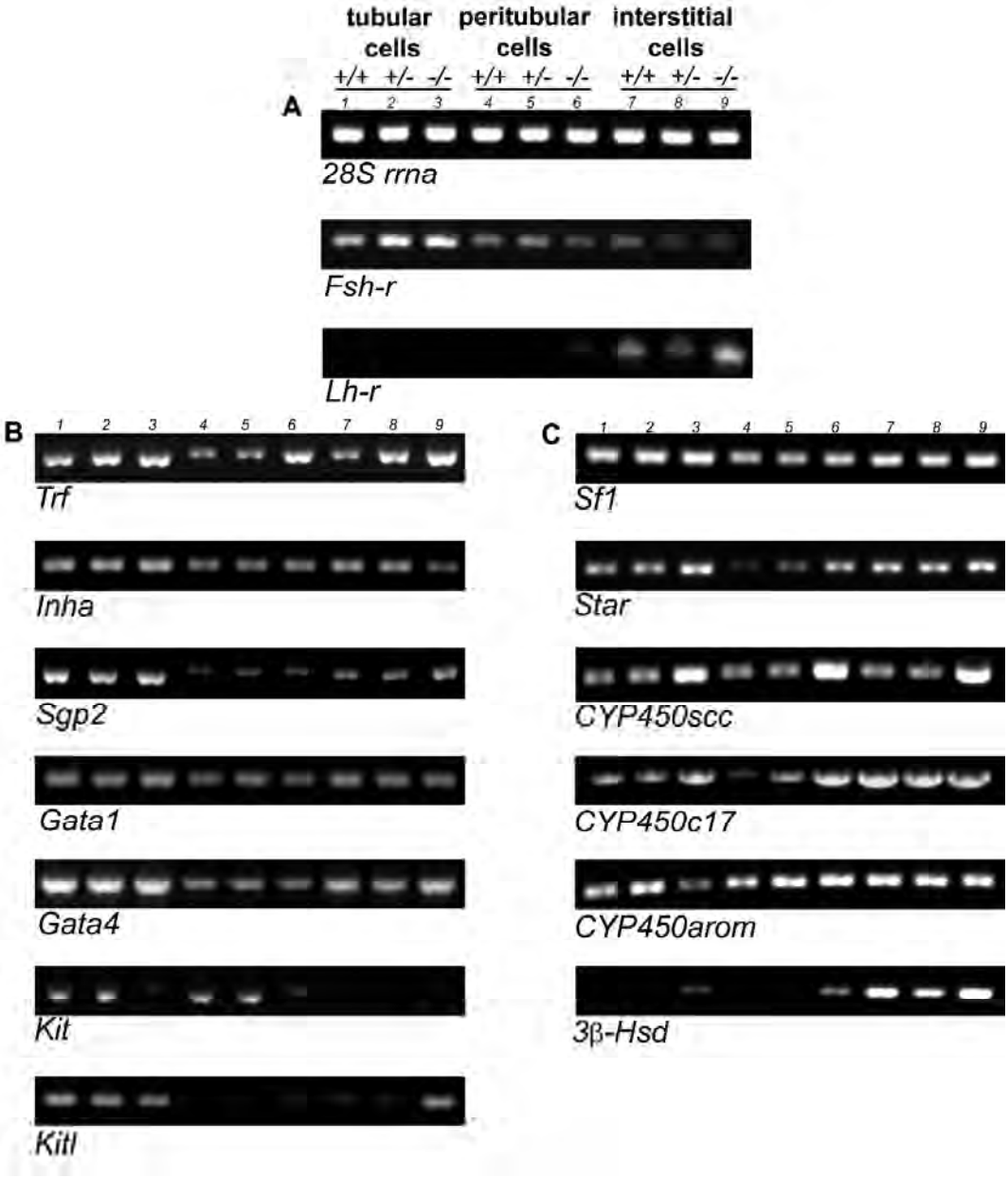

Figure 44: Semiquantitative RT-PCR analysis on mRNA of distinct testicular cell preparations of mice with different scs*Pex13* genotypes. (A) *28S rrna* as internal control; *Fsh-r*: follicle stimulating hormone receptor, *Lh-r:* luteinizing hormone receptor **(B)** Sertoli cell gene markers: *Trf:* transferrin; *Inha:* inhibin A; *Sgp2:* sulphated glycoprotein 2; *GATA1, 4:* transcription factors 1, 4; *Kit:* mast/stem cell growth factor receptor; *Kitl*: mast/stem cell growth factor receptor ligand. **(C)** Genes involved in steroidogenesis: *Sf-1:* steroidogenic factor 1; *Star:* steroidogenic acut regulator protein; *P450scc:* cytochrome P450 side cholesterol cleavage; *P450c17:* cytochrome P450c17; *P450arom*: cytochrome P450aromatas; *3β-Hsd:* 3β hydroxysteroid dehydrogenases. (+/+: scs*Pex13*WT; +/-: scs*PEX13*HTZ; -/-: scs*PEX13*KO; *tubular cells – Sertoli cells along with germ cells; peritubular cells – enriched myoid cells; interstitial cells – enriched Leydig cells).*

4.23. Measurements of the steroids reveal a strong accumulation of DHEA in the testis of scs*Pex13*KO animals

The strong Leydig cell proliferation in the interstitial space of the testis of scs*Pex13*KO animals, which developed gradually during postnatal development of the animals (from P30 to P130), already suggested that alteration of steroid synthesis might occur in scs*Pex13*KO animals. The T and androgen precursors levels were measured in serum and testis homogenates from 130 day-old mice and were compared between scs*Pex13*KO, HTZ and WT animals. Interestingly, T levels in serum revealed no significant difference between distinct mouse genotypes. The T values served further as internal standards in order to calculate relative values of other steroid precursor concentrations.

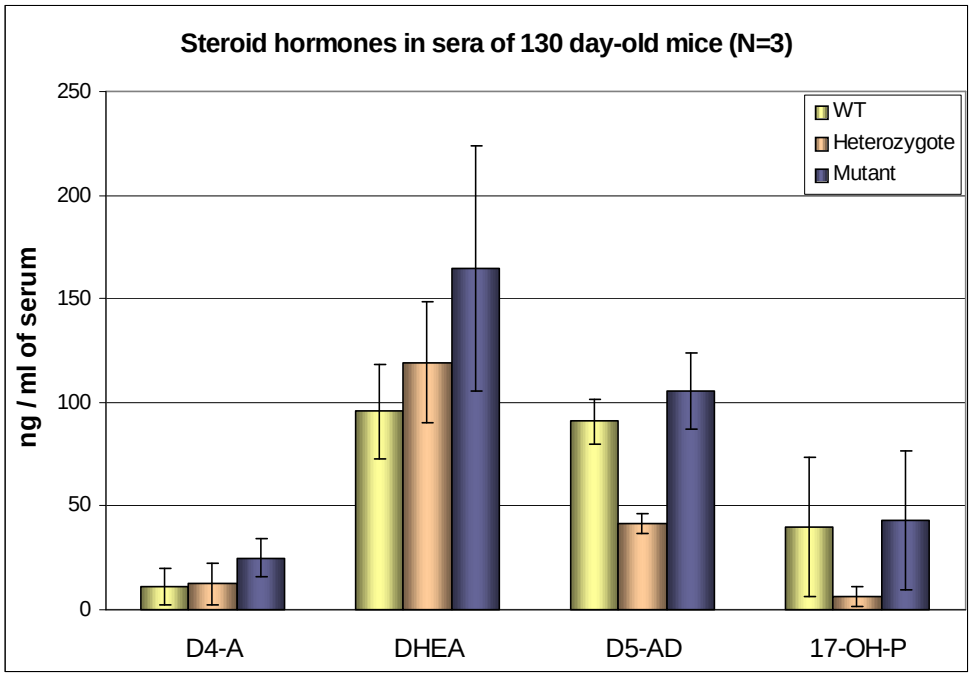

Figure 45: Steroid hormone quantification in sera of 130 day-old mice. WT: scs*Pex13*WT, HTZ: scs*Pex13* heterozygot mice, KO: scs*Pex13*KO. **(A)** Testosterone (T) quantification in the testis homogenates. **(B)** Quantification of Δ4-A: androstenedione, DEAH: dehydroepiandrosterone, Δ5-A: androstanediol, 17OH-P: 17-hydroxypregnenolone. Number of animals delaminated n=3.

Furthermore, steroid measurements were performed also in testis homogenates for the quantification of 17OH-P, 17OH-Pre, DEHA, Δ5-AD, Δ4-A, T and DHT. Again, the T concentration showed no change in testis homogenates between distinct genotypes (Fig. 46A). The T values served further as internal standards in order to calculate relative values of other steroid precursor concentrations. Among all steroid precursors which were quantified, DHEA showed a dramatic increase in concentration in testis homogenates of scs*Pex13*KO. In addition, the final steroid of the Δ5 pathway, Δ5-AD was found at a significant low level in scs*Pex13*KO testis homogenates. Levels of others steroid precursors such as 17OH-P, 17OH-Pre and Δ4-A were significant decreased in scs*Pex13*KO testis homogenates. Finally, DHT levels were not altered in testis of scs*Pex13* animals (Fig. 46B).

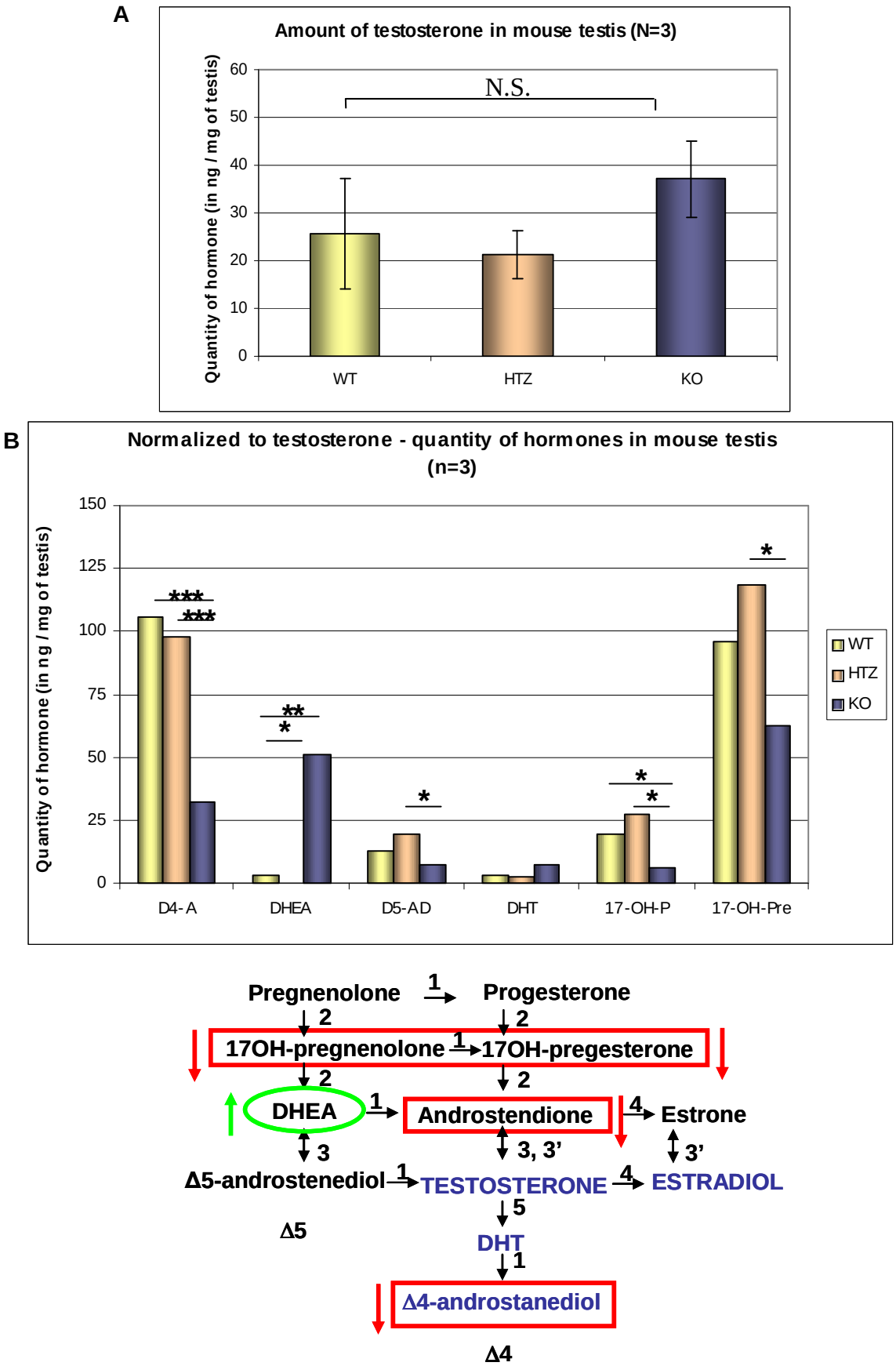

Figure 46: Steroid quantification in testis homogenates. WT: scs*Pex13*WT, HTZ: scs*Pex13* heterozygote mice, KO: scs*Pex13*KO. **(A)** Testosterone quantification in testis homogenates. (N.S no significant). **(B)** Quantification of Δ4-A: androstenedione, DHEA: dehydroepiandrosterone, Δ5-A: androstenediol, DHT: dyhydrotestosterone, 17OP: 17-hydroxypregnenolone, 17OH-Pre: 17-hydroxyprogesterone. Reaction 1: 3β-

hydroxysteroid dehydrogenase; Reaction 2: cytochrome P450 17α-hydroxylase; Reaction 3: family of 17β-hydroxysteroid dehydrogenase; Reaction 4: cytochrome P450 aromatase; Reaction 5: 5α-reductase. Number of animals used n=3. (* p ≤ 0.05, ** p ≤ 0.01, **** p ≤ 0.001).

"Virtual" activities of steroidogenic enzymes were calculated according to the different metabolite amounts and conversion rates. These calculations suggested no alterations of the CYP450 17α-hydroxylase of Δ4 pathway, whereas in the Δ5 pathway with high DHEA levels, it appeared strongly increased. The 3β-HSD of Δ5 pathway, converting 17-OH-Pre to 17-OH-P was increased in some animals, but the overall value was not significantly altered on a p ≤ 0.05 basis. In contrast, the calculalated activity of the 3β-HSD of Δ4, converting DHEA to 4-A was significantly higher in scs*Pex13*KO testis homogenates, resulting from an enhanced production of T by Δ4 pathway. Due to the strong up-regulation of the Δ4 pathway the quantity of T and DHT produced by the testis of scs*Pex13*KO was in normal range, comparable to WT and HTZ animals. The calculated strong down-regulation of the 17β–HSD would be in complete agreement with a loss of the peroxisomal 17βHSD4 (dehydrogenase function of the multi-functional protein 2) in Sertoli cells due to the *Pex13* knockout (Fig. 47).

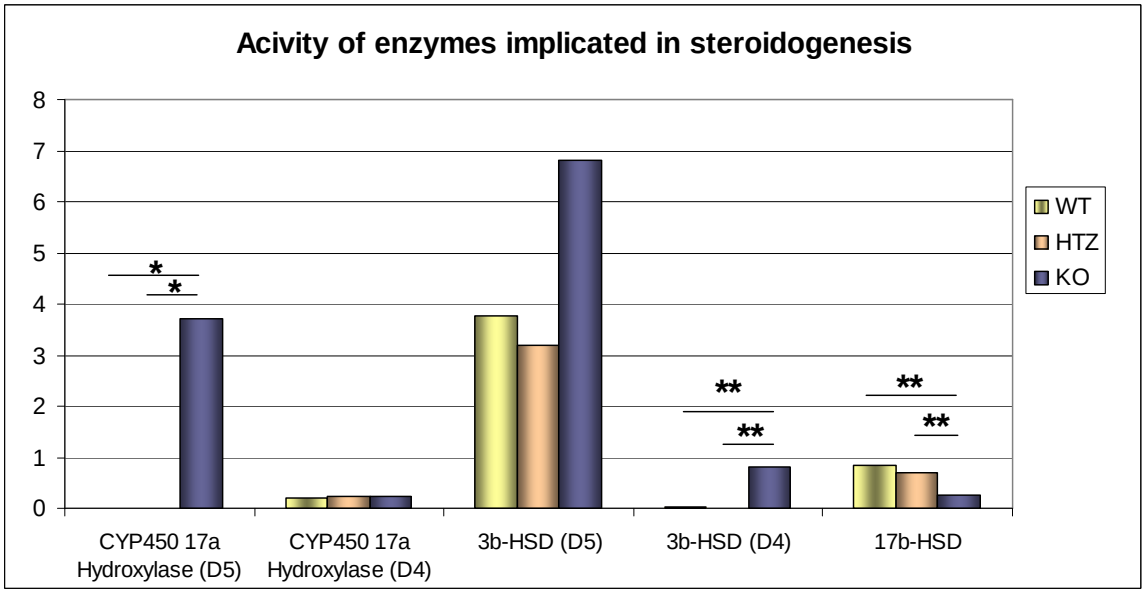

Figure 47: "Virtual calculated" activities of the steroidogenic enzymes. CYP450 17α hydroxylase / Δ5 (cytochrome P450c17 / delta 5 pathway), CYP450 17α hydroxylase / Δ4 (cytochrome P450c17 / delta 4 pathway), 3β-HSD (3β-hydroxysteroid dehydrogenase / delta 5 pathway), 3β-HSD (3β-hydroxysteroid dehydrogenase / delta 4 pathway), 17β-HSD (17β-hydroxysteroid dehydrogenase). (* p ≤ 0.05, ** p ≤ 0.01, **** p ≤ 0.001). (N=3)

4.24. Detection of reactive oxygen species (ROS) in primary Sertoli cell cultures

4.24.1 Functional peroxisomes are required for ROS homeostasis in murine Sertoli cell primary culture

Since the isolation of 98% pure and functional Sertoli cells is not possible from adult animals and only few Sertoli cells can be isolated from individual KO mice at postnatal day 15, we decided to use a *Pex13* siRNA knockdown approach in Sertoli cells of WT animals in primary

cell culture. For this purpose 15 animals at P15 were used to isolate juvenile Sertoli cells. Even though those cells are not completely comparable to the mature highly differentiated Sertoli cells, the peroxisome compartment is already well established in primary cell cultures [134]. In addition, changes of peroxisomes markers in Sertoli cells were observed in 15 day-old scs*Pex13*KO testis, showing already that ABCD3 is very weakly labeled by IF. Establishment of the conditions for the Pex13 knockdown was done with two different *Pex13* small interfering RNAs (siRNAs) over a range of 24 -96 hours with one and two subsequent transfections of the siRNA. Such long times were necessary since the half life of peroxisomes was described as three days and effects on protein levels should therefore only be visible after this time period. The optimal conditions for siRNA transfection were as follows: *Pex13* siRNA with two transfections (1st for 24 h, 2nd for 48h), harvesting the cells at 72h for protein analysis.

The juvenile Sertoli cells transfected with siRNAs specific for the *Pex13* gene showed a significant reduction in the PEX13 protein levels after 4 days of transfection (knock-down of 50% of the original value in the peroxisome enriched fraction P2 as shown by WB analyses) (Fig. 48D). Corresponding control groups without transfection (Opti-MEM) and with transfection of a non-sense scrambled siRNA (scr siRNA) revealed no effect on PEX13 protein abundance (Fig. 48D). Also in IF preparations, the PEX13 were significantly down-regulated, wherefore peroxisomes could hardly be detected anymore with the antibody against this protein in *Pex13*-siRNA transfected cells. In contrast, the organelles were clearly visible in both control preparations in a punctuated staining pattern in Sertoli cells (Fig. 48A-B). In addition to PEX13, the level of PEX14, which forms the docking complex together with PEX13 on the peroxisomal membrane, was reduced by 50% in the enriched peroxisomal fraction (P2) after siRNA transfection. Interestingly, both proteins were identified at similar levels in the P1 fraction in comparison to scr-siRNA treatment, indicating the presence of larger and old peroxisomes in the enriched heavy mitochondrial fraction P1 and the decrease of smaller organelles in the (P2) fraction (Fig. 48D). In addition, the protein levels of both ABCD1 and ABCD3 transporters were reduced by half in the (P2) fraction containing enriched peroxisomes in *Pex13* siRNA transfected cells compared to the control groups. Also peroxisomal matrix proteins were altered in a similar pattern. The peroxisomal β-oxidation enzyme ACOX1 was decreased by 50% in the (P2) fractions of *Pex13* siRNA treated cells. Finally, a reduction in CAT protein levels of more than 50% was observed in the peroxisomal fraction (P2) of the *Pex13* siRNA group (Fig.48 E). Interestingly, after the knock-down of *Pex13*, the CAT protein was observed also in the enriched heavy mitochondrial fraction P1 in a considerable amount.

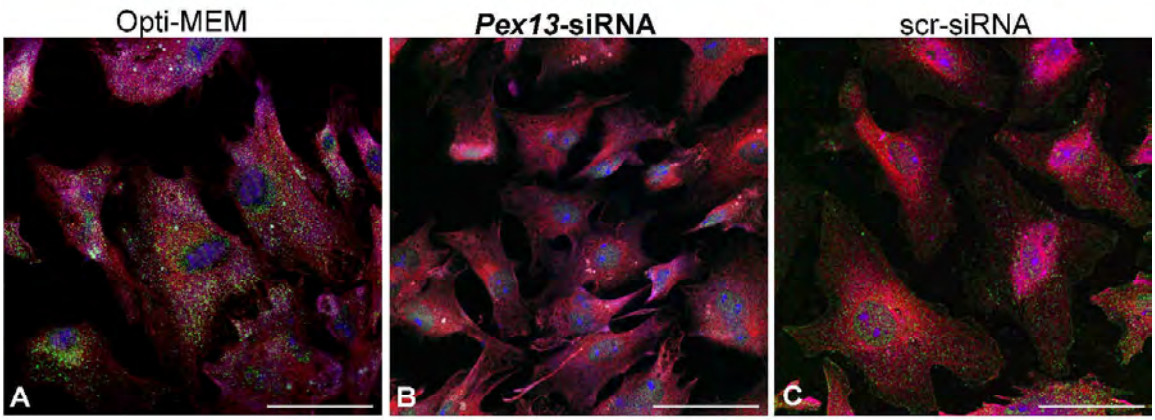

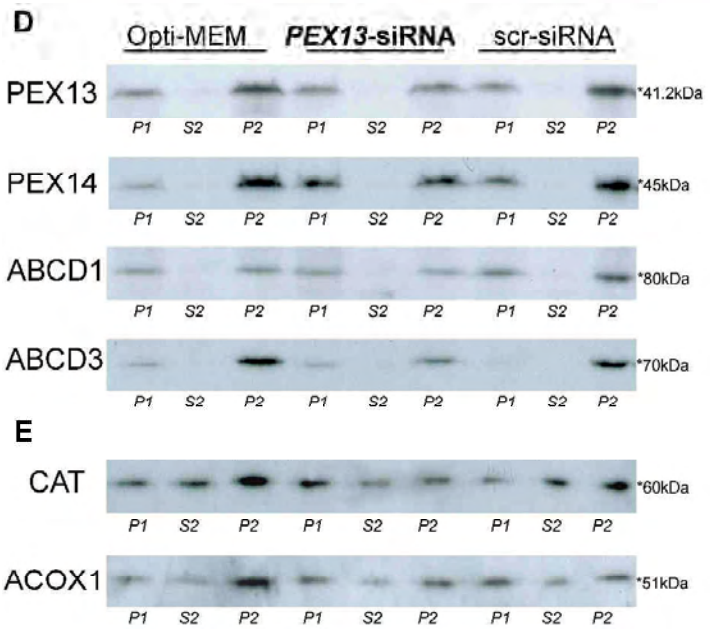

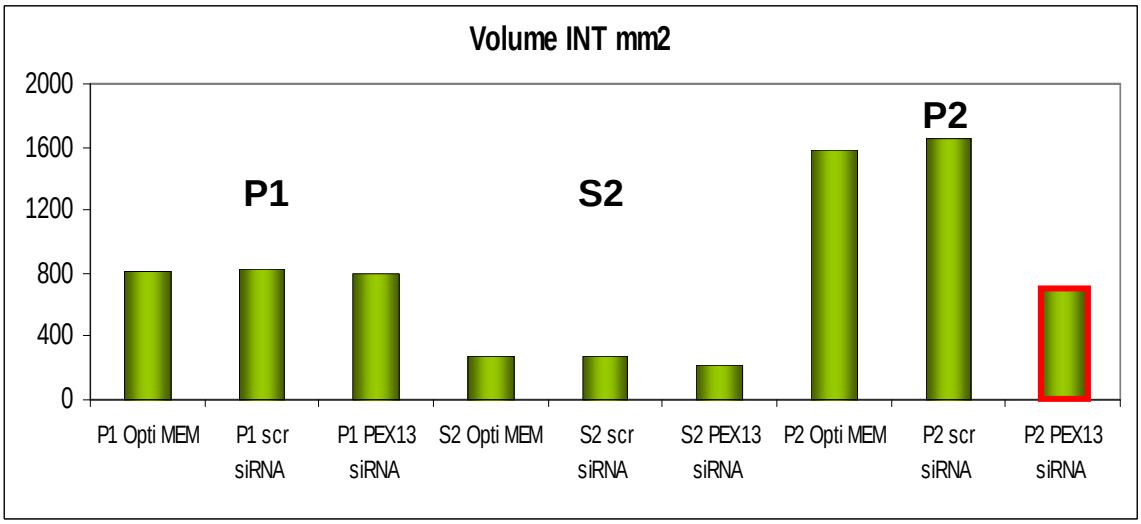

Figure 48: Effects of a *Pex13* gene knockdown on isolated Sertoli cells in primary culture. Cell cultures isolated from P15-testis, transfected twice (1st transfection for 24h, 2nd transfection for 48h) with *Pex13*-siRNA and scr-siRNA. The negative control cell culture was incubated with Opti-MEM medium only. Following the siRNA treatment the cells were fixed with 4%PFA, permeabilized and therafter used for IF analyses. **(A-C)** IF staining for PEX13 localization: **(A)** Sertoli cells incubated only with Opti-MEM. **(B)** Sertoli cells transfected with *Pex13*-siRNA. **(C)** Sertoli cells transfected with scr-siRNA. **(D-E)** Western blots analyses with specific antibodies against

different peroxisomal proteins. (5µg in each lane) **(D)** Peroxisomal membrane proteins: PEX13– peroxin 13; PEX14 - peroxin 14; ABCD1 – peroxisomal adrenoleukodystrophy protein / (ATP-binding cassette transporters, sub family D, member 1) ABCD3 – 70 kDa peroxisomal membrane protein / (ATP-binding cassette, sub family D, member 3). **(E)** ACOX1- Acyl-CoA oxidase 1, 51kDa indicates the B subunit; CAT - catalase. Bars represent in A, C 21µm and B 25µm. *(P1: nuclear and enriched heavily mitochondrial fraction; S2: supernatant with microsomes and cytosolic proteins fraction; P2: enriched peroxisomal and light mitochondria fraction).*

4.24.2. Mitochondrial ROS production is increased in Sertoli cells with *Pex13* knockdown

As shown by double-IF staining for mitochondrial SOD2 and VIM, Sertoli cells with a *Pex13*-siRNA knockdown exhibited a massive increase in the staining of the mitochondrial compartment and a proliferation of these organelles, building an extensive mitochondrial network (Fig. 49). Cells transfected with scr-siRNA only exhibited a slightly elevated SOD2 protein level, compared to control cells groups, but showed no mitochondrial proliferation. In the WB analyses a slight increase of the SOD2 protein was noted in *Pex13*-siRNA and scr-siRNA treated cultures in P1 and P2 fractions, whereas a higher amount of SOD2 was noted in S2 in *Pex13*-knockdown cells, in comparison with scr-siRNA cells. This alterations suggest that the mitochondrial network, observed in the IF analysis, was fragmented into smaller pieces during homogenization and the SOD2 protein got released into the cytoplasmic fraction of Sertoli cells. This is supported by the fact that Complex III of mitochondrial respiratory chain is increased mainly in the (P2) fraction and that no broken membranes are found in (S2) of *Pex13*-siRNA treated cells (Fig. 49D).

In the comparison to the mitochondrial SOD2, the cytoplasmic SOD1, of which a small portion is also confined under stress conditions to the peroxisomal matrix, was up-regulated at the protein level in the cytoplasmic fraction (S2) and slightly also in P1 of *Pex13*-siRNA treated primary Sertoli cells (Fig. 49D). The increase in SOD1 in the P1 fraction might indicate a shift of this protein into large peroxisomes, in a similar way as it was seen also for the peroxisomal CAT in cells with *Pex13*-siRNA knockdown (Fig. 49E).

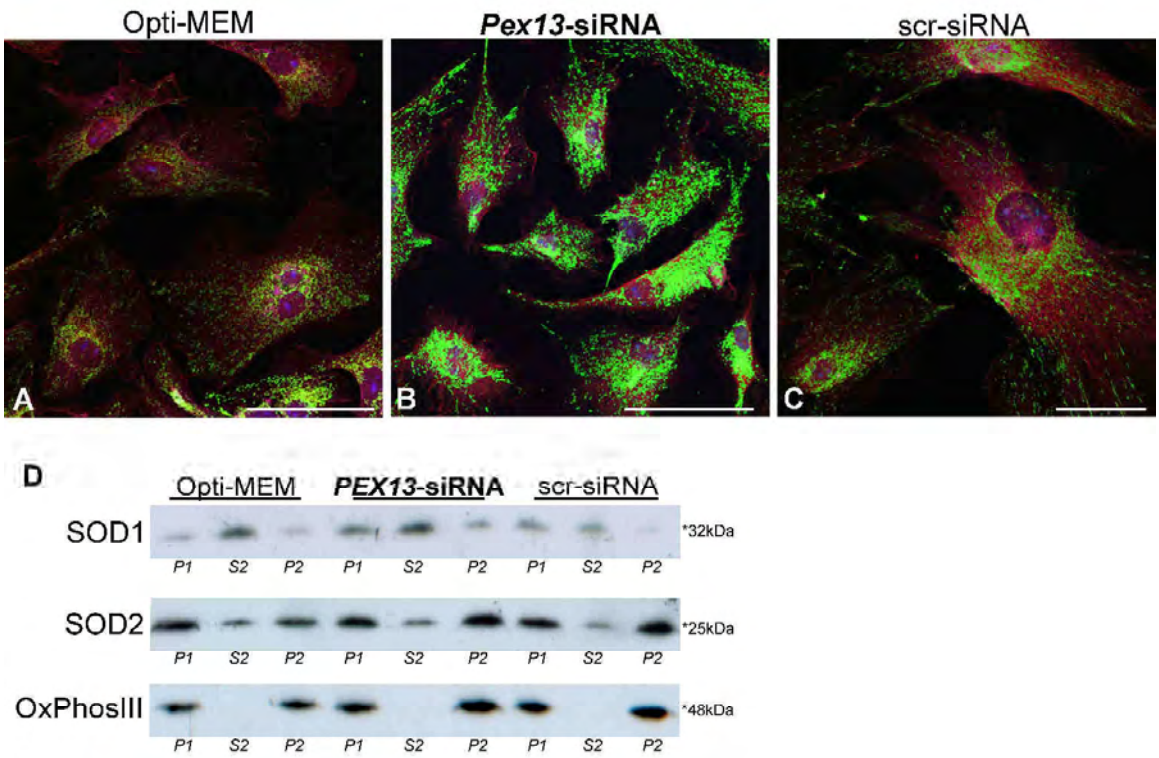

Figure 49: Increased antioxidant enzymes and proliferated mitochondria in primary Sertoli cell cultures with *Pex13* gene knockdown. Cell cultures isolated from P15-testis. The cells were transfected for tow times with *Pex13*-siRNA and scr-siRNA. The control cell cultures were incubated only with Opti-MEM medium. Following the siRNA treatment the cells were fixed with 4%PFA, permeabilized and used for IF analyses. **(A-C)** Double immunoflorescence staining for SOD2 and VIM of Sertoli cell cultures: **(A)** Sertoli cells incubated only with Opti-MEM. **(B)** Sertoli cells transfected with *Pex13*-siRNA. **(C)** Sertoli cells transfected with scr-siRNA. **(D)** Western blot analyses (cells were lysed and equivalent amounts of protein (5µg) were loaded onto 12.5% gels, separated with SDS-PAGE and elecrotransferred to PVD membranes, which were processed for immunoblot analyses, stripped several times and reprobed for: SOD1 superoxide dismutase 1; SOD2 - Superoxide dismutase 2; OxPhosIII - oxidat. phosphorylation complex III. Bars represent in A, B 25 µm and in C 18 µm. *(P1: nuclear and enriched heavy mitochondrial fraction; S2: supernatant fraction with microsomes and cytosolic proteins; P2: enriched peroxisomal and light mitochondrial fraction).*

Since mitochondria were proliferating and antioxidant proteins were up-regulated, the overall cellular ROS production was quantified by using dihydroethidium (DHE) staining in primary Sertoli cells with *Pex13*-siRNA knockdown in comparison to Opti-mem and scr-siRNA treated cells. Compared to the Opti-MEM group of cells, the ROS activity in scr-siRNA was already increased ($p<0.001$) by 50%, suggesting intracellular stress by the siRNA transfection reagent. However, in comparison with the value of scr-siRNA treated cells, *Pex13*-siRNA knock-down of the peroxisomal compartment lead to a further 80% ($p<0.001$) increase in ROS suggesting that this increase was indeed exerted by the *Pex13* knockdown (Fig. 50). The overall increase of ROS between Opti-MEM and scr-siRNA as well as between scr-siRNA and *Pex13*-siRNA treated cells was clearly visible in fluorescence pictures of DHE-stained cells (manly in perinuclear areas).

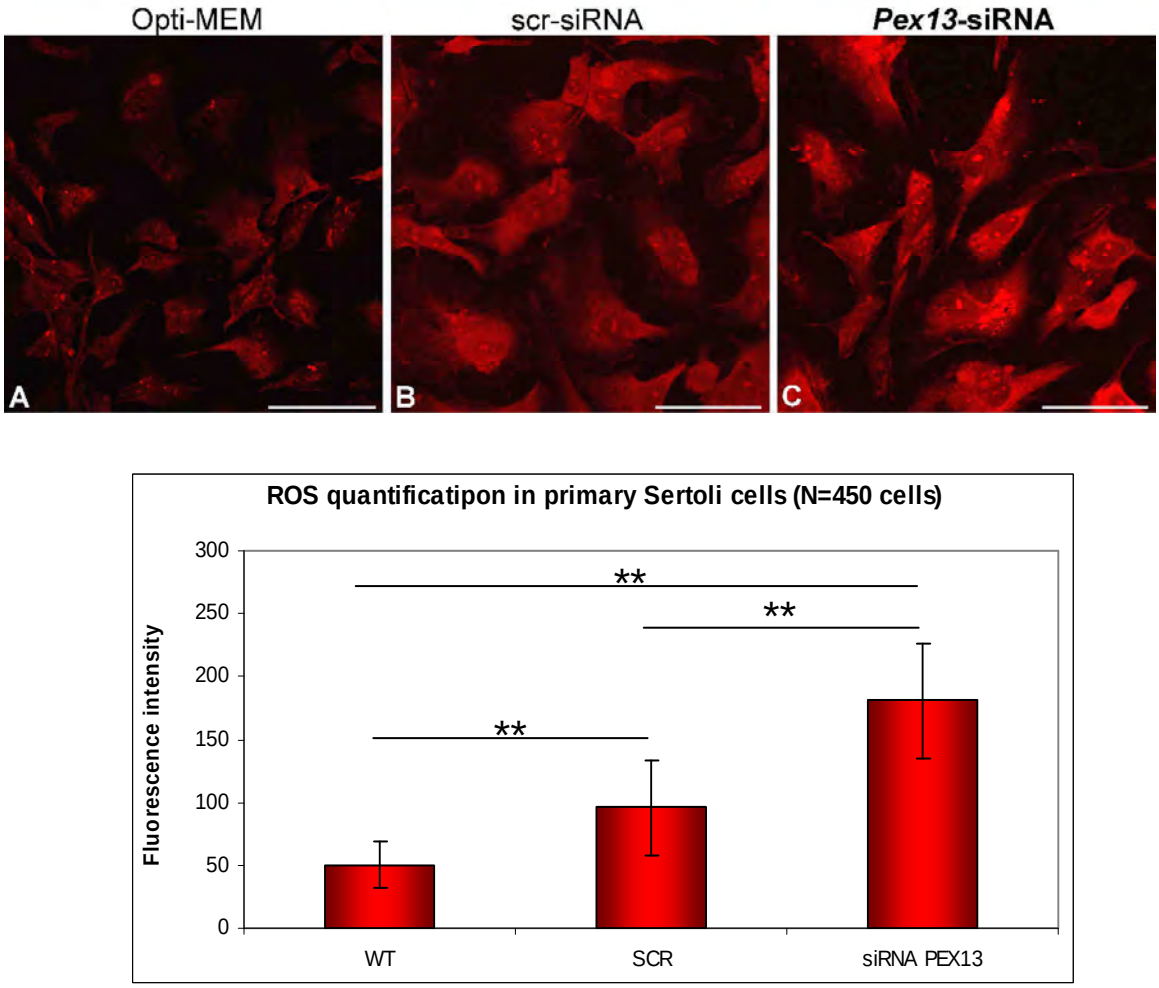

Figure 50: Measurement of ROS production by relative CLSM quantification of dihydroethidium stained Sertoli cells after different siRNA treatments. Cell cultures isolated from P15-testis. The cells were transfected two times with *Pex13*-siRNA and scr-siRNA. The control cell cultures were incubated with Opti-MEM only. **(A-C)** Following the siRNA treatment the cells were stained with DHE for 30 min. The pictures shown were captured with Leica TCS2 CLSM and the quantification of the fluorescence intensity was done with the appropriated Leica CLSM software. **(D)** Quantification of ROS production. Bars represent in A-C 25 µm. (* $p \leq 0.05$, ** $p \leq 0.01$, **** $p \leq 0.001$).

5. Discussion

The significance of peroxisomal metabolism for male fertility is accentuated by the impairment of spermatogenesis and severe testicular pathologies present in patients with peroxisomal dysfunction [251]. However, until the beginning of the experimental work of this thesis, only sparse information was available on this organelle and its physiological functions in the testis. Therefore, the protein composition of peroxisomes in distinct testicular somatic cell types was studied, as well as in germ cells, where peroxisomes were searched for, and there alteration during spermatogenesis and spermiogenesis was discovered. In addition, a new animal model for infertility due to the peroxisomal deficiency in Sertoli cells was generated with the *Cre-loxP* technology and the excision of the *exon 2* of the peroxisomal biogenesis *Pex13* gene. With the help of this model, the clear necessity of the regular peroxisomal metabolic pathways was observed for androgene precursor synthesis, Sertoli communication to other cell types as well as survival of germ cells in the seminiferous epithelium was identified. This study provides the essential evidence that peroxisomes in Sertoli cells are a prerequisite for normal male fertility.

The first part of the discussion will concentrate on peroxisome distribution and enzyme composition as well as gene regulation in normal wild type animals.

The second part of the discussion will focus on the pathological alterations excerted on various cell types in the testis as well as on metabolic, signaling and communication pathways due to *Pex13* gene knockout and peroxisome deficiency in Sertoli cells.

Part I. Peroxisomes in wild type mice and man

5.1. Peroxisomes are present in all cell types of the testis

In the testis, peroxisomes have been investigated by routine electron microscopy or by visualization of the marker protein catalase [36, 101, 287, 288]. Based on these studies peroxisomes of the testis were thought to be restricted to Leydig cells.

Because catalase is the most abundant peroxisomal protein in many tissues it is commonly used as a marker to identify peroxisomes. Using this marker, peroxisomes of the testis had been identified in Leydig cells [36, 262, 288-290]. Only recently peroxisomes were discovered also in Sertoli cells and spermatogonia by use of an alternative marker protein (ABCD3) in combination with more sensitive methods [291-293]. Due to the fact that peroxisomes could not be visualized in germ cells in later stages of spermatogenesis with this marker, the significance of these organelles for normal spermatogenesis has been questioned.

However, peroxisomes are present in all somatic cell types of the testis and all developing germ cells (except for mature spermatozoa) and they differ in their protein composition in a

cell type-specific fashion [134, 291, 293]. We have established that biogenesis proteins on the peroxisomal membrane, such as the peroxins 13 and 14 (PEX13 and PEX14), are excellent markers for the visualization of peroxisomes in the testis. Antibodies against PEX13 also allowed the identification of peroxisomes at the ultrastructural level and indeed showed a specific labelling of the membrane in cross-sectioned profiles of peroxisomes in all testicular cell types. Even very small peroxisomes of spermatids with similar size to the endoplasmic reticulum could be labeled. In addition, clusters of peroxisomes were detected in late stages of spermiogenesis (step 16 spermatids) or in residual bodies.

5.2. Peroxisomal enzyme content is heterogeneous, resulting in different metabolic functions of this organelle in distinct cell types of the testis

Peroxisomes are versatile organelles and change their enzyme compositions according to the needs of specific cell types and organs (for a review, see [234]). At least in hepatocytes the abundance and the enzyme composition of this intracellular compartment is differentiation-dependent, a process that seems to be influenced by PPARα [294]. Similarly, in the present study, significant differences in the expression of mRNAs encoding peroxisomal ABC-transporters and enzymes or in protein composition of these organelles were observed in distinct cell types of the testis. These differences were conserved between mouse and man, suggestive of a complementary or alternative function of peroxisomal metabolism in different testicular cell types. Marked differences have been observed in the protein and/or mRNA distributions of the peroxisomal ABC-transporters (ABCD1-4), the acyl-CoA oxidase 2 (ACOX2) of the β-oxidation pathway 2 and catalase (CAT).

5.3. Calatase in Leydig cells as an antioxidative enzyme for the protection of steroid synthesis?

In Leydig cells peroxisomes are often elongated as tubules and are sometimes hardly larger in diameter than dilated segments of the sER [36, 262]. As indicated also by our results, peroxisomes in Leydig cells contain the highest amount of catalase protein and are often interconnected with each other.

A network-like distribution of these organelles was already proposed by Mendis-Handagama and colleagues [262]. Interestingly, peroxisomes in Leydig cells proliferate upon LH treatment, whereas LH-deprivation results in a significant decrease in the number of these organelles. In addition, an increase of free cholesterol was noted in peroxisomes and mitochondria after LH treatment. Moreover, Mendis-Handagama and Ariyaratne (2005) speculated that testicular steroid synthesis could occur at least in part in peroxisomes and also described the presence of SCP2 in peroxisomes [79].

For steroid synthesis the high abundance of catalase may be necessary and beneficial for Leydig cells, since catalase is an antioxidant enzyme with very high capacity to metabolize H_2O_2. Increased levels of intracellular H_2O_2 in Leydig cells have been shown to inhibit steroidogenesis via blockage of the mitochondrial cytochrome P450scc activity and StAR protein expression [295]. Since peroxisomes house a variety of other antioxidative enzyme systems [296], further studies are necessary to clarify their importance in the regulation of Leydig cell functions.

5.4. Peroxisomal metabolism in cells of the seminiferous epithelium: Sertoli cell peroxisomes as protectors against lipid toxicity

The mRNAs for *Acox2* and the ABC-transporters *Abcd1* and *Abcd3* are highly expressed in isolated P14 Sertoli cells compared to other somatic cell types. In addition, *Abcd2* is much more strongly expressed in tubular cells than in peritubular cells. Furthermore, the antibody against ABCD1 stained Sertoli cells exclusively, whereas the one for ABCD3 labelled the complete basal compartment of the seminiferous tubules. These results are in agreement with the observation that in patients with X-linked adrenoleukodystrophy, the first pathological alteration seems to occur in Sertoli cells as “vacuolation” before the spermatogenetic arrest develops and Leydig cells are also affected [249]. The results of this thesis show that within the seminiferous epithelium several enzymes of the β-oxidation pathways and lipid transporters are abundant in Sertoli cells. This is in accordance with the localization of *PPARα*, a nuclear receptor and the transcriptional regulator of genes for peroxisomal β-oxidation pathway 1 enzymes in the seminiferous tubules, which also shows strong expression in Sertoli cells [297]. *PPARα*-mediated proliferation of peroxisomes could result in a rapid degradation of potential *PPARα* lipid ligands leading to the maintenance of a signaling-lipid homeostasis in the seminiferous epithelium by a feed-back mechanism. As mentioned above a precise control of the homeostasis of lipid derivatives in the seminiferous tubules seems to be essential for the survival of the seminiferous epithelium. Especially prostaglandins are potential regulators of spermatogenesis [298]. This is also of relevance to our results, since the β-oxidation enzymes of pathway 1 are able to degrade these eicosanoids (for a current review see [299]). Indeed this thesis shows that THIOLASE A is also present in germ cells in the seminiferous epithelium until late stages of spermiogenesis. With the presence of these enzymes germ cells might be able to regulate their intracellular levels of lipid signalling molecules.

5.5. Peroxisomes are present in germ cells and undergo significant alterations during spermiogenesis

Using antibodies against PEX13 and PEX14 in mouse and human testis we could show the presence of peroxisomes in germ cells up to late stages of spermiogenesis (step 16 spermatids). Co-labeling of GFP-fluorescence in peroxisomes of GFP-PTS1 transgenic mice with PEX14 in these organelles at the light-microscopical level indicates that the labelled peroxisomal membrane structures are indeed small, but import competent peroxisomes. Clear evidence for the peroxisomal nature of these particles was obtained by post-embedding protein A-gold immunocytochemistry with anti-GFP, anti-PEX13- or anti-catalase antibodies.

The presence of functional peroxisomes in maturing spermatids suggests that these organelles might be involved in the biosynthesis of plasmalogens (ether lipids) for protection of spermatids against reactive oxygen species. Azoospermia due to spermatogenic arrest at the level of spermatocytes in mice with a knockout of the *Gnpat* (DHAPAT) gene, encoding a peroxisomal enzyme of ether lipid synthesis, support this hypothesis [258]. In addition, peroxisomes in germ cells might cooperate with the endoplasmic reticulum in the synthesis of polyunsaturated fatty acids in larger quantities necessary for the integration into sphingomyelin that is essential for normal sperm function [300, 301]. Close spatial association between ER-segments and small, tubular peroxisomal profiles were frequently found in this thesis in maturing spermatids at the ultrastructural level, thus supporting this hypothesis.

Futhermore, peroxisomes in the germinal epithelium might also be involved in the control of tubular polyamine abundance or D-aspartate levels in elongated spermatids, since polyamine oxidase and D-aspartate oxidase are peroxisomal enzymes [299, 302]. In this respect for the seminiferous epithelium it is of interest that distinct polyamine levels (e.g. spermidine) are suggested to play an important role in cell proliferation and apoptosis [303].

The immunoreactivity of CAT is clearly present in spermatogonia and Sertoli cells, but could only be detected with high concentrations of antibodies in spermatocytes or early spermatids in light-microscopical preparations. Catalase immunoreactivity was clearly present in late spermatids (step 14-16) where it is localized in network-like clusters. These clusters are consistently labelled with antibodies against peroxisomal proteins (PEX13, PEX14, ABCD3, CAT, THIOLASE) and contain the imported GFP in the peroxisomal matrix in GFP-PTS1 transgenic animals. Peroxisomal profiles in these clusters are similar or often smaller in size than ER and frequently exhibit double-membraned loop structures. Clusters of small peroxisomes, peroxisomal tubular profiles with low catalase content and double-membraned loops are not new structures (for a review, see [304]). In contrast they are frequently found in tissues closely associated with lipid metabolism (such as lipid-synthesizing glands) [305,

306] in fetal tissues or in conditions associated with peroxisome proliferation (for a literature survey see discussion sections in [228, 307]). Serial section analysis revealed that double-membraned loops represent terminal cup-shaped segments of the peroxisomal compartment that are sometimes devoided of CAT but are labelled for peroxisomal membrane proteins [228, 305].

The results of this thesis show that only few, but aggregated peroxisomal clusters are present in residual bodies (Fig. 4G), most probably being phagocytosed and degraded by Sertoli cells. Selective staining of Sertoli cells for the lysosomal protein cathepsin D [293] and the autophagosomal protein LAMP2 in addition to labelling of the acrosome (Fig. 3F) supports this hypothesis. The genes involved in the regulation of the aggregation and clustering process of peroxisomes in late spermatids are unknown. However, it is known from studies with knockout animals that Pex11-proteins exert strong effects on peroxisomal abundance, size and structure. Indeed, absence of PEX11α/β leads to a decrease in peroxisomal number and an increase in the size of the particles and more interestingly overexpression of PEX11γ leads to strong reduction and clustering of almost all peroxisomes in an individual cell [308, 309]. In addition, *Pex11γ* mRNA is strongly expressed in the testis [308]. Future studies on PEX11 proteins in germ cells will reveal, whether PEX11γ is involved in the clustering process.

5.6. The heterogeneity in peroxisomal enzyme content is conserved in mouse and man

This thesis demonstrates that peroxisomes can be visualized by immunofluorescence also in Bouin-fixed, paraffin-embedded human tissue. The enzymatic heterogeneity of peroxisomes is conserved in mouse and man. The distribution pattern of peroxisomes in the human seminiferous epithelium is best recognized with PEX13 or PEX14 as well as with other marker enzymes. Comparable to the mouse the peroxisomal staining pattern is dependent on stages of the seminiferous epithelium with the peroxisomal compartment undergoing similar significant alterations during maturation of spermatids. Clusters of peroxisomal profiles also appear in late spermatids prior to segregation into residual bodies in human preparations. The cell type-specific conservation of peroxisomal metabolic pathways suggests that mouse models can indeed be used to investigate the molecular pathogenesis of peroxisome-related infertility. All described mouse models with knockout of genes involved in peroxisomal biogenesis exhibit almost identical phenotypes to those observed in corresponding patients (for a recent review, see [255]). Similar to human peroxisomal disorders, male knockout mice with single enzyme defects in peroxisomal lipid metabolism are infertile [228, 258, 259].

Part II: Physiological role of peroxisome in testis

5.7. Deficiency of peroxisomes in Sertoli cells and alterations of peroxisomal metabolic markers

All reported mice with generalized inactivation of *Pex* genes involved in PTS1- dependent matrix protein import such as *Pex5*-, *Pex2*-, *Pex13*-knockouts were described to be excellent animals models for ZS, the most severe peroxisome biogenesis disorder. Some of the features of ZS observed in patients, like cryptorchidism and testicular defects, could not be investigated in *Pex*-KO animals since they need postnatal growth and developmental of the mice. However, postnatal studies have been impossible in *Pex*-KO animals because of the lethality of mice shortly after birth. In this context generating a conditional knockout of *Pex13* specifically in Sertoli cells proved to be an indispensable necessity for functional studies of peroxisomes with impact on cell-cell interactions during testicular development and spermatogenesis. The *Pex13* gene deletion, leading to peroxisomal deficiency in Sertoli cells, was verified by a variety of methods in this thesis such as genomic PCR screening of the *Pex13* gene in different organs as testis, liver, tail and particularly in the microdissected seminiferous tubules from different phenotypes of mice. In addition IF stainings and Western blot analyses confirmed the absence of the PEX13 protein in Sertoli cells of scs*Pex13*KO animals. Futhermore, all of these methods confirmed the specificity of the *Pex13* knockout in Sertoli cells. *Cre*-mediated deletion of both alleles of *Pex13* gene in Sertoli cells showed profound effects on spermatogenesis as well as the biochemical and endocrinological alterations in animals older than three months. The expression of a single *Pex13*-allele in scs*Pex13*HTZ male animals was found to be sufficient for proper testicular homeostasis.

At the age of 130 days, the scs*Pex13*KO mice exhibit a normal developed genital tract with descended testis in the scrotum, but testes volume and weight were significantly reduced in those mice. The cryptorchidism that appears in ZS patients in comparison to scs*Pex13*KO mice can be explained by the *Pex13* gene mutation solitary in Sertoli cells with the possibility that functional other testicular cells types are compensating more severe alterations of endocrinological parameters or intercellular communication pathways.

Selective elimination of *Pex13* gene in Sertoli cells resulted in lipid accumulation, vacuolation of these cells and proliferation of the Leydig cells, histological aspects that have been reported in a variety of other testicular disorders [310] and essential fatty acid deficiency [311]. Indeed, in ZS and X-ALD/AMN patients, all these aspects have been described [251]. In addition, proliferated Leydig cells in these patients are degenerated due to severe VLCFA and fatty acid crystal accumulation since peroxisomes are absent from these cells in ZS patients. In contrast, peroxisomes in Leydig cells of scs*Pex13*KO mice protect against fatty degeneration and cell death, whereas strong accumulation of VLCFA (C24 and C26:0) occurs in Sertoli cells, leading to germ cell death. In addition, phytanic as

well as pristanic acids amounts were also increased, suggesting a metabolic defect in both α- and β-oxidation in Sertoli cells. This metabolic defect was indeed proven by the mis-targeting of β-oxidation enzymes in the Sertoli cell cytoplasm (ACOX1) or degradation of the enzymes into the cytoplasm (THIOLASE) in IF preparations and Western blot analyses.

Interestingly, in scs*Pex13*KO mice the results of the VLCFA measurements are in complete agreement with the elevated concentrations of the VLCFA observed by Aversa and colleagues in X-ALD/AMN patients [251]. The lesions described in those patients consisted of degenerative changes of seminiferous tubules including hypocellularity and mild vacuolation of seminiferous tubules, maturation arrest and Sertoli cell abnormalities associated with infertility. In addition, in these patients interstitial cells were damaged and showed lamellar lipid profiles in Leydig cells and a reduction of the number of Leydig cell clusters. [247]. In one case report of adult-onset cerebral X-ALD a severe impairment of spermatogenesis was seen with rapid progression to azoospermia [251]. In contrast, the genetic inactivation of adrenoleukodystrophy gene (*Aldp / Abcd1*) in KO mice leads to the accumulation of VLCFA in nervous tissue, but these animals do not develop a testicular phenotype. Interestingly, in the testis of *Pex7* KO mice a disorganisation of the seminiferous epithelium was described and the mice were infertile [312] and double KO mice for *Pex7:Abcd1* showed a much more severe pathology with disorganized seminiferous epithelium, Leydig cell hyperplasia and VLCFA accumulation [313]. The types of VLCFA in the testis of 60 day-old *Pex7:Abcd1* double KO mice were similar to the ones found in testis of 130 day-old scs*Pex13*KO mice in this study. The testicular defects in *Pex7:Abcd1* KO animals occur due to the generalized double knockout of the *Pex7:Abcd1* genes in all cells of the testis and as well in other tissues. The pathological alterations in those animals also occur much earlier than in *Pex7* KO testis [313]. Even though in scs*Pex13*KO mice the severe alteration of the testis developed much later, the pathological modifications in the testis are similar to *Pex7:Abcd1* KO mice suggesting that peroxisomal function specifically in Sertoli cells plays an important role in VLCFA metabolism, the degradation of other fatty acids, regulating the lipid homeostasis of the seminiferous epithelium and protecting against the fatty acid toxicity. As shown in this thesis, Sertoli cells lacking functional peroxisomes are indeed disturbed in PPAR regulation and influence intercellular communication leading to hyperplasia of the Leydig cells and influencing stereidogenesis (see later in the thesis). A recent study suggested a crucial role of plasmalogens in normal spermatocyte development and in their protection from damage caused by VLCFA accumulation [313]. Interestingly, plasmalogen levels showed a slight increase in concentration in the total testis homogenate of scs*Pex13*KO mice, suggesting that proliferated Leydig cells over-compensated plasmalogen deficiency in scs*Pex13*KO animals. Only MALDiT-TOF imaging with the possibility of spatial resolution of lipid deficiencies or accumulations could clarify the exact

nature of the lipid alterations in the testis of scs*Pex13*KO animals. However, until now only very limited knowledge is available on this technique for lipid detection and no good protocols are available for “lipid” imaging.

Previous limited studies in mice with a Sertoli cell-specific knockout of *Pex5,* encoding the cytoplasmic receptor for the import of peroxisomal matrix proteins containing a PTS1, indicated an accumulation of lipids in Sertoli cells already develops at P10 and precedes the arrest of spermatogenesis [259]. Indeed, in scs*Pex13*KO the apparition of lipid vacuoles occurred in the early pre-pubertal testis (P15) and it increased in size in the pubertal and early adult period before first signs of spermatogenic arrest were identified at P90 in scs*Pex13* animals. Accumulation of fatty acids in Sertoli cells is especially prominent in stages of the seminiferous epithelium in which the residual bodies are phagocytosed by these cells and in which peroxisomal β-oxidation is essential to degrade these lipids, since mitochondria are not capable of VLCFA activation and oxidation. Due to this fact Sertoli cells most probably are over-loaded with VLCFA in each cycle of the seminiferous epithelium, where spermatozoa are released and residual bodies are phagocytosed. Therefore, the discrete alterations in Sertoli cells in the P15 testis can easily be explained, since the first wave of sperm release occurs in the mouse testis at ~ 35 days of age.

In scs*Pex*13KO model the up-regulation of *KITL* mRNA in the interstitial cells fraction encoding a protein, known to be involved in Leydig cell proliferation, confirmed the hyperplasia of this type of cell [314]. Several studies showed that the occurrence of proliferated Leydig cells appeared to parallel the extent of loss of the Sertoli cells and also that of the thickening of the lamina propria with peritubular cells [315]. Hyperplasia of Leydig cells associated with germ cell depletion has also been reported in human and mouse infertilities. In particular, the Sertoli cell-only syndrome, a form of non-obstructive azoospermia, is the most serious male infertility, in which the patients have small testes with azoospermia caused by depletion of germ cells and frequently show Leydig cell hyperplasia [316-319]. Furthermore, it has been shown that Sertoli cells within tubules containing aberrant Leydig cells were always immature and no spermatogenesis occurred within their immediate vicinity in the adult testis [320]. Therefore, the Leydig cell hyperplasia observed in the scs*Pex13*KO mouse is likely caused by a secondary effect of the mutation of the *Pex13* gene mediated in Sertoli cells by germ cell depletion rather than direct effect of the specific peroxisomal *Pex13* gene mutation in Sertoli cells, influencing the homeostasis of Leydig cells, although the latter possibility cannot be excluded.

5.8. Alterations of peroxisomal proteins in Sertoli cells and inducible expression of the ABCD-transporters in Leydig cells of the scs*Pex13*KO

Severe modification in the abundance and distribution of peroxisomal proteins were observed in scs*Pex13*KO animals by using antibodies against various peroxisomal proteins for immunostaining or Western blot experiments. Interestingly, in addition to PEX13, PEX14, another protein of the docking complex and the cytoplasmic PTS1 receptor PEX5 were absent from the Sertoli cells suggesting that these proteins were degraded in Sertoli cells and that the PTS1 dependent import of matrix proteins was disturbed. This notion can be further supported by a strongly reduced PEX14 staining in IF preparations in Sertoli cells and by labeling of only few peroxisomal membrane ghosts around lipid droplets with antibodies against ABCD3. The mRNA of peroxisomal ABC half-transporters *Abcd2*, *Abcd3* and *Abcd4* was altered upon the *Pex13*KO in Sertoli cells. Most prominent elevations of the mRNA were observed for *Abcd4* and less strongly for *Abcd2* in Sertoli cells. The *Abcd3* mRNA level was slightly decreased in Sertoli cells. This notion can be further supported by a strongly reduced ABCD3 protein straining of preparations in Sertoli cells by labeling only few peroxisomal membrane ghosts around lipid droplets. A significant up-regulation of *Abcd3* and *Abcd4* was noted in proliferated Leydig cells in scs*Pex13*KO mice. Interestingly, in wild type animals, *Abcd3* was not highly expressed in interstitial cells – Leydig cells [134]. This is consistent with the strong staining of Leydig cells with the antibody against ABCD3 in testis sections of scs*Pex13*KO animals. Remarkably, *Abcd4* mRNA was dramatically up-regulated in Sertoli cells as well as in Leydig cells of scs*Pex13*KO mice, whereas *Abcd4* mRNA was not present in Leydig cells of scs*Pex13*WT and scs*Pex13*HTZ mice.

As reported in the literature the expression of different ABCDs can vary depending on cell type, function and metabolic conditions of the cell [134]. In human tissues the *Abcd4* mRNA is expressed at highest levels in the lung and testis, followed by the kidney [321]. However, no information is available regarding the physiological role of this peroxisomal half-transporter. In addition, in a recent study the subcellular localization of ABCD4 in peroxisomes has been questioned and its localization was attributed to the ER. The hydrophobic properties of NH2-terminal regions were suggested to determine its subcellular localization [322], indicating that ABCD4 might not reside in peroxisomal membranes. However, further morphological studies with a good antibody against this protein are needed to clarify where the endogenous ABCD4 protein is indeed localized in ER. Over-expression of the proteins using recombinant DNA technology such as used also in the mentioned publication, sometimes results in mis-targeting of the expressed proteins to incorrect sub-compartments, leading to misinterpretation of their correct localization. Over-expression has also been used to study the function of ABCD2 and ABCD3 that exhibit partial functional redundancy with ABCD1, compensating each other for VLCFA transport [321]. Others,

studies have showed that ABCD3 transports long-chain acyl-CoA (LCFA-CoA) across the peroxisomal membrane [323]. Many genes involved in lipid metabolism, including *Abcd* genes, are regulated by transcription factors like PPARs or by sterol regulatory element-binding proteins (SREBPs) involved in metabolism of fatty acids and cholesterol [324]. Indeed, the pharmacological induction of the *Abcd2* gene by fibrates through the activation of PPARα and SREBP2 has been demonstrated in rodent liver [325]. In contrast, in liver of male rodent it was shown recently that the mechanism of Abcd2 induction independently of PPARα [326]. The results from this thesis are in accordance with these publications where the *Pparα* mRNA was strongly induced in all cell types of the testis, while ABCD2 is only minor affected in peritubular and Leydig cells. In distinction with Abcd3, a PPARα dependent gene was strongly up-regulated in all cell types in scs*Pex13*KO animals. The accumulation of variety of "peroxisome-metabolized" fatty acid derivatives in Sertoli cells due to the *Pex13* knockout in combination with the increased apoptosis of germ cells seem to trigger the strong induction of the *Abcd3* and *Abcd4* genes in this cell type. The strong up-regulation of *Abcd3* and *Abcd4* transporters in Leydig cells most probably counteracts the VLCFA accumulation.

In contrast to the situation in mice, it should be noted that the human *Abcd3* gene lacks an apparent PPAR-responsive element (PPRE), suggesting that this gene must be regulated by additional mechanism [327]. This would allow hypothesizing that this might be indeed by a SREBP-mediated mechanism, which might at least partly also be responsible for the induction of the *Abcd2*, *Abcd3* and *Abcd4* and *Acox1* genes in the testis of scs*Pex13*KO mice. Interestingly, *Srebps* were mainly induced in Sertoli cells in scs*Pex13*KO animals, whereas activated *Ppars* were more widely activated, also in peritubular and Leydig cells (except for *Pparβ* in peritubular cells). The role of the distinct PPAR family members in the testis is not yet understood. However, PPARα and PPARγ have been implicated in the regulation of fatty acids metabolism in other organ systems.

Since the *Pparα* gene was induced in scs*Pex13*Ko animals, the up-regulation in tubular cells of enzymes of the *Pparα* dependent β-oxidation pathway I, such as ACOX1 and THIOLASE, can be explained. THIOLASE protein was severely decreased in tubular cells, most probably due to its mis-targeting and degradation in the cytoplasm of Sertoli cells. In contrast, ACOX1 and CAT are still present after mis-targeting in the cytoplasm. The cytoplasmic localization of enzymes in cells with peroxisome deficiency is a well-known phenomenon [328].

In contrast to the ACOX1 of the first β-oxidation pathway, the one for ACOX2, the enzyme regulating the flux in the second β-oxidation pathway involved in side-chain oxidation of cholesterol and branched-chain FA degradation, was down-regulated in both Sertoli and Leydig cells. Indeed, branched FA also accumulated in the testis of scs*Pex13*KO mice. Interestingly, already single-enzyme deficiencies in the β-oxidation pathways lead to several

alterations of male fertility. In this respect, *Acox1* KO mice showed a reduction in Leydig cell population, hypospermatogenesis, and infertility. However, no changes in Sertoli cells were reported [257]. In contrast, *Mfp2* knockouts gradually developed a complete fatty degeneration of the seminiferous epithelium, whereas Leydig cell function was preserved [259]. This KO mouse demonstrates the importance of *Mfp2* for the protection of the germinal epithelium in the tubuli of the testis. Interestingly, MFP2 enzyme is functioning in addition to FA degradation in the dehydrogenation of 17β-OH-steroids. A part of this enzyme was isolated and described as 17β-OH-HSD4, being involved in conversion of estradiol to estrone in Leydig cells [329]. A function of this enzyme in androgen synthesis has not been described until now. The results of this thesis, however, suggest that *Mfp2* might be involved in Δ5 androgen synthesis pathway since large amounts of DHEA accumulated in testis of scs*Pex13*KO animals. This could be the first evidence that peroxisomes might be essential for the regulation of streroidogenesis in different somatic cell types of testis, since a massive up-regulation of the mRNA for steroidogenic transcription factors and enzyme occurred in absence of peroxisomes in Sertoli cells. Interestingly, the accumulating DHEA and DHEA sulphate are strong inducer of peroxisome proliferation, at least in liver [330], suggesting that peroxisomes abundance might control the level of this important androgen precursor in the testis and the flux through different androgen synthesis pathways.

5.9. Functional significance of peroxisomes in steroidogenesis and alteration of related signaling pathways in scs*Pex13*KO mice

The lipid accumulation in seminiferous tubules and in proliferating Leydig cells of scs*Pex13*KO mice was associated with the up-regulation of FSH- and LH- receptors. Under normal condition FSH interaction with its receptor (FSH-R) in Sertoli cells induces an increase in cyclic AMP (cAMP) production [331], transferrin [332], α-inhibin [333] and calcium mobilization [334]. Indeed, our results show that in addition to the FSH-R up-regulation, all other autocrine and paracrine factors such as transferrin, α-inhibin and SGP-2 were increased in Sertoli cells of scs*Pex13*KO mice. Former *in vitro* studies from the literature ruled out that a direct action of the gonadotrophic hormone on Leydig cells occurs and supported the presence of a Sertoli cell-secreted nonsteroid factor that would influence testicular androgen production. To date, more than 40 factors have been described, among them inhibin and transferrin, that modulate testicular functions through autocrine, intracrine and paracrine mechanisms [42]. Therefore, it can be hypothesized that the deficiency of peroxisomes in Sertoli cells leading to pathological alterations in seminiferous tubules, will also affect the homeostasis of autocrine, intracrine and paracrine mechanisms, exerting in turn effects on Leydig cells in the testis of the scs*Pex13*KO mice.

It is well accepted that the regulation of the cAMP level is somatic cells of the testis is primary determined by hormones [335]. In addition, in the testis SF-1 is the transcription factor regulating a variety of cAMP-dependent target genes, including *Cyp450arom* and *Star* [336, 337]. Indeed, in somatic cells of scs*Pex13*KO animals *Sf-1* mRNA expression was drastically up-regulated in Sertoli cells as well as in Leydig cells, and slightly increased in peritubular cells.

In addition, the *Gata4* mRNA levels were induced in Sertoli and Leydig cells and *Gata1* in Sertoli cells of the scs*Pex*13KO testis. The GATA family of proteins is a group of transcription factors emerging as important regulators of steroidogenesis [338]. Within the gonads, GATA-4 plays a role in the steroidogenic function of somatic cells, including fetal / adult Leydig and Sertoli cells [339, 340]. Co-transfection experiments have shown that GATA-4, working alone or in concert with other transcriptional co-activators, can drive the expression of numerous genes involved in gonadal somatic cell function, including MIS [341, 342], α– and β–inhibin subunit genes [343], LH-R [344], StAR [345] P450c17 [346], 3βHSD [285] and DHEA–sulfotransferase (DHEA-S) [347]. In addition to their ability to directly stimulate the transcription of target steroidogenic promoters, GATA-4 can also regulate some of these promoters via a synergistic interaction with the nuclear receptor SF-1 [341, 342]. Both transcription factors GATA and SF-1 are up-regulated in the scs*Pex13*KO testis and appear to exert critical regulatory functions on steroidogenic enzyme gene expression in scs*Pex13*KO animals. The gene expression profiling studies indicated that increased SF-1 influences the adrenal cortex to produce more steroids and selectively modulates the steroid secretion profile by maintaining DHEA-S secretion. SF-1 in conjugation with GATA-4 induces most mRNA levels for steroidogenic enzymes (*Star, Cyp450scc and Cyp450c17, 3βHSD*) in seminiferous tubules as well as in Leydig cells. The induction of the steroidogenic enzymes in Sertoli cells of P130 scs*Pex13*KO mice is also reflected by the positive IF staining of mitochondria with an antibody against CYP450scc. The mechanism behind the strong induction of steroidogenic enzymes could indeed be explained by activation different transcription factors (SF-1, GATA-4) inducing transcription of steroidogenic enzyme gene (*Star, Cyp450scc and Cyp450c17, 3βHSD*) via the cAMP signalling pathway and via a SREBP2-mediated mechanism. Furthermore, the strong increase of non-steroidogenic factors from Sertoli cells of scs*Pex13*KO animals, such as inhibin-α, transferrin, SPG2, KITL could stimulate steroidogenesis and proliferation of Leydig cells as well. Altered Sertoli cell - Leydig cell communication and up-regulation of gonadotropin receptors in both cell types (LH-R and FSH-R) might explain this phenomenon.

In contrast to the mRNAs for all others steroidogenic enzymes, the one for *Cyp450 aromatase*, the enzyme converting androgens to estrogens was decreased in seminferous tubules, suggesting that the steroid synthesis was mainly directed from T to DHT to

guarantee constant DHT-levels in scs*Pex13*KO animals. These hypothesis is supported by the fact that all steroid precursors, except for DHEA, are decreased, whereas T and DHT levels are normal, indicating a high flux through the steroid synthesizing pathway in Sertoli cells in the direction to DHT, to keep up its the level in seminiferous tubules of scs*Pex13*KO mice. Interestingly, both RXR- and PPARγ-selective suppress *P450arom* gene expression in the ovary [348] which would perfectly fit to the results obtained in this thesis, since PPARγ was strongly induced. Furthermore, *Pparα* and *Pparβ* mRNA were also up-regulated. Aromatase knockout (ArKO) mice cannot synthesize endogenous estrogens, wherefore circulating estradiol levels was at the limit of detection and male mice exhibited severe spermatogenesis defects [349, 350]. Another important reason responsible for the low *Cyp450arom* mRNA level is the absence of germ cell in seminiferous tubules of scs*Pex13*KO testis, since *Cyp450arom* is expressed in germ cells of the mouse [336, 351]. Total body fat is also increased in 16 week-old mice in estrogen receptor α and/or β knockout mice [352]. Therefore, the question still remains whether in tubular cells of scs*Pex13*KO mice the low *Cyp450arom* levels result from the PPAR increase or not, and whether altered estradiol concentrations would contribute to germ cell death in scs*Pex13*KO animals. Unfortunately, estradiol levels could not be measured in scs*Pex13*KO testis, due to sensitivity limitations.

5.10. DHEA and estradiol conversion by peroxisome β-oxidation

Already one decade ago the molecular characterization of MFP2 was done using different antibodies against parts of the enzyme with distinct functions. Two groups cloned the cDNA of this protein, coming from two completely different directions: *a)* from isolation of a 17βHDS [97], characterizing the dehydrogenase part of the enzyme and *b)* from isolation of peroxisomal enzyme involved in β-oxidation, characterizing the hydratase part of the enzyme [353]. This enzyme also called D-bifunctional protein, working as the second enzyme in the β-oxidation pathway 2, on the D-form of fatty acid intermediates, oxidized by the acyl-CoA oxidase 2 [354-356]. However, MFP2 was shown to convert estradiol into estrone in human ovarian epithelial cells [357]. These studies proposed that the MFP2 /17βHSD4 peroxisome enzyme could play a role in the liver thereby modulating serum estradiol levels [358, 359]. In addition a former study on fish liver proposed a regulatory interplay between peroxisomes and catabolism of sexual steroids (T / estradiol) [360, 361]. Recently, it was shown that general MFP2 knockout mice exhibit normal T values in plasma of despite severe pathological alterations in the testis and development of the infertility [259]. Similarly in this thesis, normal T and DHT levels were found in the testis and in serum of scs*Pex13*KO animals. However, we noted a strong accumulation of the androgen precursor DHEA, suggesting a block in the Δ5 pathway of T synthesis at the position of 17β-HSD. This high DHEA accumulation can only be explained by the mis-targeting of MFP2 to the cytoplasm

and complete disruption of the peroxisomal β-oxidation pathway 2. Indeed as mentioned above all other androgen precursors are decreased and the 3βHSD converting DHEA to 4-A is strongly increased, suggesting that a higher flux of androgen precursors was induced via the Δ4 pathway to keep T and DHT levels constant. This hypothesis is further supported by the fact that Δ4-AD (5α androstane 3α, 17β-diol) is reduced indicating degradation product of DHT was decreased. Interestingly a significant proliferation of peroxisomes and a severe induction of CYP450 IVa were described in the liver after treatment with DHEA in perivenos zone of rat liver lobules, an “estrogen-dependent” zone in the liver [330]. In addition, DHEA was recently also described as a PPARα activator and as a pro-hormone able to mediate induction of several genes like the expression of peroxisomal ABC transporters D family in human hepatoma cells [362]. *In vitro* and *in vivo* effects of DHEA showed that *Abcd2* and *Abcd3* but not *Abcd4* genes were induced in primary culture of rat hepatocytes by DHEA-S. In addition, after 11-day treatments with DHEA, it was demonstrated that *Abcd2* and *Abcd3* are inducible in the liver of male rodents but not in brain, testes and adrenals [362]. In addition, other studies suggested that the 17βHSD4 gene is stimulated by progesterone and ligands of PPARα and is down-regulated by phorbol esters. The same study claimed that mutation of this enzyme was involved in Zellweger-like syndrome [329].

Importantly, in laboratory animals such as rats, mice, guinea pigs and dogs, the secretion of sex steroids is done exclusively in the gonads. In man, androgen precursors DHEA and DHEA-S are excreted from the adrenal glands in addition to secreting sex steroids from the gonads [363, 364]. Unlike T and estradiol, DHEA is known as a weak androgen, and does not have a known classical intracellular steroid receptor [365, 366]. As mentioned above DHEA can bind to PPARα, and most recently, it was reported that in addition it can bind to the constitutive androstane receptor [367], to which other classical peroxisomal proliferators can also bind. DHEA is an intermediate in the production of both androgens and estrogens in the peripheral tissues [368]. Previously, it was shown that recombinant human FSH in males increases the production of T in Leydig cells through Sertoli cell-released non-steroid factors. The increase in the T/Δ4 and T/DHEA ratios indicate that this factor would act by amplifying the LH response through the Δ5 pathway and the 17βHSD enzyme [369], which could be explained by the proliferation of peroxisomes that is indeed stimulated in Leydig cells by LH treatment [79].

In the prostate, DHEA effects may be further influenced by endocrine-immune interactions. For example, the DHEA-sulfatase activity is present in macrophages, thus allowing for the conversion of DHEA-S to DHEA [370]. In this thesis, the mRNA expression of this enzyme was also checked, but no signal was obtained, though the sulfates mRNA was easily amplified out of liver RNA, suggesting that the enzyme is not or only in very low levels expressed in the testis.

Administration of DHEA has been reported to have beneficial effects on ageing, diabetes, and artherosclerosis [371, 372]. The mechanism by which DHEA exerts a possible antioxidant activity has not been elucidated, although this effect seems to have some biological significance because the peroxidation of microsomal lipids are clearly reduced as shown by the decrease in thiobarbituric acid-reactive substances [372]. This antioxidative and reduced lipid peroxidation could however be explained by an increased peroxisome proliferation, organelles that contain many antioxidative enzymes and β-oxidation chains for lipid degradation. In several studies antiapoptotic and antioxidant effects of DHEA have been reported in various organs [371, 373-375]. For instance, DHEA has a beneficial anti-apoptotic effect in testicular torsion/detorsion injury in a rat model [376]. In addition, DHEA has been reported to change the fatty acid composition of mitochondrial membrane phospholipids in rats [377]. Moreover, DHEA and DHEA-S regulate apoptosis during neurogenesis in opposing ways via the *Akt* signalling pathway [378, 379] and the effects of DHEA on apoptosis appear to be determined by the cell type [379]. The protective effect of the DHEA was dose-dependent and apoptotic cells gradually decrease depending on the concentration in lymphocytes [380]. No cytotoxic effects inducing apoptotic mechanisms were observed in Leydig cells and TM4 Sertoli cells by treatment with amino-DHEA analogues. However, a necrotic effect was induced in TM4 Sertoli cells [368]. Apoptotic spermatogenic cells were always spermatogonia or spermatocytes and not Sertoli, Leydig cells or endothelial cells [381].

Apoptotic cell death in scs*Pex13*KO animals was highly pronounced in 90 day-old scs*Pex13*KO animals, showing different types of germ cells positive after TUNEL assay. In the period between 90 to 130 days almost all germ cells died in scs*Pex13*KO testis. At P130 only the rests of germ cells within the seminiferous tubules exhibited a positive TUNEL reaction. This might indicate that accumulation of lipids and strongly elevated DHEA levels are induced continuously in form of a storage disease up to a certain level (>90 days), overstepping of which leads to significant and quick death of germ cells.

In scs*Pex13*KO animals macrophages were found in high number in the interstitial space. Interestingly, it is known that macrophages can induce 3βHSD promoting conversion of DHEA into T [382]. Indeed *3βhsd* mRNA levels were up-regulated in scs*Pex13*KO testis, most probably to by-pass the 17βHSD4 block in the Δ5 pathway, leading to the higher flux of intermediates into the Δ4 synthesis pathway. The protective effect of DHEA as an anti-oxidant might have an influence until the age of 90 days in mice when the scs*Pex13*KO are fertile. Afterwards, due to the high level, DHEA might contribute to cause the apoptosis of spermatogonia.

The steroid level changes observed in scs*Pex13* animals do not seem to be related to pituitary effects since FSH values in the serum are normal, as confirmed in this thesis by an ELISA assay (data not shown).

5.11. Alterations in different subcellular compartments and ROS metabolism induced by peroxisome deficiency in scs*Pex13*KO testis

The absence of functional peroxisomes in Sertoli cells induces significant alterations in other subcellular compartment, such as mitochondria, the ER, lysosomes and the cytoplasm. In Sertoli cells of scs*Pex13*KO, mitochondria are proliferated and contain heterogeneous levels of mitochondrial complex III of the respiratory chain, increased level of the CYP450scc enzyme and dramatically up-regulated amounts of SOD2 protein, suggesting an increased ROS production. Severe alterations of mitochondria and high SOD2 levels were also described in cell types not involved in steroids synthesis such as hepatocytes, cardiomyocytes and granulocytes in *Pex5* knockout mice [328, 383]. In addition, it was shown that mitochondrial alterations in hepatocytes are not induced by external serum factors, but rather are an internal cellular problem caused by absence of peroxisomes in these cells [384]. After reintroduction of the peroxisomes by alpha-fetoprotein gene promoter dependent expression of the *Pex5* gene in hepatocytes, a mosaic pattern of the complementation of the peroxisomal biogenesis defect occurred in mice. In contrast, directly neighboring cells without peroxisome reconstitution by transgenic *Pex5* expression showed severe mitochondrial defects and strong lipid accumulation. By this approach 40% hepatocytes were found showing normal (reconstituted PEX5) peroxisomes as well mithochondria [384].

The mitochondrial alterations in Sertoli cells in scs*Pex13*KO mice would also support the notion that oxidative stress is induced in this cell type of testis. This is in line with strongly reduced of the complex III mitochondrial respiratory chain that was found by IF and WB analyses in scs*Pex13*KO mice. Interestingly, also a shift of SOD2 was noted in the cytoplasmic fractions by WB analysis, suggesting an increased mitochondrial fragility. In the literature was described that an over-expression of SOD2 is dependent on the increased or breakage of mitochondrial networks during fractionation procedure [385]. The group of antioxidant enzymes from various different subcellular compartments including SOD2, GPX1, PRDX1, 5 and 6 and CAT were increased in the testis of scs*Pex13*KO animals. SOD2 converts $O_2^{\cdot-}$ into hydrogen peroxide (H_2O_2) that may produce the highly reactive hydroxyl radical (·OH) in the presence of reduced metal atoms unless H_2O_2 is removed by the action of GPX1 or CAT. In the testis SOD1 mRNA was expressed in all cell types but no difference was observed between scs*Pex13* mouse phenotypes. In contrast, the SOD2 protein in Sertoli cells was increased in mitochondria already in 30 day-old scs*Pex13*KO and reached

its highest abundance in mitochondrial in the 130 day-old animals. However, SOD2 showed decreased immunostaining intensity in some of the proliferating Leydig cells of 130 day-old scs*Pex13*KO mice suggesting a reduced activity in pre-aged Leydig cells. Compared with control fractions the subcellular fractions of both interstitial and tubular cells from scs*Pex13*KO testis showed an enhanced mitochondrial fragility leading to the disruption release of large amounts of SOD2 into the cytosolic fraction during the homogenization procedure. SOD2 can be induced by its substrate and the superoxide anion itself [386], peroxynitrite [387] and also by pro-inflammatory mediators such as interleukins [388-390]. Since *IL-1*α and *IL-6* mRNA, both pro-inflammatory cytokines, were up-regulated in all testicular cell fractions studied and SOD2 was induced in all testicular cells, it would indicate that the *Sod2* gene is activated also by cytokines via NF-κB signaling, in addition to the leading ROS release stimulus. One of the most important cause of defective sperm maturation is the excessive ROS generation by the disruption of the antioxidant defense systems [391]. The antioxidant enzyme CAT, normally present in peroxisome, was mis-targeted due the *Pex13* knockout into the cytoplasm of Sertoli cells. This mis-targeting of CAT was visualized by both IF and WB analysis in scs*Pex13*KO mice. The presence of CAT in all cellular fractions (enriched mixed organelle fraction) suggests that CAT is bound on the outside of the organelle membranes or on peroxisomal membrane ghost structures [392]. The SOD2 increase and presence of high CAT amounts in the cytoplasm of Sertoli cells in scs*Pex13*KO animals led us to conclude that ROS production was increased and the major genes of anti-oxidant enzymes were activated in order to protect the cell and spermatogenesis against ROS toxicity.

This notion was indeed substantiated by *in vitro* experiments by a knockdown of the *Pex13* gene in primary Sertoli cell cultures. In these experiments a reduction of more than 50% of PEX13 protein was observed, leading to already described consequences on enzyme expressions and gene alteration as in comparison to the *in situ* results in testis tissue of scs*Pex13*KO mice. In addition, significant ROS production was observed in *Pex13* knockdown Sertoli cells, resulting in an enormous up-regulation of the *Sod2* gene expression and increase in SOD2 protein abundance. Extensive mitochondrial networks were observed in these Sertoli cells in IF experiments.

In addition to activation of genes of antioxidant enzymes, an increase in peroxisomal β-oxidation gene activity was also obtained in primary Sertoli cells, suggesting strong lipid accumulation and PPAR induction in the *Pex13*-siRNA cell culture experiments.

5.12. Peroxisomal dysfunction in Sertoli cells leads to induction of constitutive and inducible cyclooxygenases, production of pro-inflammatory cytokines and local testicular inflammation

Under normal conditions cytokines are involved in the development of Sertoli cells and are induced in the seminiferous tubules in later stages of spermatogenesis when the cytoplasm is shed from elongating spermatids as residual bodies (or cytopasts). These residual bodies are phagocytosed by the surrounding Sertoli cells. Ultra-thin sections of scs*Pex13*KO testis revealed large phagosomes containing rests of apoptotic germ cells. The formation of phagosomes in Sertoli cells of 130 day-old mice, was also connected to the degradation of germ cells, which might suggest a permanent cytokine induction in the scs*Pex13*KO testis. Indeed, the genes of pro-inflammatory cytokines *IL1-α* and *IL6* are induced in all testicular somatic cell preparations of scs*Pex13*KO mice. In addition, *COX1* and *COX2* are induced in the testis of 130 day-old scs*Pex13*KO mice, genes of which could be stimulated in an autocrine manner via cytokine receptor signaling cascades. Interestingly, IL-1 does not seem to stimulate intracellular ROS formation in Sertoli cells [69]. IL-1α is predominantly secreted by Sertoli cells and stimulates Sertoli cell mitosis *in vitro* and modifies the production of lactate and transferrin in those cells and is modulating the steroidogenesis in Leydig cells [393]. Indeed an increased in transferrin mRNA expression was noted in all testicular somatic cell preparations (Sertoli, peritubular and Leydig cells) from 130 day-old scs*Pex13*KO. These results are supported by *in vivo* experiments, in which Sertoli cells induced-IL-1α stimulates the production of transferrin in the mouse testis. In contrast to IL-1α which is mainly expressed in Sertoli cells, IL-6 is produced by most of testicular somatic cells: interstitial macrophages [394], Leydig cells [395], Sertoli cells [396, 397], peritubular and germ cells [398]. In addition, studies demonstrated the involvement of gonadotropins and testosterone in the regulation of IL-6 expression [398]. Furthermore, hCG induces adverse effects on germ cells which were attributed to transient testicular inflammation with high local levels of IL-1α, IL-6 and other cytokines [399]. Finally IL-1α modulats steroidogenesis in Leydig cells [393], inhibits LH-stimulated testosterone production, but can stimulate basal steroidogenesis under appropriate conditions [56].

Additionally to cytokines, the PPARs have been implicated in the regulation of inflammatory responses in cells with highly active lipid metabolism. PPARs are activated by a multitude of lipid derivatives, especially eicosanoids and prostaglandins and a variety of chemical compound, such as hypolipidemic drugs [400]. Interestingly, there is evidence suggesting that arachidonic acid and its oxygenated metabolites regulate physiological and pathological processes in reproduction [401]. In testes however, only few and controversial reports on the action of eicosanoids on spermatogenesis are available and in consequence of their possible role in spermatogenesis control are not yet well understood. One hypothesis suggests that

COX-2 could play a major role in the regulation of testicular activity in fertility disorders and aging. Previously it has been reported that COX-2 is not detected in human testicular biopsies without any evidence for morphological changes or abnormalities, whereas it is expressed in human testes with impaired spermatogenesis and male infertility [402]. COX-2 is also induced in testicular cancer [403]. In adult Leydig cells COX-2 converts arachidonic acids to prostaglandins, particularly PGE2 and PGF2a that are directly implicated in the production of pro-inflammatory cytokines such as IL-1 and IL-6 and the auto-regulation of steroidogenesis. In MA-10 mouse Leydig cells COX-2 inhibition enhanced steroidogenesis and *Star* gene expression, whereas its over-expression lead to the opposite effect [404]. Interestingly the results of this thesis show that in scs*Pex13*KO mice not only the inducible COX-2 isoform, but also the constitutive COX1 form was induced. The ubiquitous constitutive expression of COX-1 and inducible expression of COX-2 have led to the widely held belief that COX-1 produces homeostatic PGs, while PGs produced by COX-2 have primarily patho-physiological nature [405]. The alterations of the COXs expressions in scs*Pex13*KO could be exerted by different factors: 1) several cytokines (IL-1 and IL-6) are potent inducers or 2) increased ROS could stimulate the NFkB pathway and lead to COX induction, 3) their activities could be controlled differentially by regulating the amount of arachidonic acid and lipid peroxides available to the enzymes. Moreover, COX-2, but not COX-1 can use esterified fatty acids as alternative substrates [406]. In this respect the drastic accumulation of peroxisome metabolized fatty acids in scsPex13KO animals could also lead to COX-2 induction.

Most probably due to high levels of IL-1α and IL-6 secretion together with COX-1 and COX-2 up-regulation, a local inflammation with invasion of lymphocytes and Leydig cell proliferation in interstitial space was noted in the testis of scs*Pex13*KO animals. Indeed a highly elevated eicosanoid level in seminiferous tubules could result from the fact that due to the lack of peroxisomes in the Sertoli cells, prostaglandins and leukotrienes, which normally are oxidized via the L-specific β-oxidation pathway catalyzed by palmitoyl-CoA oxidase, multifunctional protein-1 and thiolase in peroxisomes [407, 408], are progressively accumulating in the scs*Pex13*KO testis.

The results indicate that the absence of functional peroxisomes from Sertoli cells on the one side leads to severe oxidative stress and on the other side to accumulation of prostaglandins which in turn induce pro-inflammatory cytokines and propagate inflammatory reactions in testicular somatic cells of scs*Pex13*KO animals.

Scheme summarizing alterations in Sertoli cells from scs*Pex13* KO testis.

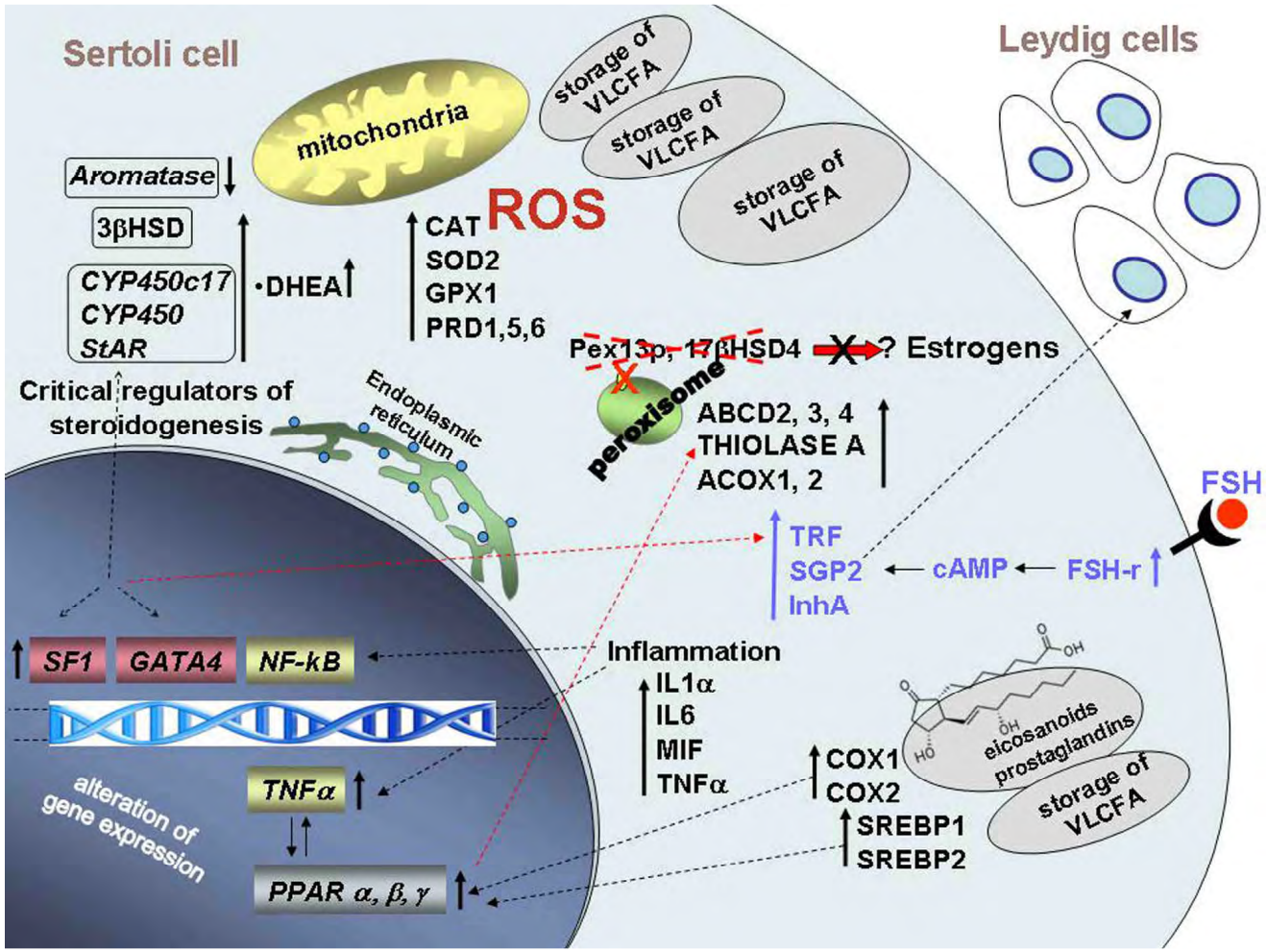

Figure 51: Deficiency of *Pex13* gene in Sertoli cells inducs a peroxisome biogenesis defects leading to defective martix protein import and disruption of α- and β-oxidation reactions which in turn leads to the accumulation of VLCFA and other peroxisome metabolized lipids. Critical regulators of steroidogenesis as well as coresponding transcription factors were altered. In addition mistargetting of MFP2 leads to DHEA acumulation. Constitutive and inducible cyclooxygeneses were induced. Hight eicosanoids, prostaglandins and interleukin levels induce inflammatory pathways. Alteration in different subcellular compartments and ROS metabolism were induced by peroxisome deficiency.

Scheme summarizing alterations in Leydig cells from scs*Pex13* KO testis.

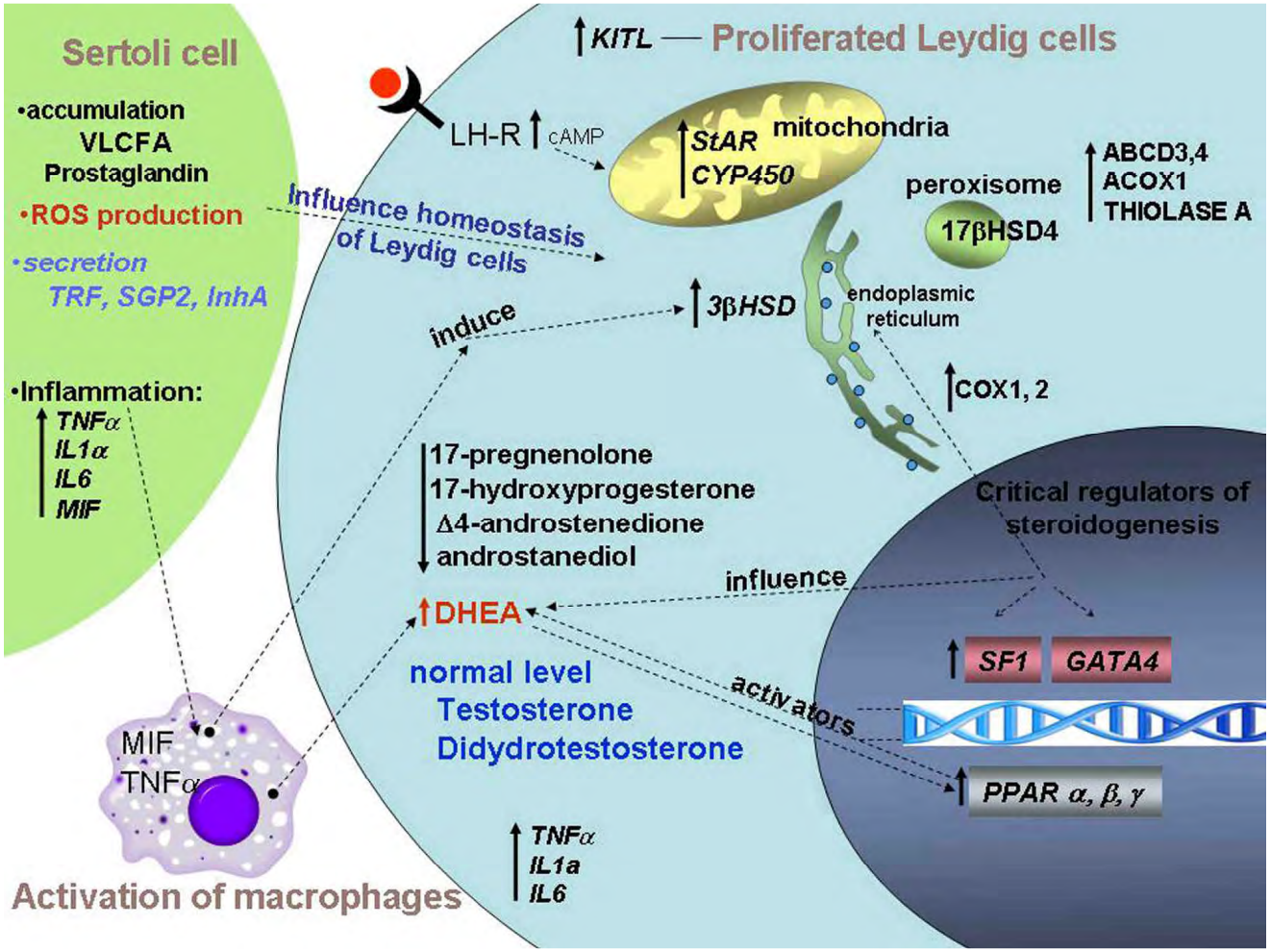

Figure 52: Hyperplasia of Leydig cells occurred in scs*Pex13*KO testis. *Pex13*KO in Sertoli cells induces the expression of the ABCD-transporters in Leydig cells. Androgen synthesies was alterated as well the related signalling pathways in Leydig cells of scs*Pex13*KO mice. Constitutive and inducible cyclooxygenases were induced. Production of pro-inflammatory cytokines was induced and local testicular inflammation occurred with activated macrophages and attraction of lymphocytes.

6. Summary

Peroxisomes are ubiquitous cell organelles with heterogeneous enzyme composition and functions, depending on the metabolic needs of different cell types, tissues and organ systems. However, until the beginning of the experimental work of this thesis hardly any knowledge was available on the metabolic functions of these cell organelles in the testis, despite the well-known severe pathological alterations in this organ in patients suffering from peroxisomal diseases. Male children with Zellweger syndrome, the most severe form of a peroxisomal biogenesis disorder, exhibit cryptorchism and patients with X-linked adrenoleukodystrophy (X-ALD), a single enzyme defect of a peroxisomal ABC transporter for lipids, show an impairment of testicular functions in 80% of the cases.

Therefore, the main goals of this thesis were to characterize the peroxisomal distribution and enzyme composition in distinct cell types of normal mouse and human testis and to analyse the molecular consequences of peroxisome deficiency and its influence on male fertility. To get a complete overview on the peroxisomal compartment and its enzyme composition in the testis in normal mice and on the alterations in scs*Pex13* knockout mice, routine histological analyses with HE-stained material, Oil red O staining on frozen sections, TUNEL, immunofluorescence and immunohistochemistry with a variety antibodies against peroxisomal and cell marker proteins, electron microscopy, laser-assisted microdissection (LAMD), isolation of different testicular cell types and primary cell culture, cell and tissue homogenisation, subcellular fractionation and organelle isolation, Western blot analysis, lipid extraction, fatty acid and steroid (androgen) analyses by GC-MS, genomic DNA isolation, PCR genotyping, total RNA isolation, RT-PCR analyses and RNAi on primary Sertoli cells were used.

The results of this thesis indicate that peroxisomes in distinct cell types of the testis exhibit specific enzyme composition and serve divers functions already under normal physiological conditions. Despite older reports from the literature on the exclusive presence of these organelles in Leydig cells, in this study peroxisomes were identified with new specific markers in all testicular cell types, including developing germ cells (except for mature spermatozoa). Peroxisomes alter their matrix protein composition, aggregate in clusters during spermiogenesis in late stages of elongated spermatids (step 14 to 16) and are transported into the cytoplasmic droplets and residual bodies, which are subsequently phagocytosed by Sertoli cells. The highest enrichment of peroxisomal lipid transporters (ABCD1 and ABCD3) as well as of ACOX2, the key regulatory enzyme of the β-oxidation pathway 2 for side-chain oxidation of cholesterol and medium levels of catalase were found in Sertoli cells, suggesting peroxisomes as protectors against lipid toxicity and oxidative stress to prevent germ cell apoptosis. Leydig cells were selectively enriched in catalase and ABCD2, indicating that peroxisomes are important also in this cell type for the protection of steroidogenesis against ROS and for lipid homeostasis. Comparative immunofluorescence analysis revealed that distribution, abundance and enyzme composition of peroxisomes were conserved between mouse and man.

To study the molecular consequences of peroxisomal dysfunction on male fertility, a Sertoli cell-specific knockout mouse was generated by AMH-cre-mediated excision of exon 2 of the *Pex13* gene, encoding a protein of the docking complex on the peroxisomal membrane involved in matrix protein import into the organelle. Due to the absence of PEX13 protein and deficient matrix protein import, all matrix proteins, such as catalase and thiolase, were mislocalized into the cytoplasm in Sertoli cells. Few peroxisomal membrane ghosts, positive for PEX14 were still present in this cell type surrounding large lipid droplets. Within 130 days of postnatal development, the scs*Pex13*KO animals developed a complete Sertoli cell only syndrome. TUNEL preparations of paraffin sections revealed that germ cell apoptosis occurred between 90 and 130 days of postnatal development. A strong increase of neutral lipids, such as triglycerides and cholesteryl esters was observed in Sertoli cells of the seminiferous tubules of P130 scs*Pex*13KO animals. The accumulation of peroxisome-metabolised fatty acids (VLCFA, pristanic and phytanic acid) in frozen testis samples suggested the deficiency of peroxisomal α- and β-oxidation. Steroid measurements revealed normal testosterone levels, but a strong accumulation of dehydroepiandrosterone (DHEA) and a decrease of all other androgen precursors, suggesting a block of the Δ5 pathway in these animals. The expression of mRNAs for the FSH- and LH-receptors was significantly increased and the ones for transcription factors (*Sf1, Gata4)* and enzymes for steroidogenesis (*Star, Cyp450scc, Cyp450c17*, *3β-Hds)* were elevated in Sertoli cells as well as in Leydig cells of scs*Pex13*KO mice. Specific Sertoli cell markers were also enhanced (*Inhα, Trf, Sgp2*). Strongly proliferated Leydig cells seemed to dramatically upregulate their peroxisomal compartment and exhibited a strong increase of peroxisomal ABCD-transporters. Ultrastructural analysis of different subcellular compartments revealed mitochondria with rearrangement of their cristae and giant whorl-like structures of SER in Leydig cells. Mitochondria in Sertoli cells were proliferated and exhibited extremely high levels of SOD2. Strong ROS production and a similar increase in mitochondrial SOD2 were detected in primary Sertoli cells with a siRNA-mediated knockdown of the *Pex13* gene. Peroxisomal dysfunction in Sertoli cells led to an induction of constitutive and inducible cyclooxygenases (COX1, COX2), production of pro-inflammatory cytokines (*Il1α, Il6, Tnfα, Mif*) and local testicular inflammation, showing infiltration of macrophages in the interstitial space of the testis in scs*Pex13*KO animals.

In conclusion, peroxisomes in Sertoli cells are essential organelles in the testis for male fertility which *(1)* regulate lipid homeostasis in the seminiferous tubules, *(2)* protect spermatogenesis against oxidative stress due to ROS increase, *(3)* are involved in androgen precursor synthesis and keep androgens in balance, and *(4)* protect against inflammation through the degradation of bioactive lipid mediators (e.g. arachidonic acid or eicosanoids).

Since peroxisomal enzyme composition is similar between mice and humans, scs*Pex13* knockout mice provide an excellent model system to study human infertility due to peroxisomal deficiency. Future studies on tissue samples from infertile patients are needed to clarify in which extent peroxisomes are involved in the pathogenesis of idiopathic infertility.

7. Zusammenfassung

Peroxisomen sind ubiquitäre Zellorganellen, die abhängig von metabolischen Anforderungen in unterschiedlichen Zelltypen, Geweben und Organsystemen eine heterogene Enzymzusammensetzung und unterschiedliche Funktionen aufweisen. Über die metabolische Funktion dieser Organellen im Hoden standen zu Beginn der experimentellen Arbeiten zu dieser Dissertation jedoch kaum Informationen in der Literatur zur Verfügung, obwohl ausgeprägte pathologische Veränderungen in diesem Organ bei Patienten mit peroxisomalen Krankheiten auftreten. So weisen Knaben mit Zellweger-Syndrom, der schwersten Form eines peroxisomalen Biogenesedefektes, Kryptorchismus auf und Patienten mit X-chromosomaler Adrenoleukodystrophie (X-ALD), einem Einzelgendefekt eines peroxisomalen ABC-Transporters für Lipide, zeigen in 80% der Fälle eine Beeinträchtigung der testikulären Funktion.

Deshalb bestanden die Hauptziele dieser Dissertation darin, die Verteilung und Enzymzusammensetzung der Peroxisomen in verschiedenen Zelltypen des Hodens der Maus und des Menschen im Vergleich zu charakterisieren sowie die molekulare Pathogenese der durch Peroxisomendefizienz ausgelösten Veränderungen zu analysieren und deren Einfluss auf die männliche Fertilität nachzuweisen. Um einen Überblick über das peroxisomale Kompartiment im Hoden von Wildtyp-Mäusen und über die Veränderungen in Sertolli-Zell-spezifischen Pex13 Knockout-Mäusen (scs*Pex13*KO) zu erhalten, wurden folgende Methoden in dieser Dissertation etabliert und angewandt: Morphologische Analyse HE-gefärbter histologischer Präparate, Ölrot O-Färbung von Gefrierschnitten, TUNEL, Immunofluoreszenz und Immunohistochemie mit unterschiedlichen Antikörpern gegen peroxisomale und zelltypspezifische Markerproteine, Elektronenmikroskopie, lasergestützte Mikrodissektion, Isolierung und Kultivierung verschiedener primärer Zellen aus Hodengewebe, Western-Blot-Analysen, Lipidextraktion, Fettsäure- und Steroidanalysen mittels GC-MS, Isolierung genomischer DNA und PCR-Genotypisierung, Isolierung von Gesamt-RNA und RT-PCR Expressionsanalysen, RNAi-Knockdown des Pex13 Gens in primären Sertolizellen, ROS-Nachweis an primären Sertoli-Zellen mittels DHE-Fluoreszenz.

Die Resultate dieser Dissertation zeigen eindeutig, dass Peroxisomen in den spezifischen Zelltypen des Hodens schon unter physiologischen Bedingungen unterschiedliche Enzymzusammensetzung besitzen und verschiedene Funktionen erfüllen. Im Gegensatz zu Literaturangaben über das Vorkommen der Peroxisomen ausschließlich in Leydig-Zellen wird in der vorliegenden Dissertation die Existenz dieser Zellorganellen in allen Zelltypen des Hodens, sogar in Keimzellen (mit Ausnahme gereifter Spermien), nachgewiesen. Peroxisomen ändern ihre Matrixproteinzusammensetzung und „clustern“ (bilden Gruppen) im Verlauf der Spermiogenese in späten Stadien elongierter Spermatiden (Stadium 14-16); sie werden in Residualkörper transportiert und durch anschließende Phagozytose in Sertolizellen abgebaut. Die höchste Anreicherung der peroxisomalen Lipidtransporter ABCD1 und ABCD3 sowie von ACOX-2, des Schlüsselenzyms des 2. β-Oxidationswegs zur Seitenkettenoxidation von Cholesterin und

auch ein relativ hohes Katalasevorkommen wurden in Sertoli-Zellen nachgewiesen. Dies deutet darauf hin, dass Peroxisomen in Sertoli Zellen vor Lipidtoxizität und oxidativem Stress schützen. Leydig-Zellen dagegen waren besonders mit Katalase angereichert und enthielten auch hohe Mengen ABCD2. Dies lässt die Schlussfolgerung zu, dass Peroxisomen in diesen Zellen die Steroidbiosynthese vor den toxischen Wirkungen von ROS schützen und die Lipidhomöostase regulieren. Vergleichende Immunofluoreszenzanalysen von murinen und humanen Proben erbrachten, dass sich Verteilung, Menge und Enzymzusammensetzung der Peroxisomen zwischen den beiden Spezies nicht grundsätzlich unterscheiden.

Um die molekularen Konsequenzen peroxisomaler Dysfunktion auf die männliche Fertilität zu untersuchen, wurde eine Sertoli-Zell-spezifische Knockout-Maus durch AMH-cre vermittelte Exzision des Exons 2 des *Pex13*-Gens hergestellt. Das *Pex13*-Gen kodiert ein Protein des Docking-Komplexes der Peroxisomenmembran, das in den Matrixproteinimport eingeschaltet ist. Durch das Fehlen des PEX13-Proteins (PEX13p) blieben alle peroxisomalen Matrixproteine, wie z.B. Katalase und Thiolase, im Zytoplasma der Sertoli-Zellen fehllokalisiert. Einige wenige Pex14p-positive peroxisomale Membranreste („ghosts“) waren um große Lipidtropfen herum detektierbar. Innerhalb von 130 Tagen in der postnatalen Entwicklung bildeten die scsPex13-Knockout-Mäuse ein komplettes „Sertoli cell only“-Syndrom aus. In TUNEL-Präparationen von Paraffinschnitten konnte der Keimzellverlust durch Apoptose innerhalb des Zeitraums zwischen 90 und 130 Tagen in der postnatalen Entwicklung nachgewiesen werden. ScsPex13 Knockout-Mäuse (P130) wiesen einen starken Anstieg neutraler Fettsäuren und von Cholesterinestern in Sertoli-Zellen der Tubuli seminiferi auf. Der Nachweis der Akkumulation von peroxisomenspezifischen Fettsäuren (sehr langkettige Fettsäuren, Pristan- und Phytansäure) in Gefrierschnitten ließ weiterhin eine Defizienz von peroxisomaler α- und β-Oxidation vermuten, was durch die Fehllokalisation von ACOX1 und Thiolase erklärt werden konnte. Steroidanalysen erbrachten normale Testosteronspiegel, jedoch eine starke Erhöhung von Dehydroepiandrosteron (DHEA) und die Verminderung aller anderen Androgenvorläufer, was durch eine Blockierung des Δ5-Stoffwechselweges auf Höhe der peroxisomalen 17β-Hydroxysteroid-Dehydrogenase (multifunktionelles Protein 2 = MFP2) in diesen Tieren erklärbar ist. Eine signifikante Erhöhung der mRNA-Expression der FSH- und LH-Rezeptoren sowie der Transkriptionsfaktoren (*Sf1, Gata4*) und der Enzyme für die Steroidsynthese (*Star*, *Cyp450scc, Cyp450c17, 3bHsd*) wurde in Sertoli- und in Leydig-Zellen festgestellt. Auch die mRNAs spezifischer Sertoli-Zell-Marker waren induziert (*Inhα, Trf, Sgp2*). Die stark proliferierten Leydig-Zellen des Interstitiums wiesen eine Vermehrung des peroxisomalen Kompartiments auf und zeigten eine starke Erhöhung der Proteinmenge von peroxisomalen ABC-Transportern. Die ultrastrukturelle Analyse verschiedener subzellulärer Kompartimente in diesen Zellen erbrachte Mitochondrien mit veränderten Cristae und große schneckennudelartige („whorl-like“) Aggregate des glatten ERs. Mitochondrien in Sertoli-Zellen wurden vermehrt aufgefunden und enthielten hohen Mengen vonn SOD2. Eine starke Induktion der ROS-Produktion und eine Erhöhung der

SOD2 konnten experimentell auch durch siRNA-ausgelösten Knockdown des *Pex13*-Gens in primären Sertoli-Zellen ausgelöst werden. Weiterhin führte die peroxisomale Dysfunktion in Sertoli-Zellen zu einer Induktion der konstitutiven und induzierbaren Formen der Cyclooxygenasen (COX1, COX2), zu der vermehrten Produktion von proinflammatorischen Cytokinen (*Il1a, Il6, Tnfα, Mif*) und einer Hodenentzündung mit Makrophageninfiltration im Interstitium in scsPex13 Knockout-Mäusen.

Zusammenfassend lässt sich feststellen, dass Peroxisomen in Sertoli-Zellen essentielle Zellorganellen zur Erhaltung der männlichen Fertilität darstellen, die *1)* die Lipidhomöostase in Tubuli seminiferi regulieren, *2)* die Spermatogenese gegen oxidativen Stress durch Erhöhung von ROS schützen, *3)* in die Androgensynthese eingeschaltet sind und das Androgengleichgewicht regulieren und *4)* vor Entzündungen des Hodens durch den Abbau von bioaktiven Lipidmediatoren (z.B.: Arachidonsäure und Eicosanoide) schützen.

Da eine ähnliche Enzymzusammensetzung im Hoden der Maus und des Menschen nachgewiesen werden konnte, stellen die scsPex13 Knockout-Mäuse ein ideales Modellsystem zum Studium männlicher Infertilität durch peroxisomale Dysfunktion dar. Zukünftige Studien mit Gewebeproben von infertilen Patienten sind jedoch notwendig, um aufzuklären, welche Rolle der peroxisomale Stoffwechsel in der Pathogenese von idiopathischer Infertilität beim Mann spielt.

8. References

1. **Pelliniemi LJ, Frojdman K, Paranko J**. Embryological and prenatal development and function of Sertoli cells. The Sertoli cell 1993; Edited by LD Russell, MG Griswold. Clearwater, Cache River Press: pp 88-113.
2. **Gubbay J, Collignon J, Koopman P, Capel B, Economou A, Munsterberg A, Vivian N, Goodfellow P, Lovell-Badge R**. A gene mapping to the sex-determining region of the mouse Y chromosome is a member of a novel family of embryonically expressed genes. Nature 1990; 346: 245-250.
3. **Sinclair AH, Berta P, Palmer MS, Hawkins JR, Griffiths BL, Smith MJ, Foster JW, Frischauf AM, Lovell-Badge R, Goodfellow PN**. A gene from the human sex-determining region encodes a protein with homology to a conserved DNA-binding motif. Nature 1990; 346: 240-244.
4. **Palmer SJ, Burgoyne PS**. In situ analysis of fetal, prepuberal and adult XX----XY chimaeric mouse testes: Sertoli cells are predominantly, but not exclusively, XY. Development 1991; 112: 265-268.
5. **Patek CE, Kerr JB, Gosden RG, Jones KW, Hardy K, Muggleton-Harris AL, Handyside AH, Whittingham DG, Hooper ML**. Sex chimaerism, fertility and sex determination in the mouse. Development 1991; 113: 311-325.
6. **Koopman P**. The genetics and biology of vertebrate sex determination. Cell 2001; 105: 843-847.
7. **Brennan J, Capel B**. One tissue, two fates: molecular genetic events that underlie testis versus ovary development. Nat Rev Genet 2004; 5: 509-521.
8. **Phillips NB, Nikolskaya T, Jancso-Radek A, Ittah V, Jiang F, Singh R, Haas E, Weiss MA**. Sry-directed sex reversal in transgenic mice is robust with respect to enhanced DNA bending: comparison of human and murine HMG boxes. Biochemistry 2004; 43: 7066-7081.
9. **Munsterberg A, Lovell-Badge R**. Expression of the mouse anti-mullerian hormone gene suggests a role in both male and female sexual differentiation. Development 1991; 113: 613-624.
10. **Lecureuil C, Fontaine I, Crepieux P, Guillou F**. Sertoli and granulosa cell-specific Cre recombinase activity in transgenic mice. Genesis 2002; 33: 114-118.
11. **Al-Attar L, Noel K, Dutertre M, Belville C, Forest MG, Burgoyne PS, Josso N, Rey R**. Hormonal and cellular regulation of Sertoli cell anti-Mullerian hormone production in the postnatal mouse. J Clin Invest 1997; 100: 1335-1343.
12. **di Clemente N, Josso N, Gouedard L, Belville C**. Components of the anti-Mullerian hormone signaling pathway in gonads. Mol Cell Endocrinol 2003; 211: 9-14.
13. **Buehr M, Gu S, McLaren A**. Mesonephric contribution to testis differentiation in the fetal mouse. Development 1993; 117: 273-281.
14. **Merchant-Larios H, Moreno-Mendoza N**. Mesonephric stromal cells differentiate into Leydig cells in the mouse fetal testis. Exp Cell Res 1998; 244: 230-238.
15. **Brennan J, Tilmann C, Capel B**. Pdgfr-alpha mediates testis cord organization and fetal Leydig cell development in the XY gonad. Genes Dev 2003; 17: 800-810.
16. **Shen WH, Moore CC, Ikeda Y, Parker KL, Ingraham HA**. Nuclear receptor steroidogenic factor 1 regulates the mullerian inhibiting substance gene: a link to the sex determination cascade. Cell 1994; 77: 651-661.
17. **Daggett MA, Rice DA, Heckert LL**. Expression of steroidogenic factor 1 in the testis requires an E box and CCAAT box in its promoter proximal region. Biol Reprod 2000; 62: 670-679.
18. **Ketola I, Rahman N, Toppari J, Bielinska M, Porter-Tinge SB, Tapanainen JS, Huhtaniemi IT, Wilson DB, Heikinheimo M**. Expression and regulation of transcription factors GATA-4 and GATA-6 in developing mouse testis. Endocrinology 1999; 140: 1470-1480.
19. **Barrionuevo F, Georg I, Scherthan H, Lecureuil C, Guillou F, Wegner M, Scherer G**. Testis cord differentiation after the sex determination stage is independent of Sox9 but fails in the combined absence of Sox9 and Sox8. Dev Biol 2008.
20. **Beau C, Rauch M, Joulin V, Jegou B, Guerrier D**. GATA-1 is a potential repressor of anti-Mullerian hormone expression during the establishment of puberty in the mouse. Mol Reprod Dev 2000; 56: 124-138.
21. **Yomogida K, Ohtani H, Harigae H, Ito E, Nishimune Y, Engel JD, Yamamoto M**. Developmental stage- and spermatogenic cycle-specific expression of transcription factor GATA-1 in mouse Sertoli cells. Development 1994; 120: 1759-1766.
22. **Lejeune H, Habert R, Saez JM**. Origin, proliferation and differentiation of Leydig cells. J Mol Endocrinol 1998; 20: 1-25.
23. **Saez JM**. Leydig cells: endocrine, paracrine, and autocrine regulation. Endocr Rev 1994; 15: 574-626.
24. **Migrenne S, Pairault C, Racine C, Livera G, Geloso A, Habert R**. Luteinizing hormone-dependent activity and luteinizing hormone-independent differentiation of rat fetal Leydig cells. Mol Cell Endocrinol 2001; 172: 193-202.
25. **O'Shaughnessy PJ, Baker P, Sohnius U, Haavisto AM, Charlton HM, Huhtaniemi I**. Fetal development of Leydig cell activity in the mouse is independent of pituitary gonadotroph function. Endocrinology 1998; 139: 1141-1146.
26. **Ge RS, Hardy MP**. Variation in the end products of androgen biosynthesis and metabolism during postnatal differentiation of rat Leydig cells. Endocrinology 1998; 139: 3787-3795.
27. **Huhtaniemi I, Pelliniemi LJ**. Fetal Leydig cells: cellular origin, morphology, life span, and special functional features. Proc Soc Exp Biol Med 1992; 201: 125-140.
28. **Vergouwen RP, Jacobs SG, Huiskamp R, Davids JA, de Rooij DG**. Proliferative activity of gonocytes, Sertoli cells and interstitial cells during testicular development in mice. J Reprod Fertil 1991; 93: 233-243.
29. **Mendis-Handagama SM, Ariyaratne HB**. Differentiation of the adult Leydig cell population in the postnatal testis. Biol Reprod 2001; 65: 660-671.
30. **Minegishi T, Kusuda S, Dufau ML**. Purification and characterization of Leydig cell luteinizing hormone receptor. J Biol Chem 1987; 262: 17138-17143.
31. **Hardy MP, Kelce WR, Klinefelter GR, Ewing LL**. Differentiation of Leydig cell precursors in vitro: a role for androgen. Endocrinology 1990; 127: 488-490.
32. **Shan L, Hardy DO, Catterall JF, Hardy MP**. Effects of luteinizing hormone (LH) and androgen on steady state levels of messenger ribonucleic acid for LH receptors, androgen receptors, and steroidogenic enzymes in rat Leydig cell progenitors in vivo. Endocrinology 1995; 136: 1686-1693.
33. **Benton L, Shan LX, Hardy MP**. Differentiation of adult Leydig cells. J Steroid Biochem Mol Biol 1995; 53: 61-68.
34. **Habert R, Lejeune H, Saez JM**. Origin, differentiation and regulation of fetal and adult Leydig cells. Mol Cell Endocrinol 2001; 179: 47-74.

35. **Ohata M**. Electron microscopic study on the testicular interstitial cells in the mouse. Arch Histol Jpn 1979; 42: 51-79.
36. **Reddy J, Svoboda D**. Microbodies in Leydig cell tumors of rat testis. J Histochem Cytochem 1972; 20: 793-803.
37. **Ichihara I, Kawamura H, Pelliniemi LJ**. Ultrastructure and morphometry of testicular Leydig cells and the interstitial components correlated with testosterone in aging rats. Cell Tissue Res 1993; 271: 241-255.
38. **Eckstein B, Borut A, Cohen S**. Metabolic pathways for androstanediol formation in immature rat testis microsomes. Biochim Biophys Acta 1987; 924: 1-6.
39. **Saunders PT**. Germ cell-somatic cell interactions during spermatogenesis. Reprod Suppl 2003; 61: 91-101.
40. **Huleihel M, Lunenfeld E**. Regulation of spermatogenesis by paracrine/autocrine testicular factors. Asian J Androl 2004; 6: 259-268.
41. **Palombi F, Filippini A, Chiarenza C**. Cell-cell interactions in the local control of seminiferous tubule contractility. Contraception 2002; 65: 289-291.
42. **Gnessi L, Fabbri A, Spera G**. Gonadal peptides as mediators of development and functional control of the testis: an integrated system with hormones and local environment. Endocr Rev 1997; 18: 541-609.
43. **Roser JF**. Regulation of testicular function in the stallion: an intricate network of endocrine, paracrine and autocrine systems. Anim Reprod Sci 2008; 107: 179-196.
44. **Sharpe RM, Maddocks S, Kerr JB**. Cell-cell interactions in the control of spermatogenesis as studied using Leydig cell destruction and testosterone replacement. Am J Anat 1990; 188: 3-20.
45. **Matsumoto AM, Bremner WJ**. Endocrine control of human spermatogenesis. J Steroid Biochem 1989; 33: 789-790.
46. **Amann RP, Hammerstedt RH, Veeramachaneni DN**. The epididymis and sperm maturation: a perspective. Reprod Fertil Dev 1993; 5: 361-381.
47. **Dunkel L, Siimes MA, Bremner WJ**. Reduced inhibin and elevated gonadotropin levels in early pubertal boys with testicular defects. Pediatr Res 1993; 33: 514-518.
48. **Ellis GB, Desjardins C, Fraser HM**. Control of pulsatile LH release in male rats. Neuroendocrinology 1983; 37: 177-183.
49. **O'Shaughnessy PJ, Baker PJ, Johnston H**. Neuroendocrine regulation of Leydig cell development. Ann N Y Acad Sci 2005; 1061: 109-119.
50. **Shan LX, Phillips DM, Bardin CW, Hardy MP**. Differential regulation of steroidogenic enzymes during differentiation optimizes testosterone production by adult rat Leydig cells. Endocrinology 1993; 133: 2277-2283.
51. **Sharpe RM**. Intratesticular control of steroidogenesis. Clin Endocrinol (Oxf) 1990; 33: 787-807.
52. **Skinner MK, Norton JN, Mullaney BP, Rosselli M, Whaley PD, Anthony CT**. Cell-cell interactions and the regulation of testis function. Ann N Y Acad Sci 1991; 637: 354-363.
53. **Spiteri-Grech J, Nieschlag E**. Paracrine factors relevant to the regulation of spermatogenesis--a review. J Reprod Fertil 1993; 98: 1-14.
54. **Avallet O, Vigier M, Perrard-Sapori MH, Saez JM**. Transforming growth factor beta inhibits Leydig cell functions. Biochem Biophys Res Commun 1987; 146: 575-581.
55. **Khan SA, Khan SJ, Dorrington JH**. Interleukin-1 stimulates deoxyribonucleic acid synthesis in immature rat Leydig cells in vitro. Endocrinology 1992; 131: 1853-1857.
56. **Svechnikov KV, Sultana T, Soder O**. Age-dependent stimulation of Leydig cell steroidogenesis by interleukin-1 isoforms. Mol Cell Endocrinol 2001; 182: 193-201.
57. **Rouiller-Fabre V, Lecref L, Gautier C, Saez JM, Habert R**. Expression and effect of insulin-like growth factor I on rat fetal Leydig cell function and differentiation. Endocrinology 1998; 139: 2926-2934.
58. **Moore A, Morris ID**. The involvement of insulin-like growth factor-I in local control of steroidogenesis and DNA synthesis of Leydig and non-Leydig cells in the rat testicular interstitium. J Endocrinol 1993; 138: 107-114.
59. **Chase RA**. The Bassett Atlas of Human Anatomy. Publisher: Benjamin Cummings 2007; ISBN-13:9780805301182.
60. **Ivell R, Bathgate RA**. Reproductive biology of the relaxin-like factor (RLF/INSL3). Biol Reprod 2002; 67: 699-705.
61. **Feng S, Ferlin A, Truong A, Bathgate R, Wade JD, Corbett S, Han S, Tannour-Louet M, Lamb DJ, Foresta C, Agoulnik AI**. INSL3/RXFP2 signaling in testicular descent. Ann N Y Acad Sci 2009; 1160: 197-204.
62. **Teerds KJ, de Boer-Brouwer M, Dorrington JH, Balvers M, Ivell R**. Identification of markers for precursor and leydig cell differentiation in the adult rat testis following ethane dimethyl sulphonate administration. Biol Reprod 1999; 60: 1437-1445.
63. **Livera G, Rouiller-Fabre V, Pairault C, Levacher C, Habert R**. Regulation and perturbation of testicular functions by vitamin A. Reproduction 2002; 124: 173-180.
64. **Boulogne B, Levacher C, Durand P, Habert R**. Retinoic acid receptors and retinoid X receptors in the rat testis during fetal and postnatal development: immunolocalization and implication in the control of the number of gonocytes. Biol Reprod 1999; 61: 1548-1557.
65. **Kastner P, Mark M, Leid M, Gansmuller A, Chin W, Grondona JM, Decimo D, Krezel W, Dierich A, Chambon P**. Abnormal spermatogenesis in RXR beta mutant mice. Genes Dev 1996; 10: 80-92.
66. **Walch L, Morris PL**. Cyclooxygenase 2 pathway mediates IL-1beta regulation of IL-1alpha, -1beta, and IL-6 mRNA levels in Leydig cell progenitors. Endocrinology 2002; 143: 3276-3283.
67. **Haour F, Kouznetzova B, Dray F, Saez JM**. hCG-induced prostaglandin E2 and F2 alpha release in adult rat testis: role in Leydig cell desensitization to hCG. Life Sci 1979; 24: 2151-2158.
68. **Cooke BA, Dirami G, Chaudry L, Choi MS, Abayasekara DR, Phipp L**. Release of arachidonic acid and the effects of corticosteroids on steroidogenesis in rat testis Leydig cells. J Steroid Biochem Mol Biol 1991; 40: 465-471.
69. **Ishikawa T, Hwang K, Lazzarino D, Morris PL**. Sertoli cell expression of steroidogenic acute regulatory protein-related lipid transfer 1 and 5 domain-containing proteins and sterol regulatory element binding protein-1 are interleukin-1beta regulated by activation of c-Jun N-terminal kinase and cyclooxygenase-2 and cytokine induction. Endocrinology 2005; 146: 5100-5111.
70. **Kovacs WJ, Olivier LM, Krisans SK**. Central role of peroxisomes in isoprenoid biosynthesis. Prog Lipid Res 2002; 41: 369-391.
71. **Song XQ, Fukao T, Yamaguchi S, Miyazawa S, Hashimoto T, Orii T**. Molecular cloning and nucleotide sequence of complementary DNA for human hepatic cytosolic acetoacetyl-coenzyme A thiolase. Biochem Biophys Res Commun 1994; 201: 478-485.
72. **Keller GA, Barton MC, Shapiro DJ, Singer SJ**. 3-Hydroxy-3-methylglutaryl-coenzyme A reductase is present in peroxisomes in normal rat liver cells. Proc Natl Acad Sci U S A 1985; 82: 770-774.

73. **Keller GA, Pazirandeh M, Krisans S**. 3-Hydroxy-3-methylglutaryl coenzyme A reductase localization in rat liver peroxisomes and microsomes of control and cholestyramine-treated animals: quantitative biochemical and immunoelectron microscopical analyses. J Cell Biol 1986; 103: 875-886.
74. **Engfelt WH, Shackelford JE, Aboushadi N, Jessani N, Masuda K, Paton VG, Keller GA, Krisans SK**. Characterization of UT2 cells. The induction of peroxisomal 3-hydroxy-3-methylglutaryl-coenzyme a reductase. J Biol Chem 1997; 272: 24579-24587.
75. **Kovacs WJ, Faust PL, Keller GA, Krisans SK**. Purification of brain peroxisomes and localization of 3-hydroxy-3-methylglutaryl coenzyme A reductase. Eur J Biochem 2001; 268: 4850-4859.
76. **Biardi L, Krisans SK**. Compartmentalization of cholesterol biosynthesis. Conversion of mevalonate to farnesyl diphosphate occurs in the peroxisomes. J Biol Chem 1996; 271: 1784-1788.
77. **Goldstein JL, Brown MS**. Regulation of the mevalonate pathway. Nature 1990; 343: 425-430.
78. **Dufau ML, Khanum A, Winters CA, Tsai-Morris CH**. Multistep regulation of Leydig cell function. J Steroid Biochem 1987; 27: 343-350.
79. **Mendis-Handagama SM, Siril Ariyaratne HB**. Leydig cells, thyroid hormones and steroidogenesis. Indian J Exp Biol 2005; 43: 939-962.
80. **Haider SG**. Cell biology of Leydig cells in the testis. Int Rev Cytol 2004; 233: 181-241.
81. **Adamski J, Husen B, Marks F, Jungblut PW**. Purification and properties of oestradiol 17 beta-dehydrogenase extracted from cytoplasmic vesicles of porcine endometrial cells. Biochem J 1992; 288 (Pt 2): 375-381.
82. **Moeller G, Adamski J**. Multifunctionality of human 17beta-hydroxysteroid dehydrogenases. Mol Cell Endocrinol 2006; 248: 47-55.
83. **Chen H, Huhtaniemi I, Zirkin BR**. Depletion and repopulation of Leydig cells in the testes of aging brown Norway rats. Endocrinology 1996; 137: 3447-3452.
84. **Stocco DM**. An update on the mechanism of action of the Steroidogenic Acute Regulatory (StAR) protein. Exp Clin Endocrinol Diabetes 1999; 107: 229-235.
85. **Papadopoulos V, Jia MC, Culty M, Hall PF, Dym M**. Rat Sertoli cell aromatase cytochrome P450: regulation by cell culture conditions and relationship to the state of cell differentiation. In Vitro Cell Dev Biol Anim 1993; 29A: 943-949.
86. **Stocco DM, Clark BJ**. Role of the steroidogenic acute regulatory protein (StAR) in steroidogenesis. Biochem Pharmacol 1996; 51: 197-205.
87. **Majdic G, Saunders PT**. Differential patterns of expression of DAX-1 and steroidogenic factor-1 (SF-1) in the fetal rat testis. Endocrinology 1996; 137: 3586-3589.
88. **Peter M, Dubuis JM**. Transcription factors as regulators of steroidogenic P-450 enzymes. Eur J Clin Invest 2000; 30 Suppl 3: 14-20.
89. **Stocco DM, Clark BJ**. Regulation of the acute production of steroids in steroidogenic cells. Endocr Rev 1996; 17: 221-244.
90. **Luo Z, He YA, Halpert JR**. Role of residues 363 and 206 in conversion of cytochrome P450 2B1 from a steroid 16-hydroxylase to a 15 alpha-hydroxylase. Arch Biochem Biophys 1994; 309: 52-57.
91. **Grover PK, Odell WD**. Correlation of in vivo and in vitro activities of some naturally occurring androgens using a radioreceptor assay for 5alpha-dihydrotestosterone with rat prostate cytosol receptor protein. J Steroid Biochem 1975; 6: 1373-1379.
92. **Labrie C, Trudel C, Li S, Martel C, Couet J, Labrie F**. Combination of an antiandrogen and a 5 alpha-reductase inhibitor: a further step towards total androgen blockade? Endocrinology 1991; 129: 566-568.
93. **Dufort I, Tremblay Y, Belanger A, Labrie F, Luu-The V**. Isolation and characterization of a stereospecific 3beta-hydroxysteriod sulfotransferase (pregnenolone sulfotransferase) cDNA. DNA Cell Biol 1996; 15: 481-487.
94. **Payne AH, Youngblood GL**. Regulation of expression of steroidogenic enzymes in Leydig cells. Biol Reprod 1995; 52: 217-225.
95. **Moller G, van Grunsven EG, Wanders RJ, Adamski J**. Molecular basis of D-bifunctional protein deficiency. Mol Cell Endocrinol 2001; 171: 61-70.
96. **Carstensen JF, Tesdorpf JG, Kaufmann M, Markus MM, Husen B, Leenders F, Jakob F, de Launoit Y, Adamski J**. Characterization of 17 beta-hydroxysteroid dehydrogenase IV. J Endocrinol 1996; 150 Suppl: S3-12.
97. **Adamski J, Carstensen J, Husen B, Kaufmann M, de Launoit Y, Leenders F, Markus M, Jungblut PW**. New 17 beta-hydroxysteroid dehydrogenases. Molecular and cell biology of the type IV porcine and human enzymes. Ann N Y Acad Sci 1996; 784: 124-136.
98. **Normand T, Husen B, Leenders F, Pelczar H, Baert JL, Begue A, Flourens AC, Adamski J, de Launoit Y**. Molecular characterization of mouse 17 beta-hydroxysteroid dehydrogenase IV. J Steroid Biochem Mol Biol 1995; 55: 541-548.
99. **Carreau S, Genissel C, Bilinska B, Levallet J**. Sources of oestrogen in the testis and reproductive tract of the male. Int J Androl 1999; 22: 211-223.
100. **Lacombe A, Lelievre V, Roselli CE, Muller JM, Waschek JA, Vilain E**. Lack of vasoactive intestinal peptide reduces testosterone levels and reproductive aging in mouse testis. J Endocrinol 2007; 194: 153-160.
101. **Zirkin BR, Santulli R, Awoniyi CA, Ewing LL**. Maintenance of advanced spermatogenic cells in the adult rat testis: quantitative relationship to testosterone concentration within the testis. Endocrinology 1989; 124: 3043-3049.
102. **Wang RS, Yeh S, Tzeng CR, Chang C**. Androgen Receptor Roles in Spermatogenesis and Fertility: Lessons from Testicular Cell-Specific Androgen Receptor Knockout Mice. Endocr Rev 2009.
103. **Bremner WJ, Millar MR, Sharpe RM, Saunders PT**. Immunohistochemical localization of androgen receptors in the rat testis: evidence for stage-dependent expression and regulation by androgens. Endocrinology 1994; 135: 1227-1234.
104. **Vornberger W, Prins G, Musto NA, Suarez-Quian CA**. Androgen receptor distribution in rat testis: new implications for androgen regulation of spermatogenesis. Endocrinology 1994; 134: 2307-2316.
105. **Shan LX, Zhu LJ, Bardin CW, Hardy MP**. Quantitative analysis of androgen receptor messenger ribonucleic acid in developing Leydig cells and Sertoli cells by in situ hybridization. Endocrinology 1995; 136: 3856-3862.
106. **Xu Q, Lin HY, Yeh SD, Yu IC, Wang RS, Chen YT, Zhang C, Altuwaijri S, Chen LM, Chuang KH, Chiang HS, Yeh S, Chang C**. Infertility with defective spermatogenesis and steroidogenesis in male mice lacking androgen receptor in Leydig cells. Endocrine 2007; 32: 96-106.
107. **Virtanen I, Kallajoki M, Narvanen O, Paranko J, Thornell LE, Miettinen M, Lehto VP**. Peritubular myoid cells of human and rat testis are smooth muscle cells that contain desmin-type intermediate filaments. Anat Rec 1986; 215: 10-20.

108. **Guldenaar SE, Pickering BT**. Immunocytochemical evidence for the presence of oxytocin in rat testis. Cell Tissue Res 1985; 240: 485-487.
109. **Maekawa M, Kamimura K, Nagano T**. Peritubular myoid cells in the testis: their structure and function. Arch Histol Cytol 1996; 59: 1-13.
110. **Skinner MK, Moses HL**. Transforming growth factor beta gene expression and action in the seminiferous tubule: peritubular cell-Sertoli cell interactions. Mol Endocrinol 1989; 3: 625-634.
111. **Skinner MK, Fetterolf PM, Anthony CT**. Purification of a paracrine factor, P-Mod-S, produced by testicular peritubular cells that modulates Sertoli cell function. J Biol Chem 1988; 263: 2884-2890.
112. **Skinner MK, Griswold MD**. Secretion of testicular transferrin by cultured Sertoli cells is regulated by hormones and retinoids. Biol Reprod 1982; 27: 211-221.
113. **Sertoli E**. Dell'esistenza di particolari cellule ramificate nei canalicoli seminiferi del testicolo umano. Morgagani 1865; 7:31-40.
114. **Clermont Y, Perey B**. Quantitative study of the cell population of the seminiferous tubules in immature rats. Am J Anat 1957; 100: 241-267.
115. **Orth JM, Gunsalus GL, Lamperti AA**. Evidence from Sertoli cell-depleted rats indicates that spermatid number in adults depends on numbers of Sertoli cells produced during perinatal development. Endocrinology 1988; 122: 787-794.
116. **Ye SJ, Ying L, Ghosh S, de Franca LR, Russell LD**. Sertoli cell cycle: a re-examination of the structural changes during the cycle of the seminiferous epithelium of the rat. Anat Rec 1993; 237: 187-198.
117. **Jean P, Hartung M, Mirre C, Stahl A**. Association of centromeric heterochromatin with the nucleolus in mouse Sertoli cells. Anat Rec 1983; 205: 375-380.
118. **de Franca LR, Ghosh S, Ye SJ, Russell LD**. Surface and surface-to-volume relationships of the Sertoli cell during the cycle of the seminiferous epithelium in the rat. Biol Reprod 1993; 49: 1215-1228.
119. **Morales C, Clermont Y, Nadler NJ**. Cyclic endocytic activity and kinetics of lysosomes in Sertoli cells of the rat: a morphometric analysis. Biol Reprod 1986; 34: 207-218.
120. **Sylvester SR, Morales C, Oko R, Griswold MD**. Sulfated glycoprotein-1 (saposin precursor) in the reproductive tract of the male rat. Biol Reprod 1989; 41: 941-948.
121. **Assaf AA, Clermont Y**. Cyclic changes of cytoplasmic components in rat sertoli cells. Anat Rec 1981; 199:12a. 1981.
122. **Lalli MF, Tang XM, Clermont Y**. Glycoprotein synthesis in Sertoli cells during the cycle of the seminiferous epithelium of adult rats: a radioautographic study. Biol Reprod 1984; 30: 493-505.
123. **Russell LD, Malone JP**. A study of Sertoli-spermatid tubulobulbar complexes in selected mammals. Tissue Cell 1980; 12: 263-285.
124. **Russell LD, Peterson RN**. Sertoli cell junctions: morphological and functional correlates. Int Rev Cytol 1985; 94: 177-211.
125. **Gilula NB, Fawcett DW, Aoki A**. The Sertoli cell occluding junctions and gap junctions in mature and developing mammalian testis. Dev Biol 1976; 50: 142-168.
126. **Russell LD, Goh JC, Rashed RM, Vogl AW**. The consequences of actin disruption at Sertoli ectoplasmic specialization sites facing spermatids after in vivo exposure of rat testis to cytochalasin D. Biol Reprod 1988; 39: 105-118.
127. **By Russell LD GM, Cache River Press, Clearwater**. “The Setoli cell”. 1993: pp.365-390.
128. **Cheng CY, Mruk DD**. Cell junction dynamics in the testis: Sertoli-germ cell interactions and male contraceptive development. Physiol Rev 2002; 82: 825-874.
129. **Russell LD**. “The Setoli cell”. ; eds. By Russell LD, Griswold MD, Cache River Press, Clearwater.1993, pp.365-390.
130. **Mruk DD, Cheng CY**. Sertoli-Sertoli and Sertoli-germ cell interactions and their significance in germ cell movement in the seminiferous epithelium during spermatogenesis. Endocr Rev 2004; 25: 747-806.
131. **Parvinen M, Pelto-Huikko M, Soder O, Schultz R, Kaipia A, Mali P, Toppari J, Hakovirta H, Lonnerberg P, Ritzen EM, et al.** Expression of beta-nerve growth factor and its receptor in rat seminiferous epithelium: specific function at the onset of meiosis. J Cell Biol 1992; 117: 629-641.
132. **Mita M, Price JM, Hall PF**. Stimulation by follicle-stimulating hormone of synthesis of lactate by Sertoli cells from rat testis. Endocrinology 1982; 110: 1535-1541.
133. **Oonk RB, Grootegoed JA, van der Molen HJ**. Comparison of the effects of insulin and follitropin on glucose metabolism by Sertoli cells from immature rats. Mol Cell Endocrinol 1985; 42: 39-48.
134. **Nenicu A, Luers GH, Kovacs W, David M, Zimmer A, Bergmann M, Baumgart-Vogt E**. Peroxisomes in human and mouse testis: differential expression of peroxisomal proteins in germ cells and distinct somatic cell types of the testis. Biol Reprod 2007; 77: 1060-1072.
135. **Chauvin TR, Griswold MD**. Characterization of the expression and regulation of genes necessary for myo-inositol biosynthesis and transport in the seminiferous epithelium. Biol Reprod 2004; 70: 744-751.
136. **Hinton BT, White RW, Setchell BP**. Concentrations of myo-inositol in the luminal fluid of the mammalian testis and epididymis. J Reprod Fertil 1980; 58: 395-399.
137. **Munell F, Suarez-Quian CA, Selva DM, Tirado OM, Reventos J**. Androgen-binding protein and reproduction: where do we stand? J Androl 2002; 23: 598-609.
138. **Roberts KP, Banerjee PP, Tindall JW, Zirkin BR**. Immortalization and characterization of a Sertoli cell line from the adult rat. Biol Reprod 1995; 53: 1446-1453.
139. **Mayo KE**. Inhibin and activin Molecular aspects of regulation and function. Trends Endocrinol Metab 1994; 5: 407-415.
140. **Matzuk MM, Finegold MJ, Su JG, Hsueh AJ, Bradley A**. Alpha-inhibin is a tumour-suppressor gene with gonadal specificity in mice. Nature 1992; 360: 313-319.
141. **Manova K, Huang EJ, Angeles M, De Leon V, Sanchez S, Pronovost SM, Besmer P, Bachvarova RF**. The expression pattern of the c-kit ligand in gonads of mice supports a role for the c-kit receptor in oocyte growth and in proliferation of spermatogonia. Dev Biol 1993; 157: 85-99.
142. **Besmer P, Manova K, Duttlinger R, Huang EJ, Packer A, Gyssler C, Bachvarova RF**. The kit-ligand (steel factor) and its receptor c-kit/W: pleiotropic roles in gametogenesis and melanogenesis. Dev Suppl 1993: 125-137.
143. **Hedger MP, Culler MD**. Comparison of LHRH-peptidase and plasminogen activator activity in rat testis extracts. Reprod Fertil Dev 1997; 9: 659-664.
144. **Vassalli JD, Sappino AP, Belin D**. The plasminogen activator/plasmin system. J Clin Invest 1991; 88: 1067-1072.

145. **Carmeliet P, Collen D**. Gene targeting and gene transfer studies of the biological role of the plasminogen/plasmin system. Thromb Haemost 1995; 74: 429-436.
146. **Cooke NE, McLeod JF, Wang XK, Ray K**. Vitamin D binding protein: genomic structure, functional domains, and mRNA expression in tissues. J Steroid Biochem Mol Biol 1991; 40: 787-793.
147. **Vernet N, Dennefeld C, Rochette-Egly C, Oulad-Abdelghani M, Chambon P, Ghyselinck NB, Mark M**. Retinoic acid metabolism and signaling pathways in the adult and developing mouse testis. Endocrinology 2006; 147: 96-110.
148. **Unni E, Rao MR, Ganguly J**. Histological & ultrastructural studies on the effect of vitamin A depletion & subsequent repletion with vitamin A on germ cells & Sertoli cells in rat testis. Indian J Exp Biol 1983; 21: 180-192.
149. **Kim KH, Griswold MD**. The regulation of retinoic acid receptor mRNA levels during spermatogenesis. Mol Endocrinol 1990; 4: 1679-1688.
150. **Livera G, Rouiller-Fabre V, Habert R**. Retinoid receptors involved in the effects of retinoic acid on rat testis development. Biol Reprod 2001; 64: 1307-1314.
151. **Paniagua R, Rodriguez MC, Nistal M, Fraile B, Amat P**. Changes in the lipid inclusion/Sertoli cell cytoplasm area ratio during the cycle of the human seminiferous epithelium. J Reprod Fertil 1987; 80: 335-341.
152. **Jutte NH, Eikvar L, Levy FO, Hansson V**. Metabolism of palmitate in cultured rat Sertoli cells. J Reprod Fertil 1985; 73: 497-503.
153. **Coniglio JG, Whorton AR, Beckman JK**. Essential fatty acids in testes. Adv Exp Med Biol 1977; 83: 575-589.
154. **Rossi G, Gasperi V, Paro R, Barsacchi D, Cecconi S, Maccarrone M**. Follicle-stimulating hormone activates fatty acid amide hydrolase by protein kinase A and aromatase-dependent pathways in mouse primary Sertoli cells. Endocrinology 2007; 148: 1431-1439.
155. **Beckman JK, Coniglio JG**. A comparative study of the lipid composition of isolated rat Sertoli and germinal cells. Lipids 1979; 14: 262-267.
156. **Furland NE, Zanetti SR, Oresti GM, Maldonado EN, Aveldano MI**. Ceramides and sphingomyelins with high proportions of very long-chain polyunsaturated fatty acids in mammalian germ cells. J Biol Chem 2007; 282: 18141-18150.
157. **Retterstol K, Haugen TB, Tran TN, Christophersen BO**. Studies on the metabolism of essential fatty acids in isolated human testicular cells. Reproduction 2001; 121: 881-887.
158. **Mullaney BP, Skinner MK**. Transforming growth factor-beta (beta 1, beta 2, and beta 3) gene expression and action during pubertal development of the seminiferous tubule: potential role at the onset of spermatogenesis. Mol Endocrinol 1993; 7: 67-76.
159. **Skinner MK**. Sertoli cells secreted regulatory factors. In Sertoli Cell Biology 2005; pp 107-120 Eds MK Skinner & MD Griswold. San Diego: Elsevier Science.
160. **Jonsson CK, Zetterstrom RH, Holst M, Parvinen M, Soder O**. Constitutive expression of interleukin-1alpha messenger ribonucleic acid in rat Sertoli cells is dependent upon interaction with germ cells. Endocrinology 1999; 140: 3755-3761.
161. **Gerard N, Syed V, Jegou B**. Lipopolysaccharide, latex beads and residual bodies are potent activators of Sertoli cell interleukin-1 alpha production. Biochem Biophys Res Commun 1992; 185: 154-161.
162. **Parvinen M, Soder O, Mali P, Froysa B, Ritzen EM**. In vitro stimulation of stage-specific deoxyribonucleic acid synthesis in rat seminiferous tubule segments by interleukin-1 alpha. Endocrinology 1991; 129: 1614-1620.
163. **Sharpe RM, Kerr JB, McKinnell C, Millar M**. Temporal relationship between androgen-dependent changes in the volume of seminiferous tubule fluid, lumen size and seminiferous tubule protein secretion in rats. J Reprod Fertil 1994; 101: 193-198.
164. **Badran HH, Hermo LS**. Expression and regulation of aquaporins 1, 8, and 9 in the testis, efferent ducts, and epididymis of adult rats and during postnatal development. J Androl 2002; 23: 358-373.
165. **Tani T, Koyama Y, Nihei K, Hatakeyama S, Ohshiro K, Yoshida Y, Yaoita E, Sakai Y, Hatakeyama K, Yamamoto T**. Immunolocalization of aquaporin-8 in rat digestive organs and testis. Arch Histol Cytol 2001; 64: 159-168.
166. **Hozawa S, Holtzman EJ, Ausiello DA**. cAMP motifs regulating transcription in the aquaporin 2 gene. Am J Physiol 1996; 270: C1695-1702.
167. **Carr I, Clegg EJ, Meek GA**. Sertoli cells as phagocytes: an electron microscopic study. J Anat 1968; 102: 501-509.
168. **Chemes H**. The phagocytic function of Sertoli cells: a morphological, biochemical, and endocrinological study of lysosomes and acid phosphatase localization in the rat testis. Endocrinology 1986; 119: 1673-1681.
169. **Morales CR, Clermont Y**. Phagocytosis and endocytosis in Sertoli cells of the rat. Bull Assoc Anat (Nancy) 1991; 75: 157-162.
170. **Shiratsuchi A, Umeda M, Ohba Y, Nakanishi Y**. Recognition of phosphatidylserine on the surface of apoptotic spermatogenic cells and subsequent phagocytosis by Sertoli cells of the rat. J Biol Chem 1997; 272: 2354-2358.
171. **Kerr JB, de Kretser DM**. Proceedings: The role of the Sertoli cell in phagocytosis of the residual bodies of spermatids. J Reprod Fertil 1974; 36: 439-440.
172. **Kerr JB, De Kretser DM**. Cyclic variations in Sertoli cell lipid content throughout the spermatogenic cycle in the rat. J Reprod Fertil 1975; 43: 1-8.
173. **Nechamen CA, Thomas RM, Cohen BD, Acevedo G, Poulikakos PI, Testa JR, Dias JA**. Human follicle-stimulating hormone (FSH) receptor interacts with the adaptor protein APPL1 in HEK 293 cells: potential involvement of the PI3K pathway in FSH signaling. Biol Reprod 2004; 71: 629-636.
174. **Walker WH, Fucci L, Habener JF**. Expression of the gene encoding transcription factor cyclic adenosine 3',5'-monophosphate (cAMP) response element-binding protein (CREB): regulation by follicle-stimulating hormone-induced cAMP signaling in primary rat Sertoli cells. Endocrinology 1995; 136: 3534-3545.
175. **Crepieux P, Marion S, Martinat N, Fafeur V, Vern YL, Kerboeuf D, Guillou F, Reiter E**. The ERK-dependent signalling is stage-specifically modulated by FSH, during primary Sertoli cell maturation. Oncogene 2001; 20: 4696-4709.
176. **Grasso P, Reichert LE, Jr.** Follicle-stimulating hormone receptor-mediated uptake of 45Ca2+ by proteoliposomes and cultured rat sertoli cells: evidence for involvement of voltage-activated and voltage-independent calcium channels. Endocrinology 1989; 125: 3029-3036.
177. **Lalevee N, Pluciennik F, Joffre M**. Voltage-dependent calcium current with properties of T-type current in Sertoli cells from immature rat testis in primary cultures. Biol Reprod 1997; 56: 680-687.
178. **Spruill WA, Zysk JR, Tres LL, Kierszenbaum AL**. Calcium/calmodulin-dependent phosphorylation of vimentin in rat sertoli cells. Proc Natl Acad Sci U S A 1983; 80: 760-764.

179. **Wu GY, Deisseroth K, Tsien RW**. Activity-dependent CREB phosphorylation: convergence of a fast, sensitive calmodulin kinase pathway and a slow, less sensitive mitogen-activated protein kinase pathway. Proc Natl Acad Sci U S A 2001; 98: 2808-2813.
180. **Gonzalez-Robayna IJ, Falender AE, Ochsner S, Firestone GL, Richards JS**. Follicle-Stimulating hormone (FSH) stimulates phosphorylation and activation of protein kinase B (PKB/Akt) and serum and glucocorticoid-Induced kinase (Sgk): evidence for A kinase-independent signaling by FSH in granulosa cells. Mol Endocrinol 2000; 14: 1283-1300.
181. **Meroni SB, Riera MF, Pellizzari EH, Cigorraga SB**. Regulation of rat Sertoli cell function by FSH: possible role of phosphatidylinositol 3-kinase/protein kinase B pathway. J Endocrinol 2002; 174: 195-204.
182. **Jannini EA, Ulisse S, Cecconi S, Cironi L, Colonna R, D'Armiento M, Santoni A, Cifone MG**. Follicle-stimulating hormone-induced phospholipase A2 activity and eicosanoid generation in rat Sertoli cells. Biol Reprod 1994; 51: 140-145.
183. **Joyce CL, Nuzzo NA, Wilson L, Jr., Zaneveld LJ**. Evidence for a role of cyclooxygenase (prostaglandin synthetase) and prostaglandins in the sperm acrosome reaction and fertilization. J Androl 1987; 8: 74-82.
184. **Verhoeven G, Cailleau J**. Testicular peritubular cells secrete a protein under androgen control that inhibits induction of aromatase activity in Sertoli cells. Endocrinology 1988; 123: 2100-2110.
185. **Blok LJ, Mackenbach P, Trapman J, Themmen AP, Brinkmann AO, Grootegoed JA**. Follicle-stimulating hormone regulates androgen receptor mRNA in Sertoli cells. Mol Cell Endocrinol 1989; 63: 267-271.
186. **Sanborn BM, Caston LA, Chang C, Liao S, Speller R, Porter LD, Ku CY**. Regulation of androgen receptor mRNA in rat Sertoli and peritubular cells. Biol Reprod 1991; 45: 634-641.
187. **Blok LJ, Hoogerbrugge JW, Themmen AP, Baarends WM, Post M, Grootegoed JA**. Transient down-regulation of androgen receptor messenger ribonucleic acid (mRNA) expression in Sertoli cells by follicle-stimulating hormone is followed by up-regulation of androgen receptor mRNA and protein. Endocrinology 1992; 131: 1343-1349.
188. **Jarow JP, Zirkin BR**. The androgen microenvironment of the human testis and hormonal control of spermatogenesis. Ann N Y Acad Sci 2005; 1061: 208-220.
189. **McLachlan RI, O'Donnell L, Meachem SJ, Stanton PG, de Kretser DM, Pratis K, Robertson DM**. Identification of specific sites of hormonal regulation in spermatogenesis in rats, monkeys, and man. Recent Prog Horm Res 2002; 57: 149-179.
190. **Lyng FM, Jones GR, Rommerts FF**. Rapid androgen actions on calcium signaling in rat sertoli cells and two human prostatic cell lines: similar biphasic responses between 1 picomolar and 100 nanomolar concentrations. Biol Reprod 2000; 63: 736-747.
191. **Sadate-Ngatchou PI, Pouchnik DJ, Griswold MD**. Follicle-stimulating hormone induced changes in gene expression of murine testis. Mol Endocrinol 2004; 18: 2805-2816.
192. **Silva FR, Leite LD, Wassermann GF**. Rapid signal transduction in Sertoli cells. Eur J Endocrinol 2002; 147: 425-433.
193. **Lindsey JS, Wilkinson MF**. Pem: a testosterone- and LH-regulated homeobox gene expressed in mouse Sertoli cells and epididymis. Dev Biol 1996; 179: 471-484.
194. **Fawcett D**. Ultrastructure and function of Sertoli cell. In: Greep RO (ed) Handbook of physiology-endocrinology, Physiol Soc Washington D.C. Vol 5 pp 21-55. 1975.
195. **Vernet N, Dennefeld C, Klopfenstein M, Ruiz A, Bok D, Ghyselinck NB, Mark M**. Retinoid X receptor beta (RXRB) expression in Sertoli cells controls cholesterol homeostasis and spermiation. Reproduction 2008; 136: 619-626.
196. **Durham LA, 3rd, Grogan WM**. Characterization of multiple forms of cholesteryl ester hydrolase in the rat testis. J Biol Chem 1984; 259: 7433-7438.
197. **Ludvigson MA, Waites GM, Hamilton DW**. Immunocytochemical evidence for the specific localization of aldose reductase in rat Sertoli cells. Biol Reprod 1982; 26: 311-317.
198. **Joseph DR, Hall SH, Conti M, French FS**. The gene structure of rat androgen-binding protein: identification of potential regulatory deoxyribonucleic acid elements of a follicle-stimulating hormone-regulated protein. Mol Endocrinol 1988; 2: 3-13.
199. **Dorrington JH, Fritz IB**. Androgen synthesis and metabolism by preparations from the seminiferous tubule of the rat testis. Curr Top Mol Endocrinol 1975; 2: 37-52.
200. **O'Shaughnessy PJ, Morris ID, Huhtaniemi I, Baker PJ, Abel MH**. Role of androgen and gonadotrophins in the development and function of the Sertoli cells and Leydig cells: Data from mutant and genetically modified mice. Mol Cell Endocrinol 2008.
201. **Mallea LE, Machado AJ, Navaroli F, Rommerts FF**. Epidermal growth factor stimulates lactate production and inhibits aromatization in cultured Sertoli cells from immature rats. Int J Androl 1986; 9: 201-208.
202. **Sierens JE, Sneddon SF, Collins F, Millar MR, Saunders PT**. Estrogens in testis biology. Ann N Y Acad Sci 2005; 1061: 65-76.
203. **Bilinska B, Wiszniewska B, Kosiniak-Kamysz K, Kotula-Balak M, Gancarczyk M, Hejmej A, Sadowska J, Marchlewicz M, Kolasa A, Wenda-Rozewicka L**. Hormonal status of male reproductive system: androgens and estrogens in the testis and epididymis. In vivo and in vitro approaches. Reprod Biol 2006; 6 Suppl 1: 43-58.
204. **Eddy EM**. Regulation of gene expression during spermatogenesis. Semin Cell Dev Biol 1998; 9: 451-457.
205. **Russell LD, Ettlin RA, Sinha Hikim AP, Clegg ED**. Histological and histopathological evolution of the testis. Cache River Press 1990; ISBN 0-9627422-0-1.
206. **Rhodin J**. "Correlation of ultrastructural organization and function in normal and experimentally changed proximal tubule cells of the mouse kidney". Doctorate Thesis. Karolinska Institutet, Stockholm. 1954.
207. **Rouiller C, Bernard W**. "Microbodies"and the problem of mitochondrial regeneration in liver cell. J Biophys Biochem Cytol 1956; (suppl 2):355-358.
208. **De Duve C, Baudhuin P**. Peroxisomes (microbodies and related particles). Physiol Rev 1966; 46: 323-357.
209. **Fahimi HD, Baumgart E**. Current cytochemical techniques for the investigation of peroxisomes. A review. J Histochem Cytochem 1999; 47:1219-1232.
210. **Lüers GH, Thiele S, Schad A, Völkl A, Yokota S, Seitz J**. Peroxisomes are present in murine spermatogonia and disappear during the course of spermatogenesis. Histochem Cell Biol 125:693-703. 2006.
211. **Holzmann E**. Peroxisomes in nervous tissue. Ann NY Acad Sci 386: 523-535. 1982.
212. **Usuda N, Reddy KM, Hashimoto T, Rao SM, Reddy JK**. Tissue specificity and species differences in the distribution of urate oxidase in peroxisomes.Lab Invest 58: 100-111. 1988.
213. **Angermuller S, Bruder G, Volkl A, Wesch H, Fahimi HD**. Localization of xanthine oxidase in crystalline cores of peroxisomes. A cytochemical and biochemical study. Eur J Cell Biol 45: 137-144. 1987.

214. **Wu XW, Lee CC, Muzny DM, Caskey CT**. Urate oxidase: primary structure and evolutionary implications. Proc Natl Acad Sci U S A 1989; 86: 9412-9416.
215. **Gorgas K**. Serial section analysis of proximal shape and membrane relationship in the mouse prepucial gland. In: HD Fahimi, H Sies (eds). Peroxisomes in Biology and Medicine. Springer-Verlag, Berlin, Heidelberg:3-17. 1987.
216. **Yamamoto L, Fahimi HD**. Three-dimensional reconstruction of a peroxisomal reticulum in regenerating rat liver: Evidence of interconnections between heterogeneous segments. J Cell Biol105: 713-722. 1987.
217. **Gorgas K**. Peroxisomes in sebaceous glands. V. Complex peroxisomes in the mouse preputial gland: serial sectioning and three-dimensional reconsruction studies. Anat Embryol 169:261-270. 1984.
218. **Fujiki Y, Fowler S, Shio H, Hubbard AL, Lazarow PB**. Polypeptide and phospholipid composition of the membrane of rat liver peroxisomes: comparison with endoplasmic reticulum and mitochondrial membranes. J Cell Biol 93: 103-110. . 1982.
219. **Van Veldhoven PP, Just WW, Mannaerts GP**. Permeability of the peroxisomal membrane to cofactors of beta-oxidation. Evidence for the presence of a pore-forming protein. J Biol Chem 262:4310-4318. 1987.
220. **Platta HW, Erdmann R**. Peroxisomal dynamics. Trends Cell Biol 2007; 17: 474-484.
221. **Distel B, Erdmann E, Gould SJ, Blobel G, Crane DI, Cregg JM, Dodt G, Fujiki Y, Goodman JM, Just WW, Kiel D JAKW, Kunau WH, Lazarow PB, Mannaerts GP, Moser HW, Osumi T, Rachubinski RA, Roscher A, Subramani S, Tabak HF, Tsukamoto T, Valle D, Klei I, Veldhoven PP, Veenhuis M**. A unified nomenclature for peroxisome biogenesis factors. J. Cell Biol. 135, pp:1-3. 1996.
222. **Baumgart E, Völkl A, Hashimoto T, HD F**. Biogenesis of peroxisomes: immunocytochemical investigation of peroxisomal membrane proteins in proliferating rat liver peroxisomes and in catalase-negative membrane loops. J Cell Biol 108:2221-2231. 1989.
223. **Girzalsky W, Platta HW, Erdmann R**. Protein transport across the peroxisomal membrane. Biol Chem 2009; 390: 745-751.
224. **Subramani S**. Protein translocation into peroxisomes. J Biol Chem 1996; 271: 32483-32486.
225. **Subramani S**. Protein import into peroxisomes and biogenesis of the organelle. Annu Rev Cell Biol 1993; 9: 445-478.
226. **Valle D, Gartner J**. Human genetics. Penetrating the peroxisome. Nature 1993; 361: 682-683.
227. **Holzinger A, Kammerer S, Berger J, Roscher AA**. cDNA cloning and mRNA expression of the human adrenoleukodystrophy related protein (ALDRP), a peroxisomal ABC transporter. Biochem Biophys Res Commun 1997; 239: 261-264.
228. **Baumgart E, Volkl A, Hashimoto T, Fahimi HD**. Biogenesis of peroxisomes: immunocytochemical investigation of peroxisomal membrane proteins in proliferating rat liver peroxisomes and in catalase-negative membrane loops. J Cell Biol 1989; 108: 2221-2231.
229. **Shani N, Jimenez-Sanchez G, Steel G, Dean M, Valle D**. Identification of a fourth half ABC transporter in the human peroxisomal membrane. Hum Mol Genet 1997; 6: 1925-1931.
230. **Gartner J, Valle D**. The 70 kDa peroxisomal membrane protein: an ATP-binding cassette transporter protein involved in peroxisome biogenesis. Semin Cell Biol 1993; 4: 45-52.
231. **Rayapuram N, Subramani S**. The importomer--a peroxisomal membrane complex involved in protein translocation into the peroxisome matrix. Biochim Biophys Acta 2006; 1763: 1613-1619.
232. **Wanders RJ**. Peroxisomes, lipid metabolism, and peroxisomal disorders. Mol Genet Metab 2004; 83: 16-27.
233. **Karnati S, Baumgart-Vogt E**. Peroxisomes in mouse and human lung: their involvement in pulmonary lipid metabolism. Histochem Cell Biol 2008; 130: 719-740.
234. **Baumgart E**. Application of in situ hybridization, cytochemical and immunocytochemical techniques for the investigation of peroxisomes. A review including novel data. Robert Feulgen Prize Lecture 1997. Histochem Cell Biol 1997; 108: 185-210.
235. **Luers GH, Nenicu A, Baumgart-Vogt E**. Peroxisomes are essential for regular spermatogenesis. Biology of male germ cells. Shaker Verlag ISBN978-3-8322-7682-9 2008.
236. **Karnati S, Baumgart-Vogt E, Immenschuh S**. Peroxisomes in mouse and human lung: their involvement in pulmonary lipid metabolism. Histochem Cell Biol 2008; 130: 719-740.
237. **Mohan R, Heyman RA**. Orphan nuclear receptor modulators. Curr Top Med Chem 2003; 3: 1637-1647.
238. **de Duve C, Palade GE**. Albert Claude, 1899-1983. Nature 1983; 304: 588.
239. **Islinger M, Luers GH, Li KW, Loos M, Volkl A**. Rat liver peroxisomes after fibrate treatment. A survey using quantitative mass spectrometry. J Biol Chem 2007; 282: 23055-23069.
240. **Hajra AK, Bishop JE**. Glycerolipid biosynthesis in peroxisomes via the acyl dihydroxyacetone phosphate pathway. Ann N Y Acad Sci 1982; 386: 170-182.
241. **Singh I, Voigt RG, Sheikh FG, Kremser K, Brown FR, 3rd**. Biochemical features of a patient with Zellweger-like syndrome with normal PTS-1 and PTS-2 peroxisomal protein import systems: a new peroxisomal disease. Biochem Mol Med 1997; 61: 198-207.
242. **Stolz DB, Zamora R, Vodovotz Y, Loughran PA, Billiar TR, Kim YM, Simmons RL, Watkins SC**. Peroxisomal localization of inducible nitric oxide synthase in hepatocytes. Hepatology 2002; 36: 81-93.
243. **Steinberg SJ, Dodt G, Raymond GV, Braverman NE, Moser AB, Moser HW**. Peroxisome biogenesis disorders. Biochim Biophys Acta 2006; 1763: 1733-1748.
244. **Wanders RJ, Waterham HR**. Peroxisomal disorders I: biochemistry and genetics of peroxisome biogenesis disorders. Clin Genet 2005; 67: 107-133.
245. **Wanders RJ, Ferdinandusse S, Brites P, Kemp S**. Peroxisomes, lipid metabolism and lipotoxicity. Biochim Biophys Acta; Epub ahead of print 2010;.
246. **Powers JM, Schaumburg HH**. Adreno-leukodystrophy (sex-linked Schilder's disease). A pathogenetic hypothesis based on ultrastructural lesions in adrenal cortex, peripheral nerve and testis. Am J Pathol 1974; 76: 481-491.
247. **Powers JM, Schaumburg HH**. The testis in adreno-leukodystrophy. Am J Pathol 1981; 102: 90-98.
248. **Kemp S, Wanders RJ**. X-linked adrenoleukodystrophy: very long-chain fatty acid metabolism, ABC half-transporters and the complicated route to treatment. Mol Genet Metab 2007; 90: 268-276.
249. **Powers JM**. Adreno-leukodystrophy (adreno-testiculo-leukomyelo-neuropathic-complex). Clin Neuropathol 1985; 4: 181-199.
250. **Brennemann W, Kohler W, Zierz S, Klingmuller D**. Testicular dysfunction in adrenomyeloneuropathy. Eur J Endocrinol 1997; 137: 34-39.
251. **Aversa A, Palleschi S, Cruccu G, Silvestroni L, Isidori A, Fabbri A**. Rapid decline of fertility in a case of adrenoleukodystrophy. Hum Reprod 1998; 13: 2474-2479.

252. **Dimmick JE**. Pathology of peroxisomal disorders. In: Organelle disease. Clinical features, diagnosis pathogenesis and management. Applegarth DA, Dimmick JE, HallJG (eds), Chapman & Hall, London, pp 211-232. 1997.
253. **Bay K, Asklund C, Skakkebaek NE, Andersson AM**. Testicular dysgenesis syndrome: possible role of endocrine disrupters. Best Pract Res Clin Endocrinol Metab 2006; 20: 77-90.
254. **Foresta C, Zuccarello D, Garolla A, Ferlin A**. Role of hormones, genes, and environment in human cryptorchidism. Endocr Rev 2008; 29: 560-580.
255. **Baes M, Van Veldhoven PP**. Generalised and conditional inactivation of Pex genes in mice. Biochim Biophys Acta 2006; 1763: 1785-1793.
256. **Fan CY, Pan J, Chu R, Lee D, Kluckman KD, Usuda N, Singh I, Yeldandi AV, Rao MS, Maeda N, Reddy JK**. Targeted disruption of the peroxisomal fatty acyl-CoA oxidase gene: generation of a mouse model of pseudoneonatal adrenoleukodystrophy. Ann N Y Acad Sci 1996; 804: 530-541.
257. **Fan CY, Pan J, Chu R, Lee D, Kluckman KD, Usuda N, Singh I, Yeldandi AV, Rao MS, Maeda N, Reddy JK**. Hepatocellular and hepatic peroxisomal alterations in mice with a disrupted peroxisomal fatty acyl-coenzyme A oxidase gene. J Biol Chem 1996; 271: 24698-24710.
258. **Rodemer C, Thai TP, Brugger B, Kaercher T, Werner H, Nave KA, Wieland F, Gorgas K, Just WW**. Inactivation of ether lipid biosynthesis causes male infertility, defects in eye development and optic nerve hypoplasia in mice. Hum Mol Genet 2003; 12: 1881-1895.
259. **Huyghe S, Schmalbruch H, De Gendt K, Verhoeven G, Guillou F, Van Veldhoven PP, Baes M**. Peroxisomal multifunctional protein 2 is essential for lipid homeostasis in Sertoli cells and male fertility in mice. Endocrinology 2006; 147: 2228-2236.
260. **Monosov EZ, Wenzel TJ, Luers GH, Heyman JA, Subramani S**. Labeling of peroxisomes with green fluorescent protein in living P. pastoris cells. J Histochem Cytochem 1996; 44: 581-589.
261. **Miller SA, Dykes DD, Polesky HF**. A simple salting out procedure for extracting DNA from human nucleated cells. Nucleic Acids Res 1988; 16: 1215.
262. **Mendis-Handagama SM, Zirkin BR, Scallen TJ, Ewing LL**. Studies on peroxisomes of the adult rat Leydig cell. J Androl 1990; 11: 270-278.
263. **Slot JW, Geuze HJ**. Sizing of protein A-colloidal gold probes for immunoelectron microscopy. J Cell Biol 1981; 90: 533-536.
264. **Grabenbauer M, Fahimi HD, Baumgart E**. Detection of peroxisomal proteins and their mRNAs in serial sections of fetal and newborn mouse organs. J Histochem Cytochem 2001; 49: 155-164.
265. **Schumacher M, Schafer G, Holstein AF, Hilz H**. Rapid isolation of mouse Leydig cells by centrifugation in Percoll density gradients with complete retention of morphological and biochemical integrity. FEBS Lett 1978; 91: 333-338.
266. **Monsees TK, Miska W, Schill WB**. Enzymatic digestion of bradykinin by rat Sertoli cell cultures. J Androl 1996; 17: 375-381.
267. **Galdieri M ZE, Palombi F, Russo MA, Stefani M.** Sertoli cell cultures: a new model for the study of somatic-germ cell interactions. J Androl, 5:249–254. 1981.
268. **Völkl A BE, Fahimi HD.** Isolation and characterization of peroxisomes. . In: Graham JM, Rickwood D (eds.), Subcellular Fractionation. Oxford: IRL Press at Oxford University Press, 143-167. 1997.
269. **Bradford MM**. A rapid and sensitive method for the quantitation of microgram quantities of protein utilizing the principle of protein-dye binding. Anal Biochem 1976; 72: 248-254.
270. **Moser HW MA**. Measurements of saturated very long chain fatty acids in plasma. in: Hommes F.A. (Ed.), Techniques in Diagnostic Human Biochemical Genetics, Wiley-Liss, New York, pp. 177-191. 1991.
271. **Geuze HJ, Slot JW, van der Ley PA, Scheffer RC**. Use of colloidal gold particles in double-labeling immunoelectron microscopy of ultrathin frozen tissue sections. J Cell Biol 1981; 89: 653-665.
272. **Fahimi HD, Baumgart E**. Current cytochemical techniques for the investigation of peroxisomes. A review. J Histochem Cytochem 1999; 47: 1219-1232.
273. **Oakberg EF**. A description of spermiogenesis in the mouse and its use in analysis of the cycle of the seminiferous epithelium and germ cell renewal. Am J Anat 99:391-409. 1956.
274. **Russel LD ER, Sinha Hikim AP, Clegg ED.** . Histological and Histopathological Evaluation of the Testis. Clearwater: Cache River Press; 1990.
275. **Bjorkman J, Tonks I, Maxwell MA, Paterson C, Kay GF, Crane DI**. Conditional inactivation of the peroxisome biogenesis Pex13 gene by Cre-loxP excision. Genesis. 2:179-80 2002
276. **Lécureuil C, Fontaine I, Crepieux P, Guillou F**. Sertoli and granulosa cell-specific Cre recombinase activity in transgenic mice. Genesis 3:114-8 2002.
277. **Bellvé AR CJ, Millette CF, O'Brien DA, Bhatnagar YM, Dym M.** Spermatogenic cells of the prepuberal mouse. Isolation and morphological characterization. J Cell Biol. 74:68-85. 1977.
278. **Ebata KT ZX, Nagano MC.** Male germ line stem cells have an altered potential to proliferate and differentiate during postnatal development in mice. Biol Reprod 5:841-7 2007.
279. **McCarrey JR, Dilworth DD, Sharp RM**. Semiquantitative analysis of X-linked gene expression during spermatogenesis in the mouse: ethidium-bromide staining of RT-PCR products. Genet Anal Tech Appl 4:117-23 1992
280. **Herschman HR, Xie W, Reddy S**. Inflammation, reproduction, cancer and all that.... The regulation and role of the inducible prostaglandin synthase. Bioessays 1995; 17: 1031-1037.
281. **Cudicini C, Lejeune H, Gomez E, Bosmans E, Ballet F, Saez J, Jegou B**. Human Leydig cells and Sertoli cells are producers of interleukins-1 and -6. J Clin Endocrinol Metab 1997; 82: 1426-1433.
282. **Lemberger T, Braissant O, Juge-Aubry C, Keller H, Saladin R, Staels B, Auwerx J, Burger AG, Meier CA, Wahli W**. PPAR tissue distribution and interactions with other hormone-signaling pathways. Ann N Y Acad Sci 1996; 804: 231-251.
283. **Corton JC, Anderson SP, Stauber A**. Central role of peroxisome proliferator-activated receptors in the actions of peroxisome proliferators. Annu Rev Pharmacol Toxicol 2000; 40: 491-518.
284. **Jegou B, Pineau C, Velez de la Calle JF, Touzalin AM, Bardin CW, Cheng CY**. Germ cell control of testin production is inverse to that of other Sertoli cell products. Endocrinology 1993; 132: 2557-2562.
285. **Martin LJ, Taniguchi H, Robert NM, Simard J, Tremblay JJ, Viger RS**. GATA factors and the nuclear receptors, steroidogenic factor 1/liver receptor homolog 1, are key mutual partners in the regulation of the human 3beta-hydroxysteroid dehydrogenase type 2 promoter. Mol Endocrinol 2005; 19: 2358-2370.
286. **Bedell MA, Mahakali Zama A**. Genetic analysis of Kit ligand functions during mouse spermatogenesis. J Androl 2004; 25: 188-199.

287. **Baumgart E, Schad A, Volkl A, Fahimi HD**. Detection of mRNAs encoding peroxisomal proteins by non-radioactive in situ hybridization with digoxigenin-labelled cRNAs. Histochem Cell Biol 1997; 108: 371-379.
288. **Reisse S, Rothardt G, Volkl A, Beier K**. Peroxisomes and ether lipid biosynthesis in rat testis and epididymis. Biol Reprod 2001; 64: 1689-1694.
289. **Zini A, Schlegel PN**. Catalase mRNA expression in the male rat reproductive tract. J Androl 1996; 17: 473-480.
290. **Ahlabo I, Barnard T**. Observations on peroxisomes in brown adipose tissue of the rat. J Histochem Cytochem 1971; 19: 670-675.
291. **Luers GH, Schad A, Fahimi HD, Volkl A, Seitz J**. Expression of peroxisomal proteins provides clear evidence for the presence of peroxisomes in the male germ cell line GC1spg. Cytogenet Genome Res 2003; 103: 360-365.
292. **Nenicu A, Baumgart-Vogt E**. Heterogeneity of peroxisomes in distinct cell types of the adult mouse testis. Eur J Cell Biol 2005; 55(suppl):58.
293. **Luers GH, Thiele S, Schad A, Volkl A, Yokota S, Seitz J**. Peroxisomes are present in murine spermatogonia and disappear during the course of spermatogenesis. Histochem Cell Biol 2006; 125: 693-703.
294. **Stier H, Fahimi HD, Van Veldhoven PP, Mannaerts GP, Volkl A, Baumgart E**. Maturation of peroxisomes in differentiating human hepatoblastoma cells (HepG2): possible involvement of the peroxisome proliferator-activated receptor alpha (PPAR alpha). Differentiation 1998; 64: 55-66.
295. **Tsai SC, Lu CC, Lin CS, Wang PS**. Antisteroidogenic actions of hydrogen peroxide on rat Leydig cells. J Cell Biochem 2003; 90: 1276-1286.
296. **Schrader M, Fahimi HD**. Peroxisomes and oxidative stress. Biochim Biophys Acta 2006; 1763: 1755-1766.
297. **Schultz R, Yan W, Toppari J, Volkl A, Gustafsson JA, Pelto-Huikko M**. Expression of peroxisome proliferator-activated receptor alpha messenger ribonucleic acid and protein in human and rat testis. Endocrinology 1999; 140: 2968-2975.
298. **Cooper DR, Carpenter MP**. Sertoli-cell prostaglandin synthesis. Effects of (follitropin) differentiation and dietary vitamin E. Biochem J 1987; 241: 847-855.
299. **Wanders RJ, Waterham HR**. Biochemistry of mammalian peroxisomes revisited. Annu Rev Biochem 2006; 75: 295-332.
300. **Wolf DE**. Lipid domains in sperm plasma membranes. Mol Membr Biol 1995; 12: 101-104.
301. **Aveldano MI, Robinson BS, Johnson DW, Poulos A**. Long and very long chain polyunsaturated fatty acids of the n-6 series in rat seminiferous tubules. Active desaturation of 24:4n-6 to 24:5n-6 and concomitant formation of odd and even chain tetraenoic and pentaenoic fatty acids up to C32. J Biol Chem 1993; 268: 11663-11669.
302. **Zaar K, Kost HP, Schad A, Volkl A, Baumgart E, Fahimi HD**. Cellular and subcellular distribution of D-aspartate oxidase in human and rat brain. J Comp Neurol 2002; 450: 272-282.
303. **Seiler N, Raul F**. Polyamines and apoptosis. J Cell Mol Med 2005; 9: 623-642.
304. **Gorgas K**. Morphogenesis of peroxisomes in lipid-synthesizing epithelia. In: Fahimi HD, Sies H (eds.), Peroxisomes in Biology and Medicine. Heidelberg: Springer Verlag; 1987;25: 3-17.
305. **Gorgas K**. Peroxisomes in sebaceous glands. V. Complex peroxisomes in the mouse preputial gland: serial sectioning and three-dimensional reconstruction studies. Anat Embryol (Berl) 1984; 169: 261-270.
306. **Gorgas K, Volkl A**. Peroxisomes in sebaceous glands. IV. Aggregates of tubular peroxisomes in the mouse Meibomian gland. Histochem J 1984; 16: 1079-1098.
307. **Baumgart E, Stegmeier K, Schmidt FH, Fahimi HD**. Proliferation of peroxisomes in pericentral hepatocytes of rat liver after administration of a new hypocholesterolemic agent (BM 15766). Sex-dependent ultrastructural differences. Lab Invest 1987; 56: 554-564.
308. **Li X, Baumgart E, Dong GX, Morrell JC, Jimenez-Sanchez G, Valle D, Smith KD, Gould SJ**. PEX11alpha is required for peroxisome proliferation in response to 4-phenylbutyrate but is dispensable for peroxisome proliferator-activated receptor alpha-mediated peroxisome proliferation. Mol Cell Biol 2002; 22: 8226-8240.
309. **Li X, Baumgart E, Morrell JC, Jimenez-Sanchez G, Valle D, Gould SJ**. PEX11 beta deficiency is lethal and impairs neuronal migration but does not abrogate peroxisome function. Mol Cell Biol 2002; 22: 4358-4365.
310. **Sharpe RM, McKinnell C, Kivlin C, Fisher JS**. Proliferation and functional maturation of Sertoli cells, and their relevance to disorders of testis function in adulthood. Reproduction 2003; 125: 769-784.
311. **Marzouki ZM, Coniglio JG**. Effect of essential fatty acid deficiency on lipids of rat Sertoli and germinal cells. Biol Reprod 1982; 27: 312-315.
312. **Brites P, Motley AM, Gressens P, Mooyer PA, Ploegaert I, Everts V, Evrard P, Carmeliet P, Dewerchin M, Schoonjans L, Duran M, Waterham HR, Wanders RJ, Baes M**. Impaired neuronal migration and endochondral ossification in Pex7 knockout mice: a model for rhizomelic chondrodysplasia punctata. Hum Mol Genet 2003; 12: 2255-2267.
313. **Brites P, Mooyer PA, El Mrabet L, Waterham HR, Wanders RJ**. Plasmalogens participate in very-long-chain fatty acid-induced pathology. Brain 2009; 132: 482-492.
314. **Yan W, Kero J, Huhtaniemi I, Toppari J**. Stem cell factor functions as a survival factor for mature Leydig cells and a growth factor for precursor Leydig cells after ethylene dimethane sulfonate treatment: implication of a role of the stem cell factor/c-Kit system in Leydig cell development. Dev Biol 2000; 227: 169-182.
315. **Mori H, Tamai M, Fushimi H, Fukuda H, Maeda T**. Leydig cells within the aspermatogenic seminiferous tubules. Hum Pathol 1987; 18: 1227-1231.
316. **Reijo R, Lee TY, Salo P, Alagappan R, Brown LG, Rosenberg M, Rozen S, Jaffe T, Straus D, Hovatta O, et al.** Diverse spermatogenic defects in humans caused by Y chromosome deletions encompassing a novel RNA-binding protein gene. Nat Genet 1995; 10: 383-393.
317. **Khalaj M, Abbasi AR, Nishimura R, Akiyama K, Tsuji T, Noguchi J, Okuda K, Kunieda T**. Leydig cell hyperplasia in an ENU-induced mutant mouse with germ cell depletion. J Reprod Dev 2008; 54: 225-228.
318. **Wikstrom AM, Raivio T, Hadziselimovic F, Wikstrom S, Tuuri T, Dunkel L**. Klinefelter syndrome in adolescence: onset of puberty is associated with accelerated germ cell depletion. J Clin Endocrinol Metab 2004; 89: 2263-2270.
319. **Lilford R, Jones AM, Bishop DT, Thornton J, Mueller R**. Case-control study of whether subfertility in men is familial. BMJ 1994; 309: 570-573.
320. **Fisher JS, Macpherson S, Marchetti N, Sharpe RM**. Human 'testicular dysgenesis syndrome': a possible model using in-utero exposure of the rat to dibutyl phthalate. Hum Reprod 2003; 18: 1383-1394.
321. **Wanders RJ, Visser WF, van Roermund CW, Kemp S, Waterham HR**. The peroxisomal ABC transporter family. Pflugers Arch 2007; 453: 719-734.

322. **Kashiwayama Y, Seki M, Yasui A, Murasaki Y, Morita M, Yamashita Y, Sakaguchi M, Tanaka Y, Imanaka T**. 70-kDa peroxisomal membrane protein related protein (P70R/ABCD4) localizes to endoplasmic reticulum not peroxisomes, and NH2-terminal hydrophobic property determines the subcellular localization of ABC subfamily D proteins. Exp Cell Res 2009; 315: 190-205.
323. **Imanaka T, Aihara K, Takano T, Yamashita A, Sato R, Suzuki Y, Yokota S, Osumi T**. Characterization of the 70-kDa peroxisomal membrane protein, an ATP binding cassette transporter. J Biol Chem 1999; 274: 11968-11976.
324. **Nagasaki S, Miki Y, Akahira J, Suzuki T, Sasano H**. Transcriptional regulation of 17beta-hydroxysteroid dehydrogenase type 12 by SREBP-1. Mol Cell Endocrinol 2009; 307: 163-168.
325. **Weinhofer I, Forss-Petter S, Zigman M, Berger J**. Cholesterol regulates ABCD2 expression: implications for the therapy of X-linked adrenoleukodystrophy. Hum Mol Genet 2002; 11: 2701-2708.
326. **Gueugnon F, Gondcaille C, Leclercq S, Bellenger J, Bellenger S, Narce M, Pineau T, Bonnetain F, Savary S**. Dehydroepiandrosterone up-regulates the Adrenoleukodystrophy-related gene (ABCD2) independently of PPARalpha in rodents. Biochimie 2007; 89: 1312-1321.
327. **Gartner J, Jimenez-Sanchez G, Roerig P, Valle D**. Genomic organization of the 70-kDa peroxisomal membrane protein gene (PXMP1). Genomics 1998; 48: 203-208.
328. **Baumgart E, Fahimi HD, Steininger H, Grabenbauer M**. A review of morphological techniques for detection of peroxisomal (and mitochondrial) proteins and their corresponding mRNAs during ontogenesis in mice: application to the PEX5-knockout mouse with Zellweger syndrome. Microsc Res Tech 2003; 61: 121-138.
329. **de Launoit Y, Adamski J**. Unique multifunctional HSD17B4 gene product: 17beta-hydroxysteroid dehydrogenase 4 and D-3-hydroxyacyl-coenzyme A dehydrogenase/hydratase involved in Zellweger syndrome. J Mol Endocrinol 1999; 22: 227-240.
330. **Beier K, Volkl A, Metzger C, Mayer D, Bannasch P, Fahimi HD**. Hepatic zonation of the induction of cytochrome P450 IVA, peroxisomal lipid beta-oxidation enzymes and peroxisome proliferation in rats treated with dehydroepiandrosterone (DHEA). Evidence of distinct zonal and sex-specific differences. Carcinogenesis 1997; 18: 1491-1498.
331. **Kangasniemi M, Kaipia A, Toppari J, Mali P, Huhtaniemi I, Parvinen M**. Cellular regulation of basal and FSH-stimulated cyclic AMP production in irradiated rat testes. Anat Rec 1990; 227: 32-36.
332. **Skinner MK, Griswold MD**. Sertoli cells synthesize and secrete transferrin-like protein. J Biol Chem 1980; 255: 9523-9525.
333. **Pineau C, Sharpe RM, Saunders PT, Gerard N, Jegou B**. Regulation of Sertoli cell inhibin production and of inhibin alpha-subunit mRNA levels by specific germ cell types. Mol Cell Endocrinol 1990; 72: 13-22.
334. **Grasso P, Joseph MP, Reichert LE, Jr.** A new role for follicle-stimulating hormone in the regulation of calcium flux in Sertoli cells: inhibition of Na+/Ca++ exchange. Endocrinology 1991; 128: 158-164.
335. **Walker WH, Daniel PB, Habener JF**. Inducible cAMP early repressor ICER down-regulation of CREB gene expression in Sertoli cells. Mol Cell Endocrinol 1998; 143: 167-178.
336. **Carreau S, Delalande C, Silandre D, Bourguiba S, Lambard S**. Aromatase and estrogen receptors in male reproduction. Mol Cell Endocrinol 2006; 246: 65-68.
337. **Zheng W, Jefcoate CR**. Steroidogenic factor-1 interacts with cAMP response element-binding protein to mediate cAMP stimulation of CYP1B1 via a far upstream enhancer. Mol Pharmacol 2005; 67: 499-512.
338. **Song KH, Park JI, Lee MO, Soh J, Lee K, Choi HS**. LH induces orphan nuclear receptor Nur77 gene expression in testicular Leydig cells. Endocrinology 2001; 142: 5116-5123.
339. **Viger RS, Mertineit C, Trasler JM, Nemer M**. Transcription factor GATA-4 is expressed in a sexually dimorphic pattern during mouse gonadal development and is a potent activator of the Mullerian inhibiting substance promoter. Development 1998; 125: 2665-2675.
340. **McCoard SA, Wise TH, Fahrenkrug SC, Ford JJ**. Temporal and spatial localization patterns of Gata4 during porcine gonadogenesis. Biol Reprod 2001; 65: 366-374.
341. **Tremblay JJ, Viger RS**. Transcription factor GATA-4 enhances Mullerian inhibiting substance gene transcription through a direct interaction with the nuclear receptor SF-1. Mol Endocrinol 1999; 13: 1388-1401.
342. **Tremblay JJ, Viger RS**. GATA factors differentially activate multiple gonadal promoters through conserved GATA regulatory elements. Endocrinology 2001; 142: 977-986.
343. **Feng ZM, Wu AZ, Zhang Z, Chen CL**. GATA-1 and GATA-4 transactivate inhibin/activin beta-B-subunit gene transcription in testicular cells. Mol Endocrinol 2000; 14: 1820-1835.
344. **Rahman NA, Kiiveri S, Rivero-Muller A, Levallet J, Vierre S, Kero J, Wilson DB, Heikinheimo M, Huhtaniemi I**. Adrenocortical tumorigenesis in transgenic mice expressing the inhibin alpha-subunit promoter/simian virus 40 T-antigen transgene: relationship between ectopic expression of luteinizing hormone receptor and transcription factor GATA-4. Mol Endocrinol 2004; 18: 2553-2569.
345. **Hiroi H, Christenson LK, Strauss JF, 3rd**. Regulation of transcription of the steroidogenic acute regulatory protein (StAR) gene: temporal and spatial changes in transcription factor binding and histone modification. Mol Cell Endocrinol 2004; 215: 119-126.
346. **Fluck CE, Miller WL**. GATA-4 and GATA-6 modulate tissue-specific transcription of the human gene for P450c17 by direct interaction with Sp1. Mol Endocrinol 2004; 18: 1144-1157.
347. **Kiiveri S, Liu J, Westerholm-Ormio M, Narita N, Wilson DB, Voutilainen R, Heikinheimo M**. Differential expression of GATA-4 and GATA-6 in fetal and adult mouse and human adrenal tissue. Endocrinology 2002; 143: 3136-3143.
348. **Nakanishi T**. Endocrine disruption induced by organotin compounds; organotins function as a powerful agonist for nuclear receptors rather than an aromatase inhibitor. J Toxicol Sci 2008; 33: 269-276.
349. **Jones ME, Thorburn AW, Britt KL, Hewitt KN, Misso ML, Wreford NG, Proietto J, Oz OK, Leury BJ, Robertson KM, Yao S, Simpson ER**. Aromatase-deficient (ArKO) mice accumulate excess adipose tissue. J Steroid Biochem Mol Biol 2001; 79: 3-9.
350. **Murata Y, Robertson KM, Jones ME, Simpson ER**. Effect of estrogen deficiency in the male: the ArKO mouse model. Mol Cell Endocrinol 2002; 193: 7-12.
351. **Nitta H, Bunick D, Hess RA, Janulis L, Newton SC, Millette CF, Osawa Y, Shizuta Y, Toda K, Bahr JM**. Germ cells of the mouse testis express P450 aromatase. Endocrinology 1993; 132: 1396-1401.
352. **Ohlsson C, Hellberg N, Parini P, Vidal O, Bohlooly YM, Rudling M, Lindberg MK, Warner M, Angelin B, Gustafsson JA**. Obesity and disturbed lipoprotein profile in estrogen receptor-alpha-deficient male mice. Biochem Biophys Res Commun 2000; 278: 640-645.

353. **Dieuaide-Noubhani M, Asselberghs S, Mannaerts GP, Van Veldhoven PP**. Evidence that multifunctional protein 2, and not multifunctional protein 1, is involved in the peroxisomal beta-oxidation of pristanic acid. Biochem J 1997; 325 (Pt 2): 367-373.
354. **Dieuaide-Noubhani M, Novikov D, Baumgart E, Vanhooren JC, Fransen M, Goethals M, Vandekerckhove J, Van Veldhoven PP, Mannaerts GP**. Further characterization of the peroxisomal 3-hydroxyacyl-CoA dehydrogenases from rat liver. Relationship between the different dehydrogenases and evidence that fatty acids and the C27 bile acids di- and tri-hydroxycoprostanic acids are metabolized by separate multifunctional proteins. Eur J Biochem 1996; 240: 660-666.
355. **Nguyen SD, Baes M, Van Veldhoven PP**. Degradation of very long chain dicarboxylic polyunsaturated fatty acids in mouse hepatocytes, a peroxisomal process. Biochim Biophys Acta 2008; 1781: 400-405.
356. **van Grunsven EG, van Berkel E, Ijlst L, Vreken P, de Klerk JB, Adamski J, Lemonde H, Clayton PT, Cuebas DA, Wanders RJ**. Peroxisomal D-hydroxyacyl-CoA dehydrogenase deficiency: resolution of the enzyme defect and its molecular basis in bifunctional protein deficiency. Proc Natl Acad Sci U S A 1998; 95: 2128-2133.
357. **Nagayoshi Y, Ohba T, Yamamoto H, Miyahara Y, Tashiro H, Katabuchi H, Okamura H**. Characterization of 17beta-hydroxysteroid dehydrogenase type 4 in human ovarian surface epithelial cells. Mol Hum Reprod 2005; 11: 615-621.
358. **Corton JC, Bocos C, Moreno ES, Merritt A, Cattley RC, Gustafsson JA**. Peroxisome proliferators alter the expression of estrogen-metabolizing enzymes. Biochimie 1997; 79: 151-162.
359. **Fan LQ, You L, Brown-Borg H, Brown S, Edwards RJ, Corton JC**. Regulation of phase I and phase II steroid metabolism enzymes by PPAR alpha activators. Toxicology 2004; 204: 109-121.
360. **Castro LF, Rocha MJ, Lobo-da-Cunha A, Batista-Pinto C, Machado A, Rocha E**. The 17beta-hydroxysteroid dehydrogenase 4: Gender-specific and seasonal gene expression in the liver of brown trout (Salmo trutta f. fario). Comp Biochem Physiol B Biochem Mol Biol 2009; 153: 157-164.
361. **Batista-Pinto C, Rocha E, Castro LF, Rodrigues P, Lobo-da-Cunha A**. Seasonal and gender variation of peroxisome proliferator activated receptors expression in brown trout liver. Gen Comp Endocrinol 2009; 161: 146-152.
362. **Poczatkova H, Bogdanova K, Uherkova L, Cervenkova K, Riegrova D, Rypka M, Vesely J**. Dehydroepiandrosterone effects on the mRNA levels of peroxisome proliferator-activated receptors and their coactivators in human hepatoma HepG2 cells. Gen Physiol Biophys 2007; 26: 268-274.
363. **Labrie F, Belanger A, Cusan L, Candas B**. Physiological changes in dehydroepiandrosterone are not reflected by serum levels of active androgens and estrogens but of their metabolites: intracrinology. J Clin Endocrinol Metab 1997; 82: 2403-2409.
364. **Belanger B, Belanger A, Labrie F, Dupont A, Cusan L, Monfette G**. Comparison of residual C-19 steroids in plasma and prostatic tissue of human, rat and guinea pig after castration: unique importance of extratesticular androgens in men. J Steroid Biochem 1989; 32: 695-698.
365. **Widstrom RL, Dillon JS**. Is there a receptor for dehydroepiandrosterone or dehydroepiandrosterone sulfate? Semin Reprod Med 2004; 22: 289-298.
366. **Labrie F, Luu-The V, Belanger A, Lin SX, Simard J, Pelletier G, Labrie C**. Is dehydroepiandrosterone a hormone? J Endocrinol 2005; 187: 169-196.
367. **Fujita A, Furutama D, Tanaka T, Sakai R, Koyama A, Hanafusa T, Mitsuhashi T, Ohsawa N**. In vivo activation of the constitutive androstane receptor beta (CARbeta) by treatment with dehydroepiandrosterone (DHEA) or DHEA sulfate (DHEA-S). FEBS Lett 2002; 532: 373-378.
368. **Bazin MA, Travert C, Carreau S, Rault S, El Kihel L**. First synthesis of 7alpha- and 7beta-amino-DHEA, dehydroepiandrosterone (DHEA) analogues and preliminary evaluation of their cytotoxicity on Leydig cells and TM4 Sertoli cells. Bioorg Med Chem 2007; 15: 3152-3160.
369. **Levalle O, Zylbersztein C, Aszpis S, Aquilano D, Terradas C, Colombani M, Aranda C, Scaglia H**. Recombinant human follicle-stimulating hormone administration increases testosterone production in men, possibly by a Sertoli cell-secreted nonsteroid factor. J Clin Endocrinol Metab 1998; 83: 3973-3976.
370. **Hennebold JD, Daynes RA**. Regulation of macrophage dehydroepiandrosterone sulfate metabolism by inflammatory cytokines. Endocrinology 1994; 135: 67-75.
371. **Khalil A, Lehoux JG, Wagner RJ, Lesur O, Cruz S, Dupont E, Jay-Gerin JP, Wallach J, Fulop T**. Dehydroepiandrosterone protects low density lipoproteins against peroxidation by free radicals produced by gamma-radiolysis of ethanol-water mixtures. Atherosclerosis 1998; 136: 99-107.
372. **Tamagno E, Aragno M, Boccuzzi G, Gallo M, Parola S, Fubini B, Poli G, Danni O**. Oxygen free radical scavenger properties of dehydroepiandrosterone. Cell Biochem Funct 1998; 16: 57-63.
373. **Aksoy Y, Yapanoglu T, Aksou H, Yildirim AK**. The effect of dehydroepiandrosterone on renal ischemia-reperfusion-induced oxidative stress in rabbits. Urol Res 2004; 32: 93-96.
374. **Aragno M, Brignardello E, Tamagno E, Gatto V, Danni O, Boccuzzi G**. Dehydroepiandrosterone administration prevents the oxidative damage induced by acute hyperglycemia in rats. J Endocrinol 1997; 155: 233-240.
375. **Ayhan S, Tugay C, Norton S, Araneo B, Siemionow M**. Dehydroepiandrosterone protects the microcirculation of muscle flaps from ischemia-reperfusion injury by reducing the expression of adhesion molecules. Plast Reconstr Surg 2003; 111: 2286-2294.
376. **Aksoy H, Yapanoglu T, Aksoy Y, Ozbey I, Turhan H, Gursan N**. Dehydroepiandrosterone treatment attenuates reperfusion injury after testicular torsion and detorsion in rats. J Pediatr Surg 2007; 42: 1740-1744.
377. **Mohan PF, Cleary MP**. Short-term effects of dehydroepiandrosterone treatment in rats on mitochondrial respiration. J Nutr 1991; 121: 240-250.
378. **Zhang L, Li B, Ma W, Barker JL, Chang YH, Zhao W, Rubinow DR**. Dehydroepiandrosterone (DHEA) and its sulfated derivative (DHEAS) regulate apoptosis during neurogenesis by triggering the Akt signaling pathway in opposing ways. Brain Res Mol Brain Res 2002; 98: 58-66.
379. **Jiang Y, Miyazaki T, Honda A, Hirayama T, Yoshida S, Tanaka N, Matsuzaki Y**. Apoptosis and inhibition of the phosphatidylinositol 3-kinase/Akt signaling pathway in the anti-proliferative actions of dehydroepiandrosterone. J Gastroenterol 2005; 40: 490-497.
380. **Takahashi H, Nakajima A, Sekihara H**. Dehydroepiandrosterone (DHEA) and its sulfate (DHEAS) inhibit the apoptosis in human peripheral blood lymphocytes. J Steroid Biochem Mol Biol 2004; 88: 261-264.
381. **Hadziselimovic F, Geneto R, Emmons LR**. Increased apoptosis in the contralateral testes of patients with testicular torsion as a factor for infertility. J Urol 1998; 160: 1158-1160.

382. **Arnold JT, Blackman MR**. Does DHEA exert direct effects on androgen and estrogen receptors, and does it promote or prevent prostate cancer? Endocrinology 2005; 146: 4565-4567.
383. **Baumgart E, Vanhorebeek I, Grabenbauer M, Borgers M, Declercq PE, Fahimi HD, Baes M**. Mitochondrial alterations caused by defective peroxisomal biogenesis in a mouse model for Zellweger syndrome (PEX5 knockout mouse). Am J Pathol 2001; 159: 1477-1494.
384. **Janssen A, Gressens P, Grabenbauer M, Baumgart E, Schad A, Vanhorebeek I, Brouwers A, Declercq PE, Fahimi D, Evrard P, Schoonjans L, Collen D, Carmeliet P, Mannaerts G, Van Veldhoven P, Baes M**. Neuronal migration depends on intact peroxisomal function in brain and in extraneuronal tissues. J Neurosci 2003; 23: 9732-9741.
385. **Robinson BH**. The role of manganese superoxide dismutase in health and disease. J Inherit Metab Dis 1998; 21: 598-603.
386. **Liu R, Buettner GR, Oberley LW**. Oxygen free radicals mediate the induction of manganese superoxide dismutase gene expression by TNF-alpha. Free Radic Biol Med 2000; 28: 1197-1205.
387. **Jackson RM, Parish G, Helton ES**. Peroxynitrite modulates MnSOD gene expression in lung epithelial cells. Free Radic Biol Med 1998; 25: 463-472.
388. **Poswig A, Wenk J, Brenneisen P, Wlaschek M, Hommel C, Quel G, Faisst K, Dissemond J, Briviba K, Krieg T, Scharffetter-Kochanek K**. Adaptive antioxidant response of manganese-superoxide dismutase following repetitive UVA irradiation. J Invest Dermatol 1999; 112: 13-18.
389. **Sato M, Sasaki M, Hojo H**. Antioxidative roles of metallothionein and manganese superoxide dismutase induced by tumor necrosis factor-alpha and interleukin-6. Arch Biochem Biophys 1995; 316: 738-744.
390. **Nogae C, Makino N, Hata T, Nogae I, Takahashi S, Suzuki K, Taniguchi N, Yanaga T**. Interleukin 1 alpha-induced expression of manganous superoxide dismutase reduces myocardial reperfusion injury in the rat. J Mol Cell Cardiol 1995; 27: 2091-2099.
391. **Sheweita SA, Tilmisany AM, Al-Sawaf H**. Mechanisms of male infertility: role of antioxidants. Curr Drug Metab 2005; 6: 495-501.
392. **Schriner SE, Linford NJ, Martin GM, Treuting P, Ogburn CE, Emond M, Coskun PE, Ladiges W, Wolf N, Van Remmen H, Wallace DC, Rabinovitch PS**. Extension of murine life span by overexpression of catalase targeted to mitochondria. Science 2005; 308: 1909-1911.
393. **Guazzone VA, Jacobo P, Theas MS, Lustig L**. Cytokines and chemokines in testicular inflammation: A brief review. Microsc Res Tech 2009.
394. **Bryniarski K, Szczepanik M, Ptak M, Ptak W**. Modulation of testicular macrophage activity by collagenase. Folia Histochem Cytobiol 2005; 43: 37-41.
395. **Boockfor FR, Wang D, Lin T, Nagpal ML, Spangelo BL**. Interleukin-6 secretion from rat Leydig cells in culture. Endocrinology 1994; 134: 2150-2155.
396. **Cudicini C, Kercret H, Touzalin AM, Ballet F, Jegou B**. Vectorial production of interleukin 1 and interleukin 6 by rat Sertoli cells cultured in a dual culture compartment system. Endocrinology 1997; 138: 2863-2870.
397. **Rival C, Theas MS, Guazzone VA, Lustig L**. Interleukin-6 and IL-6 receptor cell expression in testis of rats with autoimmune orchitis. J Reprod Immunol 2006; 70: 43-58.
398. **Potashnik H, Elhija MA, Lunenfeld E, Potashnik G, Schlatt S, Nieschlag E, Huleihel M**. Interleukin-6 expression during normal maturation of the mouse testis. Eur Cytokine Netw 2005; 16: 161-165.
399. **Thorsson AV, Christiansen P, Ritzen M**. Efficacy and safety of hormonal treatment of cryptorchidism: current state of the art. Acta Paediatr 2007; 96: 628-630.
400. **Mangelsdorf DJ, Thummel C, Beato M, Herrlich P, Schutz G, Umesono K, Blumberg B, Kastner P, Mark M, Chambon P, Evans RM**. The nuclear receptor superfamily: the second decade. Cell 1995; 83: 835-839.
401. **Ahsan S, Lacey M, Whitehead SA**. Interactions between interleukin-1 beta, nitric oxide and prostaglandin E2 in the rat ovary: effects on steroidogenesis. Eur J Endocrinol 1997; 137: 293-300.
402. **Frungieri MB, Weidinger S, Meineke V, Kohn FM, Mayerhofer A**. Proliferative action of mast-cell tryptase is mediated by PAR2, COX2, prostaglandins, and PPARgamma : Possible relevance to human fibrotic disorders. Proc Natl Acad Sci U S A 2002; 99: 15072-15077.
403. **Hase T, Yoshimura R, Matsuyama M, Kawahito Y, Wada S, Tsuchida K, Sano H, Nakatani T**. Cyclooxygenase-1 and -2 in human testicular tumours. Eur J Cancer 2003; 39: 2043-2049.
404. **Wang X, Dyson MT, Jo Y, Stocco DM**. Inhibition of cyclooxygenase-2 activity enhances steroidogenesis and steroidogenic acute regulatory gene expression in MA-10 mouse Leydig cells. Endocrinology 2003; 144: 3368-3375.
405. **Rouzer CA, Marnett LJ**. Cyclooxygenases: structural and functional insights. J Lipid Res 2009; 50 Suppl: S29-34.
406. **Kozak KR, Rowlinson SW, Marnett LJ**. Oxygenation of the endocannabinoid, 2-arachidonylglycerol, to glyceryl prostaglandins by cyclooxygenase-2. J Biol Chem 2000; 275: 33744-33749.
407. **Mannaerts GP**. [Lipid degradation by way of beta and alpha oxidation in peroxisomes of mammals]. Verh K Acad Geneeskd Belg 1999; 61: 65-89.
408. **Van Veldhoven PP**. New insights in peroxisomal beta-oxidation. Implications for human peroxisomal disorders. Verh K Acad Geneeskd Belg 1998; 60: 195-214.

Acknowledgment

I would like in this section to thank all the persons who supported me during the whole period of my doctoral thesis.

I am very grateful to Prof. Dr. Eveline Baumgart-Vogt who established the subject of the thesis and for having directed my study within the working group. She is also greatly acknowledged for her constructive remarks and for discussions about the progress of this work and for having guided me through the fascinating world of microscopy. Her way of explaining cell biology really helped me to learn a lot about cell metabolism and, in particularly, about peroxisomes.

I would like to thanks as well Dr. Werner Kovacs for having given me good tips for my molecular biology experimental work. I enjoyed our scientific and personal discussions.

Many thanks also to Dr. B. Ahlemeyer for our good discussions, scientific ones as well as private ones.

From the Giessen Veterinary Anatomy Department, thanks to Dr. Ralph Brehm (now in Hannover) for the kind explanations about animal breeding strategy.

My warm thanks are going to Mrs. Thiele for her availability and her patience. She explained to me in a kind and friendly way the method of isolation and culturing of the cells.

Many thanks as well to Mrs. Richter, who had the patience to go together with me through the literature of Leydig cells methodology isolation and to help me in establishing the protocol for this type of cells. She also taught me the Western Blot method and so many other things that I cannot list everything here!

I also thank Mrs. Gottwald, Mrs. Snips and Mrs. Pfeiffer who welcomed me at the very beginning of my time in this department, in the morphology laboratories and gave me the basic hints, but very important ones for preparation and sectioning of tissues.

Thank you to the doctoral and master students for nice discussion and for the cosmopolitan atmosphere, making me to discover different cultures.

Vielen Dank to both nice secretaries, Mrs Hellmann who contributed to my learning of this “not so easy” German language and to Mrs. Heller who contributed to my way of speaking German and let me believe that I can speak this language…

The International PhD Program of the University of Giessen, the DFG Reproductive Science and KFO 181 Reproductive Group are greatly acknowledged for the financial support.

I thank my family and my friends, especially for their encouragement emails which meant very much to me during all this time of my life, particularly Anca with her jokes which I miss since I left Romania. Thanks to my sister, Bianca and Oliver for delightful phone and video calls.

I thank Etienne for his continuous support and being so lovely and patient with me!

Finally, I thank very much my parents for their comprehension, encouragement, and for their financial support during my studies.

PROFESSIONAL EXPERIENCE

2009 - now

Research Fellow, DFG project, Clinical Research Group “Male Factor Infertility”, KLIFO 181/Project 3 “Peroxisomes and infertility” (Associated with the Section 6 “Reproduction in Man and Animals” in the International Giessen Graduate School for the Life Sciences

Department of Anatomy and Cell Biology II, Medical Cell Biology. Justus-Liebig University, Giessen, Germany. Group of Prof. Dr. E. Baumgart-Vogt (Director)

2004 - 2009

Doctoral Researcher, Department of Anatomy and Cell Biology II, Medical Cell Biology. Justus-Liebig University, Giessen, Germany. Group of Prof. Dr. E. Baumgart-Vogt (Director)

2003 - 2004

Research Fellow, Department of Internal Medicine. Justus-Liebig University, Giessen, Germany. Group of Prof. Dr. W. Seeger (Director)

2000-2003

Veterinary Medicine Doctor, National Institute of Diagnosis and Animal Health, Bucharest, Romania, Group of Dr. Stefan Nicolaie (Director)

2000

Veterinary Medicine Doctor, Sterilization and vaccination of stray dogs. Foundation "Four Paws" and Department of Animal Surgery, City Hall Bucharest, Romania

PRIZES AND AWARDS

- Young Investigator Award 2009 (2nd prize) – 5th International Workshop of Molecular Andrology (Giessen, Germany)
- Larry Ewing Memorial Trainee Travel Fund Grant 2009 – 42nd Annual Meeting of the Society for the Study of Reproduction (Pittsburgh, PA, USA)
- Selection of Image for the "2008/2009 Calendar from Biology of Reproduction", Page: September 2008, *Figure 2D* from Nenicu et al 2007 (see below)

SCIENTIFIC PUBLICATIONS AND PRESENTATIONS

Publications

Nenicu A, Lüers GH, Kovacs W, David M, Zimmer A, Bergmann M, and Baumgart-Vogt E (2007) Peroxisomes in Human and Mouse Testis: Differential expression of peroxisomal proteins in germ cells and distinct somatic cell types of the testis. Biol Reprod 2007; 77:1060-1072.

Lüers GH, **Nenicu A**, and Baumgart-Vogt E (2008) Peroxisomes are essential for regular spermatogenesis. In: Biology of male germ cells, Editors: Glander HJ, Grunewald S, Paasch U, Shaker Publisher GmbH, Aachen, Germany, ISBN: 978-3-8322-7682-9

Nenicu A, Hartmann MF, Wudy SA, Okun JG, Guillou F, Crane DI, Baumgart-Vogt E (2010) Peroxisomes and infertility: Molecular pathogenesis of male infertility due to peroxisomal deficiency in Sertoli cells (scsPex13 knockout). (article in preparation for Cell Metabolism)

Selected Oral Presentations on Congresses

Nenicu A, Kovacs W, and Baumgart-Vogt E (2006) *Peroxisomes in the human and mouse testis,* European Peroxisome Meeting, September 18-19th 2006 Leuven, Belgium

Nenicu A, Crane DI, Guillou F, and Baumgart-Vogt E (2008) *Sertoli Cell-Specific Knockout of Pex13 effects integrity and function of adult testis in the mouse,* 103rd Annual Meeting of the Germany Society for Anatomy, March 14-17th 2008, Innsbruck, Austria

Nenicu A, Okun JG, Wudy SA, Hartmann FM, Guillou F, Crane DI and Baumgart-Vogt E *The PEX13 knockout in Sertoli cells leads to infertility due to alterations in steroid precursor metabolism, lipid toxicity and oxidative stress*, International Congress – Molecular Andrology, Stem Cells – Somatic Cells – Germ Cells, May 8-10th 2009, Giessen, Germany

Abstracts and Posters

Nenicu A and Baumgart-Vogt E (2005) *Heterogeneity of peroxisomes in distinct cell types of the adult mouse testis.* Eur J Cell Biol Volume 84S1 p58, Annual Meeting of the German Society for Cell Biology, March 16-19th 2005, Heidelberg

Nenicu A, Bergmann M, and Baumgart-Vogt E (2005) *Important role of peroxisomes in lipid metabolism of this testicular cell type.* Andrologia 2005 Dec;37(6):197-249, 4th International Workshop of Molecular Andrology, Oct 7-9th 2005, Giessen

Nenicu A, Kovacs W, Bergmann M, and Baumgart-Vogt E (2006) *Peroxisomes in the human and mouse testis.* 23rd Annual workshop of the German Society for Anatomy, Sept 27-29th 2006, Würzburg

Nenicu A, Lüers GH, Bergmann M, and Baumgart-Vogt E (2007) *Peroxisomal heterogeneities in distinct cell types of the testis – stage dependent alteration of the peroxisomal compartment in seminiferous tubules.* 102nd Annual Meeting of the Germany Society for Anatomy, March 30th - April2nd 2007, Giessen
Annual Meeting of the German Society for Cell Biology, March 14-17th 2007, Frankfurt

Nenicu A, Lüers GH, Bergmann M, and Baumgart-Vogt E (2007) *Stage-dependent alterations of the peroxisomal compartment during spermatogenesis in seminiferous tubules of the testis. Special role of Seroli cells in peroxisome removal.* Eur J Cell Biol Volume 86S1 p, Annual Meeting of the German Society for Cell Biology, March 14-17th 2007, Frankfurt

Nenicu A, Okun JG, Wudy SA, Hartmann FM, Guillou F, Crane DI and Baumgart-Vogt E (2009) *Molecular pathogenesis of infertility in mice with Sertoli-cell-specific peroxisome dysfunction.* 104th Annual Meeting of the Germany Society for Anatomy, March 27-30th 2009, Antwerpen, Belgium

Nenicu A, Okun JG, Hartmann MF, Wudy SA, Guillou F, Crane DI, Baumgart-Vogt E (2009) *Molecular pathogenesis of male infertility due to peroxisome dysfunction in Sertoli cells.* 42nd Annual Meeting of the Society for the Study of Reproduction (Pittsburgh, PA, USA)

TEACHING EXPERIENCE

In charge of the organization of a practical course for the International Giessen Graduate School for the Life Sciences (GGL-Section Reproductive Medicine), theoretical and experimental parts, June 11th-13th 2008.

Teacher and Practical Advisor for: Isolation of primary Sertoli cells, cultivation of the cells, and characterization of the purity of Sertoli cells by immunofluorescence staining, isolation of subcellular fractions from Sertoli cells, Western blot analysis.

International Workshop Molecular Andrology

Stem Cells • Somatic Cells • Germ Cells

Young Investigator Award 2009

2nd Prize

Anca Nenicu

This award was presented during the 5th International Workshop MOLECULAR ANDROLOGY in Giessen, Germany, for scientific excellence.

Prof. Dr. Mark Hedger
Chair Prize Committee

Prof. Andres Meinhardt
Convenor

Giessen 10th May 2009

SOCIETY FOR THE STUDY OF REPRODUCTION 4327

Anca Nenicu

Check Number: 4327
Check Date: Jul 18, 2009

Check Amount: $235.00

Item to be Paid - Description	Discount Taken	Amount Paid
2009 LEMTTF Travel Award		235.00

SOCIETY
for the
STUDY OF REPRODUCTION

ADMINISTRATIVE OFFICES
Judith Jansen, Executive Director
1619 Monroe Street
Madison, Wisconsin 53711-2063
Voice 608.256.2777
Fax 608.256.4610

17 July 2009

MEMO

TO: Recipients of Larry Ewing Memorial Trainee Travel Fund Grants

FROM: Kristin Happ Molitoris

Enclosed, please find a check representing your travel grant from the Larry Ewing Memorial Trainee Travel Fund (LEMTTF). This grant is meant to defray expenses incurred by your participation in the 42nd Annual Meeting of the Society for the Study of Reproduction, July 18–22, in Pittsburgh, Pennsylvania. The LEMTTF is supported by donations from SSR members, by the sale of commemorative t-shirts at each annual meeting, and a grant from the Eunice Kennedy Shriver National Institute of Child Health and Human Development.

We are looking forward to your presentation.

Enclosure: one check in the amount of US $235.00

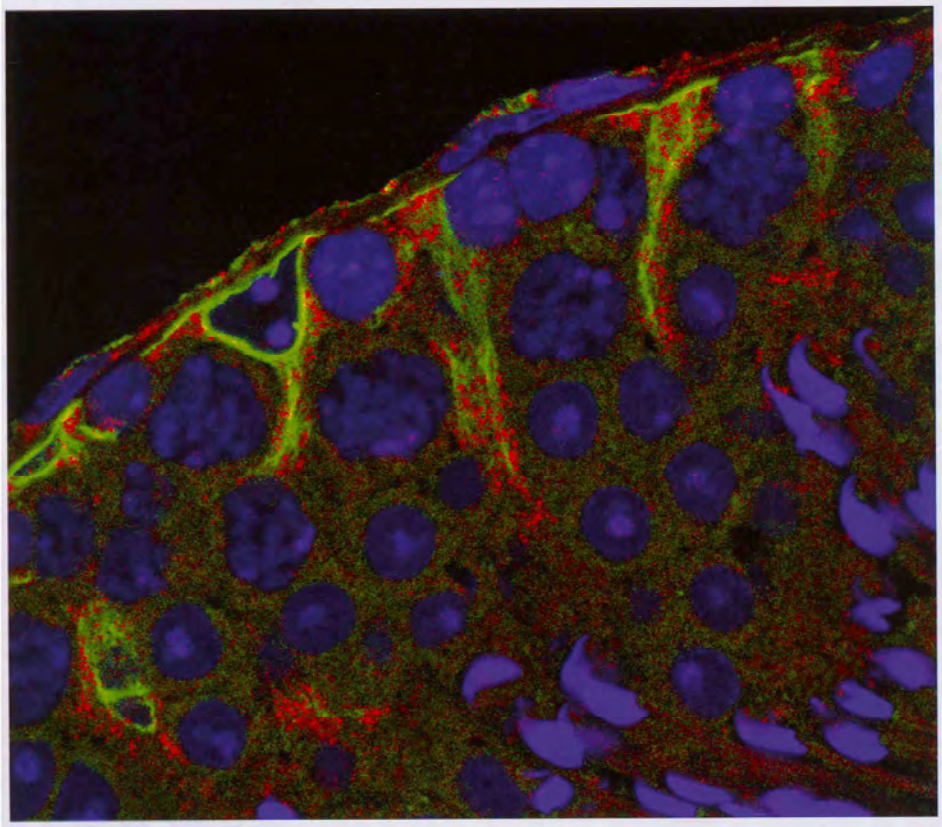

Peroxisomal and mitochondrial proteins in adult mouse testis detected using double immunofluorescence for ABCD1 (red) and vimentin (green), and counterstained with TOTO-3 iodide (blue).
Nenicu et al., *Biology of Reproduction* December 2007.

SEPTEMBER 2008

SUNDAY	MONDAY	TUESDAY	WEDNESDAY	THURSDAY	FRIDAY	SATURDAY
♂ ♀	SSR Office Closed 1	2	3	4	5	6
7	8	9	10	11	12	13
14	15	16	17	18	19	20
21	22	23	24	25	26	27
28	29	30				

Got *BOR* in your library?
Check, and let your libraries know that you want *BOR*!

Society for the Study of Reproduction: http://www.ssr.org
Biology of Reproduction: http://www.biolreprod.org
Online Manuscript Processing System: http://submit.biolreprod.org
SUBMIT YOUR BEST MANUSCRIPTS TO *BIOLOGY OF REPRODUCTION*

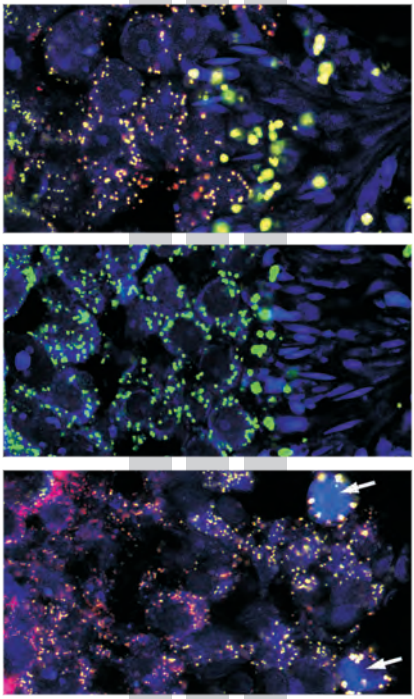

édition scientifique
VVB LAUFERSWEILER VERLAG

VVB LAUFERSWEILER VERLAG
STAUFENBERGRING 15
D-35396 GIESSEN

Tel: 0641-5599888 Fax: -5599890
redaktion@doktorverlag.de
www.doktorverlag.de

ISBN: 978-3-8359-5617-9